A STUDY OF FORCE-MOTION AND VIBRATION TRANSMISSION PROPERTIES OF SEATED BODY UNDER VERTICAL VIBRATION AND EFFECTS OF SITTING POSTURE

Wenping Wang

A Thesis

in

The Department

of

Mechanical and Industrial Engineering

Presented in Partial Fulfillment of the Requirements
for the Degree of Doctor of Philosophy (Mechanical Engineering) at
Concordia University
Montréal, Québec, Canada

December 2006

Your file Votre référence
ISBN: 978-0-494-30145-6
Our file Notre référence
ISBN: 978-0-494-30145-6

ABSTRACT

A Study of Force-Motion and Vibration Transmission Properties of Seated Body Under Vertical Vibration and Effects of Sitting Posture

Wenping Wang, Ph.D.
Concordia University, 2006

Seated occupant perception of whole-body vibration is attributed to physical responses of the tissues and muscles to vibration, such as stresses, strains and power absorption within the tissues. Such physical biodynamic responses are related to sensation of discomfort, fatigue and health and safety risks due to vibration exposure. The physical responses of the seated body to vibration are strongly influenced by various factors in a highly complex manner. These include the frequency content and magnitudes of transmitted vibration, individual factors (age, build, body mass, body mass index, physical fitness, gender, etc.), seat design factors, postural supports, etc. Owing to extreme complexities associated with quantifying the physical biodynamic responses, the overall biodynamic responses involving the force-motion relationship at the body-seat interface have been mostly measured and studied. A few studies have also investigated the nature of vibration transmitted to various segments of the body. A number of biodynamic models have also been developed on the basis of these measures. The force-motion and vibration transmission properties, however, have been derived in different laboratories using subjects of varying masses and most likely under different conditions. While the reported data clearly show extreme variabilities, the corresponding models differ most significantly in the structure as well as responses.

This dissertation research concerns with characterization of the biodynamic responses of seated human body to vibration in terms of force-motion and vibration

transmission properties. The force-motion biodynamic responses were measured considering the primary driving-point (seat-buttock interface) using 13 male and 14 female subjects under different postural and excitation conditions. The force-motion data were also analyzed to derive the power absorbed within the vibration-exposed body, apart from the apparent mass (APMS). The measured data are interpreted to demonstrate the significant effects of sitting postures, involving variations in backrest support, hands position and seat geometry, on the biodynamic responses. The results revealed most significant effect of the body mass. The results attained from ANCOVA further show that the primary resonant frequency and bandwidth of the biodynamic responses are strongly influenced by the combined effects of hands position and back support condition, while the peak magnitude is further affected by the seat height. Owing to the limitations of the single-driving point force-motion relationships, experiments were undertaken to measure both the force-motion and transmission of seat vibration to the head simultaneously. A secondary driving-point, formed by the backrest and upper body, is also incorporated for fully characterizing the force-motion biodynamics of the body seated with a back support. An adjustable head-strap comprising a three-axes acceleration measurement system was developed to measure the vibration transmitted to the seated subjects' head. These experiments were performed with 12 adult male subjects and the data were analyzed to derive the biodynamic responses in terms of seat-to-head transmissibility (STHT), total apparent mass measured at the seat pan, cross-axis apparent mass of the upper body reflected at the back support. The results attained were used to characterize the roles of various contributing factors, such as back support condition, hands position and excitation magnitude. The results reveal the non-linearities in the APMS and STHT

responses. The results of the ANOVA further show the strong influences of the three back support conditions on both vertical and fore-and-aft STHT responses over the entire frequency ranges. The vertical APMS magnitudes in the vicinity of the secondary resonance tend to be higher for the back supported postures.

The mechanical equivalent models of the seated body are further attempted on the basis of observed biodynamic responses. Owing to the significant effects of the back support conditions, one-and two-dimensional models are formulated to simulate the APMS and STHT responses for all three back support conditions. The target datasets, however, are limited to those representing mean body mass of 75.58 kg in the excitation of $1 m/s^2$ rms acceleration (0.5-15 Hz). A 4-DOF one-dimensional model is developed using simultaneously measured vertical APMS and STHT response. The model parameters are identified for the three back support conditions respectively to emphasize the significance of back support conditions. The model parameter analysis suggest that both the force-motion and motion-motion measures need to be satisfied in order to obtain a more reliable model parameter set. The two-dimensional 5-DOF model allows for the consideration of the upper body interactions with the inclined backrest support. The identified models show good agreements with the measured target responses in APMS measured at the seat pan and the backrest, and vertical STHT.

The model validity is further demonstrated in terms of the absorbed power property of the seated body. Considering that the physical responses of the tissues are more directly related to localized responses, alternate methods that can predict the distributed absorbed power property in body segment are realized in both one-dimensional and two-dimensional models.

ACKNOWLEDGEMENTS

Firstly, the author is profoundly grateful to her supervisors, Dr. Subhash Rakheja and Dr. Paul-Émile Boileau, for their scholarly guidance, enthusiastic dedication and financial support throughout the doctoral work. The author will be forever indebted to their diligent efforts for the publications and dissertation.

The author is also greatly thankful for that the initiation of doctoral research and scientific publication is attributed to receiving the extensive data from earlier studies at CONCAVE under the leadership of Dr. Rakheja.

The author would like to acknowledge the technical support provided by Mr. Danius Juras, José Esteves, and Jerome Boutin during the experimental setup at CONCAVE and IRSST respectively.

Particularly, the author would like to express her most sincere gratitude to all of those who have rendered gratuitous assistance with participation of human vibration experiments.

Finally, the author conveys her deepest sense of gratitude to her husband, Changqing Zhang, and their lovely son, Zhiyuan Zhang, for their inspiration and encouragement through the doctoral study.

TABLE OF CONTENTS

LIST OF FIGURES

LIST OF TABLES

LIST OF ABBREVIATIONS AND SYMBOLS

ABBREVIATIONS

ANOVA	Analysis of variance
ANCOVA	Analysis of covariance
APMS	Apparent mass
BIF	A flat pan with back supported by an inclined backrest
BVF	A flat pan with back supported by a vertical backrest
BVF	A flat pan with back supported by a vertical backrest
BIP	An inclined seat pan and back supported by the inclined backrest
DPMI	Driving point mechanical impedance
LAP	Hands-in-lap posture
LBP	Low back pain
ISO	International Standard Organization
IBS	Inclined backrest support
NBS	No back support
NVF	A flat pan with back not supported
NVP	An inclined pan with back not supported
rms	Root mean square
SD	Standard deviation
STHT	Seat to head transmissibility
VBS	vertical backrest support
WBV	Whole body vibration
WBVVS	Whole-body vehicle vibration simulator

SYMBOLS

α, β, γ	weighting factors applied to the APMS and STHT functions
ϕ	inclination angle of the seat pan with respect to horizontal axis
ω	angular frequency (rad/s)
χ	model parameter vector
μ_i	the fraction of model mass to the total body mass
λ_i	the weighting factors applied to the modulus of biodynamic function
ψ_i	the weighting factors applied to the phase of biodynamic function
ζ_i	relative motion across a damping element in lumped parameter models
θ	the rotational motion of entire upper body in 5-DOF model
γ_z	coherence of vertical STHT
γ_x	coherence of fore-and-aft STHT
τ	the time lag between the force and velocity signal
a, b, c, d	the distances from the greater trochanteric point to each body mass in 5-DOF model
$a(j\omega)$	the driving point acceleration
$a_i(j\omega)$	body segment acceleration response
$C_{vF}(\omega)$	coincident spectral density between the force and velocity

c_1, c_2, c_3, c_4	viscous damping coefficients (Ns/m)
c_{b1}, c_{b2}	viscous damping coefficients (Ns/m)
c_t	rotational viscous damping coefficients (Nms/rad)
$E(\chi)$	squared errors resulting from the biodynamic responses
F_d	the damping force developed by the linear viscous element
F_v	the force measured at the seat base in the vertical direction
F_b	the force measured normal to the backrest
$\widetilde{F}(t)$	driving force at the human-seat interface
$F(j\omega)$	complex driving force at the human-seat interface
$G_{aF}(j\omega)$	one-sided cross-spectral densities of acceleration and force
$G_{vF}(j\omega)$	one-sided cross-spectral densities of velocity and force
$G_a(j\omega)$	one-sided auto-spectral density of the vertical seat acceleration
$G_v(j\omega)$	one-sided auto-spectral density of the vertical seat velocity
$H_i(s)$	displacement transfer function relating the human seat interface motion (x) to that of body mass m_i (x_i)
$H_i(j\omega)$	complex displacement transfer function relating the human seat interface motion (x) to that of body mass m_i (x_i)
$H_{\dot{\zeta}_1}(j\omega)$	complex relative velocity transfer function
k_1, k_2, k_3, k_4	stiffness coefficients (N/m)

k_{b1}, k_{b2}	stiffness coefficients (N/m)
k_t	rotational stiffness coefficients (Nm/rad)
$M(j\omega)$	complex APMS function
M_v	vertical APMS
M_{vb}	cross-axis APMS
$M_v(j\omega)$	complex 'vertical APMS' function
$M_{vb}(j\omega)$	complex 'cross-axis APMS' function
m_0, m_1, m_2, m_3, m_4	model masses
m_s	sitting mass in the model
M_T	total body mass in the model
$\overline{M}(s)$	normalized APMS transfer function
N	the number of discrete frequencies selected in the 0.5 to 15 Hz range
NC	total number of viscous damping elements in the model
$p_i(\omega)$	absorbed power density in each viscous damping element (Nms^{-1}/Hz)
$Q_{vF}(\omega)$	quardrature spectral density between the force and velocity
r_i $(i=1,2,3,4)$	relative motion of body masses in 5-DOF model
R_i $(i=1,2,3,4)$	Laplace transformation of r_i
X	motion at the driving point (4-DOF model)
x_i $(i=1,2,3,4)$	motion of body masses in 4-DOF model
X_i $(i=1,2,3,4)$	Laplace transformation of x_i
X	Laplace transformation of x

$S_{aF}(j\omega)$	cross-spectral densities of acceleration and force
$S_{vF}(j\omega)$	cross-spectral densities of velocity and force
$S_a(j\omega)$	auto-spectral density of the vertical seat acceleration
$S_v(j\omega)$	auto-spectral density of the vertical seat velocity
$S_{\ddot{x}_H\ddot{z}}(j\omega)$	cross spectral densities of the head acceleration along the x direction
$S_{\ddot{z}}(j\omega)$	auto-spectral density of the vertical seat acceleration
$S_{\ddot{z}\,H\ddot{z}}(j\omega)$	cross spectral densities of the head acceleration along the z direction
$S_{\ddot{z}}(j\omega)$	auto-spectral density of the vertical seat acceleration
$S_{\ddot{x}_H}(j\omega)$	auto-spectral density of the fore-and-aft head acceleration
$S_{\ddot{z}F_V}(j\omega)$	cross-spectral densities of acceleration and force
TF_x	fore-and-aft STHT
TF_z	vertical STHT
$T(j\omega)$	complex seat-to-head transmissibility
$T(s)$	vertical STHT transfer function
$T_x(s)$	fore-and-aft STHT transfer function
$\widetilde{V}(t)$	driving force at the human-seat interface
$\ddot{Z}$	acceleration at the human-seat interface in the vertical direction

CHAPTER 1

INTRODUCTION AND SCOPE OF DISSERTATION

1.1 General

Depending on the type and design of road and off-road vehicles, the seated vehicle occupants are exposed to considerable levels of low-frequency vibration originating primarily from the vehicle–terrain interactions. Prolonged exposure to such whole-body type of vibration has been related to discomfort, reduced working efficiency, and various health effects [1].

Many studies have suggested that the exposure to whole-body vibration (WBV) can affect the lumbar spine and the connected nervous system [2,3]. Epidemiological studies have suggested the associations between the WBV exposure encountered in vehicles and adverse effects among the professional drivers [4-7]. A critical evaluation of the epidemiologic literature on the effects of long-term WBV exposure on the spinal system indicated that low back pain (LBP), early degeneration of the lumbar spine system and herniated lumbar disc were the most frequently reported adverse effects in workers exposed to WBV. There are also many chronic health problems and adverse physiological and psychophysical effects associated with long-term occupational exposure to vibration in the 0.5-80 Hz frequency range, including abdominal pain digestive and vision problems *etc.*[1, 7-9].

In view of the severe health effects resulting from exposure to vibration environment of on-and-off road vehicles, knowledge of the manners in which vibration is transmitted to and through the human body is a prerequisite for understanding of the cause-effect relationship between WBV and health, comfort and performance. The

human response to vibration has been mostly characterized by the biodynamic responses expressed either in terms of motion-motion relationships between the anatomical locations of the seated body and the human–seat interface, or by the force-motion relationships at the driving-point [9-11]. The biodynamic responses related to the motion-motion and force-motion relationships have been widely investigated to enhance an understanding of the human responses to vibration and to develop mechanical equivalent models for applications in seating dynamics [1,12].

The human response to vibration has been widely investigated under a variety of test conditions, involving differences in subjects' mass, sitting posture, excitation frequency and magnitude, and type of excitation [9-11]. Body posture in a vehicular environment is a complex function of many seat and work-station design parameters, such as seat height, footrest position with respect to the seat, hands position (in the lap or on a steering wheel), backrest angle, and seat pan dimensions and angle. The International Standard, ISO-5982 [12], defines the range of biodynamic responses of the seated occupants exposed to vertical vibration, which are applicable only for sitting postures without a back support. Therefore, the range of idealized values presented in ISO-5982, and the ensuing biomechanical model are not likely applicable for the seated vehicle occupants during typical vehicular vibration exposure.

This dissertation research firstly explores the force-motion behavior of the seated occupant at a single measurement point while exposed to vertical vibration. Furthermore, the motion-motion biodynamic response of the seated occupant is also measured along with the force-motion biodynamic response and both functions are analyzed in terms of the apparent mass and seat-to-head vibration transmissibility. The mechanical equivalent

models of the occupants satisfying both functions are finally proposed and validated to characterize the simultaneous force-motion and motion-motion behavior of vehicle occupants under vertical WBV.

1.2 Human response to whole-body vibration

Whole-body vibration (WBV) arises where the body is supported on a vibrating surface. When sitting on a vibrating seat, standing on a vibrating floor, or lying on a vibrating bed, humans are subjected to WBV. Heavy road and off road vehicles, due to their interactions with uneven terrains, are known to yield considerable levels of whole body vibration to the driver and the passengers. Prolonged exposure to vehicular whole body vibration has been related to discomfort, reduced working efficiency, and various health and safety risks. In an attempt to enhance the understanding of the seated body and potential injury mechanisms, considerable efforts have been made to characterize the biodynamic responses of seated human body under WBV exposure.

It has been well-established that the occupant dynamics contribute considerably to the overall vibration attenuation performance of seats. Figure 1.1 illustrates the comparison of acceleration transmissibility of an automotive seat, loaded with equivalent rigid mass and human subjects [13]. The seated occupant response to vibration contributes considerably in shaping the vibration transmission performance of a seat, which may be attributed to dissipation/absorption of vibration energy by the biological system. It is necessary for the designer of preventative measures to take into account the fact that the biodynamic properties of the human body can interact with and affect the characteristics of a vibration isolation system. Knowledge of the biodynamic

characteristics of the human body may also find applications in establishing meaningful laboratory vehicle seat testing procedures based on the applicable biodynamic data [1,13].

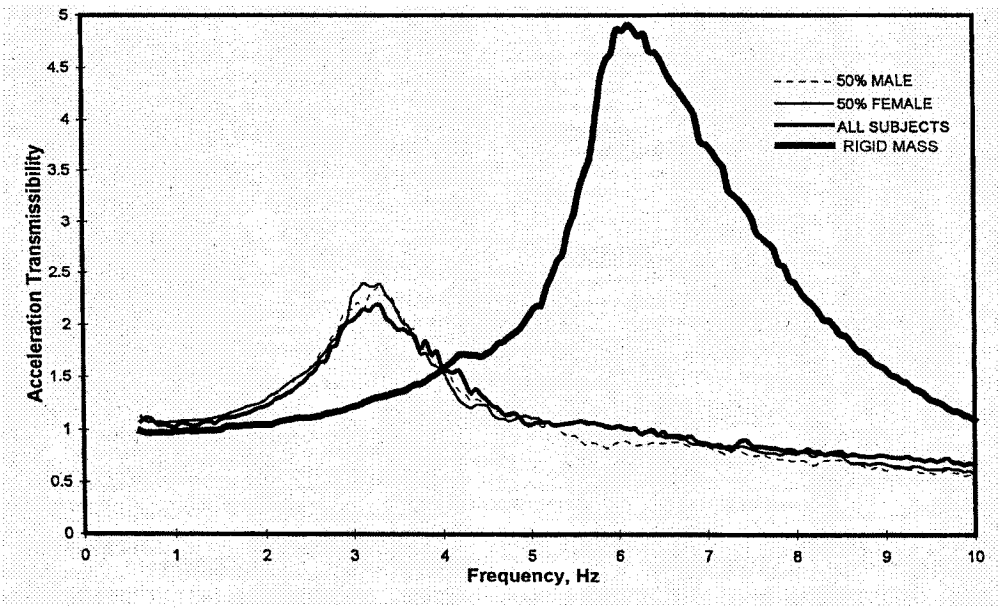

Figure 1.1: Comparison of acceleration transmissibility of an automotive seat loaded with human subjects and an equivalent rigid mass [13].

Biodynamic responses of seated occupants to whole-body vibration can be broadly categorized into two types. The first category (force-motion relationship) is only concerned with measurements of force and motion at the 'driving point' (i.e. the vibrating surface that the subject is in contact with). The second category (motion-motion or 'transmissibility' relationship) is only concerned with acceleration measurements made at multiple sites such as measurements at the driving-point combined with measurements at the body segments.

The driving-point response functions such as the driving-point mechanical impedance (DPMI), and the apparent mass (APMS) which are ratios between the force

and the motion at the human-seat interface have been widely used to represent the dynamic characteristics of the body. Mathematically, these two force-motion relationships are given by:

$$Z(j\omega) = \frac{F(j\omega)}{V(j\omega)} \tag{1.1}$$

$$M(j\omega) = \frac{F(j\omega)}{a(j\omega)} = \frac{Z(j\omega)}{j\omega} \tag{1.2}$$

In the above equation, $Z(j\omega)$ is the complex DPMI, $M(j\omega)$ is the complex apparent mass and, $F(j\omega), V(j\omega)$, and $a(j\omega)$ are the driving point force, and driving point velocity and acceleration, respectively. ω is the angular frequency, and $j = \sqrt{-1}$ is the complex phasor. The magnitude of DPMI can be obtained by multiplying the APMS by the angular frequency, thus tending to make the resonant peaks appear more apparent at high frequencies, than if they were represented in terms of APMS. From the definitions of DPMI and APMS, it is apparent that DPMI leads the APMS by 90 degrees.

The absorbed power, another type of force-motion relationship, could be simultaneously acquired from the same measurement as DPMI/APMS, which could be estimated from:

$$P(t) = \tilde{F}(t)\tilde{V}(t) \tag{1.3}$$

Where $\tilde{F}(t)$ and $\tilde{V}(t)$ are the dynamic force and velocity at the human-seat interface respectively. The power can be obtained, in the frequency domain, by calculating the cross-spectrum density of the force and velocity [14]. Because of the phase difference between the measured force and motion at the driving-point, the cross-spectrum density is normally complex, which can be generally expressed as follows [14]:

$$P(j\omega) = C_{vF}(\omega) - jQ_{vF}(\omega) \tag{1.4}$$

In the above equation, $P(j\omega)$ is the complex rate of vibration energy with the unit Nms^{-1}/Hz. $C_{vF}(\omega)$ is the coincident spectral density function, or the co-spectrum, and $Q_{vF}(\omega)$ is the quadrature spectral density function, or the quad-spectrum. The real component of the power determines the energy absorbing part, due to the transformation into heat by internal friction within the tissues. The imaginary component determines the energy storing part within the human body. Unlike the other two driving point dynamic functions, the absorbed power can be used to measure a vibration 'dose', as it increases with vibration magnitude and duration. Absorbed power might be a good quantity for assessing the risk of injury due to WBV exposure, and thus is increasingly attracting more attention [3,15-18].

Vibration transmissibility is defined as the complex ratio measured at the point at which the vibration enters the body (e.g., on a seat) and the point at which the vibration is measured on the body segment (e.g., head, pelvis, spine, viscera).

$$T(j\omega) = \frac{a_i(j\omega)}{a(j\omega)} \tag{1.5}$$

$T(j\omega)$ is the complex seat to body segment transmissibility function and $a_i(j\omega)$ is the body segment acceleration response. Unlike the force-motion biodynamic responses, the motion-motion biodynamic responses involve two measurement points. In view of the measurement challenges arising from mounting accelerometer on the surface of the skin, measurement of the vibration transmission to the head, referred to as seat-to-head transmissibility (STHT), has been widely performed to characterize the motion-motion biodynamic responses [10,11].

The above four functions have been invariably employed to characterize the human biodynamic response to WBV by performing measurements under a variety of test conditions. These include the individual anthropometric parameters, sitting posture and nature of vibration (magnitude and frequency) [10,11]. Based on the measured biodynamic data, a number of mechanical-equivalent biodynamic models have also been proposed in the literature for the purpose of providing a mathematical summary of measured biodynamic responses, estimating the magnitudes of the forces and motion transmitted to particular subsystems within the body (e.g. the spine) and establishing potential damage mechanisms, and assessing the tolerance to vibration under the exposure to intensive vibration levels [12,19-21].

1.3 Review of published biodynamic data on whole body biodynamic responses

In this section, the published data on whole-body biodynamic response characteristics are reviewed together with the test conditions. Table 1.1 summarizes the objectives and experimental conditions of various reported studies on DPMI/APMS, absorbed power, and vibration transmissibility. In many of the earlier studies, such as those conducted by Coermann [22] and Miwa [23], the number of subjects included was usually small and there were few considerations of the many factors affecting the measured biodynamic characteristics, such as the sitting postures, the subject characteristics, and vibration excitations. The majority of the studies have employed limited number of male subjects, while input vibration frequencies have been limited to below 20 Hz.

Table 1.1: Summary of experimental conditions employed in different studies.

Authors	Subject			Excitation			Reported Functions
	Number and gender	Body mass (kg)	Posture	Type	Level	Frequency Range(Hz)	
Coermann (1960)[22]	8 males	70-99	Standing, sitting with feet not supported, no backrest	Sine	0.1, 0.2 and 0.3g	1-20	DPMI and STHT
Vogt et al., (1969)[24]	10 males	79(mean)	Erect sitting, loosely restrained, feet supported, but not vibrated	Sine	0.5g with increased gravity of 1, 2 and 3g	2-15	DPMI, STHT
Suggs et al., (1970)[25]	11 males	58-90	Sitting upright with hands in lap, feet supported, no backrest	Sine	0.10g peak to peak	1.75-10	DPMI
Miwa (1974)[23]	5 males	50-76	Standing; kneeling;sitting erect and relaxed, feet not vibrated	Sine	0.1g r.m.s	3-200	DPMI
Griffin (1975)[26]	12 males	60-88	No backrest	Sine	0.2-0.4m s^{-2} r.m.s	7-75	STHT
Cohen et al., (1977)[27]	6 males	55-82	Comfortable neutral sitting posture; Tractor non-cushioned seat; no backrest	Sine	0.69 ms^{-2} r.m.s	2.5-5	STHT
Mertens (1978)[28]	6 males 3 females	57-90	Upright sitting with feet not supported	Sine	0.4g r.m.s with increased gravity of 1,2, 3 and 4g	2-20	DPMI STHT
Griffin et al., (1978)[29]	56 males 28 females 28 children	Not stated	Sitting, increasing height of footrest, no backrest	Sine	1 ms^{-2} r.m.s	4 and 16	STHT
Griffin et al., (1979)[30]	18 males 18 females	Not stated	Comfortable; upright; relaxed; stiff, Increasing height of footrest, no backrest	Sine	1 ms^{-2} r.m.s	1-100	STHT

Table 1.1: Summary of experimental conditions employed in different studies (continued).

Sandover (1982)[31]	6	52.7-87.2	Erect with various conditions of feet and arms	Random	1.2 and 2.3 ms^{-2} r.m.s	1-25	APMS
Donati and Bonthoux (1983)[32]	15 males	49-74	Erect, feet supported, hands on steering wheels	Sine and Broadband random	1.6 ms^{-2}	1-10	DPMI
Hagena et al., (1986)[33]	9 males 2 females	Not stated	Erect sitting posture no backrest	Sine	0.2g	3-40	STHT
Hinz and Seidel (1987)[34]	4 males	56-83	Moderately erect sitting no backrest	Sine	1.5 and 3.0 ms^{-2} r.m.s	2-12	DPMI, STHT
Paddan and Griffin (1988)[35]	12 males	58-81	Two postures: sitting with backrest and without backrest	Random	1.75 ms^{-2} r.m.s	0.25-20	STHT
Fairley and Griffin (1989)[36]	24 males 24females 12children	Not stated	Upright, no backrest, footrest Vibrating, hands in lap	Random	1ms^{-2} r.m.s	0.25-20	APMS
Fairley and Griffin (1989)[36]	8 males	57-85	4 seated postures: Normal, upright erect, upright tense upright back supported; Feet supported on footrest moving with platform	Random	0.25,0.5,1.0, 2.0 ms^{-2} r.m.s	0.25-20	APMS
Smith (1993)[37]	3 males 2 females	64-86	Sitting upright with back support and constraint	Sine and random	1 and 2 ms^{-2} r.m.s	3-21	DPMI

Table 1.1: Summary of experimental conditions employed in different studies (continued).

Seidel (1996)[38]	37 males	49-103	Hard seat without backrest feet supported and vibrated	Random	0.7,1.0 and 4 ms^{-2} r.m.s	0-20	DPMI
Zimmermann and Cook (1997) [39]	30	77.6	Not stated	Sine	1 ms^{-2}	4.5-16	STHT
Boileau and Rakheja (1998) [40]	7 males	54-80.9	Erect back not supported, erect back supported, sloughed back not supported	Sine sweep and broad band random	1, 1.5, 2.0 ms^{-2} rms	0 – 10	DPMI
Kitazaki and Griffin (1998) [41]	8 males	74.6 (Mean)	Hard seat without backrest	Random	1.7 ms^{-2} r.m.s	0.5-35	APMS, seat-to-body segment transmissibility
Matsumoto and Griffin (1998) [42]	8 males	63-83	Flat rigid seat, no back support	random	1.0 ms^{-2} r.m.s	0.5-20	APMS, seat-to-body segment transmissibilty
Lundstron and Holmlund (1998)[43]	15 males 15 females	54-93	Relaxed and erect upper body posture	Sine	0.25-1.4 ms^{-2}	1.13-80	Absorbed power
Mansfield and Griffin (1998) [44]	12 males	74.5	Comfortable upright posture, without backrest	Random	Six level: 0.25-2.5 ms^{-2} r.m.s	0.2-20	Absorbed power
Mansfield and Griffin (2000)[45]	12 males	60-85	Comfortable upright posture, without backrest	Random	Six level:0.25-2.5 ms^{-2} r.m.s	0.2.-20	APMS and seat-to-body segment transmissibility
Holmlund et al., (2000)[46]	15 males 15 females	57-92 54-93	Relaxed and erect upper body	Sine	0.5,0.7,1.0,1.4 ms^{-2} r.m.s	2-100	DPMI

Table 1.1: Summary of experimental conditions employed in different studies (continued).

Hinz et al. (2001) [47]	39 males	48-131	Suspended seat with/without backrest, hands on steering wheel	Random	0.6 ms^{-2} r.m.s	0-10	STHT
Rakheja et al. (2002)[48]	12 males 12 females	48-111.4	Hard seat with backrest; hand in lap/ hands on steering wheel	Random	0.25,0.5,1.0 ms^{-2} r.m.s	0-40	APMS
Demic et al. (2002) [49]	30	85.9	Back support	Random	0.55, 1.75, 2.25 ms^{-2} rms	0-10	STHT
Nawayseh and Griffin (2003) [50]	12 males	63-103	Feet hanging, maximum thigh contact, average thigh contact, and minimum thigh contact, No back support	Random	0.125,0.25,0.625, 1.25 ms^{-2} r.m.s	0.25-15	APMS
Nawayseh and Griffin (2005) [51]	12 males	62-106	Feet hanging, maximum thigh contact, average thigh contact, and minimum thigh contact, Vertical back support	Random	0.125,0.25,0.625, 1.25 ms^{-2} r.m.s	0.25-20	APMS
Nawayseh and Griffin (2005) [52]	12 males	57-106	feet hanging, maximum thigh contact, average thigh contact, and minimum thigh contact, Vertical back support	Random	0.125,0.25,0.625, 1.25 ms^{-2} r.m.s	0.25-20	Absorbed power
Nawayseh and Griffin (2005) [53]	12 males	65-103	Vertical back support	Random	0.125,0.25,0.625, 1.25 ms^{-2} r.m.s	0.25-15	APMS

From the review of the reported studies, it is evident that although all these studies have significantly contributed to the understanding of the human biodynamic responses, most of the reported studies have been performed with subjects seated with either no back support or with back supported against a vertical backrest, while hands resting on the lap. Such a sitting posture would hardly represent that encountered in vehicle driving. Moreover, all of the studies have focused only on a single measurement point when investigating the force-motion relationship, with the exception of a few recent studies that involved the measurement of the dynamic force imparted on a purely vertical backrest [51-53]. Only a few studies have included the postural variations arising from inclined pan or cushion, inclined backrest, low seat height and full backrest support, which are encountered in a typical vehicular sitting situations [48,54].

Despite the insufficiencies in the reported biodynamic data, the influence of various factors on the biodynamic responses has been investigated in a number of studies. These include the subjects related factors, such as body mass, height, body built, and gender; the excitation characteristics, such as vibration type (sine, random), magnitude (r.m.s, peak magnitude), frequency range [9-11]. Very little effects, however, have been made to study the role of seat characteristics, such as seat height geometry, and effects of the body mass and seat design factors, which are discussed in the following sub-sections.

1.3.1 Influence of subject mass

The reported data, on the APMS/DPMI, or absorbed power of the seated body shows considerable variability between subjects, which could be partly attributed to differences in the static body masses supported on the seat pan or platform. The static

mass has often been considered to represent the measured value of APMS at or near 0.5 Hz [36]. Fairley and Griffin [36] have reported the APMS responses of 60 seated subjects including 24 males, 24 females and 12 children, which revealed large scatter in the data due to the variations in the subject masses. The scatter in magnitude response at lower frequencies was reduced considerably by normalizing with respect to the static seated mass of each subject. The DPMI characteristics, reported by Seidel [38] for a total of 37 male subjects assuming an erect sitting posture, were grouped into four sets based upon different ranges of subject mass, namely less than 60kg, between 60-70kg, between 70-80kg, and higher than 80kg. Figure 1.2 illustrates the DPMI magnitude response of subjects in different mass ranges as reported by Seidel [38].

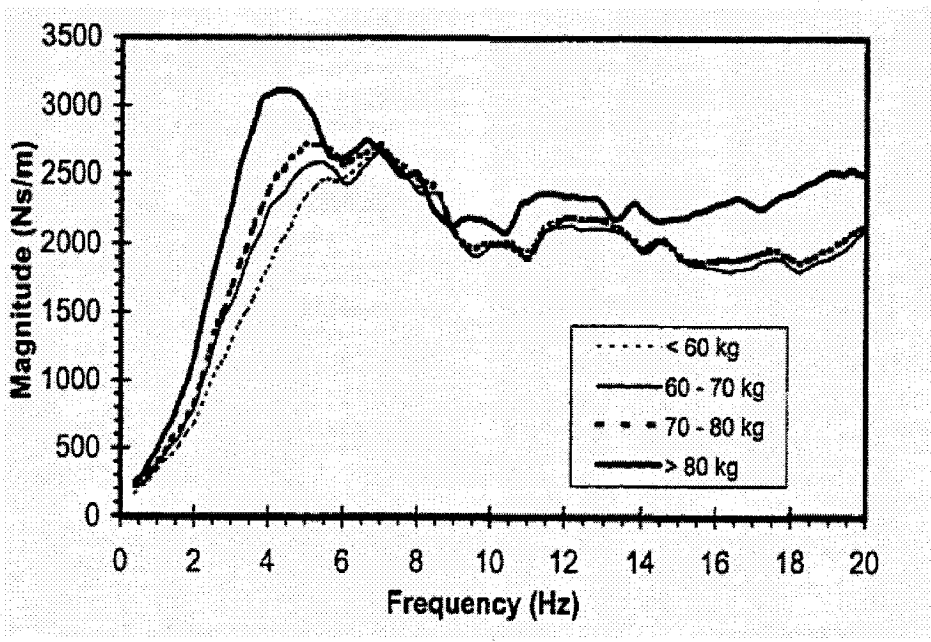

Figure 1.2: The effect of body mass on the DPMI magnitude (Seated erect without back support) [38].

The strong dependence of the response on the body mass has been further demonstrated in the study by Rakheja et al. [48] using 24 individuals (12 females and 12 males). This study grouped the measured data into four different mass ranges for subjects adopting automotive seating postures. Figure 1.3 illustrates the effect of body mass on the APMS magnitude, which clearly illustrates considerably larger differences in the peak APMS magnitudes for different mass groups. A higher body mass, in general, yields higher peak magnitude response and lower corresponding frequency, as illustrated in Figure 1.4. The study further suggested considerable influence of the hands position, as illustrated in Figure 1.3. The hands on the steering wheel posture resulted in lower peak magnitude and the corresponding frequency, when compared with those attained with hands in lap posture.

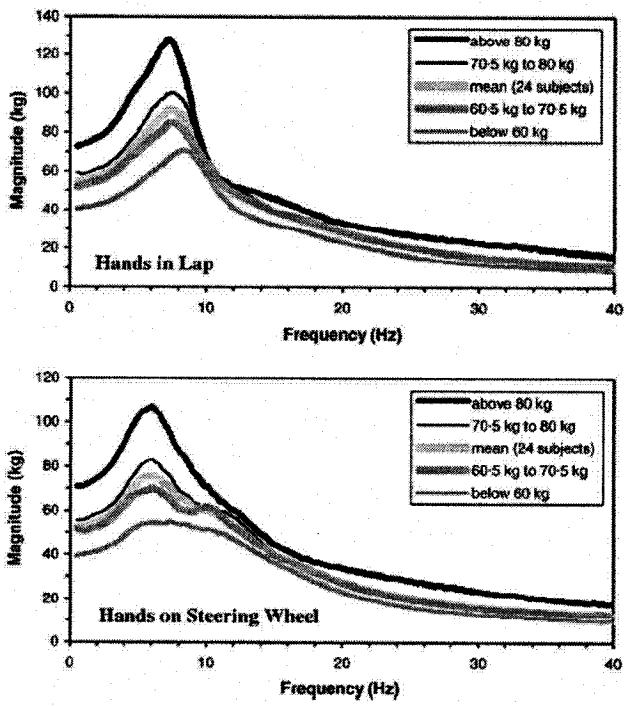

Figure 1.3: The effect of body mass on the vertical APMS magnitude (Seated with the inclined backrest support; excitation magnitude: 0.25—1.0 m/s^2 rms) [48].

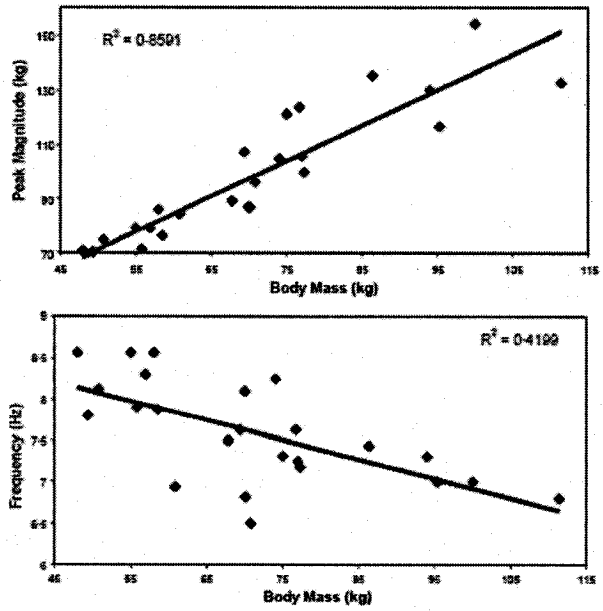

Figure 1.4: Dependence of peak APMS magnitude and corresponding frequency on the body mass (Seated with the inclined backrest support with hands on steering wheel posture) [48].

Lundstrom and Holmlund [43] reported the absorbed power characteristics of 30 seated subjects exposed to vertical sinusoidal vibration. Figure 1.5 suggests that the total amount of absorbed power is linearly dependent on the sitting weight irrespective of the excitation level, seated posture, and gender. The figure shows that the responses for four different excitation (0.5, 0.7, 1.0, 1.4 m/s^2 rms) in the 2-100 Hz frequency range. The result also suggested that quantity of vibration energy dissipated within the body increase most significantly with the magnitude of vibration excitation.

Only a few studies have explored the influence of variation in the body mass and size on the STHT magnitude [11,29]. A definite influence of such factors, however, could not be established due to the considerable variations in the measured STHT responses of individuals.

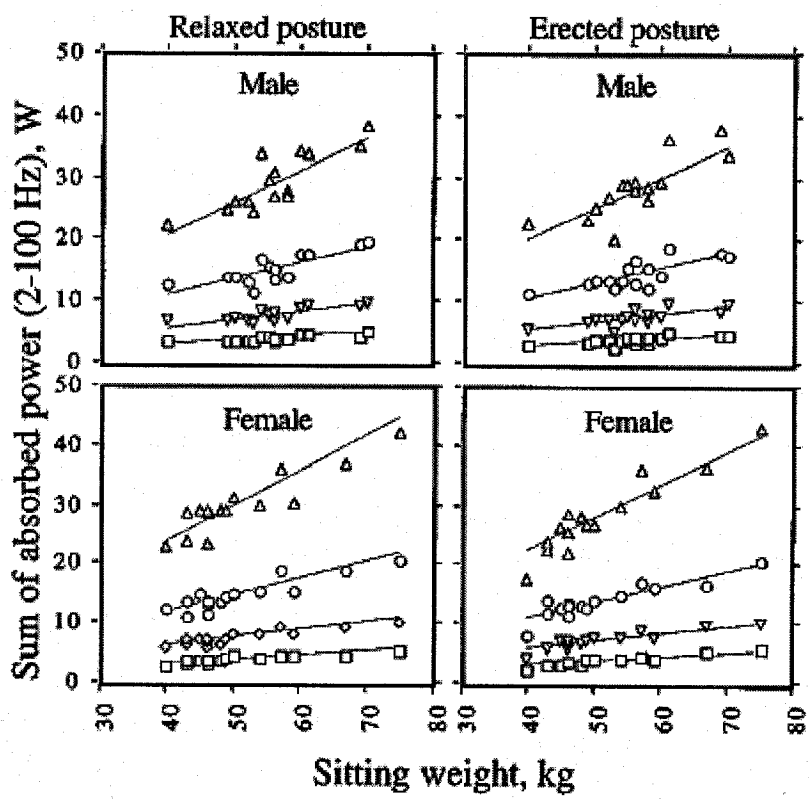

Figure 1.5: Absorbed power-sum for the frequency range 2-100 Hz for four different stimulus acceleration levels (0.5-1.4 m/s^2 rms) in relation to sitting weight [43].

1.3.2 Influence of excitation magnitude and frequency

The biodynamic response characteristics of the seated human body under different types and levels of whole body vibration excitations have been investigated in several studies. The human body shows a highly nonlinear response to vibration. A common finding associated with the driving-point biodynamic functions is a reduction in the primary resonance frequency with increase in the vibration magnitude [34,36,41,43-45]. This phenomenon is also known as a 'softening effect' of the seated body under increased WBV. Using sinusoidal vibration over the 2-12 Hz frequency range, Hinz and Seidel [34]

reported a decrease in the DPMI resonance frequency from 4.5 to 4 Hz, and a decrease in the STHT resonance frequency from 5.0 to 3.8 Hz, when the vibration magnitude was increased from 1.5 to 3.0 m/s^2 rms. These results are shown in Figure 1.6. Under exposure to random vibration, Fairley and Griffin [36] reported a decrease in the apparent mass resonance frequency from 6 to 4 Hz with, an increase in vibration magnitude from 0.25 to 2.0 m/s^2 rms. Mansfield and Griffin [45] also reported a similar nonlinear phenomenon, as shown in Figure 1.7. Lundstrom and Holmlund [43] reported the absorbed power characteristics of 30 seated subjects exposed to vertical vibration. The absorbed power was found to be strongly dependent on the magnitude of acceleration due to vibration. The study by Lundstrom and Holmlund [43] further showed that the power absorbed by the seated body was strongly dependent upon the excitation magnitude, as shown in Figure 1.8. The power absorbed under exposure to vertical whole body vibration at six different magnitudes of random vibration (0.25, 0.5, 1.0, 1.5, 2.0, 2.5 m/s^2 rms) was also measured by Mansfield and Griffin [44] using 12 male subjects. The results showed that the largest absorbed power occurred at about 5 Hz, and the frequency of the peak value decreased with increasing vibration magnitude, as shown in Figure 1.8, in term of median normalized absorbed power. The total absorbed power increased approximately in proportion to the square of the acceleration magnitude.

Seat-to-body segment transmissibilities have also revealed the non-linear response behavior similar to those observed in the driving-point biodynamic functions. Matsumoto and Griffin [42] measured the transmissibility of the vibration to the head, the pelvis and six locations on the spine (T1, T5, T10, L1, L3, L5) in three orthogonal axes in the sagittal plane using five different vibration magnitudes. A nonlinear behavior in response

was observed at most measurement locations. For example, when the vibration magnitude increased from 0.125 to 2.0 m/s^2 rms, the resonance frequency associated with the vertical transmissibility to L3 reduced from 6.25 to 4.75 Hz.

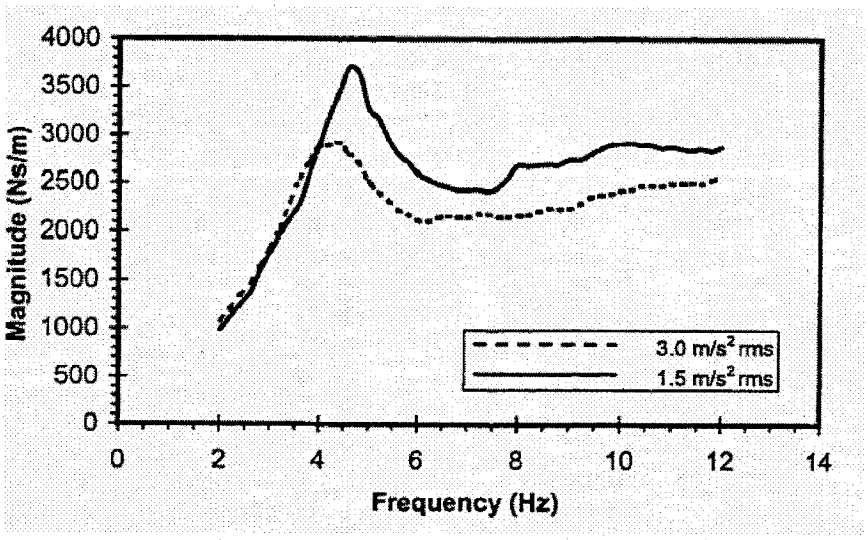

(a)

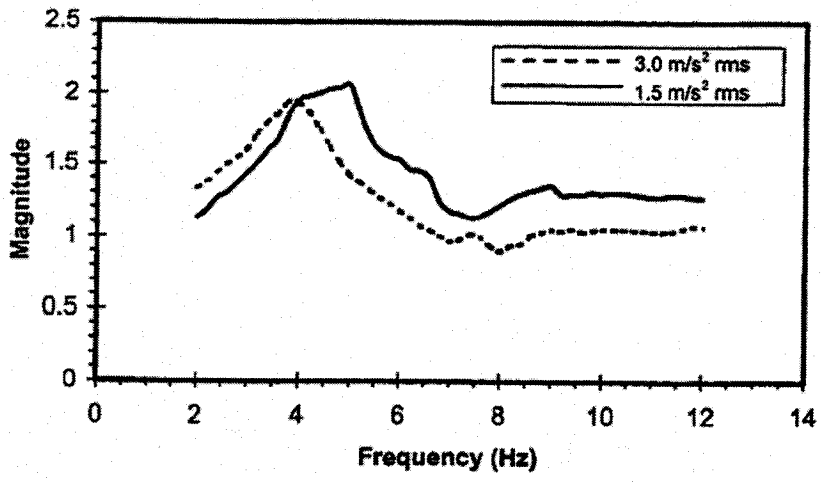

(b)

Figure 1.6: Effect of excitation magnitude on: (a) the mean DPMI, (b) STHT response of four male subjects [34].

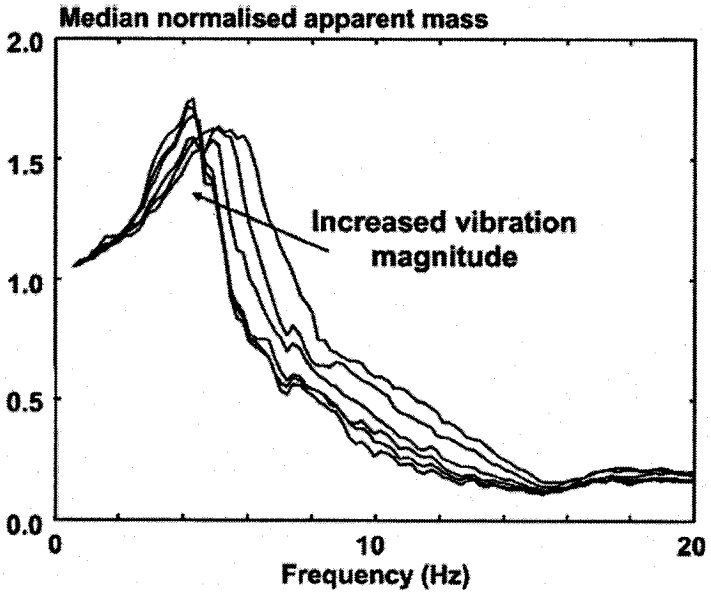

Figure 1.7: Effect of excitation magnitude on the median normalized APMS response of 12 male subjects [45].

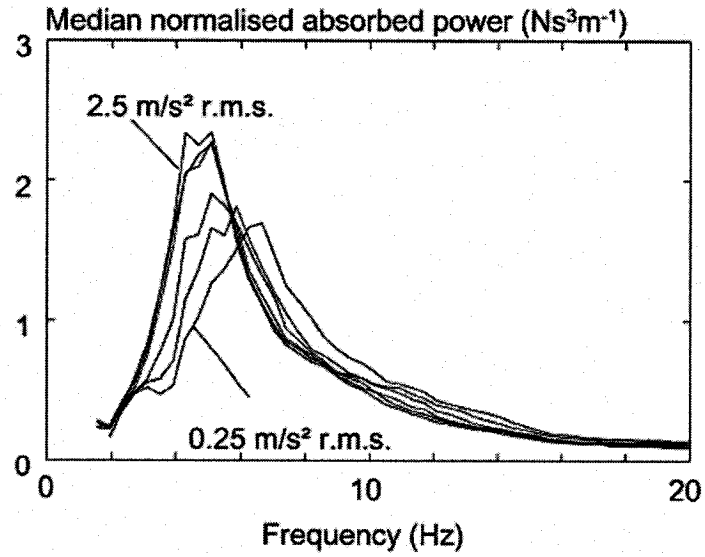

Figure 1.8: Median normalized absorbed power responses of 12 subjects exposed to vertical vibration of different magnitudes (0.25, 0.5, 1.0, 1.5, 2.0 and 2.5 m/s^2 rms acceleration) [44].

The influence of the excitation magnitude on the STHT, however, may be considered to be small, in comparison with the inter and intra-subject variations of the measured data. Only one exceptional study by Hinz and Seidel [34] revealed the non-linearity of the STHT responses under relatively higher sinusoidal excitation magnitudes. Variations in the back support and head inclination are known to cause greater effects on STHT than those caused by variations in the magnitude of the vibration [1]. This may be partly attributed to the great variations in the reported data, or insufficiencies in the measured data.

1.3.3 Influence of sitting posture on the biodynamic responses

The influence of body posture on the biodynamic response has not been thoroughly assessed [10,11]. Researchers have attempted to characterize the postural variations on the biodynamic responses from different perspectives. Several factors are known to influence the upper body posture including the muscle tension, body and seat geometry, work-station configuration *etc.*. The lower body posture is mostly influenced by the use of footrest, leg position, seat height *etc.*.

Most studies have characterized the biodynamic responses of the seated subjects with 8 "erect (stiff)" or "slouched (relaxed)" postures [23,32,36,41,43,44]. Miwa [23] reported that an erect sitting posture yields higher magnitudes of DPMI in the vicinity of the observed resonant frequencies (7 Hz and 15 Hz) than those attained with a relaxed sitting posture. A higher resonant frequency of the occupant sitting with a more erect posture has also been reported in many other studies [36,43,44]. Fairley and Griffin [36] investigated the effects of posture and muscle tension separately using a population of

eight subjects adopting four different postures, referred to as "normal", "erect", "backrest contact" and "tense". Their results showed a higher resonant frequency for the "erect" and "tense" postures than that for a "normal" posture. Kitazaki and Griffin [36] also showed an increase in the mean resonant frequency from 4.4 to 5.2 Hz when the posture of subjects changed from 'slouched' to 'erect'. Similar tendencies have also been observed in the absorbed power responses under WBV. Absorbed power of the seated occupants exposed to vertical vibration, as measured by Lundstrom and Holmlund [43], indicated a relatively higher resonant frequency when sitting with an erect posture as opposed to a relaxed posture. All of the above studies suggest an increase in the primary resonant frequency of the seated body when the upper body posture is varied from a slouched (or relaxed) to an erect (or stiff), suggesting an increase in body stiffness when the muscle tension is increased.

Some other studies have also characterized the biodynamic responses based upon the variations in the lower-body support. Fairley and Griffin [36] have reported that the apparent mass at low frequencies increased with increased in the height of a stationary footrest. The apparent mass magnitude, however, decreased with increased height of a footrest moving in phase with the seat. A footrest may further affect the vibration transmissibility. As for the STHT measurements performed by Griffin et al. [30] revealed that presence of a footrest (normal height) does not considerably influence the STHT. Nawayseh and Griffin [50,51] found that fore-and-aft cross-axis apparent mass (the ratio of the fore-and-aft force on the seat to vertical acceleration) depended on support for the lower legs on a moving footrest. The variations in the fore-aft position of the footrest with respect to the seat, however, did not affect the force-motion biodynamic response of

subjects seated under an automotive posture while maintaining contact with an inclined backrest, as reported by Rakheja et al. [48].

The influences of a backrest and variations in its inclination angle have been investigated by Boileau and Rakheja [40], involving a total of 7 male subjects. In this study, the measurement was performed for three sitting postures: 1) sitting erect with back unsupported, referred to as the 'erect back not supported' (ENS) posture; 2) sitting erect with most of the back in contact with the backrest, also referred to as 'erect back supported' (EBS) posture; and 3) sitting in a slouched (SLO) posture, the upper body having a more pronounced inclination towards the front than with the ENS posture, while the lower back is in contact with the backrest. The measurements were performed with two different seat backrest angles of 0° and 14° with respect to the vertical axis. The mean DPMI magnitude and phase responses, illustrated in Figure 1.9, revealed significant influence of the sitting posture. The results suggested a suppression and smoothing of the impedance magnitude around the resonances when the backrest angle was increased to 14°. Furthermore, an EBS posture yields higher DPMI magnitudes at frequencies above 6 Hz.

The vibration transmissibility of the body segments is also affected by the presence of a backrest, although only a few studies have attempted to study the role of back support condition. Paddan and Griffin [35,55-57,] investigated the influence of backrest support on seat-to-head transmissibility using six directions of excitation (vertical, fore-and-aft, lateral, roll, pitch and yaw) and six directions of head movement. Under vertical excitation, the responses reveal a decrease in the inter-subject variability when the subjects sat while

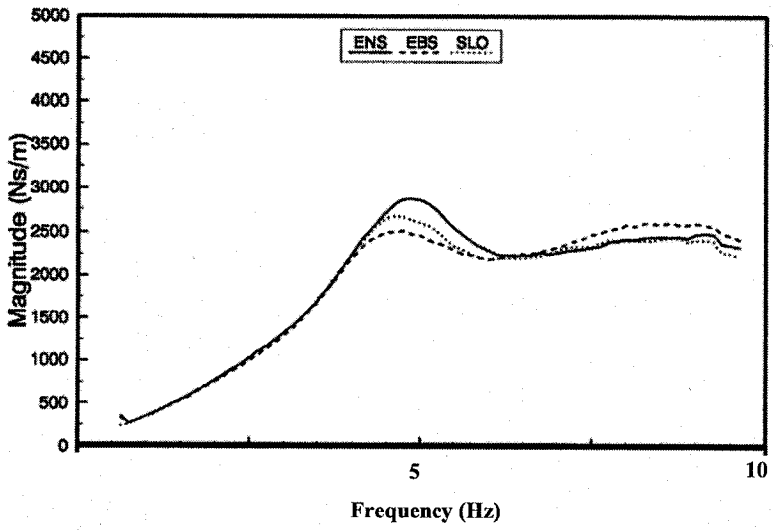

Figure 1.9: Influence of posture on the DPMI magnitude response under sine sweep excitations (1.0,1.5, 2.0 m/s^2 rms acceleration)[48].

leaning against an upright backrest. The magnitude of head vibration increased with the back support, especially in the mid-sagittal plane in the frequency range 0.25–20 Hz. Figure 1.10 illustrates the mean vertical STHT response characteristics of 12 subjects with and without an upright backrest. The results clearly show that the use of a backrest yields significant increase in vertical vibration transmission at frequency above 4.5 Hz. The use of backrest also resulted in higher resonant frequency, which increased from 4.2 Hz for no back support to 6.2 Hz. These results may also be associated with different orientation of the head and neck, which results in the difference in the orientation of the bite-bar head acceleration measurement system. The STHT response, in general, exhibit excessively large inter-subject variabilities, when compared to those observed in the force-motion based biodynamic response functions. Only a few studies, however, have reported the inter-subject variability of the data [35,39,47].

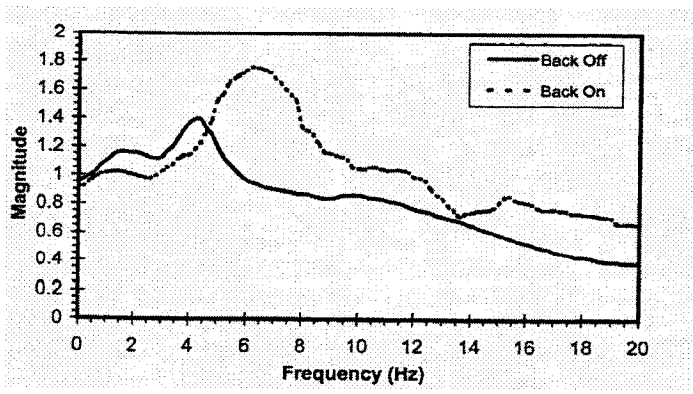

Figure 1.10: Effect of contact with a rigid flat backrest on the mean STHT response of 12 subjects [43].

Mansfield [58] reported an increase in pelvis rotation at resonance when a backrest was used, with a corresponding increase in the inter-subject variability in contrast with the seat-to-head transmissibility results reported by Paddan and Griffin [35]. The use of backrest was also reported to contribute to attenuation of vibration at the third lumbar vertebra reported by Magnusson et al. [59].

Fairley and Griffin [36] found that the use of a backrest caused an increase in the resonant frequency of the body and higher apparent mass magnitude at frequencies above resonance, while subjects were asked to maintain four different postures, referred to as "normal", "erect", "backrest contact" and "tense". Mansfield [58] also found an increase in the apparent mass above resonance when using a backrest but found no significant differences between the resonance frequencies with a normal upright posture and a back-on posture (i.e. the back in contact with the backrest). Similar observations were also made on the basis of absorbed power responses, reported by Nawayseh and Griffin [52].

All of the above studies have considered sitting conditions involving back not supported or supported against a vertical backrest, and hands in the lap or crossed against

the chest. Occupants of different vehicles, however, may assume a variety of postures. For example, the car drivers usually sit with an inclined backrest while the drivers of industrial trucks usually sit with a more upright back posture. The vehicle driver also may maintain their hands in contact with a steering wheel. The effects of inclined backrest and hands position on APMS responses have been presented in a recent study by Rakheja et al. [48]. The measurements were performed using 24 adult subjects seated with full contact with the inclined back support and two different hands positions (in lap, representing a passenger-like posture, and on the steering wheel, representing a driver-like posture), while being exposed to three different levels of broad band (0.25, 0.5 and 1.0 m/s^2 rms acceleration) vibration in the 0.5-40 Hz frequency range, and a track-measured vibration spectrum (1.07 m/s^2 rms acceleration). The results suggested considerable effect of the hands position on the APMS magnitudes, while maintaining an automotive posture as illustrated in Figure 1.11. The observed differences in the peak magnitude and corresponding frequency are also believed to e caused by very low seated height.

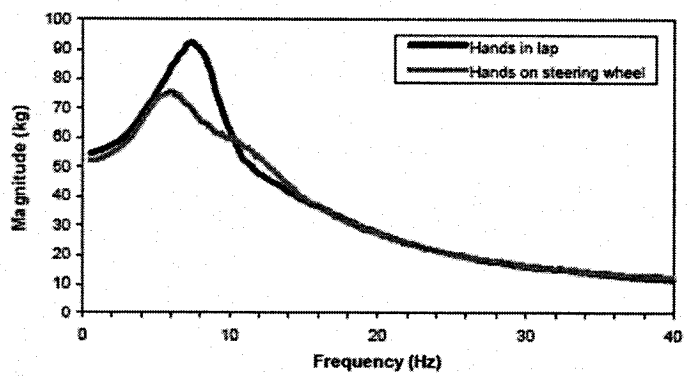

Figure 1.11: Comparison of mean APMS responses attained for different hands positions for a seated automotive posture [48].

1.3.4 Influence of gender

A few studies have specifically investigated the influence of gender on the biodynamic response of the seated human body exposed to vertical vibration [29, 37, 43,46, 48, 59,62]. Griffin et al. [60], and Parsons and Griffin, [61] have concluded the gender effect to be mostly insignificant. Fairley and Griffin [36] reported insignificant gender effect on the biodynamic response based upon measurements performed with 24 males, 24 females and 12 children. Another study performed with 15 males and 15 females also reported insignificant gender effect on the basis of energy absorption of the seated occupants [43]. Similar conclusions were also reached by Rakheja et al., [48] by comparing the mean APMS responses of 12 males and 12 females exposed to typical automotive vibration environment. However, a few other studies have drawn contradictory conclusions on gender effects. Griffin and Whitham [37] observed a trend toward higher sensitivity at higher excitation frequencies (above 16 Hz) of vertical seat vibration in female subjects, when compared to that in the data attained for the male subjects. On the basis of the measured vibration transmissibility of a cushion seat with occupants, it was concluded that the vibration transmissibility of a seat-occupant system is strongly affected by the gender [62]. It may be necessary to further investigate the influence of gender on the biodynamic response characteristics of the seated human occupants by considering the anthropometric factors, such as body mass.

1.3.5 Summary of reported biodynamic response characteristics

Experimental studies exhibit a consistent finding for the vertical response of the seated human body exposed to whole-body vertical vibration. A primary resonance has

been found between 4 and 6 Hz in both the force-motion biodynamic responses [22-24, 34,36,43,46], and motion-motion biodynamic responses [22,24,26,27,34]. A second resonance has been found between 8 and 12 Hz in some investigations [36,46], but it is less clear and the variability between investigations and between subjects is larger. The second resonance at about 8 Hz corresponded to pitching modes of the pelvis and the second visceral mode, as suggested by Kitazaki and Griffin [41].

The findings of all of the studies referred to in this section were made on the basis of either force-motion or motion-motion biodynamic response functions (DPMI/APMS, STHT), while the two function have been measured in separate tests. Only a few studies, such as those of Hinz and Seidel [34], Matsumoto and Griffin [42] and Mansfield and Griffin [45], have reported simultaneous measures of force-motion and motion-motion biodynamic responses. The motion-motion responses in these studies, however, revealed excessively large inter-subject variability. A relationship, between the force-motion and motion-motion responses has not yet been attempted. Synthesis of the measured data in the ISO-5982 [12] and data reported in different studies generally exhibit considerable differences corresponding to peak APMS and STHT magnitudes [10,11]. These may, in-part, be attributed to variations in the test conditions used in two independent measurements. Further effects are thus needed to thoroughly investigate the relation under simultaneous measurements of the APMS and STHT responses.

The STHT responses reported in different studies show extreme differences which may be attributed to differences in various factors, such as measurement and analysis methods, experimental designs, subject anthropometry, nature of WBV and muscle tension [1, 11]. The reported studies on STHT characteristics of the seated body exposed

to vertical or horizontal vibration have been thoroughly reviewed by Paddan and Griffin [11]. The results reported in 46 different studies on the transmissibility of vertical seat vibration to the head were analyzed to define the median range of STHT. The synthesis included data from those involving 6 or more subjects. Figure 1.12 (a) illustrates comparisons of mean STHT responses reported by different investigators, which clearly demonstrate extreme variabilities among the datasets. Another synthesis was also conducted by Boileau et al. [10], which formed the basis of the ISO-5982 standard [12]. The synthesis included datasets acquired under relatively narrow ranges of experimental conditions, particularly those reported for the mean body mass of test subjects in the 49-94 kg range, vertical vibration excitation magnitude below 5 m/s^2 (sinusoidal or random) and test subject posture being erect without a back support. The study also considered datasets reporting STHT within the 0.5-20 Hz frequency range. The study proposed the range of idealized STHT characteristics of seated subjects under defined conditions on the basis of a total of 8 datasets. Figure 1.12 (b) presents the datasets used for defining the range of idealized STHT responses in ISO-5982. The results again show large variability despite the narrow range of the chosen experimental conditions. Such variabilities further suggest that the seat-to-head vibration transmissibility is strongly influenced by many factors, such as sitting posture, muscle tension, and type, magnitude and frequency of vibration excitation.

Effect of the sitting posture on the biodynamic response has been a complex issue. The differences in the body postural variations result in considerable variability of the measured biodynamic data. Although it has been reported that the frequency of the primary resonance tends to decrease when subjects change their postures from erect to

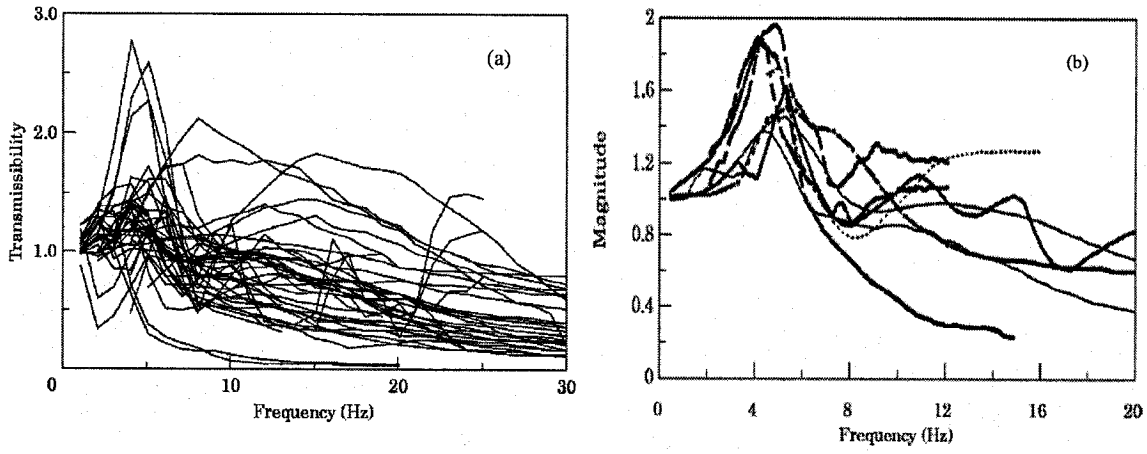

Figure 1.12: Variations in the mean STHT transmissibility characteristics reported in different reported studies (a) synthesized data by Paddan & Griffin [11]; and (b) synthesized data by Boileau et al.. [10].

relaxed [23,32,36,41,43,44]. Occupants of different vehicles may assume a variety of upper-body postures depending on the seat-geometry and work-station. The postural variation arising from seat geometry (backrest and pan inclination) has been partly investigated in a few reported studies [48, 54]. Role of seat design and work-station design parameters (backrest, pan inclination and seat height) on the force-motion and motion-motion biodynamic behavior has not been clearly characterized. There exist multiple points of vibration entry even if only vertical excitation is applied, depending on the back support condition, the hands position and the feet position. The characterization of the human response to vertical WBV thus requires the consideration of multiple vibration entry points, which is a formidable task when the complexities of the biological system of seated body are added.

The reported studies including the ISO-5982 standard ignore the body interactions with the backrest. The backrest in the car seat contributes to decrease the muscle tensions

and helps maintain a controlled sitting posture in driving [48,54]. The changes in body posture when leaning against a backrest may alter the vibration modes of the body, especially the pitch mode, and thus the vibration transmissibility and human perception of vibration.

1.4 Review of biodynamic models

'Biodynamics' is the science of the physical, biological and mechanical properties or responses of the body, in which its tissues, organs, parts and systems are either with reference to forces or motion, or related to the body's own mechanical activity. Biodynamic models may enhance the understanding of how the body moves, summarize biodynamic measurements, and provide predictions of the effects of motion on human health, comfort or performance.

The reported biodynamic models can be categorized into three types: lumped parameters, continuum models and discrete models. In the lumped parameter models, the mass of the body structure is concentrated into a few lumped masses interconnected by springs and dampers. The majority of the reported models fall within this group of models. The discrete and continuum models consider distributed parameters of the human body and component characteristics in two-and three-dimensions.

The development of mechanical-equivalent models of the seated human body is known to pose considerable difficulties associated with the identification of model structures and properties of the biological system. Biodynamic models constitute the basis for developing anthropodynamic manikins which can effectively be used for the assessments of the coupled seat occupant system [21,63,64]. A number of lumped-

parameter mechanical-equivalent models have been proposed on the basis of the measured biodynamic responses [19], where the mechanical properties of the biodynamic system are represented by one or more lumped masses, and energy restoring and dissipative elements. The model parameters are usually identified from the measured biodynamic response data using either curve-fitting or optimization based system identification techniques.

Coerman [22] proposed a SDOF model of the human body, as shown in Figure 1.13. The mass of the subject, including the upper torso and head, supported by the seat is lumped and linked to the base through parallel spring and damping elements. Damping coefficient c is due to the spine and the adjacent tissues. Stiffness coefficient k represents the restoring property of the spine. The model parameters were identified to match the DMPI responses measured with subjects sitting without their feet and back supported under sinusoidal excitation only.

Fairly and Griffin [36] proposed a two-DOF, as shown in Figure 1.14. This seated body model involved two masses: m_1 is the mass of the upper body moving relative to the platform, and m_2 is the mass of the lower body and the legs supported on the platform but not moving relative to the platform. The mass of the legs m_3 was included in the model only when the feet were supported on a stationary footrest. The model parameters were identified to fit the measured mean APMS of 60 subjects, including 24 males, 24 females and 12 children, sitting erect without back support. The APMS was measured under 1.0 m/s^2 rms random vibration in the frequency range 0.25-20 Hz.

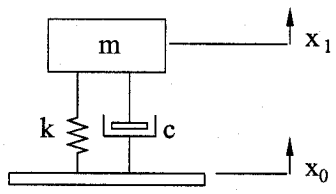

$f_n = 6.3\ Hz \quad \xi = 0.57 \quad k = 131181 N/m \quad$ *'Erect'*

$f_n = 5.2\ Hz \quad \xi = 0.65 \quad k = 84180 N/m \quad$ *'Relaxed'*

Figure 1.13: SDOF model by Coerman [22].

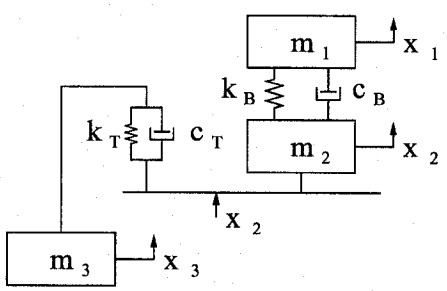

$m_1 = 45.6\ kg$

$m_2 = 6\ kg$

$m_3 = 11.5\ kg$

$\xi = 0.475$

$c_B = 1360\ Nm/s$

$f_{nB} = 5\ Hz$

Figure 1.14: Two-DOF model proposed by Fairly and Griffin [36].

Suggs et al. [25] proposed a two-DOF biodynamic model of the human body to characterize the human body response behavior over a frequency range comprising the first two resonant frequencies of the body (Figure 1.15). The model parameters were identified from the measured DPMI characteristics of 11 male subjects seated upright with feet supported, hands in lap, and exposed to sinusoidal vibration of 2.54 mm amplitude in the 1.75 to 10 Hz frequency range. The lumped masses of the model consisted of m_1, representing the pelvis and the abdomen; m_2, representing the head and the chest; and m_0, representing the spinal column. Similarly, Allen [65] developed

another two-DOF biodynamic model of the human body, as shown in Figure 1.16. This model characterizes the upper body response and the head response. The lumped masses m_0 and m_1 represent the upper body and the head of the body, respectively.

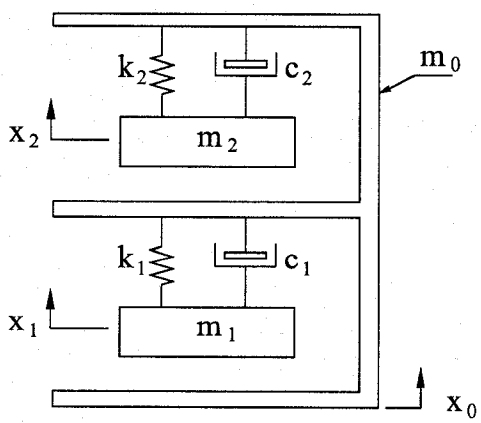

$m_0 = 5.7\ kg$
$m_1 = 36.4\ kg$
$m_2 = 18.6\ kg$
$k_1 = 25968\ N/m$
$k_2 = 41549\ N/m$
$c_1 = 485\ Ns/m$
$c_2 = 884\ Ns/m$

Figure 1.15: Two-DOF model proposed by Suggs *et al.* [25].

$m_0 = 50.0\ kg$
$m_1 = 5.0\ kg$
$\xi_0 = 0.3$
$\xi_1 = 0.05$
$f_{n0} = 5.0\ Hz$
$f_{n1} = 17.0\ Hz$

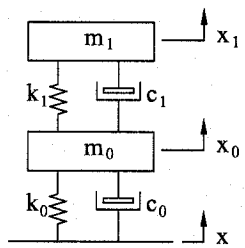

Figure 1.16: Two-DOF model proposed by Allen [65].

A number of multi-DOF models of the seated human subjects have been proposed by many researches. Payne and Band [66] proposed a 4-DOF lumped-parameter biodynamic model, as shown in Figure 1.17. The proposed model comprises mass m_1

representing the buttocks and pelvis; m_2 representing the viscera; and m_4 representing the neck and the head. The model parameters were identified from the DPMI response only.

$m_1 = 29kg$
$m_2 = 6.8kg$
$m_3 = 21.8kg$
$m4 = 5.45kg$
$\xi_1 = 0.25$
$\xi_2 = 0.5$
$\xi_3 = 0.1$
$\xi_4 = 0.15$
$k_2 = 2838N/m$
$k_4 = 204820N/m$
k_1, k_3 *adjusted*

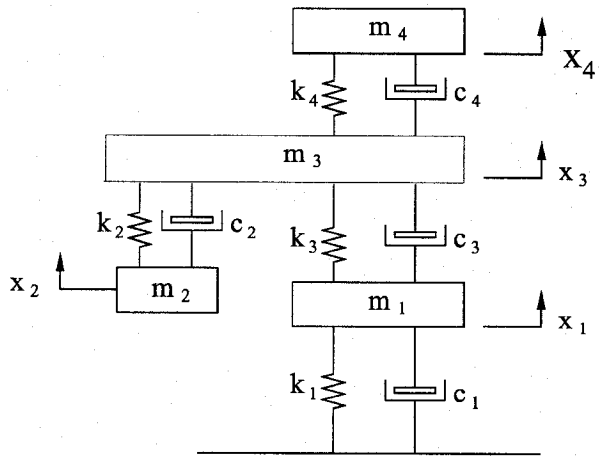

Figure 1.17: Four-DOF model proposed by Payne and Band [66].

Boileau [40] proposed a four-DOF model, as shown in Figure 1.18, consisting of four masses, coupled by linear elastic spring and viscous-damping elements. In this model, the mass m_1 represents the head and neck; the mass m_2 represents the chest and upper torso; the mass m_3 represents the lower torso; and the mass m_4 represents the thighs and pelvis in contact with the seat. The mass of lower legs and the feet are not considered in this model, assuming their negligible contributions to the biodynamic response of the seated human body. The model is proposed for a seated subject maintaining en erect posture without back support. The model parameters were identified such that the model response matches both the target DPMI and STHT magnitude and phase responses.

Mertens [28] developed a comprehensive biodynamic model involving the comparison of both the impedance and vibration transmissibility magnitude and phase characteristics with experimental results. The model comprised of five lumped masses representing the legs, buttocks, abdominal system, chest system and head. The study was intended for ejection seat applications.

Wu [9,12] proposed a three DOF model (Figure 1.19), which consists of four masses, coupled by linear elastic springs and viscous-damping elements. The masses m_1, m_2 and m_3 are introduced with an objective to describe the biodynamic behavior related to two resonant peaks observed in the APMS and STHT magnitude responses near frequencies of 5 Hz and 10 Hz, respectively. The lower mass m_0 is brought to increase the flexibility for tuning the model parameters without increasing the number of DOF. The model parameters were identified such that the model response matches both the target APMS and STHT magnitude and phase responses. The masses of the model did not correspond to any physiological structures within the body.

A comparative study of one-dimensional lumped parameter models, ranging from single-degree-freedom (SDOF) to multi-degree-freedom (MDOF) was conducted by Boileau et al. [19]. In this study, 11 different biodynamic models representing the seated human body were selected from the published studies. Among the 11 models considered, only three of these models were identified to satisfy both DPMI and STHT, these being multi-DOF models proposed by Mertens [28], by ISO CD 5982 (1993) [67], and by Boileau [40]. The remaining models considered in the study involved the Dynamic Response Index (DRI) by Coermann [22], an improved DRI model was proposed by Payne [68], 5DOF model by Amirouche and Ider [69] and a non-linear model defined by

Patil and Palanichamy [70]. These models were solely based on either individual force-motion or motion-motion biodynamic response functions for parameter identification.

$m_1 = 5.31\ kg$
$m_2 = 28.49\ kg$
$m_3 = 8.62\ kg$
$m_4 = 12.78\ kg$
$\sum_{i=1}^{4} m_i = 55.2\ kg$
$k_1 = 310\ kN/m$
$k_2 = 183\ kN/m$
$k_3 = 162.8\ kN/m$
$k_4 = 90\ kN/m$

$c_1 = 400\ Ns/m$
$c_2 = 4750\ Ns/m$
$c_3 = 4585\ Ns/m$
$c_4 = 2064\ Ns/m$

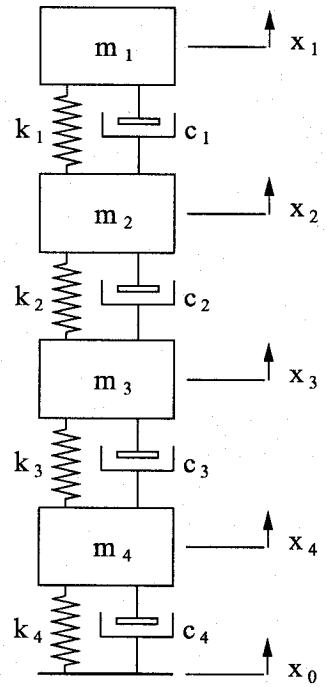

Figure 1. 18: Four-DOF model proposed by Boileau [40].

$m_0 = 2\ kg$
$m_1 = 6\ kg$
$m_2 = 2\ kg$
$m_3 = 45\ kg$
$k_1 = 9.99 \times 10^3\ N/m$
$k_2 = 3.44 \times 10^4\ N/m$
$k_3 = 3.62 \times 10^4\ N/m$
$c_1 = 387\ Ns/m$
$c_2 = 234\ Ns/m$
$c_3 = 1.39 \times 10^3\ N/m$

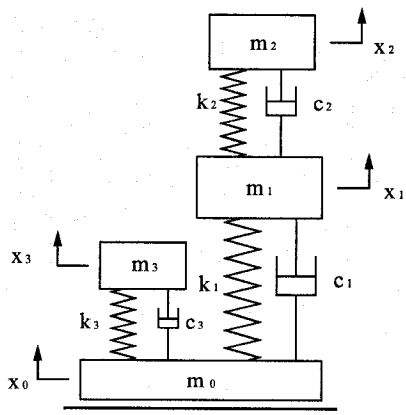

Figure 1.19: Three-DOF model proposed by Wu [9] and included in the ISO 5982 [12].

The majority of lumped parameter models are one-dimensional. Majority of the above models can provide useful approximate input-output relationships, under the experiment conditions considered, which cannot be considered applicable for automotive seating. Vehicle driving usually involves different postures (leaning against a backrest, sitting erect or sitting with a slouched posture), hands in contact with a steering wheel, and feet supported either on the floor or on pedals, while the vibration excitation is random in nature. All of the above-mentioned models have been derived on the basis of the biodynamic response data acquired for subjects seated without a back support.

In addition to the above one-dimensional models, a couple of two-dimensional lumped parameter models were reported in recent years. Matsumoto and Griffin [71] proposed a two dimensional lumped parameter model, which could reveal rotational motion. Figure 1.20 shows this mechanistic model, in which model masses represented segments of the seated human body. Masses 1-4 represent legs, pelvis, upper-body and viscera mass respectively. Masses 1, 2 and 3 of Matsumoto–Griffin model are connected by revolute joints and rotational spring-dampers. Masses 1 and 4 can move only in vertical direction. The models were validated by using the apparent mass and transmissibilities measured by Matsumoto and Griffin [71]. This model was developed to have similar characteristics to measured data in the apparent mass and transmissibilities at some body parts, and then to reveal the dynamic mechanism associated with the primary resonance of the seated human body. It may be concluded that the resonance of the apparent mass at about 5 Hz may be attributed to a vibration mode consisting of vertical motion of the pelvis and legs and a pitch motion of the pelvis, both of which

cause vertical motion of the upper-body above the pelvis, a bending motion of the spine, and vertical motion of the viscera. But this model cannot depict the head motion.

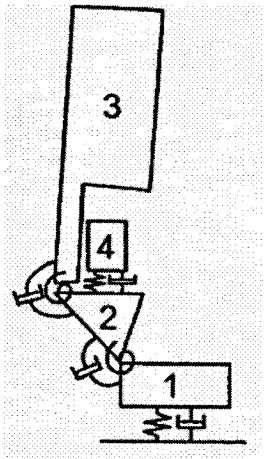

Figure 1.20: Lamped parameter models of seated human body proposed by Matsumoto and Griffin [71]

Zhang [54] propose a two-dimensional structure of the four-DOF model of the seated occupant with inclined pan and back support in order to investigate the relative interactions of the seated occupants with an inclined backrest at the two driving-points formed by the buttock-seat pan and the upper body-backrest under exposure to broad-band and road-measured vertical vibration. This model structure incorporates the geometric effects of a typical automotive seat, and comprises three masses coupled by linear elastic and damping elements constrained to translate along the axes shown in the Figure 1.21. The rotational stiffness and damping characteristics of the body are neglected, and therefore only masses are coupled while considering the two-dimensional dynamic interactions of the seat. This model gives some insight into building up two-dimensional of anthropodynamic manikins.

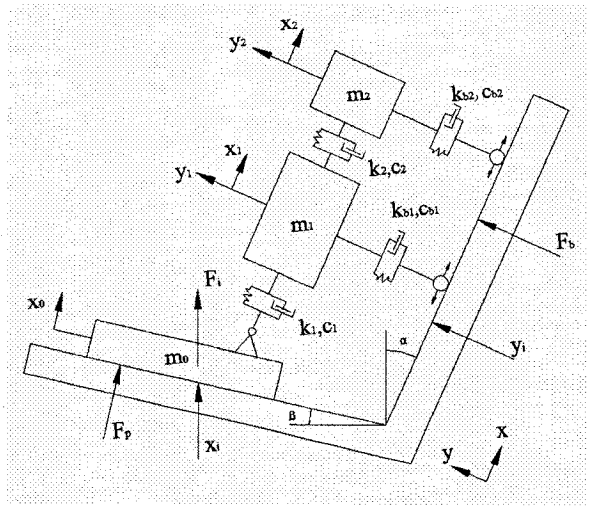

Figure 1.21: Mechanical-equivalent biodynamic model of the seated occupant with back support by Zhang [54].

The other two types of human models, namely discrete models and continuum models, are formulated to better describe and predict the motion of human body in the two-dimensional space or the three-dimensional space. The discrete models consider the spine as a layered structure of rigid elements, representing the vertebral bodies, and deformable elements representing the inter-vertebral discs. The continuum models assume the spine as a homogeneous rod beam. Kitazaki and Griffin [66] proposed a two-dimensional space finite element model of the human body, as shown in Figure 1.22. This model was entirely linear and includes 134 elements and 87 degrees-of-freedom. This model, was employed to model the spine, viscera, head, pelvis and buttocks tissue, using beam, spring and mass elements. The model was verified by comparison of the vibration mode shapes with those measured in the laboratory. The entire spinal column was modeled by 24 beam elements, representing all the inter-vertebral discs between the

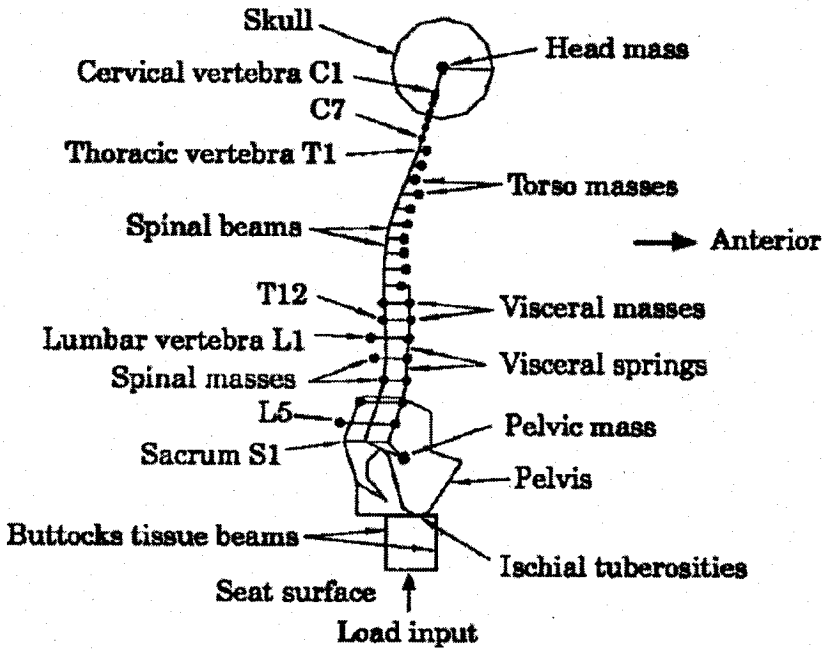

Figure 1.22: The two-dimensional biomechanical model in the normal posture [72].

vertebral C1 and the sacrum S1. Mass elements for the torso were located anterior to the spine in the region between the T1 and T10 levels by mass-less rigid links, such that model the eccentric inertial loading of the torso on the spine. Below the T10 level (the diaphragm level), the spinal masses and the visceral masses were modeled by separate mass elements. The sum of the spinal and the visceral masses at each vertebral level corresponded to the torso mass, with its mass center also located anterior to the spine. The visceral column in the abdominopelvic cavity was modeled by seven mass elements from T11 to L5 interconnected by elastic elements. The bottom of the visceral column was connected to the pelvis mass by a mass-less rigid link, and top connected to the spinal beam at the T10 level, also by a mass-less rigid link representing the pair of the lowest complete ribs. The interaction between the visceral and the spine was modeled by

horizontal elastic elements interconnecting the visceral masses and the spinal beams. The head was simply modeled by connecting to the top of the spinal beam at the C1 level by a beam element representing the atlanto-occipital joint. The pelvis was modeled by a mass element and connected to the bottom of the spinal beam at the S1 level by a mass-less rigid link. A total of seven modes were computed for a normal body posture below 10 Hz, and the mode shapes of the model agreed well with those obtained from laboratory measurements.

Finite element modeling may offer the better suited approach to predict the internal forces acting on lumbar vertebrae during whole-body vibration and shock. The model may be closely related to human anatomy in order to reflect adequately the complexity of human biodynamics. However, Finite element modeling tends to be overly complex for the prediction of the average force-motion behavior compared with lumped parameter modeling.

1.5 Scope of the dissertation research

A quantity of biodynamic data have been generated by different investigators to characterize the biodynamic responses of the seated human subjects under whole-body vibration while using different measurement methods and conditions. This has resulted in considerable discrepancies among the reported data by different investigators. The contents and interpretation of biodynamic data have been a great concern in characterizing human responses to vibration.

The ranges of idealized values presented in the ISO 5982 standard [12] may not apply to the seated vehicle occupants exposed to a vehicular environment, since they are based upon data acquired with no back support and under relatively high magnitudes of

vertical vibration. The biodynamic measurements, which, to a large extent, could reflect the seating and body posture of seated vehicle occupants in a vehicular environment, are still not sufficient.

The human response to vibration is strongly dependent upon the support conditions provided by the seat and the workstation configuration. These may include the back supported against an inclined backrest and hands resting on a steering wheel. The dynamic interactions between the body and the supports other than the seat pan have been characterized only in a few recent studies [43-45, 65]. The international standard, ISO-5982 [12], defines the ranges of DPMI of seated occupants exposed to vertical vibration, which are applicable only for sitting postures without a back support. The seated human interactions with the backrest have been studied in a recent study, where the backrest is considered to be perfectly vertical [43-45]. Considering that the automotive seats are designed with inclined seat pan and backrest to provide comfortable and controlled sitting posture, the reported data for a vertical backrest may not be considered applicable.

Compared to APMS/DPMI and STHT, only a few studies have investigated the absorbed power quantity of seated human body exposed to WBV. However, the energy-absorption approach may offer the advantages over the use of DPMI/APMS. The relationship between the absorbed power and APMS/DPMI is still not clear. Whether the absorbed power is a good quantity for characterizing the influence of anthropometric parameters, the role of seat geometry and sitting posture as well as assessing the risk of injury due to WBV exposure have not been thoroughly investigated.

The biodynamic responses have been mostly characterized in terms of force-motion relationships at the body-seat interface or at the point of entry of vibration, but

force-motion relationships do not yield information on the transmission of vibration to different segments of the body. Considerable efforts have also been made to study the transmission of vibration to the head and different segments of the body. Seat-to-head vibration transmissibility (STHT), has been used to gain a better understanding of transmission of vibration through the seated body [1]. It has also been shown that STHT can be directly related to the normalized APMS response to WBV, when the response can be characterized by that of a single-degree-of-freedom system [73]. The measurements of vibration transmitted to the head have been performed using a bite-bar or a helmet mounted system. The STHT responses reported in different studies show extreme differences, which may be attributed to differences in various factors, such as measurement and analysis methods, experiment designs, subject anthropometry *etc.*. Owing to the extreme variations observed in the reported data on STHT and lack of sufficient knowledge on the contributions of specific seat and vibration related factors, it is desirable to undertake further measurements on STHT of seated subjects exposed to vertical WBV. The additional data could facilitate interpretations on the human response to WBV, and the role of back support and sitting posture. The additional datasets are further expected to contribute to the standardization efforts for defining the ranges of idealized values of STHT, and on-going efforts in deriving satisfactory biodynamic models and anthropodynamic manikins for the seated body for efficient assessment of seats [54,55].

Furthermore, the force-motion relationship has been widely examined at a single measurement point, the buttock-seat interface with the exception of a single recent study that attempted the measurement of dynamic force imparted on a vertical backrest [51-53].

By measuring the forces at the two points, namely at the vertical human-seat interface and the backrest, cross-axis force-motion relationship may be derived and characterized. Cross axis force-motion relationship may not only enhance the understanding of 'to the body' vibration characteristics but also enhance the significance of seating dynamics on the biodynamic response during WBV exposure. Considering that the automotive seats are designed with inclined seat pan and backrest to provide comfortable and controlled sitting posture, the reported force-motion biodynamic data for a vertical backrest may not be considered applicable. Moreover, the identification of cross-axis responses would permit fro development of more reliable two-dimensional biodynamic model.

The reported studies have mainly focused on the force-motion only or motion-motion only to study the biodynamic responses under different experimental conditions. These studies may not thoroughly characterize the biodynamic responses of the seated body. Only a few of studies [34,42,45] have simultaneously measured the APMS and vibration transmissibility. These data exhibit differences in the frequencies corresponding to peak APMS and STHT magnitude although both are believed to represent the primary resonance of the seated body. It is believed that simultaneous measurements of both responses could yield the identical primary resonant frequency. Moreover, these measurements were limited only to 'no back support' posture, which is not sufficient to characterize the biodynamic responses of vehicle occupants seated with an inclined back support and hands on the steering wheel posture. Simultaneous derivation of force-motion and motion-motion relationships in terms of APMS and STHT may provide a sound approach to identify the target values of biodynamic responses and thus may provide the basis for deriving biodynamic models.

The human body, comprising a complex combination of visco-elastic properties of muscles, bones, joints *etc.*, responds to whole-body vibration in a highly complex manner. The widely reported mechanical-equivalent models are, solely based on the force-motion or motion-motion biodynamic response functions [19]. Only a few models have been proposed to satisfy the two biodynamic response functions. Furthermore, only a few mechanical equivalent models include the contributions due to both anthropometry and body posture.

The dissertation research is expected to yield considerable contributions to the whole-body biodynamics in view of measurement, analysis and modeling. The outcome of the research work will provide a design and analysis tool for potential applications in assessment of coupled occupant system and design of automotive seat. The knowledge of whole-body biodynamics is vital to realize better seat design and testing.

1.6 Objective of the dissertation research

The overall objective of this proposed dissertation research is to focus on the characterization of biodynamic responses of seated occupants exposed to vertical vibration as a function of posture and seat design factors, and on the model development of seated vehicle occupants under whole-body vertical vibration exposure. The specific objectives of the proposed research are as follows:

- Derive the force-motion biodynamic response applicable to a single measurement point.
- Simultaneously measure the multiple force-motion and motion-motion biodynamic response functions applicable to seated subjects under test conditions representative of vehicular vibration environment and configurations.

- Characterize the force-motion relationship for seated vehicle occupants exposed to vertical WBV in terms of apparent mass; Identify the influence of nature and magnitude of excitation, seat geometry factors, hands position, sitting posture, anthropometry, gender *etc.* via statistical tools.
- Characterize the force-motion biodynamic responses of seated vehicle occupants exposed to vertical WBV in terms of absorbed power; Identify the influence of nature and magnitude of excitation, seat geometry factors, hands position, sitting posture, anthropometry, gender *etc.* via using statistical tool.
- Investigate both force-motion and motion-motion biodynamic responses corresponding to body support interaction as a function of various intrinsic and extrinsic variables.
- Identify the target values of simultaneous force-motion and motion-motion biodynamic responses under vertical WBV.
- Develop the seated occupant models taking into account the seating geometry and anthropometry, on the basis of force-motion, motion-motion and combination of the two responses.
- Validate the seated-occupant models taking into account the seating geometry and anthropometry on the basis of the identified target curves.

1.7 Organization of the dissertation

This dissertation is organized into six chapters. The literature is reviewed in the first chapter while highlighting the research contributions on the various subjects such as to formulate the scope and objective of the dissertation. The first chapter also presents the

results of a complete review of published data on whole-body biodynamic response and seated human body models. Chapter 2 presents the detailed experimental design, test methodology and data analysis used in this dissertation. Chapter 3 reports the individually measured force-motion biodynamic responses. The role of seat geometry, anthropometry and various factors on the measured APMS response and indirectly derived absorbed power are thoroughly characterized. Chapter 4 provides the results and discussions of simultaneously measured biodynamic responses, and furthermore propose the target data for the model development. Chapter 5 presents the work of model development. A seated human body model taking into account anthropometry and seat geometry is proposed based on the simultaneously measured force-motion and motion-motion biodynamic response data. Finally, the highlights of the dissertation research, conclusions and the recommendations for future studies are presented in Chapter 6.

CHAPTER 2

EXPERIMENTAL AND DATA ANALYSES METHODS

2.1 Introduction

The methods for measuring the biodynamic responses of seated occupants exposed to vibration have been well established in the reported studies. The approach invariably considers a rigid seat, free from resonances in the frequency range of interest, idealised band limited vibration, either deterministic (harmonic) or random in nature, and a single driving-point at the seat pan [36,46,48,74]. However, the seated occupants in vehicular environment tend to lean against the backrest. The support against a backrest may change both 'to the body' and 'through the body' biodynamic behaviour of the seated body. The total characterization of the seated body biodynamic response to vertical vibration may thus require consideration of body interactions with both the seat pan and the backrest. In this case, the characterization of the force-motion relationship would involve consideration of two driving-points and measurements of dynamic forces at both the seat pan and seat backrest interfaces. The majority of the studies have considered seating without back support, and only a few recent studies [48,51-54,] have considered the measurements at the backrest while the data have been used to characterize cross-axis biodynamic response applicable only for vertical backrests. While the force-motion relationships at the driving-point have been successfully measured using seat-mounted force sensors and accelerometers, the measurement of motion-motion relationship are known to pose extreme challenges associated with the sue of skin-mounted sensors. Different methods have thus been applied to quantify the motion-motion relations, which invariably exhibit excessive inter-subject variabilities [75-78].

Moreover, the data acquired by different researchers exhibit greater discrepancies [75-78]. Alternate measurement methods are thus needed to obtain more repeatable and reliable measures of the motion-motion relationships, such as STHT.

This chapter mainly describes the experimental methods for simultaneously measuring the force-motion and motion-motion biodynamic responses, while the force-motion measurements involve multiple driving points. The measured responses are represented by apparent mass and seat-to-head transmissibility. The individual APMS measurements are also briefly introduced along with the simultaneous measurement, and the measured data are applied to derive the absorbed power responses using direct and indirect approach. The data acquisition and signal analyses methods are further described for deriving both the STHT and the apparent mass responses of the seated vibration-exposed human occupants.

2.2 Head accelerometer mounting, seat and measurement system

2.2.1 Head accelerometer mounting

In the literature, two methods have been widely reported for measuring the vibration transmitted to the head including helmet-mounted accelerometer or bite-bar. The "bite-bar" method relies on the use of the teeth to grip a rigid bar to which accelerometers are secured. This method has been shown to provide repeatable results over a wide range of frequencies (up to 100 Hz) [1]. Paddan and Griffin [35] proposed the use of a dental mould to reduce the discomfort sensation of the subjects holding the bite bar and the variabilities in the data. The data acquired using a bite-bar, however, show considerable variability, as reported by Paddan and Griffin [35] and Matsumoto and

Griffin [71]. Figures 2.1 and 2.2 illustrated the results of these two studies. The great variabilities may be considered as the significant contributions due to angular motions of the head [1]. Furthermore, the alignment of the bite-bar mounted accelerometers along a target coordinate system could pose considerable difficulties.

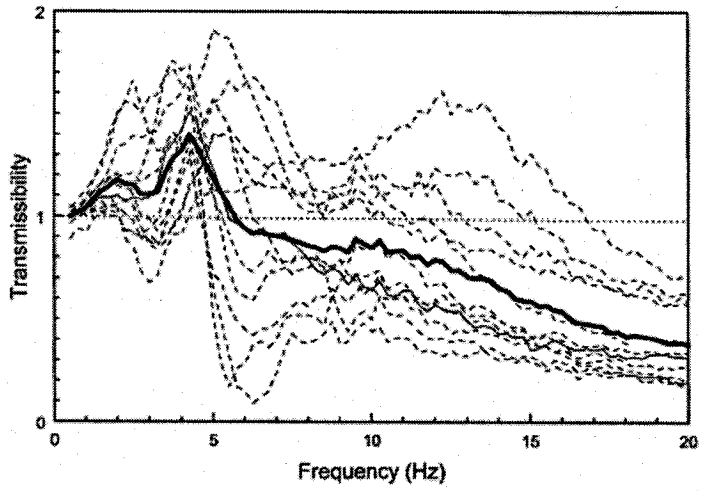

Figure 2.1: The seat-to-head vertical transmissibilities of 12 subjects (- - - - -) and the corresponding average response (——). Data from Paddan and Griffin [35].

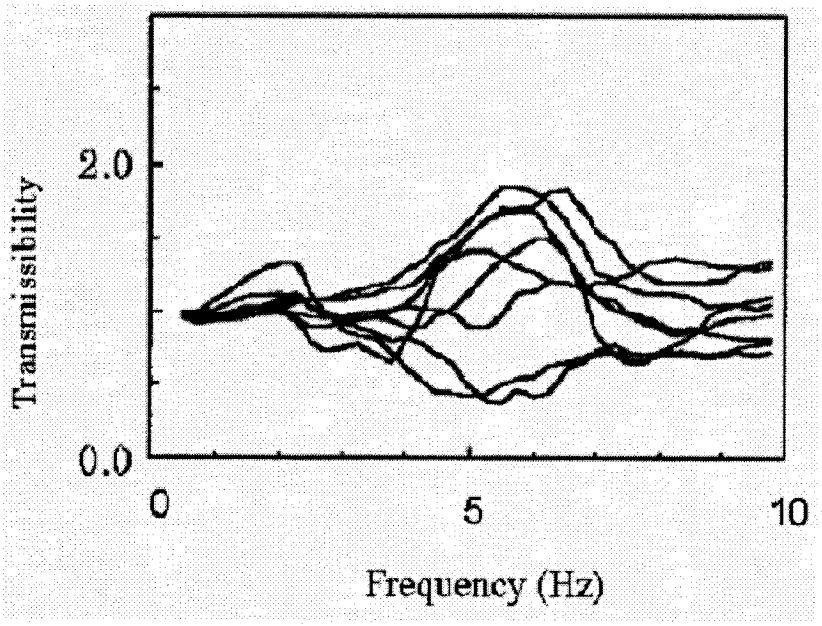

Figure 2.2: The seat-to-head vertical transmissibilities of 8 subjects. Data from Matsumoto and Griffin [71].

As an alternative, vibration transmitted to the head has been measured using helmet-mounted accelerometers [79-81]. The relative movement of the helmet with respect to the head is believed to alter the nature of vibration transmitted to the head and contribute to the high variability in the measured data [79-81]. The mass and mass moments of inertia of the helmet mounting system could further affect the nature of transmitted vibration. The adverse effects of the helmet mass and its relative movements could be reduced by utilizing an adjustable strap alone instead of the helmet. In this study, a strap typically used in safety helmets was used to measure the vibration transmitted to the head. The strap shown in Figure 2.3, comprises a ratchet mechanism to adjust the tension around the head, and weighs only around 300 grams. A three-axis accelerometer (Analog Devices Model ADXL05 EM-3) was mounted on the center of the buckle of the over-the-head strap (Figure 2.3). This type of mounting further facilitated for adequately adjusting and monitoring the accelerometer orientation. The helmet-strap accelerometer mounting system was calibrated in the laboratory to ensure its flat frequency response in the frequency range of interest, which was chosen as 0-15 Hz in the experiments. For this purpose, a human head-shaped fixture was designed, as shown in Figure 2.3.

2.2.2 Simultaneous biodynamic measurement system and experimental method

Figure 2.4 provides a schematic representation of the experimental setup used in simultaneous biodynamic measurement. Figure 2.4 (a) illustrates the schematic setup of force-motion measurement system, and Figure 2.4 (b) illustrates the schematic of motion-

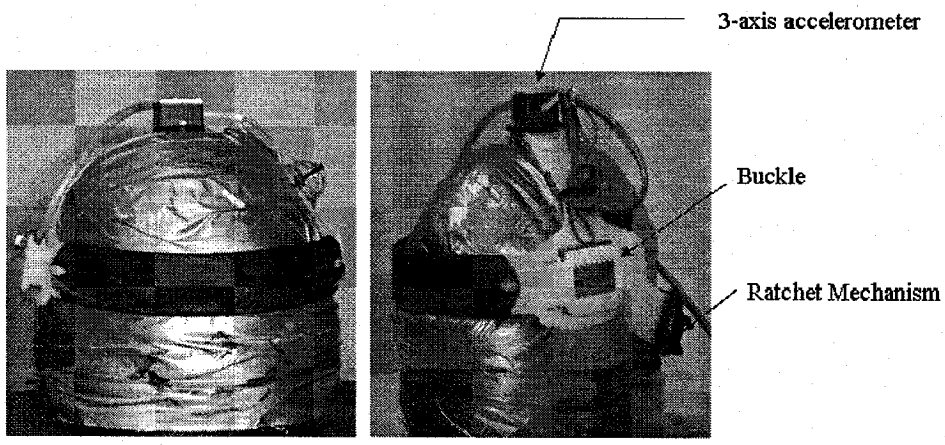

Figure 2.3: Head accelerometer mounting system used in this study.

motion measurement setup. The test fixture involves the use of a whole-body vehicle vibration simulator (WBVVS) capable of producing vertical vibration of deterministic as well as random nature. The WBVVS comprises two vertical electro-hydraulic actuators with a number of safety control loops that limit the peak displacement, peak force and peak acceleration to preset levels. A steering column is installed on the WBVVS to allow for experiments to be conducted under a driver-like sitting posture.

A rigid seat is designed using hollow square-section steel bars to reduce its total weight. Its configuration is to realize geometry representative of the automotive seats. The 450 mm x 450mm seat pan is rigidly fixed on the truss structure at an angle of 77° with respect to the z-axis. While the backrest may be mounted on the truss structure, along with two load cells and force plate, which are installed to measure the total dynamic force exerted by the driver to the backrest. The backrest provides an oval support surface of 220mm x 300mm. Two different backrest configurations were realized

in this setup. These included an upright backrest and an inclined backrest forming an angle of 24° with respect to the z axis.

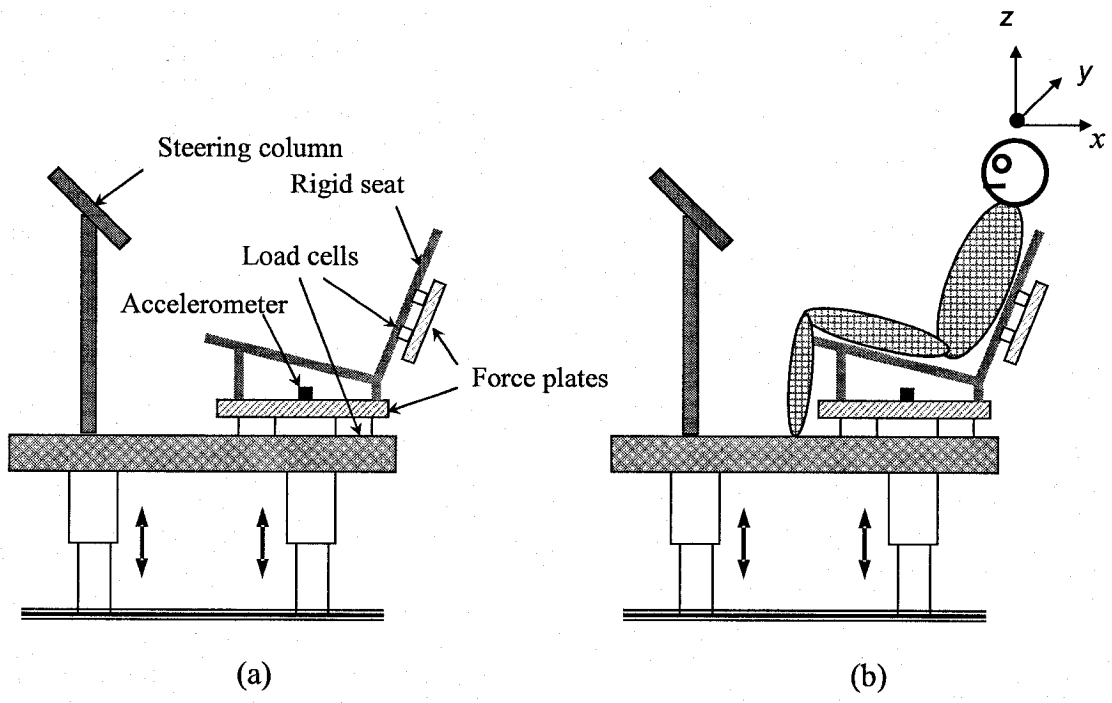

Figure 2.4: Schematic diagram of the seat, force platform and accelerometer arrangements for simultaneous measurement.

The seat assembly is instrumented to measure the total body force acting on the seat base along the z-axis. The force-plate at the seat base was fabricated using four Kistler load cells with a summing junction. Two identical 222 N force transducers (Sensotec, model 41), together with a summing junction were also installed between the backrest and the tubular support structure of the seat to measure the forces along an axis normal to the back support surface. Figure 2.4 (a) illustrates the location of the load cells supporting the seat. The seat and the force platform were positioned to achieve the overall centre of gravity of the seat-occupant system near the geometric centre of the force sensors. A single-axis accelerometer (Analog Devices Model ADXL05 EM-1) was

installed on the platform of a vertical vibration simulator to measure the acceleration due to vertical vibration at the driving point. The primary resonance frequency of the assembly comprising seat with its support structure, and the vibration platform with the steering column was measured as 21 Hz.

As illustrated in Figure 2.4 (b), to examine how the vertical vibration at the seat is transmitted to the head, the same accelerometer used in force-motion measurement was employed at the seat base. A three-axis accelerometer, as illustrated in Figure 2.3, was used in the helmet-strap mounting system to acquire the head vibration along the three translational axes.

A total of 12 healthy adult male volunteers, aged between 21-39 years, took part in the experiment. The subjects had no prior known history of musculo-skeletal system disorders. The subjects' mass ranged from 66.4 kg to 99.6 kg, with mean mass of 77.3 kg and standard deviation of the mean of 10.1 kg. The standing height of the subjects varied from 1.64 m to 1.83 m. The physical characteristics of test subjects are summarized in Table 2.1. Prior to the tests, each subject was informed about the purpose of the study, experimental set up and usage of a hand-held emergency stop, which could suppress the platform motion in a ramp-down manner when activated. Each subject was given written information about the experiment and was requested to sign a consent form that was previously approved by a Human Research Ethics Committee.

Table 2.1: Physical characteristics of test subjects involved in simultaneous measurement.

N=12	Mean	SD	Minimum	Maximum
Age (years)	30.75	6.02	25	39
Weight (kg)	77.26	10.12	66.4	99.6
Height (m)	1.74	0.06	1.83	1.64

The measurements were performed for each subject assuming three different sitting postures, as illustrated in Figure 2.5. The variations in sitting postures were realized by different back support conditions: (i) sitting with no back support, NBS; (ii) Sitting with upper body supported against a vertical backrest, VBS; and (iii) sitting against the inclined backrest, IBS. Under each back support condition, the subjects were also asked to assume two types of hand positions: hands in lap (referred to as "LAP") representing a passenger-like sitting posture, and hands on the steering wheel (referred to as "SW") representing the driver-like sitting posture.

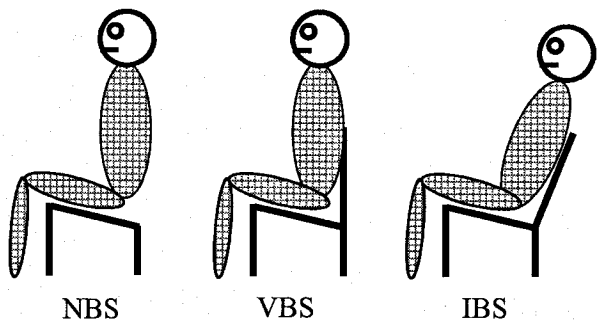

Figure 2.5. Schematic representation of three back support conditions used in the simultaneous measurements.

In present study, random excitations were synthesized for both individual and simultaneous measurements. The biodynamic response characteristics of the participants were measured under different levels of constant acceleration spectral density random excitations. For simultaneous measurement, three different magnitudes denoted by the overall rms accelerations were obtained by selected three different controller gains. The magnitudes of random excitations were chosen to achieve overall rms accelerations of

0.25 m/s^2, 0.5 m/s^2 and 1.0 m/s^2, Figure 2.6 illustrates the power spectral densities of three white-noise random excitation signals in the 0.5-15 Hz frequency range. The results show nearly flat acceleration spectrum in the 0.5-15 Hz frequency range.

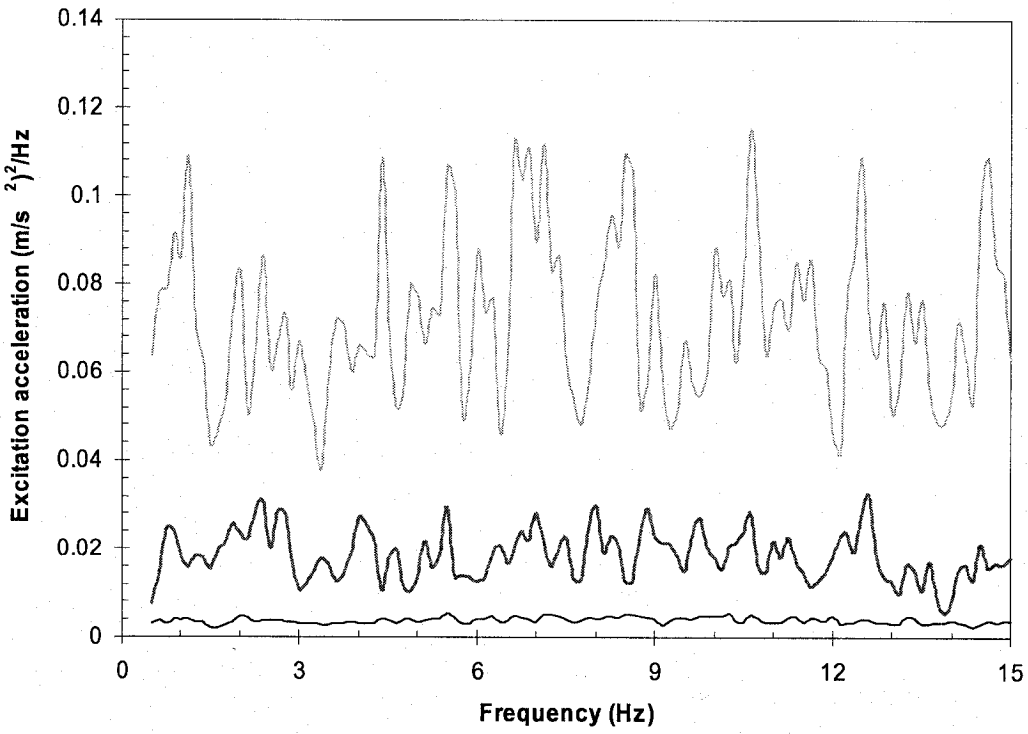

Figure 2.6: Excitation auto-spectral density used in simultaneous measurement—— 0.25 m/s^2 rms —— 0.5 m/s^2 rms ..... 1.0 m/s^2 rms.

Table 2.2 summarizes the test matrix used in simultaneous biodynamic measurements, and involves combinations of three excitation levels, two hands position and three back support conditions. Each measurement was repeated three times to examine the repeatability of the measurement and intra-subject variabilities.

Table 2.2: Test matrix used in simultaneous measurement.

White noise excitation	0.25 0.5 1.0 m/s^2 rms (0.5-15Hz)	0.25 0.5 1.0 m/s^2 rms (0.5-15Hz)	0.25 0.5 1.0 m/s^2 rms (0.5-15Hz)
Back support condition	No back support	Vertical back support	Inclined back support
Hands position	LAP, SW	LAP, SW	LAP, SW

2.2.3 Experimental procedure: simultaneous measurements

The purpose of simultaneous biodynamic measurement in this thesis is to derive both the APMS and STHT biodynamic responses at the same time under identical experimental conditions. Due to the limitation of the available analyzer channels, the measurements were performed in two sessions. The first session involved the APMS measurement, while the second session acquired the STHT data. To maintain the relatively consistent sitting posture, the back force was strictly monitored in both sessions for the back supported postures. For the same posture, the time interval of two sessions of measurements was generally less than one hour. The static force signals acquired from the seat base and backrest force sensors, were recorded prior to and after each test, and were compared to examine the consistency in the subject posture. The trial was repeated when difference in the static forces acquired before and after a test exceeded 10%. The mean values of the two measurements were thus taken as the body masses supported by the two supporting surfaces. The acceleration and force signals at the seat base and backrest were acquired in four-channel signal analyzer.

For the STHT measurement session, each subject was asked to wear the head-accelerometer band and adjust its tension to ensure a tight but comfortable fit. The

experimenter made the necessary adjustments to ensure appropriate orientation of the head accelerometer using a level. Each subject was asked to sit assuming the desired posture, while keeping a steady head position by staring straight ahead at his self-image in a mirror, which was located on the wall around 4 meters away from the test subject. Meanwhile the subject's posture during each trial was visually checked by the experimenter to ensure consistency.

2.2.4 Individual force-motion biodynamic response experimental method

Owing to the limitations of the measurement techniques, the force-motion and motion-motion biodynamic relationships of seated body under WBV have been measured separately in most of reported studies. In this dissertation, the force-motion measurements were conducted using 27 subjects to study the role of seat geometry along with hand position, pan angle, and sitting height on the force-motion biodynamic behaviour.

The experiments were conducted using a specially designed rigid seat considered to provide a typical seat geometry, and the adjustability to realize different postural configurations. The seat could be adjusted to realize three different sitting heights, measured from the pan to the floor: 510mm (H1), 460mm (H2) and 410mm (H3); two different inclinations of the backrest (0° and 12°); and two different pan angles (0° and 7.5°). The variations in the seat height and geometry were selected on the basis of ranges defined in ISO-4253[82], which recommends cushion and backrest inclinations in the 3-12° and 5-15° ranges, respectively, for off-road vehicle seats. The standard also recommends seat height in the 510-525 mm with reference to seat index point. The

postural variations were also considered for two different hand positions: hands in lap (referred to as "LAP") representing a passenger-like sitting posture, and hands on the steering wheel (referred to as "SW") representing the driver-like sitting posture. Similar to the previous session, Figure 2.7 provides a schematic view of measurement system used in the single force-motion biodynamic response measurement which illustrates the location of the main components of the measurement system. Unlike the simultaneous force-motion measurement setup, four identical force sensors (Sensotec, model 41), each rated at 444 N, were mounted under the base plate of the seat to measure the total vertical force developed at the seat base. A summing junction was used to sum the signals from the four load cells. Since the primary resonance frequency of the assembly comprising seat with its support structure, and the vibration platform with the steering column was measured as 45 Hz, the excitation frequency range was selected in the 0.5-40 Hz. Besides, the test seat geometry and steering column is different from what was employed in the simultaneous measurement study.

Apart from the three seated heights and two different hand positions, the biodynamic responses are characterized for six different seat-dependent posture (Figure 2.8): (i) seated on an inclined seat pan and back supported by the inclined backrest (BIP); (ii) inclined pan with back supported by a vertical backrest (BVP); (iii) a flat pan with back supported by a vertical backrest (BVF); (iv) a flat pan with back supported by an inclined backrest (BIF); (v) inclined pan with back not supported (NVP); and (vi) flat pan with back not supported (NVF). The combinations of these seat designs and hands positions

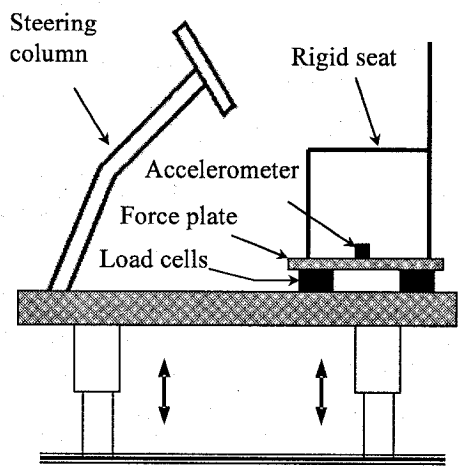

Figure 2.7: Schematic diagram of the seat, force platform and accelerometer arrangements for single force-motion measurement.

resulted in a total of 36 different postural configurations. Two different magnitudes denoted by the overall rms accelerations were obtained by selecting three different controller gains. The magnitudes of random excitations were chosen to achieve overall rms accelerations of 0.5 m/s^2 and 1.0 m/s^2, as illustrated in the Figure 2.9. A white noise random signal was synthesized to yield flat acceleration spectrum in the 0.5-40 Hz frequency range. Table 2.3 summarizes the test matrix used in the study.

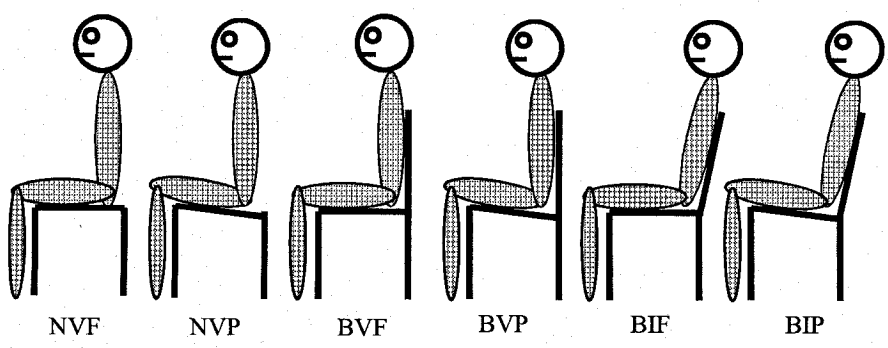

Figure 2.8: Schematic representations of different sitting postures used in single-force motion biodynamic responses.

A total of 27 subjects, 13 males and 14 females, participated in the experiments. All subjects were considered to be healthy with no known signs of musculo-skeletal system disorders. Prior to the test, each subject was given written information about the experiment and was requested to sign a consent form previously approved by a Human Research Ethics Committee. Table 2.4 summarizes the physical characteristics of the subjects in terms of mean, standard deviation (S.D.), minimum and maximum values of subject age, height and body mass. The body mass of the participants ranged from 47.5 kg to 110.5 kg with mean of 70.8 kg.

Table 2.3: Physical characteristics of the test subjects involved in single driving-point force-motion measurement.

	Mean, Standard Deviation, Minimum, and Maximum values		
	Male	Female	All subjects
Population	13	14	27
Age (years)	38.1, 8.4, 21.0, 53.0	41.0, 8.7, 26.0, 52.0	39.6, 8.5, 21.0, 53.0
Height (cm)	175.5, 4.89, 165.0, 181.0	166.6, 6.3, 153.0, 175.0	170.9, 7.13, 153.0, 181.0
Body mass (kg)	75.8, 14.3, 49.5, 97.6	66.2, 16.5, 47.5, 110.5	70.8, 16.0, 47.5, 110.5
Body mass index (kg/m*m)	24.49, 3.98, 18.1, 32.2	23.64, 4.93, 18.9,26.5	24.05,4.43,18.1, 32.2
Body fat (%)	21, 9, 6, 39	31, 11, 19, 54	26, 11, 6, 54

Table 2.4: Test matrix used in single force-motion biodynamic measurement.

rms acceleration due to excitation (m/s^2)						
Hands position	LAP			SW		
Sitting posture	Seat height					
	510mm	460mm	410mm	510mm	460mm	410mm
NVF	0.5,1.0	0.5,1.0	0.5,1.0	0.5,1.0	0.5,1.0	0.5,1.0
BVF	0.5,1.0	0.5,1.0	0.5,1.0	0.5,1.0	0.5,1.0	0.5,1.0
BIF	0.5,1.0	0.5,1.0	0.5,1.0	0.5,1.0	0.5,1.0	0.5,1.0
NVP		0.5,1.0			0.5,1.0	
BVP		0.5,1.0			0.5,1.0	
BIP		0.5,1.0			0.5,1.0	

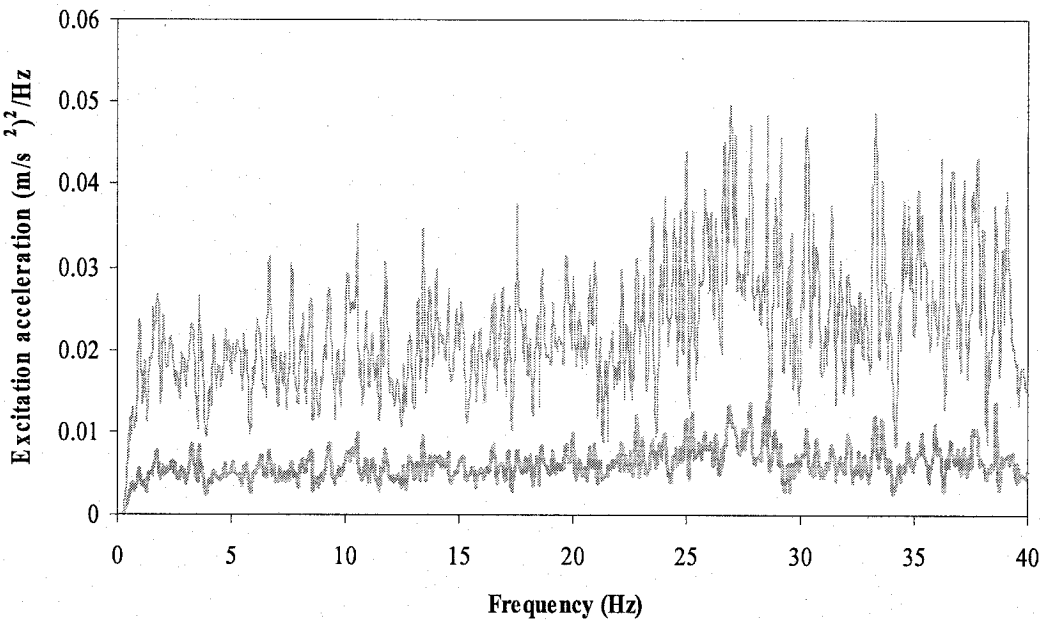

Figure 2.9: Excitation auto-spectral density employed in the single force-motion measurement; —— 0.5 m/s^2 rms; and —— 1.0 m/s^2 rms.

2.3. Data analysis

The acceleration signals measured at the seat base (vertical) and the head (vertical and fore-and-aft direction) were acquired in a multi-channel data acquisition and analysis system (Brurel & Kjær Pulse 6.0 system). Similarly, the force signals measured at the seat base (vertical) and the backrest (normal to the backrest) were also acquired from the analyzer system. It should be noted that the side-to-side head motion was not acquired due to its very low magnitude. The data corresponding to each measurement were acquired over a period of 56s (25 averages using Hanning window and an overlap of 75%). The data analyses were performed using a bandwidth of 100 Hz and resolution of 0.125 Hz. Each experiment was performed twice, and the results were compared to

ensure reasonable repeatability. Additional trials were performed, when the deviations between the peak magnitudes of the head acceleration and the corresponding frequency observed during the two trials exceeded 15%. The static body weights supported by the seat base and backrest were recorded before and after each trial. A particular trial was repeated if the static values acquired after the test difference from those acquired prior to the test by more than 10%.

The acquired data were analyzed using the CPB (constant percentage band width) and FFT (Fast Fourier Transform) analyzers of the pulse system. The following post-processing functions were displayed on the screen using the pulse software to monitor the results:

- Magnitude and phase of the APMS response that was derived from the force and acceleration measured at the seat base.
- Magnitude of cross-axis APMS response that was derived from the force measured at the backrest and acceleration measured at the seat base.
- Magnitude and phase of the vertical STHT response that was derived from the acceleration measured at the head in the vertical direction and acceleration measured at the seat base.
- Magnitude and phase of the fore-and-aft STHT response that was derived from the acceleration measured at the head in the fore-and-aft direction and acceleration measured at the seat base.
- Coherence function of the vertical head acceleration and acceleration signals at the seat base.
- Coherence function of the force and acceleration signals at the seat base.

- Coherence function of the force and acceleration signals at the backrest.
- Third-octave band spectra of the seat base acceleration.

The measured APMS responses and cross-spectra were stored in terms of their real and imaginary components for further analyses. The APMS and the cross-axis APMS response of the seat alone were acquired prior to the test with each subject, and stored to perform inertial corrections of the responses of the seat with subject.

Identical test methodology was employed for measuring force-motion biodynamic response in either individual or simultaneous measurement. Figure 2.10 schematically illustrate the quantity of measured physical parameter with two back supported postures. F_v is the force measured at the seat base in the vertical direction, and F_b is the force measured normal to the backrest. Acceleration is measured at the seat base in the vertical direction ($\ddot{z}$). Two forces were analyzed relative to the vertical acceleration, resulting in the two biodynamic measures. The two force-motion biodynamic responses were produced in the frequency domain, namely:

$$M_v(j\omega) = S_{\ddot{z}F_v}(j\omega) / S_{\ddot{z}}(j\omega) \qquad (2.1)$$

$$M_{vb}(j\omega) = S_{\ddot{z}F_b}(j\omega) / S_{\ddot{z}}(j\omega) \qquad (2.2)$$

Where $M_v(j\omega)$ is referred to as 'vertical APMS' and $M_{vb}(j\omega)$ is referred to as 'cross-axis APMS'. ω *is* corresponding to the excitation frequency of ω. $S_{\ddot{z}F_v}(j\omega)$ is the cross-spectral density of the total force measured at the seat base along the vertical *z*-axis the acceleration due to excitation $\ddot{z}$. $S_{\ddot{z}F_b}(j\omega)$ is the cross-spectral density of the

force measured normal to the seat back and the acceleration due to excitation $\ddot{z}$, and $S_{\ddot{z}}$ is input acceleration auto spectral density.

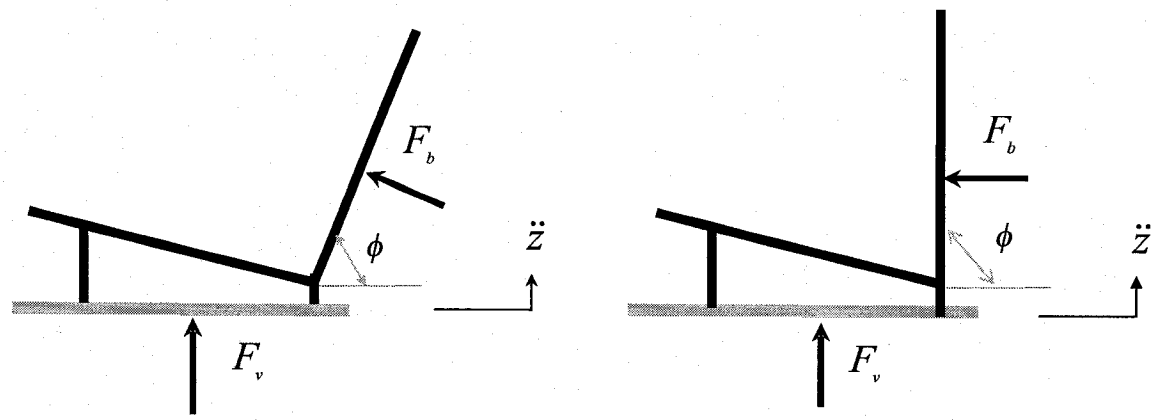

Figure 2.10: Schematic diagram of the force-motion measurement point for the back supported postures.

The coherence response between the forces and accelerations, and force and velocities were constantly monitored during experiments performed with subjects to ensure adequate signals. A measurement was rejected when coherence value was observed to be below 0.9 within the entire frequency range. The analyzer software was also programmed to continually display the rms acceleration due to excitation in the third-octave frequency bands, which was monitored to ensure consistent excitation.

Two APMS responses were initially measured with test seat alone, which will be used to perform the inertia cancellation of the measured biodynamic response. Figure 2.11 illustrate the 'vertical APMS' and cross-axis APMS" for the seat alone with the inclined backrest (measured at 1.0 m/s^2 rms). The results show nearly constant magnitude of the APMS in the concerned frequency range representing the masses due to the entire seat assembly and the backrest support, respectively. To calculate the biodynamic

responses of seated body, the real and imaginary parts of the transfer function measured without a subject were subtracted from the corresponding real and imaginary parts of the transfer function measured with the subjects. Finally, the two complex biodynamic responses of the seated subjects were derived, in terms of the APMS magnitude and phase responses.

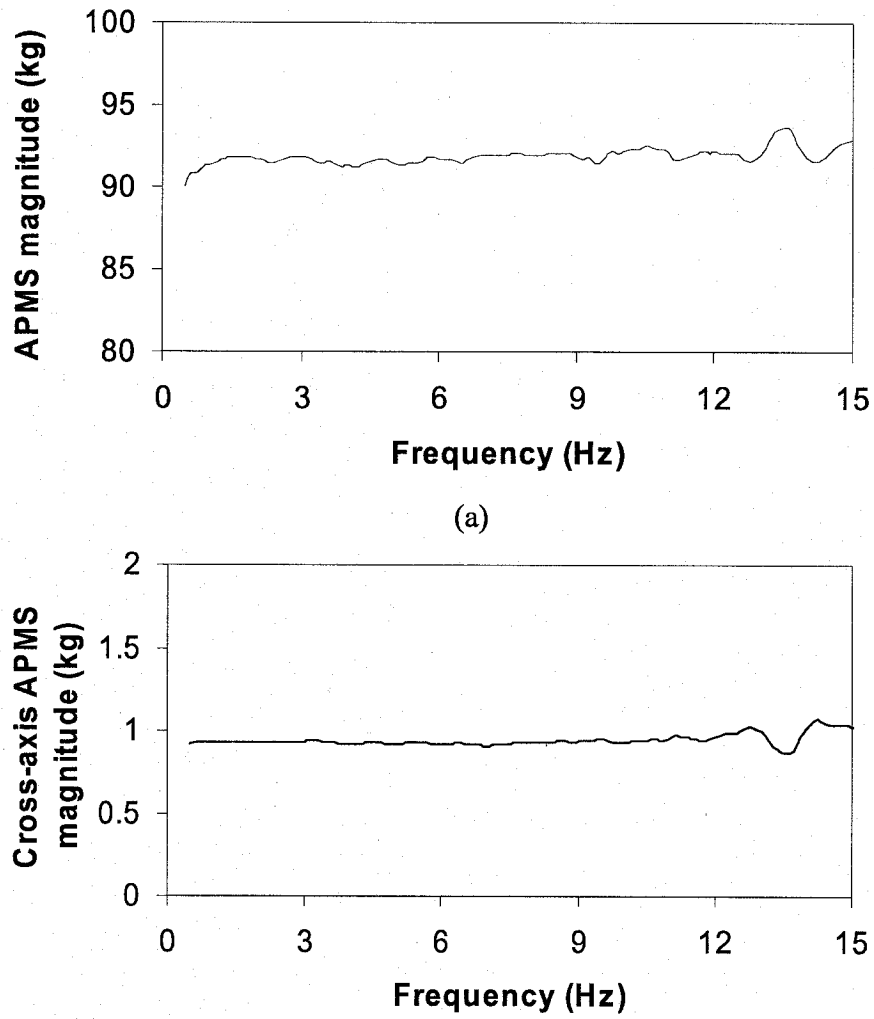

Figure 2.11: The measured APMS magnitude of the seat alone for the inclined back support: (a) entire seat assembly; (b) the backrest.

The seat-to-head transfer function in both vertical (TF_z) and fore-and-aft directions (TF_x) were derived from spectral analysis method. Namely, the transfer function, the complex ratio of cross-spectral density between the seat acceleration and head acceleration (vertical or fore-and-aft direction), and the auto-spectral density of vertical seat acceleration, such that:

$$TF_z = \frac{S_{\ddot{z}_H \ddot{z}}(j\omega)}{S_{\ddot{z}}(j\omega)} \tag{2.3}$$

$$TF_x = \frac{S_{\ddot{x}_H \ddot{z}}(j\omega)}{S_{\ddot{z}}(j\omega)} \tag{2.4}$$

Where $S_{\ddot{z}_H \ddot{z}}$ and $S_{\ddot{x}_H \ddot{z}}$ are the cross spectral densities of head acceleration along the z and x directions with the vertical seat base acceleration $\ddot{z}$, and $S_{\ddot{Z}}$ is auto-spectral density of the vertical seat acceleration.

It should be noted that the magnitude of head acceleration along the lateral axis (y) was observed to be very small and thus not presented in the study. For each transfer function, the coherence γ^2 between the two signals being analyzed was computed to examine the correlation between the seat acceleration and the head acceleration during each trial. The coherence provides a value ranging from 0 to 1, and represents the ratio of the square of the absolute value of cross-spectral density to the product of auto-spectral density of the seat acceleration and head acceleration in both vertical and fore-and-aft directions [14]:

$$\gamma_z^2 = \frac{\left|S_{\ddot{z}_H \ddot{z}}(j\omega)\right|^2}{S_{\ddot{z}_H}(j\omega) S_{\ddot{z}}(j\omega)} \tag{2.5}$$

$$\gamma_x^2 = \frac{\left|S_{\ddot{x}_H \ddot{z}}(j\omega)\right|^2}{S_{\ddot{x}_H}(j\omega) S_{\ddot{z}}(j\omega)} \tag{2.6}$$

Where γ_z and γ_x are the coherence of the vertical and fore-and-aft head acceleration with respect to the seat base acceleration, respectively, and $S_{\ddot{x}_H}$ is the auto spectral density of the fore-and-aft head acceleration.

The experiments were initially performed to examine the frequency response characteristics of the head accelerometer mounted on the head-shaped fixture. The head accelerometer mounting system was placed on the platform of the WBVVS, which was subject to a white noise random vibration in the 0.5-15 Hz range (0.5 m/s^2). The vertical acceleration of the platform and the head accelerations along the three-axes (x, y and z) were acquired and analyzed to determine the magnitude response in the concerned frequency range. Figure 2.12 presents the measured frequency response characteristics of the head acceleration measurement system in terms of TF_x, TF_y and TF_z in the 0.5-15 Hz frequency range. The results show nearly flat response and close to unity value of the magnitude ratio along the vertical direction, and thus confirm the validity of the proposed measurement system. The vibration transmissibility magnitude in the fore-and-aft direction is around 0.05, and even smaller in the lateral direction, which was believed to be caused by slight orientation errors.

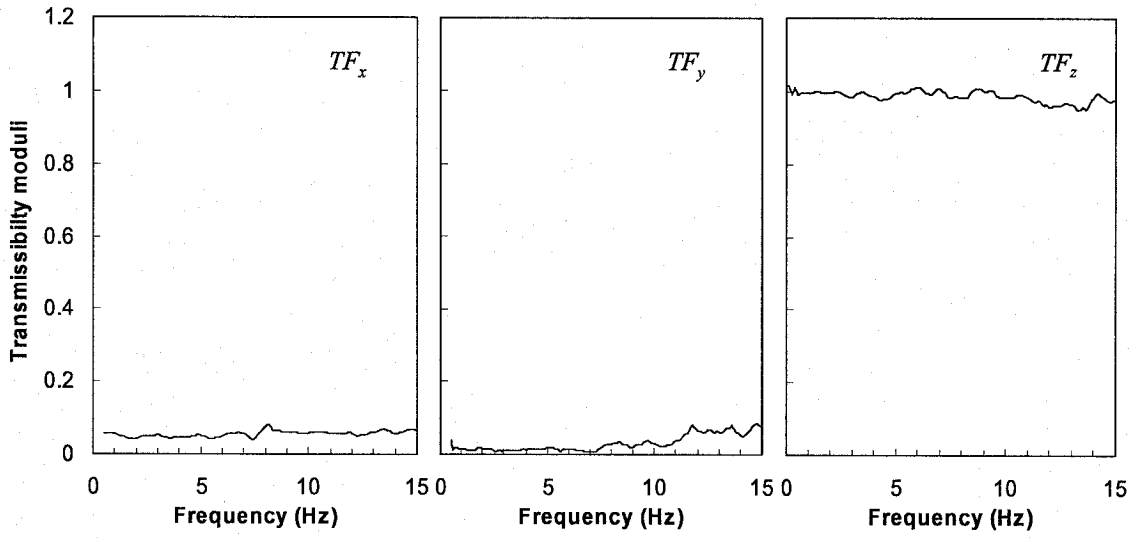

Figure 2.12: The three-axes frequency response characteristics of the head acceleration mounting system under vertical vibration.

2.4 Absorbed power: mathematical formulation

A vast majority of the reported APMS/DPMI data are based upon measured motion, usually acceleration, and the dynamic force at the driving point, to determine the 'to the body' force-motion relationship at the human-seat interface. Mathematically these functions are expressed in terms of one-sided power spectral density functions [14]:

$$M(j\omega) = S_{aF}(j\omega)/S_a(j\omega) \tag{2.7}$$

$$Z(j\omega) = S_{vF}(j\omega)/S_v(j\omega) \tag{2.8}$$

Where $M(j\omega)$ and $Z(j\omega)$ are the complex APMS and DPMI functions respectively corresponding to excitation frequency ω. $S_{aF}(j\omega)$ and $S_{vF}(j\omega)$ are the cross-spectral densities of acceleration $a(t)$ and force $F(t)$, and velocity $v(t)$ and force respectively; $S_a(j\omega)$ and $S_v(j\omega)$ are the auto-spectral densities of excitation acceleration and velocity.

Upon consideration of one-sided spectral density $(0,\infty)$, the above relationship could be expressed as:

$$M(j\omega) = G_{aF}(j\omega)/G_a(j\omega) \tag{2.9}$$

$$Z(j\omega) = G_{vF}(j\omega)/G_v(j\omega) \tag{2.10}$$

Where $G_{aF}(j\omega)$ and $G_{vF}(j\omega)$ are the one-sided cross-spectral densities of acceleration $a(t)$ and force $F(t)$, and velocity $v(t)$ and force respectively; $G_a(j\omega)$ and $G_v(j\omega)$ are one-sided the auto-spectral densities of excitation acceleration and velocity.

The vibration power transferred to the seated human body over the exposure interval T is computed from:

$$P_{avg} = \frac{1}{T}\int_0^T v(t)F(t)dt \tag{2.11}$$

In order to analyze the transferred power in the frequency domain, it is necessary to introduce the cross-correlation function in the time domain, such that:

$$R_{vF}(\tau) = \frac{1}{T}\int_0^T v(t)F(t+\tau)dt \tag{2.12}$$

Where τ is the lag between the force and velocity signal, and R_{vF} is the cross–correlation function. The averaged transferred power can be determined by letting τ=0, which yields:

$$P_{avg} = R_{vF}(0) \tag{2.13}$$

The application of Wiener-Khinchine relations yields [14]:

$$S_{vF}(j\omega) = \frac{1}{2\pi}\int_{-\infty}^{\infty} R_{vF}(\tau)e^{-j\omega\tau}d\tau \tag{2.14}$$

$$R_{vF}(\tau) = \int_{-\infty}^{\infty} S_{vF}(j\omega) e^{j\omega\tau} d\omega \tag{2.15}$$

The complex spectral density in the above relation can also be expressed using single-sided cross spectral density:

$$G_{vF}(j\omega) = C_{vF}(\omega) - jQ_{vF}(\omega) \tag{2.16}$$

Where $C_{vF}(\omega)$ is the coincident spectral density function, or the co-spectrum, and $Q_{vF}(\omega)$ is the quadrature spectral density function, or the quad-spectrum. The above cross-correlation function may thus be expressed as [14]:

$$R_{vF}(\tau) = \int_{0}^{\infty} [C_{vF}(\omega)\cos\omega\tau + Q_{vF}(\omega)\sin\omega\tau]d\omega \tag{2.17}$$

Equations (2.13) and (2.17) yield the averaged transferred power in terms of the co-spectrum function by letting τ=0;

$$P_{avg} = \int_{0}^{\infty} C_{vF}(\omega) d\omega \tag{2.18}$$

The above formulations suggest that the amount of transferred energy per unit time at the driving point could be derived in the frequency domain from the real part of the cross-spectrum of the driving force and the velocity. The imaginary component of the cross-spectrum has been related to the energy restoring properties of the biological system [83].

Considering that both the APMS/DPMI and absorbed power function derive from the force-motion behavior at the driving-point, a clear relation between two measures exists. It can be ascertained that the real part of the DPMI directly relates to the power absorbed by the human body exposed to vibration. From the DPMI definition described

in Equation (2.10), the cross-spectrum of force response and excitation velocity can be expressed as:

$$G_{vF}(j\omega) = Z(j\omega)G_v(j\omega) \tag{2.19}$$

The co-spectrum or real component of the cross-spectral density may also be computed from the DPMI as follows:

$$C_{vF}(\omega) = \mathrm{Re}[Z(j\omega)]G_v(j\omega) \tag{2.20}$$

Where '*Re*' designates the real component. Upon substituting for $C_{vF}(\omega)$ from the above in Equation (2.18), the averaged absorbed power may be obtained as:

$$P_{avg} = \int_0^\infty \mathrm{Re}[(Z(j\omega)]G_v(j\omega)d\omega \tag{2.21}$$

In a similar manner, the averaged absorbed power could also be related to the APMS response function. Both the APMS and DPMI functions represent the same biodynamic behaviour, and can be related as:

$$M(j\omega) = Z(j\omega)/j\omega \tag{2.22}$$

The auto-spectral density relationship between the excitation velocity and acceleration could be expressed as:

$$G_v(j\omega) = G_a(j\omega)/(j\omega)^2 \tag{2.23}$$

The co-spectrum $C_{vF}(\omega)$ in Equation (2.20) may further be derived as:

$$C_{vF}(\omega) = \mathrm{Im}[M^*(j\omega)]G_a(j\omega)/\omega \tag{2.24}$$

Where '*Im*' designates the imaginary component of the conjugate of the complex APMS, $M^*(j\omega)$.

The averaged absorbed power can thus be related to the APMS response function as:

$$P_{avg} = \int_0^{\infty} \frac{\mathrm{Im}[(M^*(j\omega))]G_a(j\omega)}{\omega} d\omega \qquad (2.25)$$

The above equation defines the relationship between the APMS function and the absorbed power, which may be applied to determine the energy dissipation properties of seated occupants exposed to WBV using the well-documented APMS data. The measured force, acceleration and APMS data were applied to compute the average absorbed power using the indirect method, described by Equation (2.25).

2.5 Experimental validation of the indirect method for absorbed power

The validity of the indirect method was also examined by comparing the computed absorbed energy response with that derived from the direct method, described by Equation (2.18). This comparison was performed for the data acquired from a single subject seated on a flat pan with no back support (NVF) and hands in LAP posture. The measurements and data analysis for this purpose were performed under three different levels of random excitations (overall rms accelerations 0.25, 0.5 and 1.0 m/s2 in the frequency range of 0.5-20 Hz).

Figure 2.13 illustrates a comparison of the absorbed power density derived from the measured force and acceleration using direct as well as indirect methods corresponding to the selected posture (NVF) and three different excitation levels (0.5, 1.0, 1.5 m/s^2 rms acceleration). The results are presented in terms of absorbed power density, directly attained from the force-velocity co-spectrum. The results show very good agreement between the direct and indirect methods of analyses, irrespective of the

excitation magnitude, with the exception of only slight deviation in the low frequency bands. The magnitudes of absorbed power density are comparable with those reported by Mansfield and Griffin [44] corresponding to comparable magnitudes of excitation and sitting posture.

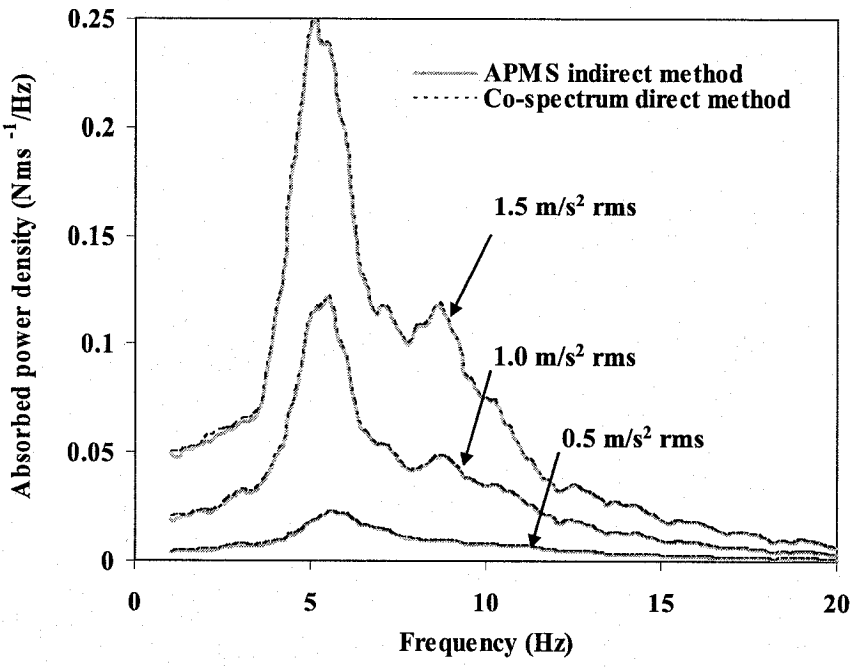

Figure 2.13: Comparisons of absorbed power characteristics computed using direct and indirect methods under different levels of rms acceleration.

In view of the good agreement between the indirect and direct methods, the indirect method is applied to study the characteristics of absorbed power responses of seated occupants from the measured APMS responses. The average absorbed power is computed in the constant percentage bandwidth analysis (1/3 octaves), and response characteristics are presented corresponding to each 1/3 octave center frequency, such that:

$$P_{avg}(\omega_c) = \int_{\omega_l}^{\omega_u} C_{vF}(\omega) d\omega \tag{2.26}$$

Where ω_l and ω_u are the lower and upper limits of the chosen frequency band, and ω_c is the center frequency of the band.

2.6 Statistical data analysis

Owing to considerable inter-subject and within-subject variabilities obtained in different experimental conditions, statistical analyses are performed to characterize the measured force-motion and motion-motion biodynamic responses.

In this dissertation, the determination of mean and standard deviation, regressions analysis, analysis of variance (ANOVA) and analysis of covariance (ANCOVA) were employed to analyze the measured data using SPSS 11.5 software. The main purposes of different statistical analyses summarize as: the investigation of significance of various factors contributing to postural variations of force-motion biodynamic responses, such as hands position, seat height, pan and backrest orientation, back support conditions; the investigation of linear dependence between the biodynamic response and anthropometry factors, such as body mass, body mass index, body height and body fact; the investigation of excitation magnitudes and frequency on the biodynamic responses. The significance of the contributing factors is stated based on the p values less than 0.05.

2.7 Summary

This chapter describes the design of measurement system, experimental design and measurement methods employed for individual force-motion, and simultaneous force-motion and motion-motion measurements.

The single force-motion biodynamic response characteristics of 13 male and 14 female seated subjects, exposed to vertical vibration, were measured under different postural conditions. The measurements were performed for a total of 36 different sitting postural configurations realized through variations in hands position (in lap and on steering wheel), seat heights (510mm, 460 mm and 410 mm), and seat design factors involving pan (0° and 7.5°) and backrest (0° and 12°) orientations and different back support conditions. The measured data, were derived in terms of the vertical apparent mass (APMS), and then the absorbed power response was calculated from the APMS data using the indirect method in the study. The derived apparent mass and absorbed power responses are analyzed to characterize the role of seat geometry (pan orientation, back support condition and seat height) and postures (hands position) on the force-motion biodynamic responses under vertical WBV vibration.

Simultaneous force-motion and motion-motion measurements were performed using 12 adult male subjects exposed to whole-body vertical random vibration in the 0.5-15 Hz frequency range while exposed to three magnitudes of excitation (0.25, 0.5 and 1.0 m/s^2 rms acceleration). The seat geometry in simultaneous measurement is quite different from the single force-motion measurement, such as lower seat height, relatively higher pan (12°) and backrest (0° and 24°) inclination. The measured force-motion biodynamic responses, are derived in terms of the 'vertical APMS and 'cross-axis APMS'.

A helmet-strap-mounted accelerometer mounting system was designed to measure the head acceleration motions along the three translational axes. The proposed approach to measuring the head motion could facilitate the adjustment and monitoring of the accelerometer orientation, while reducing the discomfort caused by a 'bite-bar' system,

and the inertial force contributions arising from the helmet-mounted measurement systems. The measured motion-motion biodynamic responses, are derived in terms of 'vertical STHT' and 'fore-and-aft STHT'.

The effects of back support conditions on both APMS and STHT biodynamic responses were investigated by considering three back support conditions (No back support, vertical back support, and inclined back support), two different hands positions (hands in lap and hands on the steering wheel) and three excitation levels.

CHAPTER 3

MEASUREMENT OF SINGLE DRIVING-POINT FORCE-MOTION CHARACTERISTICS

3.1 Introduction

The characterization of vibration transmitted to the body segments poses considerable measurement challenges. The reported data exhibit extreme differences in the responses, even though they have been performed under comparable and controlled experimental conditions [11,33,35,41,42,75-77]. Alternatively, the functions based upon 'to-the-body' measurement, namely DPMI/APMS and absorbed power, are conveniently used to characterize the human responses to vibration. The measurements of these force-motion functions require instrumentation at the driving-point surfaces and thus yield more repeatable data with relatively lower inter-subject variabilities.

The APMS has the advantage that it can be obtained directly from the measured acceleration and force. Furthermore, Newton's second law of motion gives APMS a simple intuitive meaning: "The rate of change of momentum of a body is proportional to the force acting on it and is in the direction of the force". When the human body is effectively rigid (e.g. at very low frequencies in the vertical axis) the apparent mass of the body is equal to its static mass and the force and acceleration are in phase. As the frequency of motion increases, the presence of one or more resonances and/or the visco-elastic properties of the biological system tend to alter the APMS response and introduce a phase difference between the force and the acceleration. At higher frequencies the upper body is only loosely coupled, the dynamic force is thus dominated by the masses near the driving point resulting in lower magnitude of the APMS.

The absorbed power could either be directly derived from real part of the cross-

spectrum density between the force and velocity [43, 88-89] or indirectly from the imaginary part of APMS. As the absorbed power is a function of vibration magnitude, it makes the quantity sensitive to vibration input spectral content. Furthermore, the absorbed power will increase in magnitude as the magnitude of the vibration increases. This is in contrast with the property of apparent mass, which is not directly proportional to the input excitation magnitude.

Since the APMS indicates the body mass at low frequency, it is strongly dependent upon the body mass, and absorbed power was found to have the similar characteristics, as reviewed in section 1.3.1 [43]. The force-motion biodynamic response may also be associated with other anthropometry variables, like body height, body mass index and body fat. Although the strong influence of sitting postures on both the APMS and absorbed power has been recognized in only a few studies [43,52], the effects of variables influencing posture have not been systematically assessed.

In this chapter, the APMS biodynamic response of 13 male and 14 female seated subjects, exposed to whole-body vertical random vibration in the 0.5-40 Hz frequency range are measured under two different postural conditions. The measurements are performed for a total of 36 different sitting postural configurations realized through variations in hands position LAP (in lap) and SW (on steering wheel), three seat heights (H1:510mm, H2: 460mm and H3: 410mm), and seat design factors involving two different pan orientations (0° and 7.5°). The measured data, in terms of the vertical apparent mass (APMS) and absorbed power computed from the APMS dataset, are analyzed to study the role of seat geometry on the biodynamic response under whole-body vertical vibration using statistical methods and tools.

3.2 The role of seat geometry and posture on the APMS characteristics

3.2.1 APMS response characteristics and body mass dependence

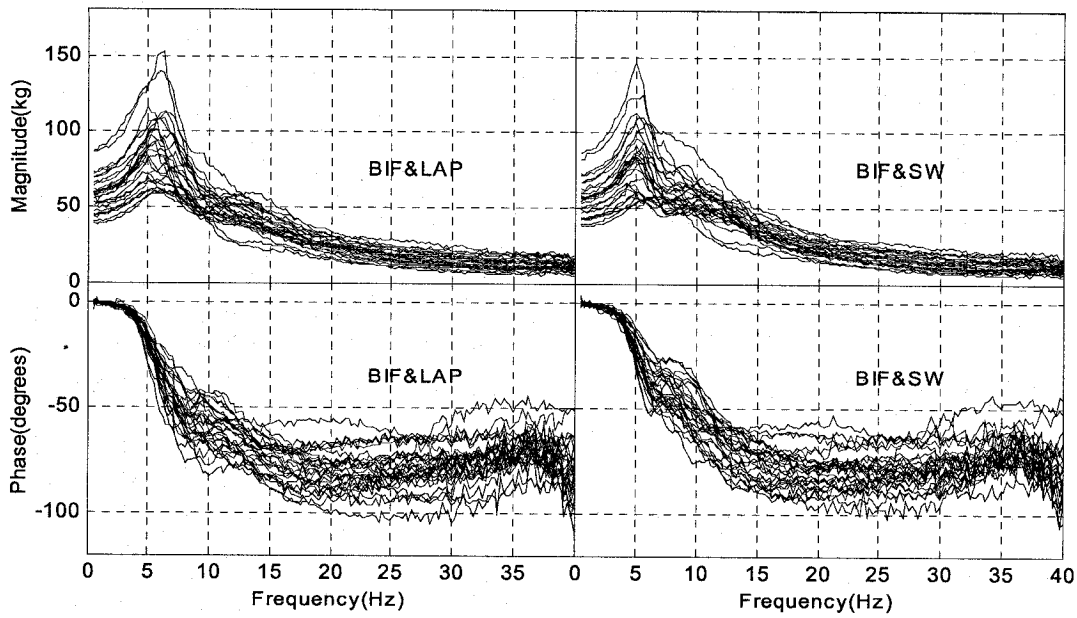

Figure 3.1: APMS magnitude and phase responses of 27 subjects (seat height: 460mm; excitation: 1.0 m/s^2 rms).

Figure 3.1 illustrates, as an example, the variations in measured APMS magnitude, and phase responses of 27 subjects obtained for the medium seat height (H2), two hands positions (LAP and SW) and BIF (inclined back support and flat pan) posture, while exposed to 1.0 m/s^2 rms vertical white-noise vibration. The results show considerable scatter in the magnitude response at frequencies below 20 Hz, but at frequencies above 20 Hz the variations tend to diminish considerably irrespective of the hands position. The corresponding scatter in the phase response, however, presents the opposite trend. Despite the significant variations, the magnitude responses peak in the 5 to 6.5 Hz frequency range for all subjects, often referred to as the primary resonant frequency of the seated body. The identified range of primary resonant frequencies is somewhat higher than 5 Hz, which has been widely reported [12,28,32,37]. The difference in the primary

resonance frequency is mainly due to relatively low excitation magnitude applied in this study, and partly to the differences in the sitting posture; the back being supported on an inclined backrest as opposed to a straight back without backrest support. A higher primary resonant frequency of occupants seated against an inclined backrest has also been observed in another study involving automotive seat postures and lower excitation magnitude [40].

The dispersion in the measured data is widely believed to be caused by variations in the body masses [36,38,40], while little is known on the nature of the dependence. The measured data is thus analyzed to study the correlation between the APMS magnitude and the body mass as a function of the excitation frequency. Figure 3.2 presents the results obtained from the regression analysis between the measured APMS magnitude at selected frequencies (3, 6 and 12 Hz), which represent the frequencies below, close to and above the primary resonance, and the body mass corresponding to specific sitting postures considered, The results suggest linear dependence of the APMS magnitude on the body mass at the selected frequencies, irrespective of the postural configuration considered. The results show higher linear correlation (R^2 >0.9) at 3 Hz, reasonably good correlation around the primary resonance (R^2 > 0.8), and relatively poor correlation (R^2 < 0.6) at frequency beyond the resonance. The results suggest that the APMS magnitude above 12 Hz is less sensitive to body mass variations. The results attained for other excitation and seat heights also revealed similar tendencies. The regression analysis also reveals the fact that the apparent mass measurement has the advantage of indicating subject weight at low frequencies when the human body acts similar to a rigid mass [28,67].

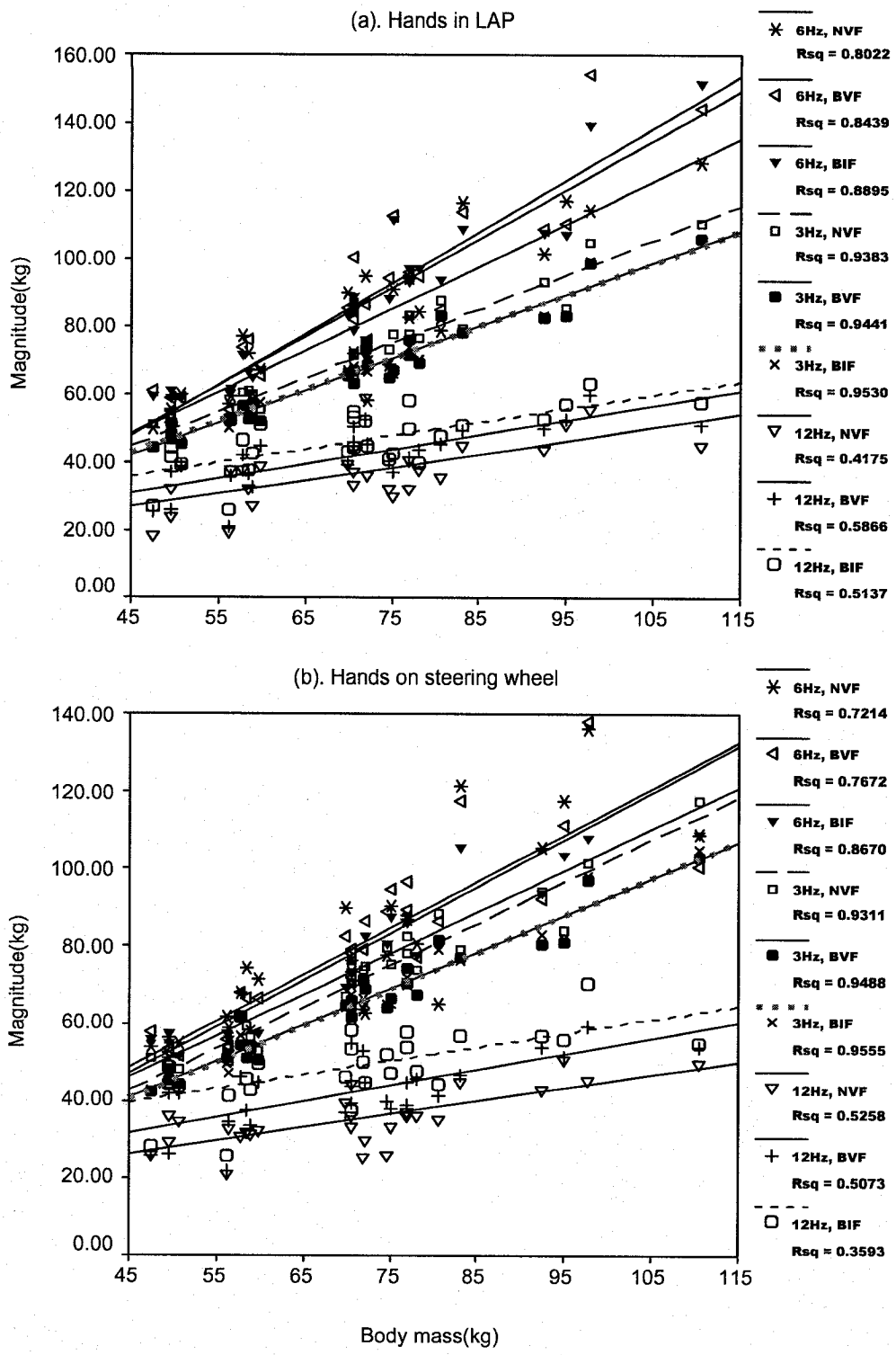

Figure 3.2: Dependence of APMS magnitude responses on body mass at selected frequencies and under different sitting postures (seat height: 460mm; excitation: 1.0 m/s^2 rms).

The variations in the APMS responses of different subjects could thus be attributed to differences in body masses and the sitting posture. The current ISO 5982 standard presents the mean DPMI and APMS responses for three groups of seated occupants with different mean masses, namely 55 kg, 75 kg and 90 kg. These values have been established on the basis of a proposed seated human occupant model [8,12]. A study of the biodynamic responses of 24 subjects assuming automotive seating postures and exposed to vertical vibration demonstrated the body mass effect by grouping the measured data in different mass ranges, such as below 60 kg, 60.5 to 70 kg, 70.5 to 80 kg, and above 80 kg [40]. This grouping method can also be found in the study by Seidel [30]. Such an approach would permit the study of other contributing factors for a sample of subjects within a narrow mass range, while the number of datasets would be considerably small. The grouping of the data performed in this study resulted in a total of 10, 4, 7 and 6 subjects in the mass range below 60 kg, 60.5 to 70.5 kg, 71 to 80 kg and above 80 kg, with mean body masses being 54.5, 70.4, 75.1 and 93.2 kg, respectively. Figure 3.3 shows the mean APMS magnitude responses of subjects within four mass groups assuming different seat-dependent postures at seat height H2, while exposed to 1 m/s^2 rms broad band random excitation. The results show considerable variability in the mean apparent mass responses, starting in the neighborhood of primary resonant frequency up to 20 Hz. Considering only small variations in the body mass within each group, the results suggest the influence of postural variations on the apparent mass response, which primarily occurs within this frequency range. The results attained under other excitations and seat heights also confirmed the same trends.

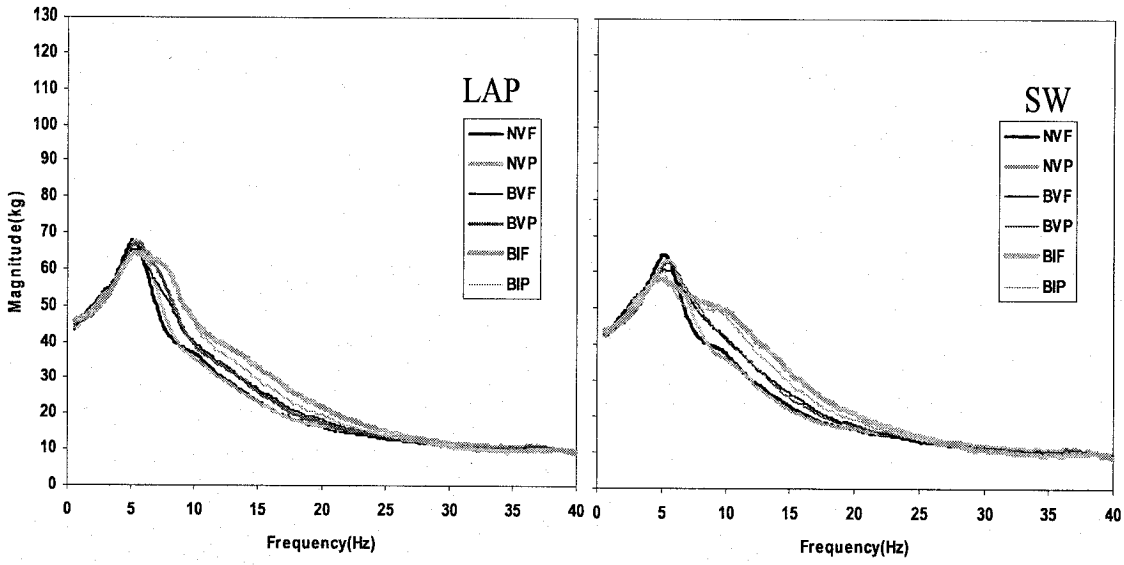

(a)

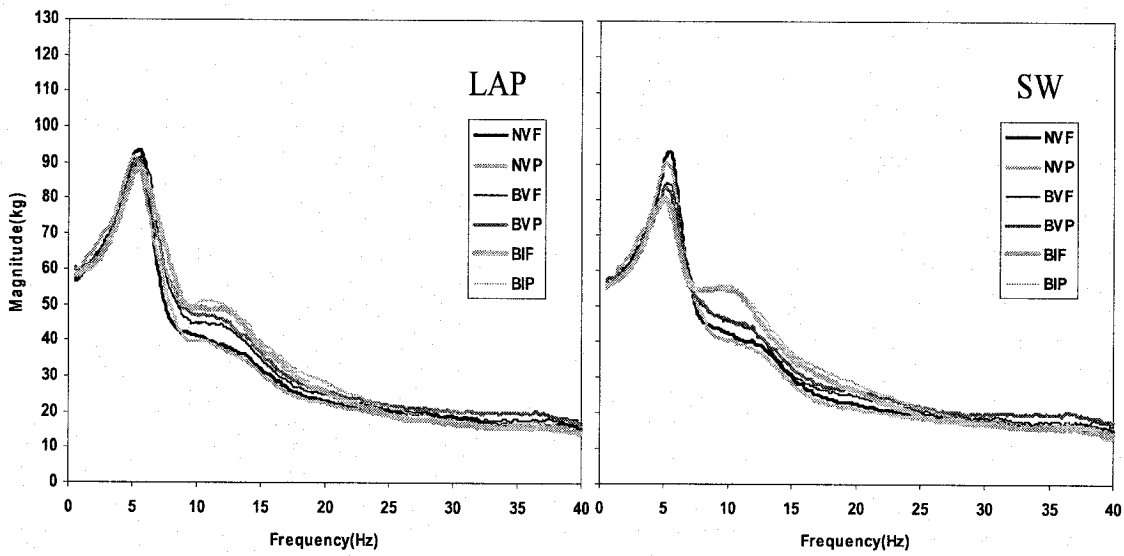

(b)

Figure 3.3: Mean APMS magnitude responses of subjects in four different mass groups corresponding to different sitting postures, (a) below 60kg; (b) 60.5-70.5kg (Continued).

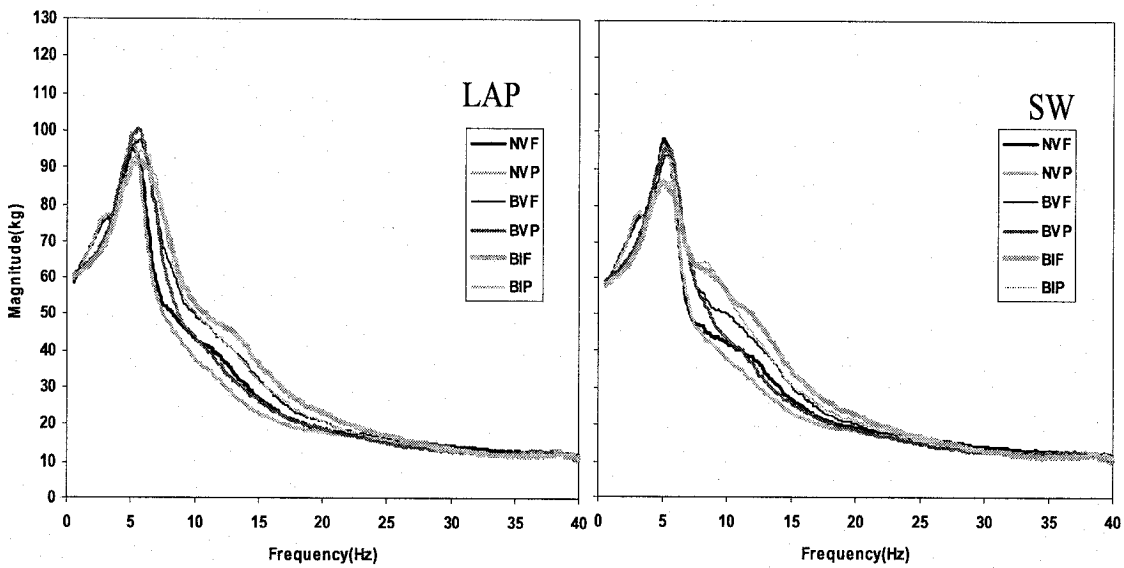

(c)

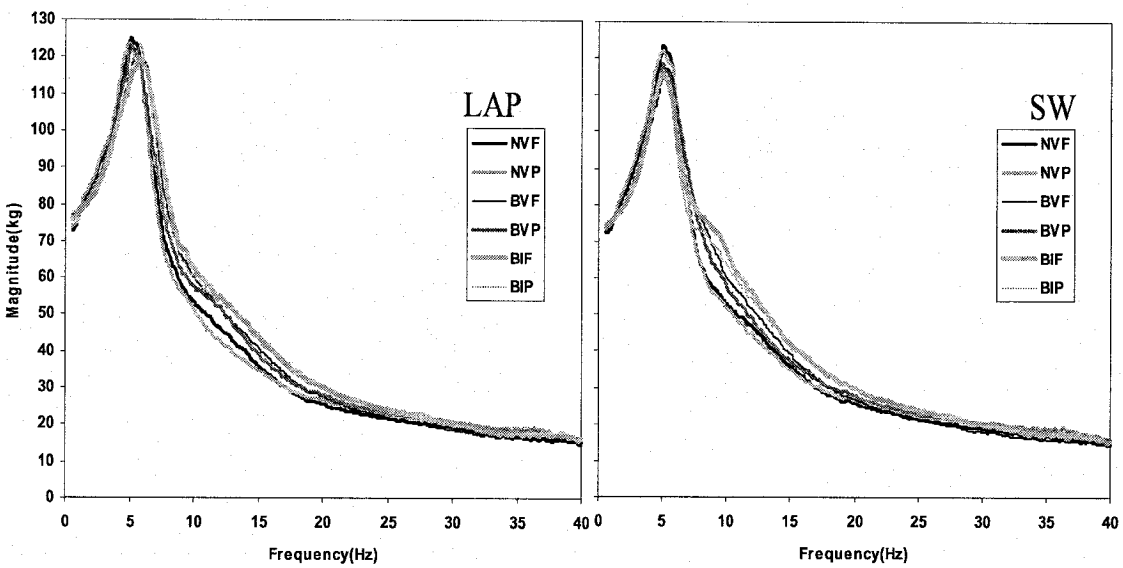

(d)

Figure 3.3: Mean APMS magnitude responses of subjects in four different mass groups corresponding to different sitting postures, (c) 71-80kg; (d) above 80kg (seat height: 460mm; excitation: 1.0 m/s^2 rms).

Alternatively, normalized biodynamic response data has been considered to greatly reduce the body mass dependent variability between subjects [28,38]. The measured data for each subject corresponding to each posture were normalized with respect to the respective static mass supported by the seat. Figure 3.4 illustrates, as an example, normalized APMS of subjects within four different mass groups assuming BIF postures with hands in lap and on the steering wheel, and seat height H2, while exposed to 1 m/s^2 rms excitation. The results show that a considerable scatter among the four groups still exists after normalization, and suggest that the normalization alone could not eliminate the strong effects of the body mass.

3.2.2 Variations in static APMS with postural differences

Due to the differences in anthropometric characteristics of the subjects, considerable variability of APMS between subjects could be accounted for by the different static masses supported by the platform, which is considered to correspond to the measured value of APMS at 0.5 Hz. This static value of the mass for specific subject and sitting posture agreed very well with the static force imposed on the seat, measured before and after each test. The variations in the static mass are evaluated in terms of the percent of body weight supported by the seat pan for all 27 subjects as a function of the sitting posture using mean values and standard deviations of the mean static forces measured before and after each test. The results, summarized in Table 3.1 for subjects with all the postural configurations constitute the basis for the subsequent dynamic APMS analysis. The results suggest that the body mass supported by the seat increases with increasing seat height, while the higher seat height yields larger variations in the

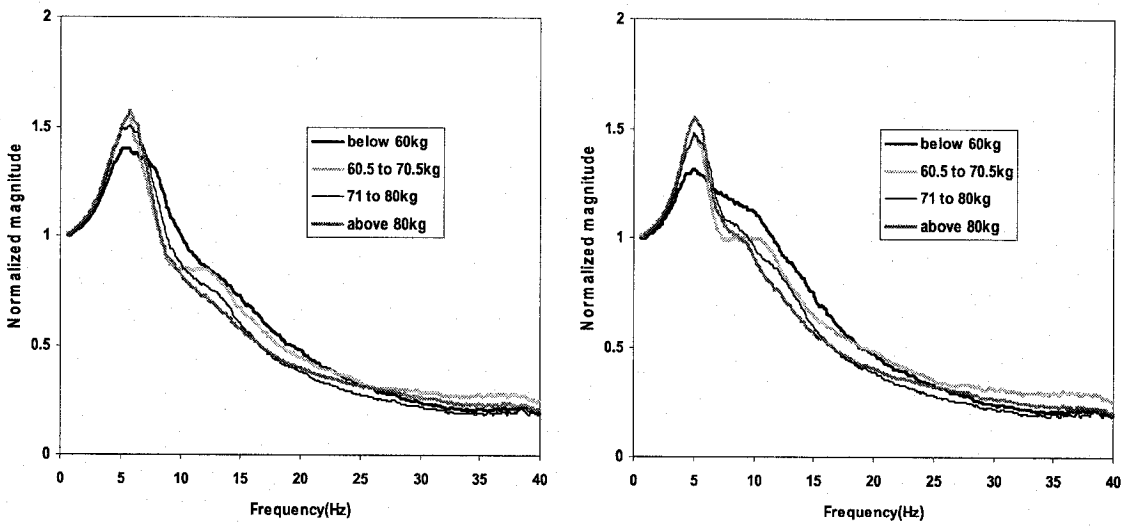

Figure 3.4: Mean normalized APMS magnitude responses of four mass group subjects corresponding to sitting posture BIF (seat height: 460mm; excitation: 1.0 m/s^2 rms) (a) hands in LAP; (b) hands on SW.

seated mass for all postures as observed from the standard deviations. For the higher seat height, considerable variations may be further caused by differences in individual subjects' heights, which may result in partial feet support or partial thigh contact etc.. The results also show that the body mass supported by the seat is lowest for no back support postures and highest for the inclined back support postures.

Table 3.1: Mean and standard deviation of the percent of body weight supported by the seat under different seated postures.

Hand position	LAP			SW		
Seat-dependent posture (defined in Figure 2.6)	Seat Height					
	H1	H2	H3	H1	H2	H3
NVF	84.8 ± 6.4	79.5 ± 5.4	73.4 ± 4.1	83.4 ± 7.8	78.1 ± 4.5	73.0 ± 3.3
BVF	85.7 ± 5.7	81.6 ± 4.0	77.2 ± 2.9	83.5 ± 5.1	79.3 ± 4.1	75.2 ± 2.6
BIF	88.7 ± 5.5	82.6 ± 4.1	77.1 ± 3.0	85.1 ± 5.8	79.8 ± 4.0	74.3 ± 2.6
NVP		80.7 ± 4.5			78.1 ± 4.1	
BVP		82.2 ± 4.0			79.7 ± 3.5	
BIP		82.8 ± 4.1			79.1 ± 3.9	

3.2.3 Influence of pan angle on APMS

The seats employed in automobiles and commercial vehicles exhibit considerable variations in the inclination of their pan. The measured data acquired for 0° and 7.5° inclinations are analyzed to study the influence of seat pan angle on the biodynamic response. The results presented in Table 3.1 reveal very little difference in the static APMS observed between the postures involving inclined and flat pans, such as NVF vs. NVP, BVF vs. BVP and BIF vs. BIP (measured only for seat height H2). Figure 3.5 illustrates a comparison of mean APMS magnitude responses of 27 subjects obtained for different postures involving flat and inclined pans of medium seat height (H2: 460 mm) and exposure to 1.0 m/s^2 rms. the results show negligible effect of the seat pan variations considered in this study, irrespective of the hands position and the seat-dependent posture.

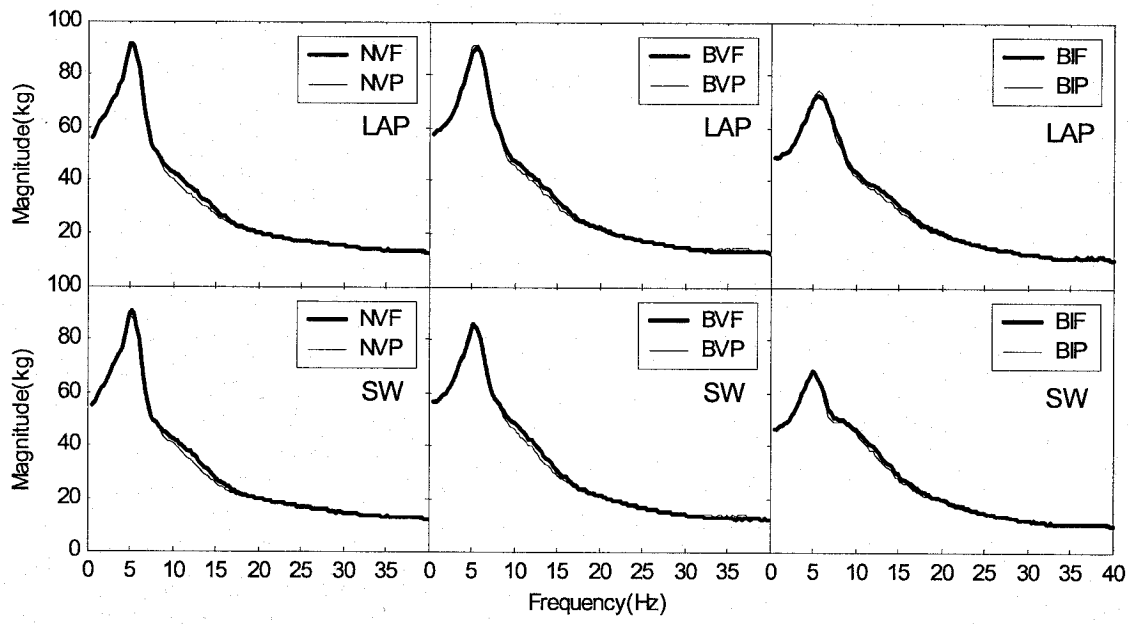

Figure 3.5: Effect of seat pan inclination on the mean APMS magnitude response of 27 subjects for different postures (height: 460mm; excitation: 1.0 m/s^2 rms).

In view of the above results, the seat-dependent postural variations can be reduced from six to three for the subsequent analysis. These include the variations in the backrest inclination or support condition, such as NVF, BVF and BIF. Considering the two hands position, a total of six sitting postures are considered for a given seat height in the subsequent analysis.

3.2.4 Statistical analysis method

Since the strong influence of body mass on force-motion biodynamic function has been recognized, as discussed in previous section, the analysis of covariance (ANCOVA), a combination of regression analysis with an analysis of variance, is used when a response variable y, in addition to being affected by the treatments, is also linearly related to another variable x [84]. The use of the analysis of covariance design was prompted by a desire to sharpen the analysis by reducing within-treatment variability. The use of ANCOVA with the body mass as covariant could thus permit the analysis of influences of contributing factors other than the body mass, such as hands position, back support condition and seat height.

ANCOVA performed in this study, considered the individual subject's responses at selected discrete frequencies over the frequency range 0.5-40 Hz. The significance values of main and interaction effects of postural variable were extracted from the corresponding analysis. Pairwise comparison procedures followed with ANCOVA analysis were further conducted to check the effects of each two postural variations with other factors fixed.

3.2.5 Influence of the back support condition and hands position on APMS

As shown in Table 3.1, the body mass supported by the seat with hands on steering wheel is lower than that with the hands in lap postures, irrespective of the seat height. The percent body mass supported by the seat pan for the posture involving a vertical backrest is higher than that for no back support, but lower than that for the inclined backrest support for all three seat heights. Figure 3.6 shows a comparison of mean magnitude responses of 27 subjects obtained for six different postures involving a flat pan. The mean magnitude responses attained for no back support (NVF), and support against a vertical (BVF) and an inclined backrest (BIF) are compared for two different hands position in Figure 3.6 (a). The effect of hands position on the mean magnitude response for each back support condition is further shown in Figure 3.6 (b).

The results show that the hands position becomes relevant only for postures involving back support conditions. The APMS response of subjects seated without back support exhibits relatively sharp resonant response for both hands positions. Under the hands in lap position, the bandwidth of the peak response increases when the back is supported. This bandwidth increases further when the back is supported by an inclined backrest (BIF). The response under sitting postures with back supported and hands on the SW shows an increase in the system damping associated with the first mode alone, which tends to be more significant for the inclined back support. Back supported on an inclined backrest coupled with hands on SW yields a more pronounced secondary mode near 10 Hz. This secondary mode has also been observed in a reported study [40]. The effect of hands position on the magnitude response, however, is not evident at frequencies above 12 Hz.

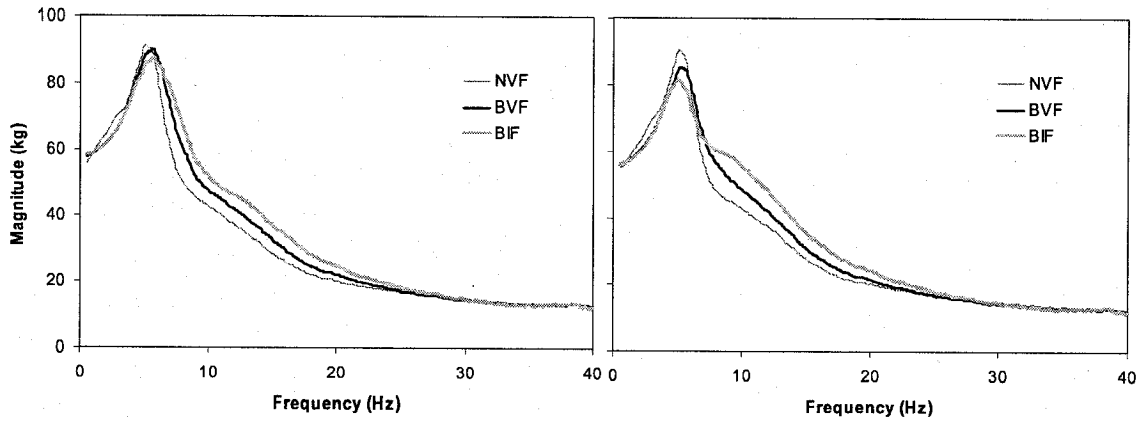

(a) Hands positions

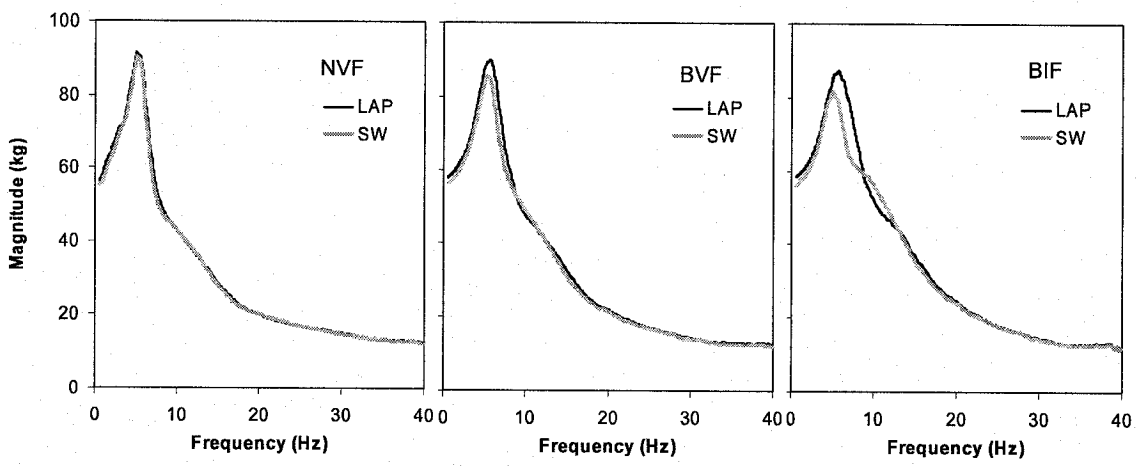

(b) Back support condition

Figure 3.6: Influence of hands position and back support condition on the mean APMS magnitude response of 27 subjects (seat height: 460mm; excitation: 1.0 m/s^2 rms.)

Two factors ANCOVA followed by multiple comparisons were performed to analyze the statistical significance of the influence of hands position and back support conditions over the measured frequency range. Tables 3.2, 3.3 and 3.4 provide the

detailed results on the influence of hands position and back support condition on the mean APMS responses.

The results attained from the pairwise comparison of hands position (LAP vs SW), summarized in Table 3.2, show that the frequency range of significant p value with respect to three postures is more or less consistent irrespective of the seat height. The mean APMS response would be relatively insensitive to the hands position when seated without backrest support ($p > 0.05$), as it is also evident from Figure 3.5 (b). The hands position is observed to be significant around primary resonance ($p < 0.005$) in the 5.125 to 7 Hz frequency range, when seated with vertical back support (BVF). For the inclined backrest (BIF), the hands position is strongly significant at the primary resonance around 6 Hz ($p < 0.0001$), and somewhat significant around the second resonant mode near 10 Hz ($p < 0.05$).

For the comparison between vertical back support (BVF) and unsupported back (NVF), the results presented in Table 3.3 indicate that significant differences in the mean APMS response start to occur at relatively lower frequencies for the hands in lap position (LAP) than for the hands on the steering wheel (SW) position, namely 6 Hz for LAP position, and 6.875 Hz for SW position. The range of significance in both cases ends at a frequency more or less close to 18 Hz. The results shown in Table 3.4 for the comparison between the inclined back support (BIF) and vertical back support (BVF) also indicate a similar trend, although the frequency effect is relatively smaller.

It may be concluded that the hands position influences the APMS response only when the back is supported on an inclined backrest and at frequencies within the primary

Table 3.2: p values derived from pairwise comparison of LAP vs SW, extracted from two-way ANCOVA with respect to three seat heights.

Frequency (Hz)	H1			H2			H3		
	BIF	BVF	NVF	BIF	BVF	NVF	BIF	BVF	NVF
1	+	-	-	-	-	-	-	-	-
3, 4, 5	-	-	-	-	-	-	-	-	-
5.125	-	+	-	-	-	-	++	-	-
5.375	+	+	-	-	-	-	+	+	-
5.625	++	++	-	+	-	-	++	+	-
5.75	+++	++	-	++	+	-	+++	+	-
5.875	+++	++	-	++	+	-	+++	++	-
6	+++	++	-	+++	+	-	+++	++	-
6.125	+++	++	-	+++	+	-	+++	+	-
6.375	+++	++	-	+++	++	-	+++	+	-
6.875	+++	+	-	+++	+	-	+++	+	-
7	+++	+	-	+++	+	-	+++	-	-
7.375	+++	-	-	+++	+	-	++	-	-
7.875	+	-	-	++	-	-	-	-	-
8	-	-	-	+	-	-	-	-	-
9	-	-	-	-	-	-	-	-	-
10	+	-	-	+	-	-	++	-	-
11	+	-	-	+	-	-	+	-	-
12,15,20,40	-	-	-	-	-	-	-	-	-

$p>0.05$ -; $p<0.05$ +; $p<0.005$ ++; $p<0.0001$ +++

Table 3.3: p values from pairwise comparison of BVF vs NVF, extracted from two-way ANCOVA with respect to three seat heights.

Frequency (Hz)	LAP			SW		
	H1	H2	H3	H1	H2	H3
1	-	-	-	-	-	-
2	-	-	+	-	-	-
3	-	-	-	++	+	+
4.625	-	-	-	+	-	-
4.875,5,5.125,	-	-	-	+	+	+
5.375	-	-	-	-	-	+
5.875	+	-	-	-	-	-
6	+	+	+	-	-	-
6.125	++	+	+	-	-	-
6.375	++	++	+	-	-	-
6.875	+++	+++	++	+	+	-
7.375	+++	+++	+	+	+	+
7.875	++	+++	++	+	+++	++
8	++	+++	+	++	++	++
9	++	++	+	+++	++	+++
10, 11	+	+	+	+++	++	+++
12, 15	+	+	+	++	+	+
16, 17	+	+	+	+	-	+
18	+	-	+	-	-	-
20	-	-	+	-	-	-
22, 40	-	-	-	-	-	-

$p>0.05$ -; $p<0.05$ +; $p<0.005$ ++; $p<0.0001$ +++

Table 3.4: p values derived from pairwise comparison of BIF vs. BVF extracted from two-way ANCOVA (Hands by Seat) under three seat heights.

Frequency (Hz)	LAP			SW		
	H1	H2	H3	H1	H2	H3
1-5	-	-	-	-	-	-
5.625	-	-	-	-	+	+
5.75	-	-	-	-	-	+
5.875	-	-	-	-	+	+
6, 6.125	-	-	-	-	-	+
7	+	-	-	-	-	-
7.375	+	+	-	-	-	-
7.875, 8	+++	++	-	+	-	-
9	+++	+	-	+++	++	+
10	+++	+	+	+++	+++	+++
11	+++	+	+	+++	+++	++
12, 13	++	+	+	+++	++	++
14, 15	++	+	+	++	+	++
16	++	++	+	++	++	++
17, 18	++	++	+	++	++	+
20	+	+	+	+	+	-
22	-	+	-	-	+	-
32, 40	-	-	-	-	-	-

$p>0.05$ -; $p<0.05$ +; $p<0.005$ ++; $p<0.0001$ +++

resonant frequency range. Furthermore, the influence of back support, irrespective of hands position, is significant generally after the primary resonance to 18 Hz. The apparent mass magnitudes tend to increase with the back support within this frequency range.

3.2.6 Influence of seat height on APMS

The seated height affects the sitting posture and the portion of the body weight supported by the seat. As shown in Table 3.1, a higher seat height leads to higher percent of body mass supported by the seat, irrespective of the sitting posture and hands position. Figure 3.7 illustrates a comparison of the mean APMS magnitude responses of 27 subjects measured on seats with three different heights considered in the study. The

results are presented for three different seat-design postures and two hands positions. For a given posture, the effect of seat height on the primary resonant frequency is observed to be minimal. The peak magnitude response, however, tends to be slightly higher under a higher seat height, which may be attributed to the increased body mass supported by a higher seat. A lower seat height generally yields lower magnitude response over most of the frequency range.

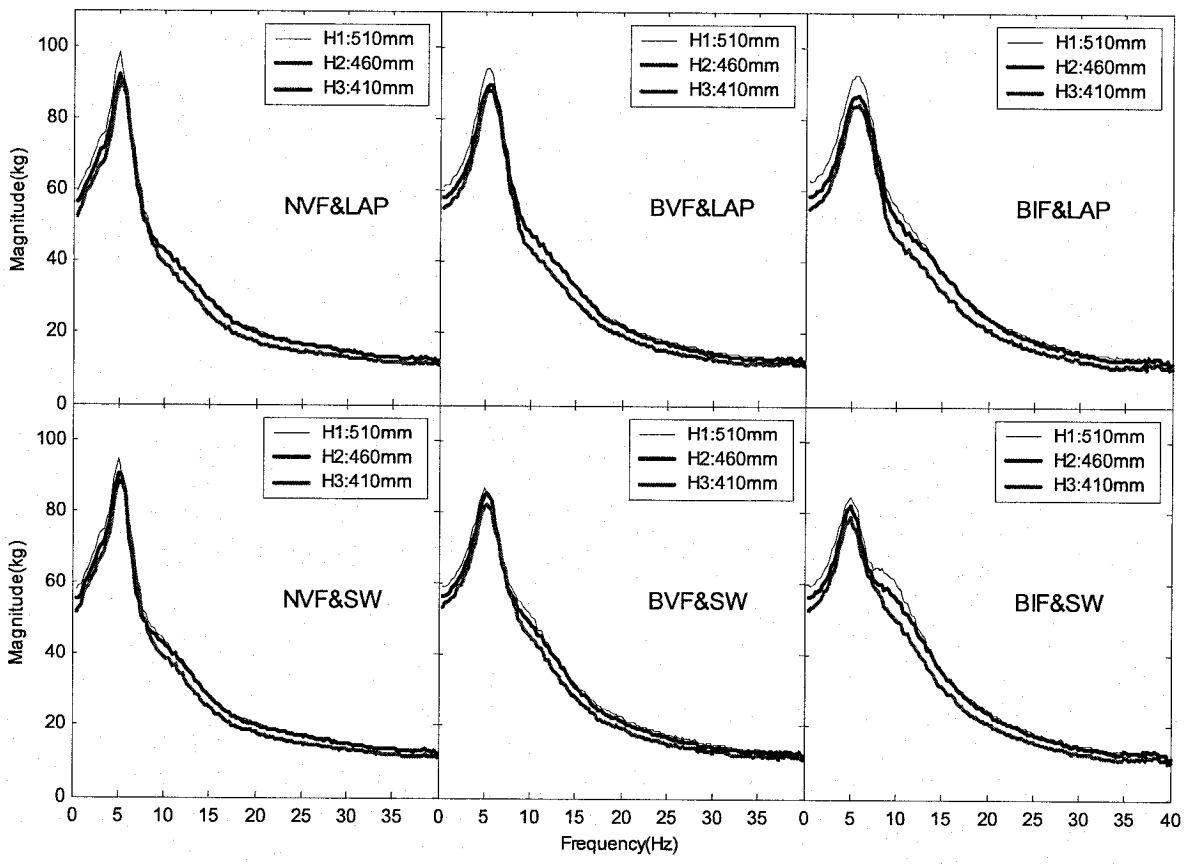

Figure 3.7: Effect of seat height on the mean APMS magnitude response of 27 subjects for different postures (excitation: 1.0 m/s^2 rms).

Table 3.5 shows the results of one-way ANCOVA with the body mass as the covariate. Further multiple comparisons between three seat height levels reveal that a significant difference ($p < 0.005$) of magnitude response can be found between the H1 and H3 in most of the frequency range except in the narrow frequency range just after the peak response under all six postures. However the pairwise comparisons of H1 vs H2, H2 vs H3 did not show a significant difference within the frequency range considered. Referring to Table 3.1, it can be seen that the body mass supported by the seat on the average increases by approximately 5% when seat height is increased from H3 to H2 or from H2 to H1 for all postures considered. The corresponding increase when the seat height increases from H3 to H1 is of the order of 10%. These results suggest that a 100 mm difference in the seat height would result in around 10% difference in body mass supported by the seat, and thus affect the APMS magnitude response significantly, while a difference of 50 mm or less may have negligible effect.

The results shown in Table 3.5 also show that the level of significance arising from the seat height for the inclined backrest support posture (BIF) is higher than that for other postures. This is attributable to relatively larger difference of body mass supported by the seat under an inclined backrest posture when compared with no back or vertical back support postures, as evident from Table 3.1.

3.2.7 Peak response variations on APMS

The measured data are further analyzed to identify the influences of postural variations on the peak APMS responses and the primary resonance. A strong linear correlation ($R^2 > 0.8$), between the peak apparent mass magnitude and the body mass

Table 3.5: p value obtained from three seat height dependency test (ANCOVA) subject to six postures.

Frequency (Hz)	NVF		BVF		BIF	
	LAP	SW	LAP	SW	LAP	SW
1,2,3	+++	+++	+++	+++	+++	+++
4	++	+	+++	++	+++	+++
4.375	+	+	+++	+	+++	++
4.625,4.875	+	+	++	+	+++	+++
5	+	+	++	+	+++	++
5.125	+	+	++	-	+++	+++
5.375	-	-	+	-	+++	++
5.625	-	-	-	-	+++	++
5.75	-	-	-	-	++	++
5.875,6,6.125	-	-	-	-	++	+
6.375	-	-	-	-	+	-
6.875,7,7.375	-	-	-	-	-	-
7.875	-	-	-	-	-	+
8	-	-	-	-	-	++
9	+	-	+	+	+++	+++
10	+	+	++	++	+++	+++
11	+	-	++	+	+++	+++
12,13	+	-	+	+	+++	+++
14,15,16	+	+	+	+	+++	+++
17	++	+	+	+	+++	+++
18	++	+	++	++	+++	+++
20	++	++	++	++	+++	+++
22	+	+	++	++	+	++
25	+	+	+	+	+	++
32	+	+	++	+	+	+
40	-	+	-	-	+	-

$p>0.05$ -; $p<0.05$ +; $p<0.005$ ++; $p<0.0001$ +++

under different postures is clearly evident in Figure 3.8, irrespective of the postural factors considered (hands position, back support condition and seat height). Such a correlation between the body mass and the primary resonant frequency, however, was not observed. Furthermore, the regression results suggest that the rate of change of peak APMS magnitude with body mass tends to vary with the sitting postures; the larger variations occur under higher seat and hands on steering wheel posture.

Three factors analysis of covariance and variance were performed to analyze the effects of sitting posture on the peak magnitude and primary resonance, respectively. The results presented in Table 3.6 indicate that the main effect of seat height ($p < 0.0001$) on

peak magnitude is quite strong, while the influence on primary resonance is not significant ($p > 0.05$). The strong effect of seat height on peak APMS magnitude can also be observed from Figure 3.8, where a relatively higher linear correlation ($R^2 > 0.9$) was revealed under the lower seat height H3 compared with the other seat heights.

Since the significant interaction ($p < 0.005$) between two hands position and three back support conditions were obtained from the analysis (Table 3.7), the multiple comparisons with Sidak adjustment followed by three factor analysis are employed to reveal the effects of two hands position and three back support condition on the peak

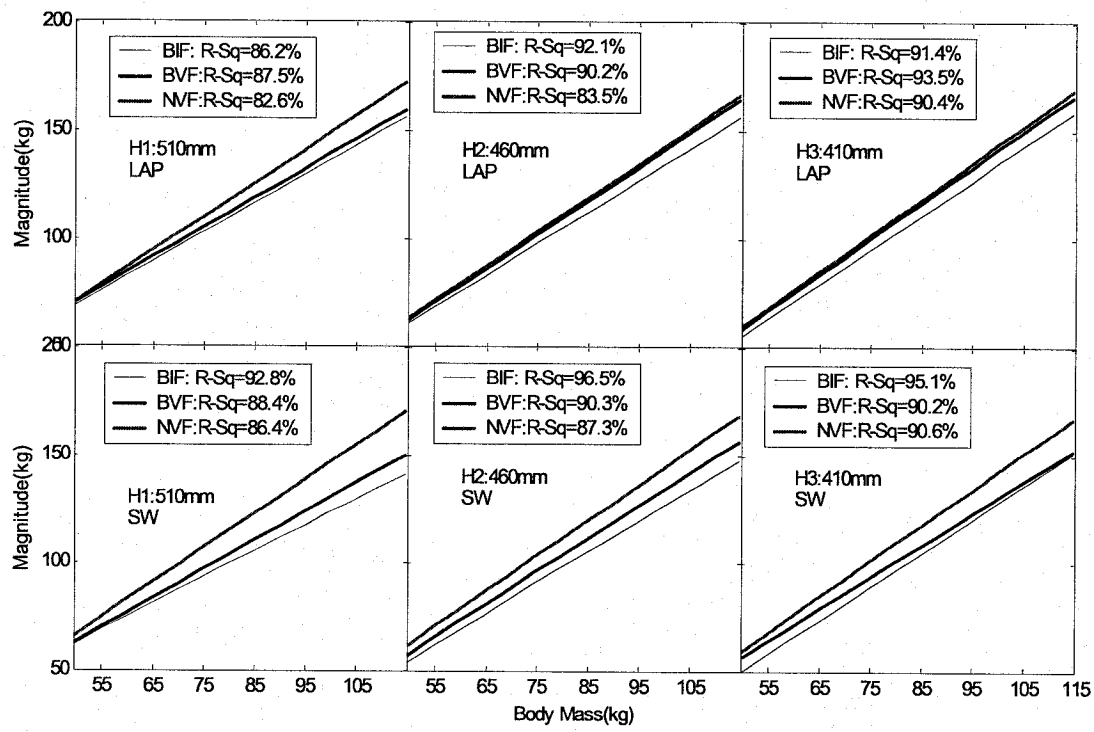

Figure 3.8: Dependence of peak APMS magnitude on the body mass under different sitting postures.

Table 3.6: p values obtained from three factor statistical analysis, HP=hands position (LAP, SW); B=back support conditions (BIF, BVF, NVF), SH= seat height (H1,H2,H3).

	HP	B	SH	HP*B	HP*SH	B*SH	HP*B *SH
Peak magnitude	*0.000*	*0.000*	*0.000*	*0.004*	0.267	0.789	1.000
Primary resonance	*0.003*	*0.027*	0.312	*0.000*	0.965	0.364	0.973

Table 3.7: p values obtained from pairwise comparison of two hands position corresponding to different seat heights and back support conditions.

	H1			H2			H3		
	BIF	BVF	NVF	BIF	BVF	NVF	BIF	BVF	NVF
Peak magnitude	*0.000*	*0.000*	0.122	*0.004*	*0.012*	0.699	*0.004*	*0.015*	0.772
Primary Resonance	*0.010*	0.656	0.923	*0.002*	0.981	0.555	*0.001*	0.791	0.782

Table 3.8: p values obtained from peak magnitude pairwise comparisons corresponding to different seat heights and hands positions.

	H1		H2		H3	
	LAP	SW	LAP	SW	LAP	SW
BIF vs. BVF	0.866	0.526	0.360	0.177	0.215	0.076
BVF vs. NVF	0.208	*0.001*	0.852	*0.013*	0.839	*0.012*

magnitude and primary resonance responses. The results (Table 3.8) show that the effect of hands position on peak APMS is consistent for all postures in view of the peak magnitude as well as the primary resonance. Under no back support condition, no difference could be found between two hands position, while a significant difference exists between the two hands position for both the peak magnitude ($p < 0.005$), and the primary resonance ($p < 0.05$) under an inclined back support. The posture involving vertical back support revealed significant difference ($p < 0.05$) between the two hands position for peak magnitude, while the difference for primary resonance was

insignificant. The results from the pairwise comparison presented in Table 3.8 also show that back support condition is consistent for hands in the lap position. No significant difference could be observed when the seated occupants altered their sitting posture from no back support to vertical back support, or from vertical back support to inclined back support. A significant difference between the no back and vertical back support, however, was evident for all three seat height levels ($p < 0.005$), when the hands are placed on the steering wheel.

Considering that the primary resonance is not greatly influenced by the seat height, the resonant frequency is further characterized using descriptive statistics (mean values and their standard deviations) and analysis of variance for the six sitting postures. As shown in Figure 3.9, hands in lap posture coupled with inclined backrest support yields primary resonance, which is 0.6 Hz larger than that attained with hands on the SW. This value is significant ($p < 0.0001$). This difference was not observed for the vertical back support and no back support. For the hands in lap position, the BIF posture yields primary resonance that is 0.4 Hz higher than that with the BVF posture, while the primary resonance of the BVF posture is approximately 0.13 Hz higher than the NVF posture. With the hands on steering wheel, no significant difference of primary resonance could be observed for the BVF vs NVF, or BVF vs NVF postures.

It may be concluded that the peak APMS magnitude is strongly affected by the hands position and seat height, while the primary resonance is affected only by the hands position. The main effect of back support condition for either peak magnitude or primary resonance is relatively smaller.

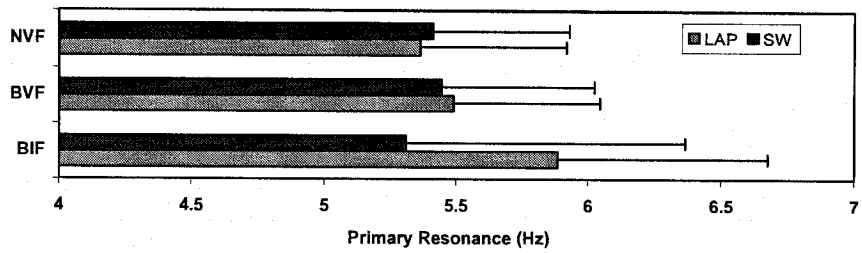

Figure 3.9: Mean and standard deviations of the primary resonant frequency under six different sitting postures.

3.2.8 Effect of gender on APMS

In this study, the influence of gender on the APMS response is investigated through analysis of selected data pertaining to male and female subjects with similar mean body mass in an attempt to reduce the contributions due to differences in body masses. The APMS data attained for a total of 10 subjects, including 5 male (mean body mass = 71.4 ± 7.4kg) and 5 female (mean body mass = 71.7 ± 3.0kg), were thus selected from the ensemble of 27 subjects. Figure 3.10 illustrates comparisons of mean APMS magnitude responses of the selected male and female subjects for different postures. The results show the presence of a more clear second resonance in the frequency range above 15 Hz, and higher APMS magnitude response at higher frequencies for the female subjects. An ANCOVA analysis of 27 subjects on the gender dependency also revealed that gender effect could be observed only in the frequency range above 15 Hz for all postures ($p < 0.05$).

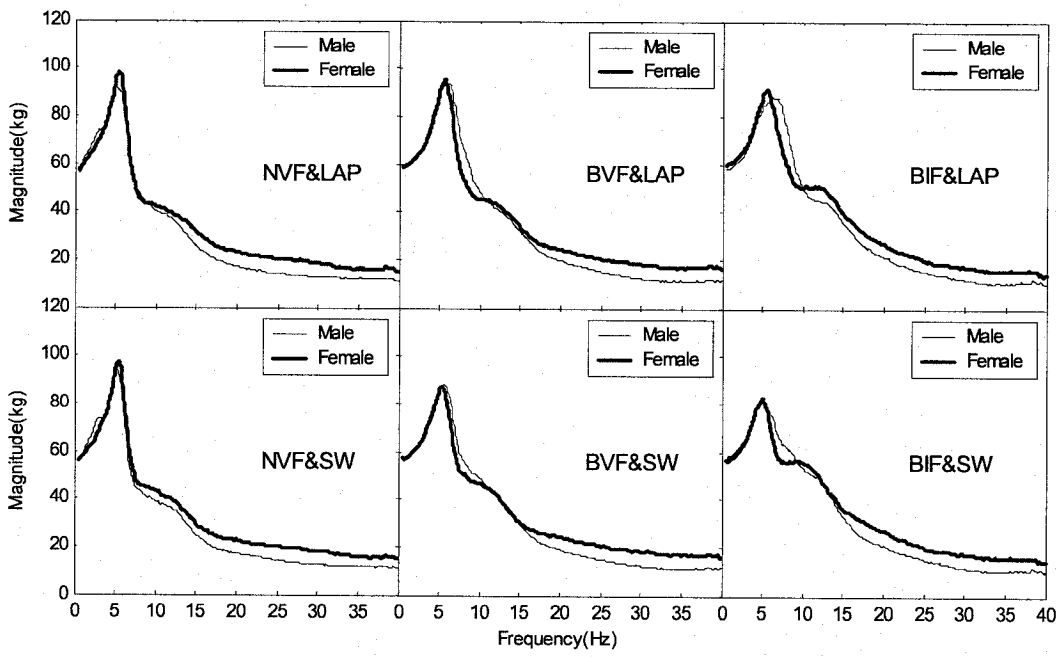

Figure 3.10: Influence of gender (5 male, 5 female) on the mean APMS magnitude response (seat height: 460mm; excitation: 1.0 m/s^2 rms)

3.2.9 Effect of magnitude of vertical vibration excitation on APMS

Most studies have concluded that the APMS response depends upon the vibration magnitude, and a "softening' of the body with increasing excitation magnitude [34,36,41,43-45]. The effect of magnitude of excitation on the biodynamic responses of occupants seated assuming a typical automotive posture was observed to be slightly more important for the passenger posture (hands in lap) than for the driving posture (hands on steering wheel) [48]. The comparisons of mean magnitude response of 27 subjects exposed to two different magnitudes of vibration excitation, employed in this study, corresponding to six seat dependent postures shows that hands in lap postures are relatively more sensitive to vibration excitation magnitude (Figure 3.11). The APMS

magnitudes in general tend to decrease with an increase in excitation magnitude. The body "softening" effect tends to be more apparent under no back support posture, irrespective of the hands position. In this particular case, the results shown in Figure 3.12 indicate that the primary resonance reduces by 0.5-0.6 Hz with increasing excitation magnitude from 0.5 to 1.0 m/s^2 rms, which is found to be significant ($p < 0.005$). The corresponding reductions in primary resonance under vertical back and inclined back support postures were found to be in the order of 0.3 Hz ($p < 0.05$) and less than 0.2 Hz ($p > 0.05$).

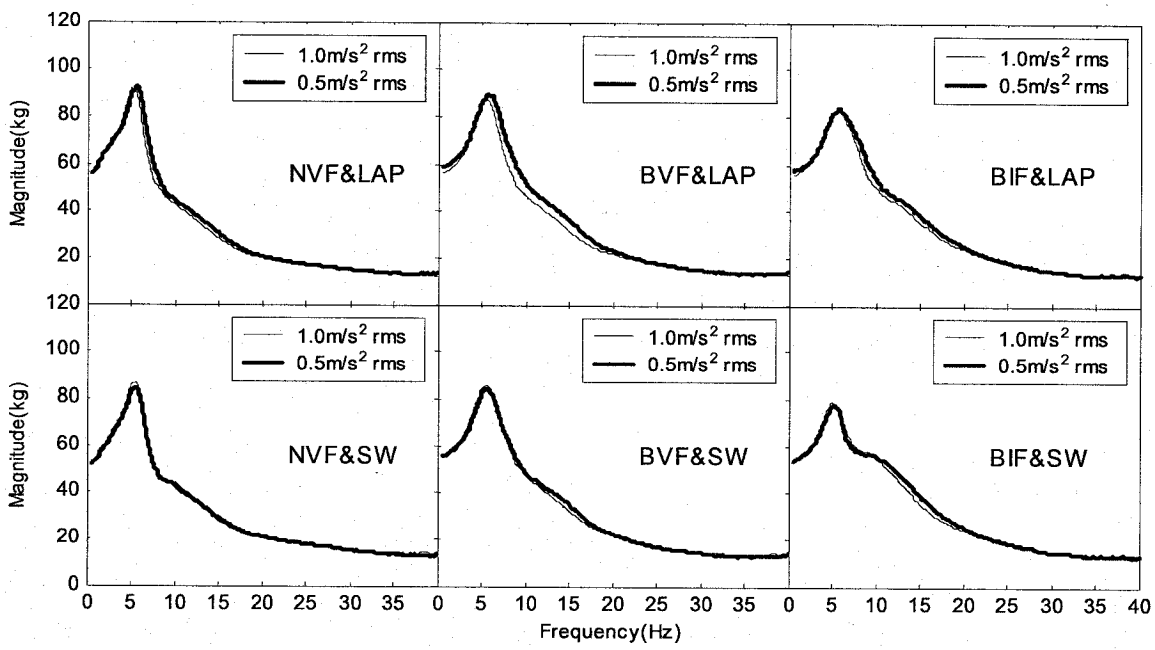

Figure 3.11: Influence of excitation magnitude on the mean APMS magnitude response (seat height: 460mm).

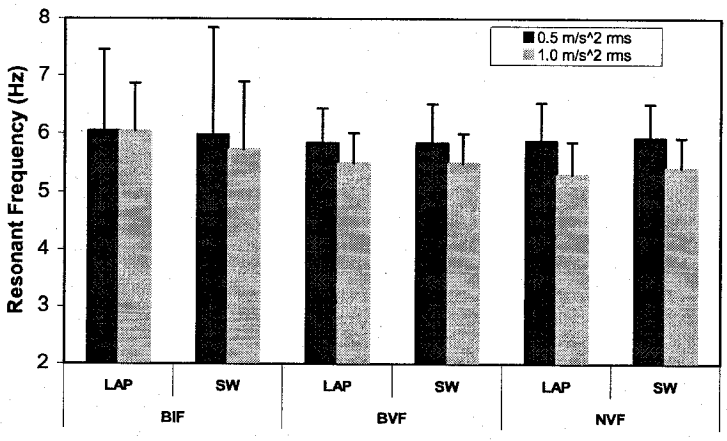

Figure 3.12: Influence of excitation magnitude on primary resonance for different postures (seat height: 460mm).

3.3 The role of seat geometry and posture on the absorbed power properties

The measured data are further analyzed to compute the biodynamic responses using the methodology described in section 2.4. The absorbed power characteristics are thoroughly evaluated to study the influence of seat geometry and postures.

3.3.1 Absorbed power response characteristics

Figure 3.13 illustrates, as an example, the variations in the absorbed power computed from the measured force-motion responses of 27 subjects seated on the medium height seat (H2), with flat pan and back supported on the inclined backrest (BIF) under two different hands positions (LAP and SW), while exposed to 1.0 m/s^2 rms vertical white-noise excitation. The results derived in the third-octave frequency bands show considerable scatter in the computed absorbed power over most of the frequency range, specifically in the 4-16 Hz frequency bands. Despite the significant variations in

the data acquired for different subjects, the maximum amount of energy absorption occurs in the frequency bands centered around 5 to 16 Hz bands for both hands positions.

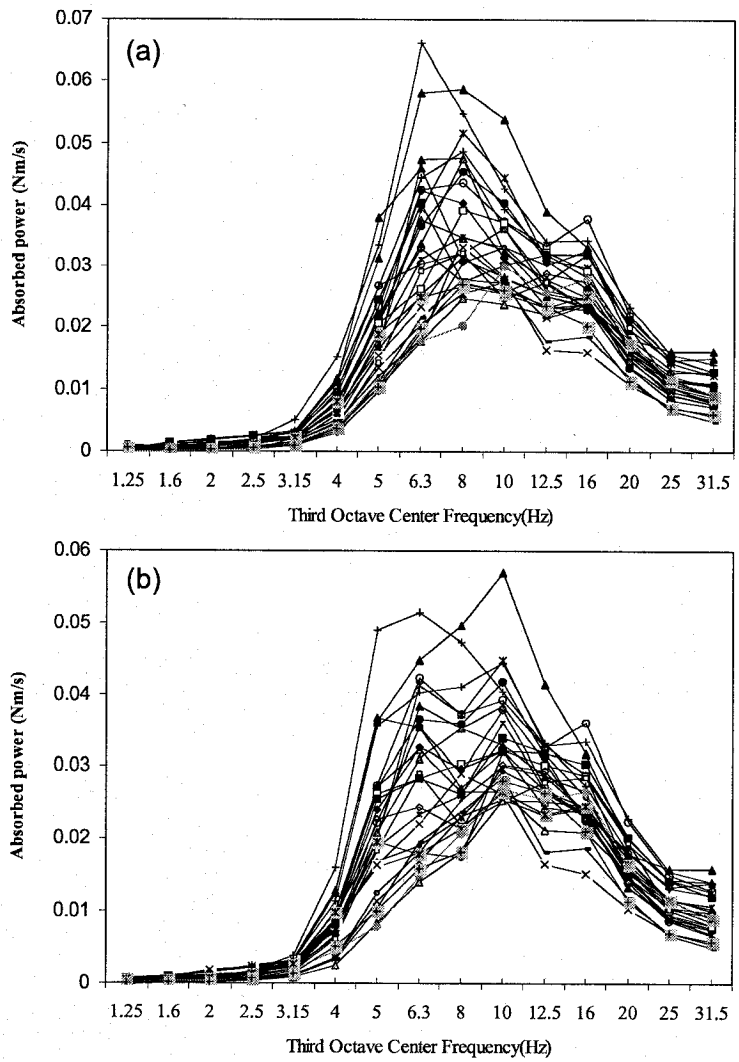

Figure 3.13: Comparison of absorbed power responses of 27 subjects (a) hands in lap; and (b) hands on steering wheel (BIF posture; seat height: 460mm; excitation: 1.0 m/s^2 rms).

The frequency corresponding to peak response, however, is higher for the hands on steering wheel posture, as has also been observed in the previous APMS responses. The scatter in the absorbed power data appears to be more than that observed in the APMS

responses reported in many studies [36,46,48]. Moreover, the frequencies corresponding to the peak power responses are also slightly higher than those corresponding to the peak APMS responses. Similar scatter of absorbed power were also observed from the data attained for different sitting posture and seat height combinations. The total amount of vibration energy absorption in the 4-16 Hz frequency bands, derived from the summation of the energy in the individual bands, was observed to be in the order of 80 % of the total energy absorption measured over the entire frequency range (0.5-40 Hz) for all the sitting posture and seat height combinations considered.

The dispersion in the data presented for a particular seat height and posture (Figure 3.13) is believed to be caused by variations in the individual anthropometric variables, particularly the body mass. The strong effect of body mass on the APMS magnitude has been widely reported [36,48],while a few studies have also shown the effect on the absorbed power [43,44]. Apart from the body mass, variations in seat geometry, seat height and sitting postures strongly affect the energy dissipation properties of the vibration exposed body, while little is known on the nature of the dependence of the absorbed power on these factors. The acquired data is thus analyzed to study the correlations between the absorbed power and factors related to anthropometry and sitting posture as a function of the excitation frequency.

3.3.2 Absorbed power vs. excitation magnitude

Theoretically, the energy absorption depends upon the input auto-spectral density, as defined for the indirect method in Equation (2.23). The reported studies [43,44] consistently concluded that the total absorbed power increased approximately in

proportion to the square of the excitation magnitude. The results shown in Figure 2.11 for a single subject also reveal that the peak absorbed power density is linearly dependent upon the square of the excitation level. The results also exhibit that the peak absorbed power density occurs in the 5-5.875 Hz range. The frequency corresponding to the peak response tends to decrease with increasing vibration magnitude, suggesting a softening trend that has been widely observed from the APMS responses [36]. The APMS responses of the seated body under vertical vibration, however, show relatively small effect of vibration magnitude, and thus do not provide information relevant to severity of the vibration exposure.

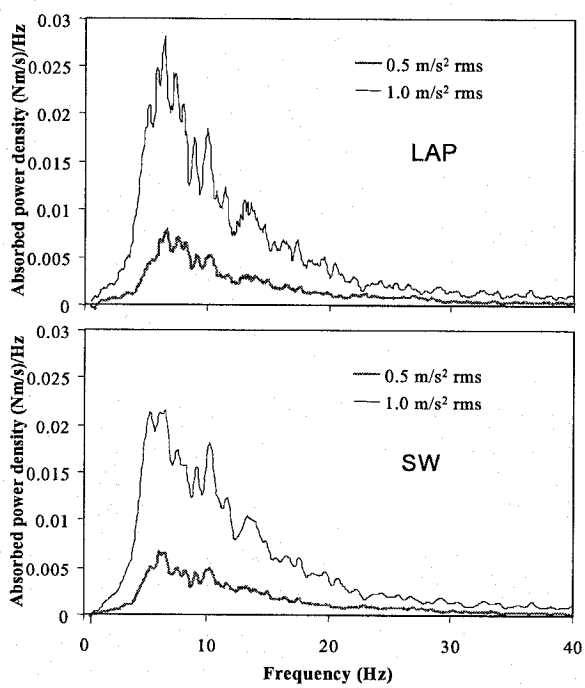

Figure 3.14: Comparisons of mean absorbed power responses of 27 subjects under different excitation levels (BIF posture; seat height: 460mm).

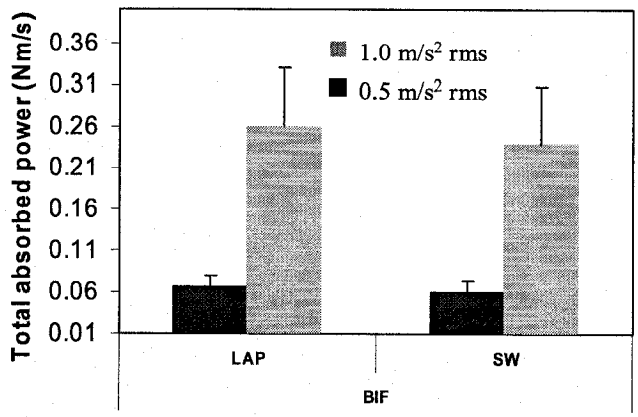

Figure 3.15: Comparisons of mean total absorbed power of 27 subjects under different excitation levels (BIF posture; seat height: 460mm).

The strong effect of vibration magnitude on the mean absorbed power is further shown in Figure 3.14. The Figure illustrates comparisons of the mean absorbed power density responses of 27 subjects attained under 0.5 and 1.0 m/s^2 excitations, while seated on the medium-height (H2) seat assuming BIF posture with two different hands positions. The mean magnitudes of the absorbed power density are significantly smaller than those obtained for the single subject (Figure 2.13) under the same levels of rms accelerations. It should be noted that the results presented in Figure 3.14 correspond to 0.5 and 1.0 m/s^2 rms accelerations based upon white noise random excitations in the 0.5 to 40 Hz band, while those presented in Figure 2.11 correspond to excitations in the 0.5-20 Hz band. The effective overall rms accelerations of excitations with flat power spectral density in the 0.5 to 40 Hz range is approximately one-half of that in the 0.5 to 20 Hz range. Consequently, the power density magnitudes of the single subject data are almost 4 times those of mean responses for a given level of rms acceleration. The mean total absorbed power is further computed for both excitation levels and same postures, and compared in Figure 3.15. Comparisons suggest that the total absorbed power under 1.0 m/s^2 rms

excitation is approximately 4 times that attained under 0.5 m/s^2 rms excitation within the frequency range considered, irrespective of the hands position. The results clearly show that the peak absorbed power density and total energy absorption of seated human body increases nearly quadratically with the exposure level, while hands on steering wheel posture (SW) yields slightly lower power absorption.

3.3.3 Absorbed power and anthropometry

The computed data are analyzed to study the influence of some of the anthropometry related parameters, such as body mass, body mass index, standing height and body fat percentage, on the total absorbed power. The total absorbed power in the entire frequency range is evaluated under different sitting postures through summation of energy values within individual one-third octave bands, having center frequencies from 1.25 Hz to 31.5 Hz. The relationships between the total absorbed power and selected anthropometric variables were also explored through a series of linear regression analyses.

Table 3.9 shows the coefficients of determination (R-Squared values) obtained from single-factor regression analyses between the total absorbed power and the selected anthropometric variable, and the corresponding *p* values derived from the single-factor ANOVA. The results summarized in the table have been derived from the datasets obtained for the 12 sitting postures, medium seat height (H2: 460mm) and 1.0 m/s^2 rms acceleration excitation. The total absorbed power exhibits highest correlation with the body mass ($R^2>0.94$), irrespective of the sitting posture and hands position. While the correlation with the standing height is relatively poor ($0.32<R^2<0.43$), the subject height

was observed to be a significant factor (p<0.0001) in view of the total absorbed power. The correlation of the total absorbed power with the standard BMI, which represents the ratio of body mass to the square of the standing height, is observed to be excellent (R^2>0.84), irrespective of the sitting posture and hands positions (p<0.0001). Lowest correlation is observed with the body fat (0.18<R^2<0.26) with p<0.05. The datasets obtained for other seat height and excitation level combinations also revealed identical trends. The results in general revealed that the larger body mass and body mass index generally yields much greater total absorbed power. Higher standing body height and percentage of body fat also revealed relatively larger energy absorption within the seated human body. As an example, Figure 3.16 illustrates the strong linear dependence between the total absorbed power and the body mass, and the BMI, obtained for medium seat height (H2), two hands positions (LAP and SW) and BIF (inclined back support and flat pan) posture. The figure shows excellent correlation of the total power with both selected variables under both the applied excitation levels. The total absorbed power within the body increases linearly with the body mass as well as BMI for both the excitation levels.

Table 3.9: R-Square values (%) obtained from single regression analysis between total absorbed power (1.25-31.5Hz) and anthropometric variables, and corresponding p values (Seat height: 460mm; excitation 1.0 m/s^2 rms).

Anthropometric variables	Posture											
	LAP						SW					
	BIF	BIP	BVF	BVP	NVF	NVP	BIF	BIP	BVF	BVP	NVF	NVP
Body mass (kg)	94.5^a	97.4^a	96.1^a	97.4^a	93.8^a	96.1^a	95.7^a	97.6^a	95.7^a	96.9^a	96.0^a	97.4^a
Body mass index (kg/m^2)	84.6^a	92.1^a	85.7^a	91.5^a	86.0^a	93.1^a	85.5^a	91.2^a	84.7^a	90.5^a	86.7^a	92.9^a
Standing height (cm)	40.9^a	35.4^b	41.9^a	36.0^b	37.7^b	32.2^b	40.8^b	31.6^b	42.6^a	30.6^b	40.4^a	34.3^b
Body fat (%)	22.8^c	23.8^c	25.3^c	22.8^c	19.7^c	26.4^c	20.6^c	21.9^c	18.8^c	25.7^c	19.7^c	25.3^c

Note: Values are coefficient of determination with the unit %.
Superscript: a: p<0.0001; b: p<0.005; c: p<0.05;

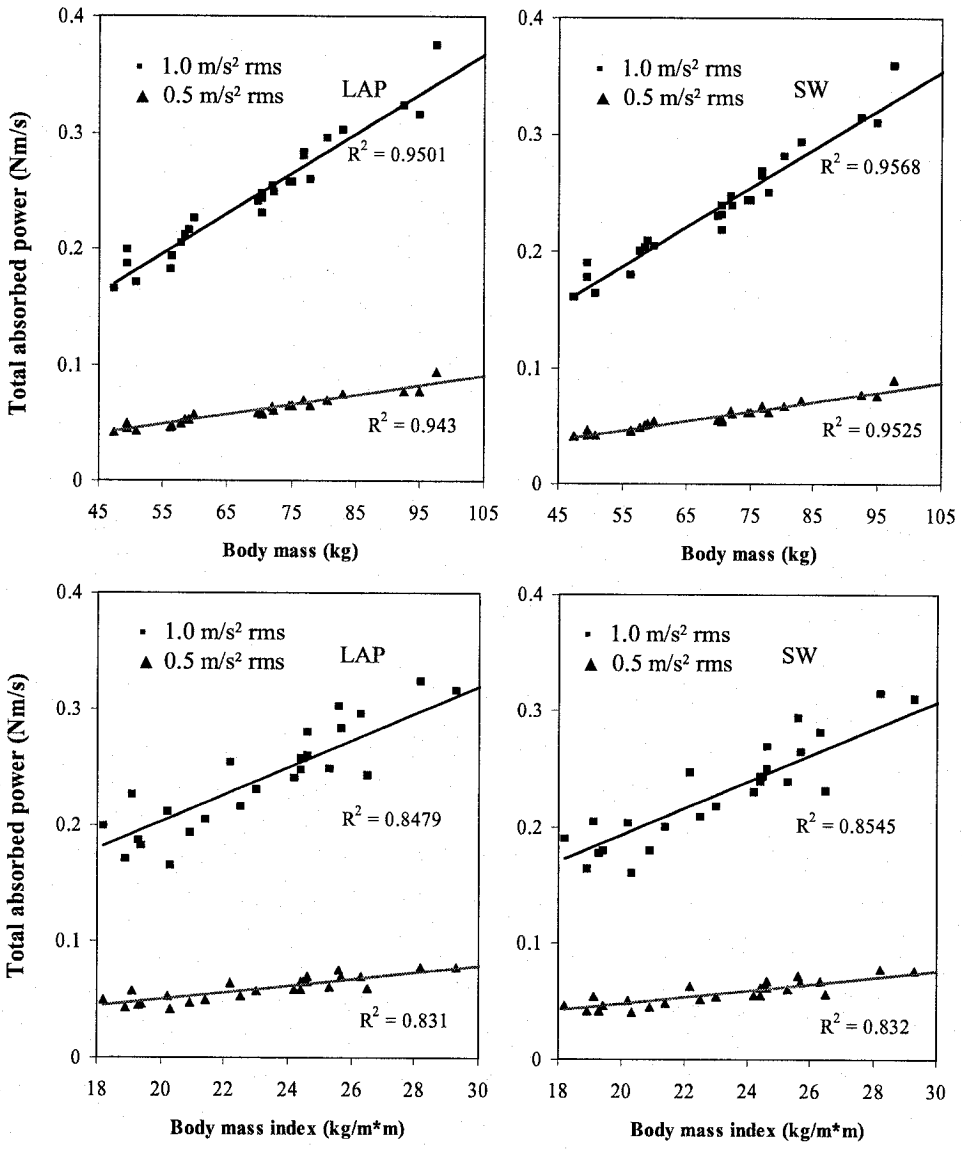

Figure 3.16: Linear dependence between total absorbed power in the frequency range considered and subjects' body mass and body mass index.

The rate of increase in total power with respect to body mass under the larger excitation (1.0 m/s^2 rms) is approximately four times that obtained under the lower excitation (0.5 m/s^2 rms), irrespective of the hands position. The ratio of rates of increase in power with the BMI under the two levels of excitation is also of the same order. The results further

show that energy absorption of seated human body is increasing quadratically with the exposure level. Owing to the strong dependence of the power with the exposure level, the absorbed power could serve as an effective measure of the vibration 'dosage'.

3.3.3 Absorbed power and sitting posture

The sitting posture assumed by a subject depends upon the seat geometry (inclinations of the pan and backrest), seat height, and back support condition, as described in section 2.2.4. The measured data are analyzed to assess the influence of sitting posture as determined by the seat geometry, height and hands position on the power absorption characteristics of the seated human body exposed to vertical vibration. Owing to the strong dependence of the absorbed power on the body mass and body mass index, the analyses are performed for a subset of datasets containing the data acquired for a smaller subject population of comparable body mass and BMI. For this purpose, the data acquired for a total of 10 subjects with body mass ranging from 70.5 to 78 kg (mean= 73.7 kg; standard deviation =2.96 kg) and BMI ranging from 22.2 to 25.7 kg/m^2, (mean= 24.5 kg/m^2; standard deviation=1.23 kg/m^2) are selected from the ensemble of 27 subjects in order to examine the influence of postural factors variations. The analyses based on this selected subset of data are expected to eliminate the strong inter-subject variability arising from variations in the anthropometric variables, such as the body mass and BMI. The effects of postural variations arising from the pan angle, seat height, backrest support condition and hands position are discussed below.

3.3.4 Influence of pan angle on absorbed power

The reported studies on biodynamic responses of seated human occupants exposed to vertical vibration, with only one exception, have considered seats with flat pans [36,43,46]. The influence of seat pan angle on absorbed power characteristics is evaluated through analyses of the data acquired for 0° and 7.5° inclinations of the seat pan. The results showed minimal influence of the pan angle on the spectral distribution of the absorbed power. Figure 3.17 illustrates comparisons of the mean total power responses attained for 10 subjects seated on the medium-height seat assuming different postures involving flat and inclined pans, namely NVF vs. NVP, BVF vs. BVP and BIF vs. BIP, and exposed to 1 m/s^2 excitation. The results show negligible effect of the seat pan variations considered in this study, irrespective of the hands position and the seat-dependent posture. The seat-dependent postural variations can thus be reduced from six to three for the subsequent analysis, as it was observed for the APMS analysis. These include the variations in the backrest inclination or support condition, such as NVF, BVF and BIF. Considering the two hands positions, a total of six sitting postures are considered for a given seat height.

3.3.6 Influence of hands position and seat geometry on absorbed power

Figure 3.18 shows comparisons of mean absorbed power responses in the third-octave frequency bands, derived from data acquired for 10 selected subjects assuming six different postures (NVF, BVF and BIF coupled with two hands positions) and exposed to 1 m/s^2 rms excitation. The mean responses attained for the two hands positions are presented in Figure 3.18 (a) for the no back support (NVF), and support against a vertical

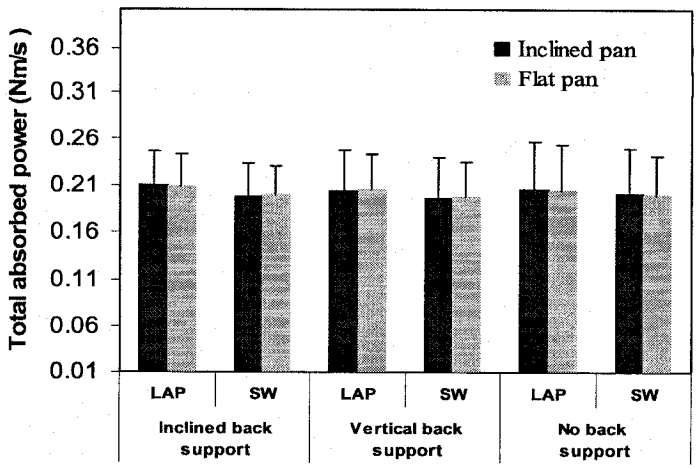

Figure 3.17: Effect of seat pan inclination on the mean absorbed power response of 10 subjects for different postures (seat height: 460mm; excitation: 1.0 m/s^2 rms).

(BVF) and an inclined backrest (BIF). The effect of hands position for each back support condition is further shown in Figure 3.18 (b). For the NVF and BVF postures, the peak energy absorption occurs in the 6.3 Hz frequency band, while that for the BIF posture it is shifted to the 8 Hz band. All the three postures coupled with hands on the steering wheel (SW) also yield a secondary peak in the 10 Hz band, while the response for the NVF posture exhibits rapid decline in magnitude in frequency bands following the frequency band of peak response (6.3 Hz). Irrespective of the hands positions, the unsupported back posture (NVF) results in higher energy absorption in the lower frequency bands prior to the resonance (considered to be the center frequency of the band corresponding to peak magnitude), while less energy absorption occurs for the inclined backrest posture (BIF). However, the seated body tends to absorb more energy with the inclined backrest in the frequency bands beyond the resonant frequency, which is attributed to the presence of the secondary resonance around 10 Hz. The results also show that the hands position becomes relevant in the frequency bands close to the resonance, irrespective of the back

support condition; the hands in lap postures (LAP) cause higher energy absorption in the vicinity of the resonant frequency.

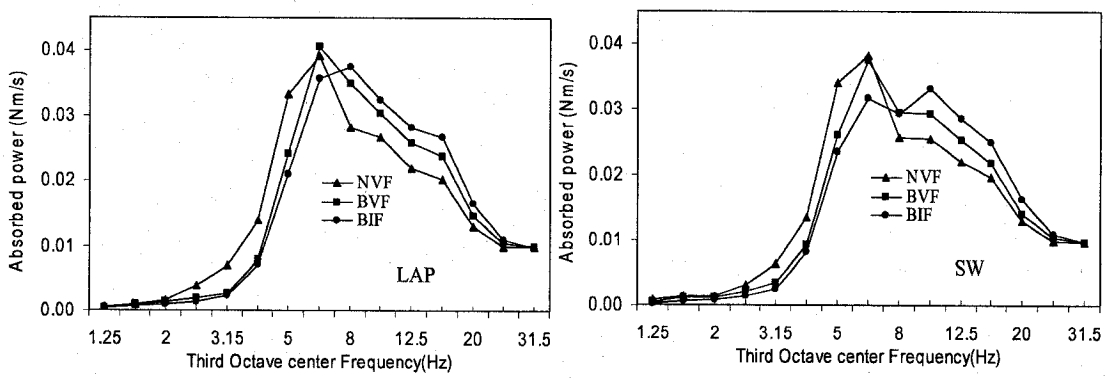

(a) Back support condition

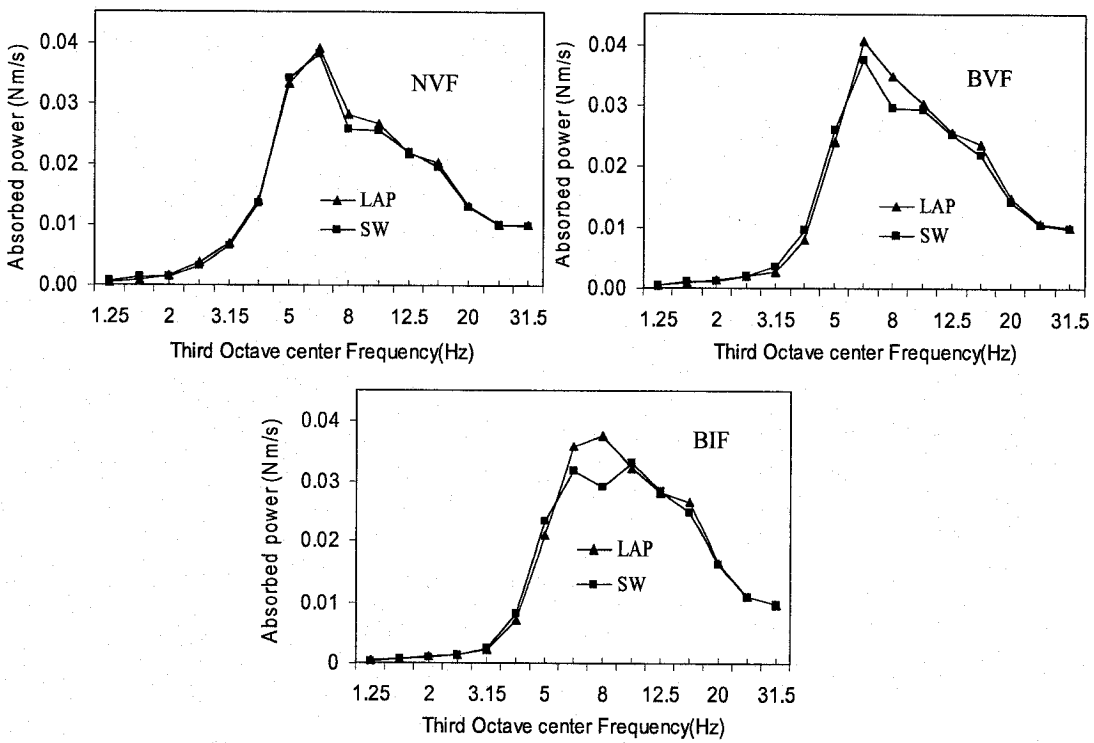

(b) Hands position

Figure 3.18: Influence of back support condition and hands position on mean absorbed power responses of 10 subjects (seat height: 460mm; excitation: 1.0 m/s^2 rms).

To further examine the influence of hands position and back support condition, the total absorbed power responses derived for the 10 selected subjects are synthesized. Figure 3.19 illustrates the mean and standard deviation of the total absorbed power quantity under six postures. The results further show that hands in lap postures yield higher power absorption within the body, irrespective of back support condition. Meanwhile irrespective of the hands position, inclined backrest support tends to absorb less energy than the vertical back support condition, while no back support condition causes highest energy absorption. It may thus be concluded that the inclined back support condition with hands on steering wheel would cause the least amount of energy absorption within the body, despite the presence of the secondary resonant peak.

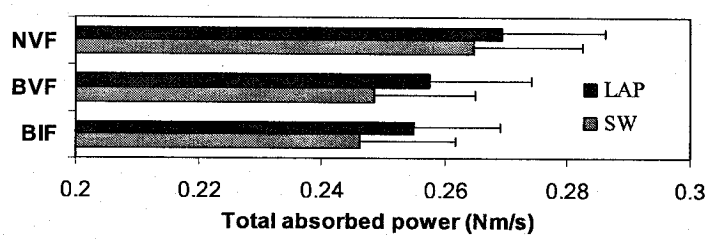

Figure 3.19: Mean and standard deviations of the total absorbed power computed for the 10 subjects under six different sitting postures.

3.3.7 Influence of seat height on absorbed power

The seated height affects the sitting posture and the proportion of the body weight supported by the seat. A higher seat leads to a higher percentage of body mass supported by the seat pan (Table 3.1). Figure 3.20 illustrates comparisons of the mean absorbed power responses of the 10 subjects in the third-octave frequency bands, synthesized from the data acquired for three different heights considered in the study. Similar to APMS

magnitude responses (Figure 3.7), the effect of postural variation arising from seat height is more notable for inclined backrest support (BIF) than for other postures. The BIF posture thus reveals relatively larger differences in absorbed power under three seat heights, especially around the resonant frequencies. Figure 3.21 further illustrates the effect of seat height on the mean total power absorbed by the body under six different sitting postures. The results show that the total absorbed power under BIF posture with hands in lap tends to be higher than those attained for BVF and NVF postures.

3.3.8 Peak absorbed power response variations

The computed data are further analyzed to identify the influences of postural variations on the peak absorbed power response. A strong linear correlation ($R^2 > 0.74$), between the peak absorbed power magnitude and the body mass under different postures is clearly evident in Figure 3.22 (a), irrespective of the postural factors considered (hands position, back support condition and seat height), meanwhile a strong linear correlation ($R^2 > 0.62$) between the peak absorbed power magnitude and the body mass index is also evident in Figure 3.22 (b). Furthermore, the regression results suggest that the rates of change of peak absorbed power with both body mass and body mass index tend to vary with the sitting postures. A larger variation occurs under hands on steering wheel posture, irrespective of the seat height and back support condition. It may thus be concluded that the peak-absorbed power is strongly affected by the hands position.

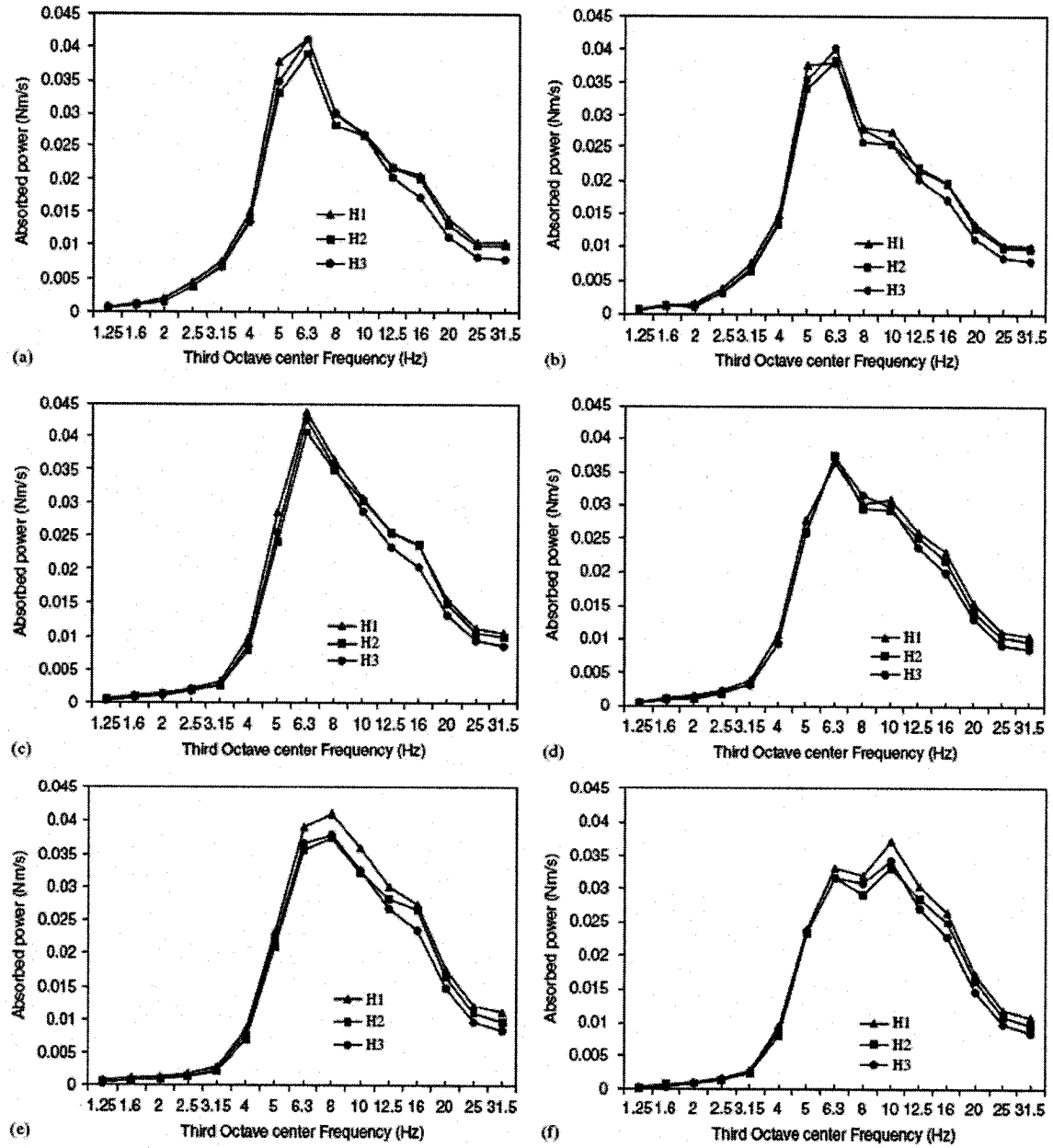

Figure 3.20: Effect of seat height on the mean absorbed power response of 10 subjects for different sitting postures (excitation: 1.0 m/s^2 rms). (a) NVF&LAP; (b) NVF&SW; (c) BVF&LAP; (d) BVF&SW; (e) BIF&LAP; (f) BIF&SW

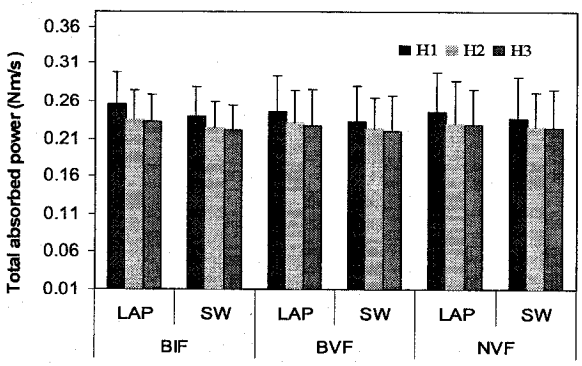

Figure 3.21: Effect of seat height on the mean total absorbed power response of 10 subjects for different sitting postures (excitation: 1.0 m/s^2 rms).

Table 3.10 summarizes the results attained from single linear regression between the peak absorbed power and selected anthropometry variables, body mass and body mass index. The results suggest that peak energy absorption rates with body mass (mW/kg) and body mass index ($mW/kg/m^2$) vary with the sitting posture and seat height. Results suggest that an inclined back support condition tends to reduce the peak energy absorption rate, irrespective of the hands positions, when compared to those for the NVF and BVF postures. Hands on SW posture cause less energy absorption rate at the primary resonance, irrespective of the seat height and back support condition. The NVF posture yields largest energy absorption rate near primary resonance, while the effect of hands position is very small. The results also show that back supported postures yield lower energy absorption rate with higher seat, while this trend is evident for the medium seat height for the NVF posture.

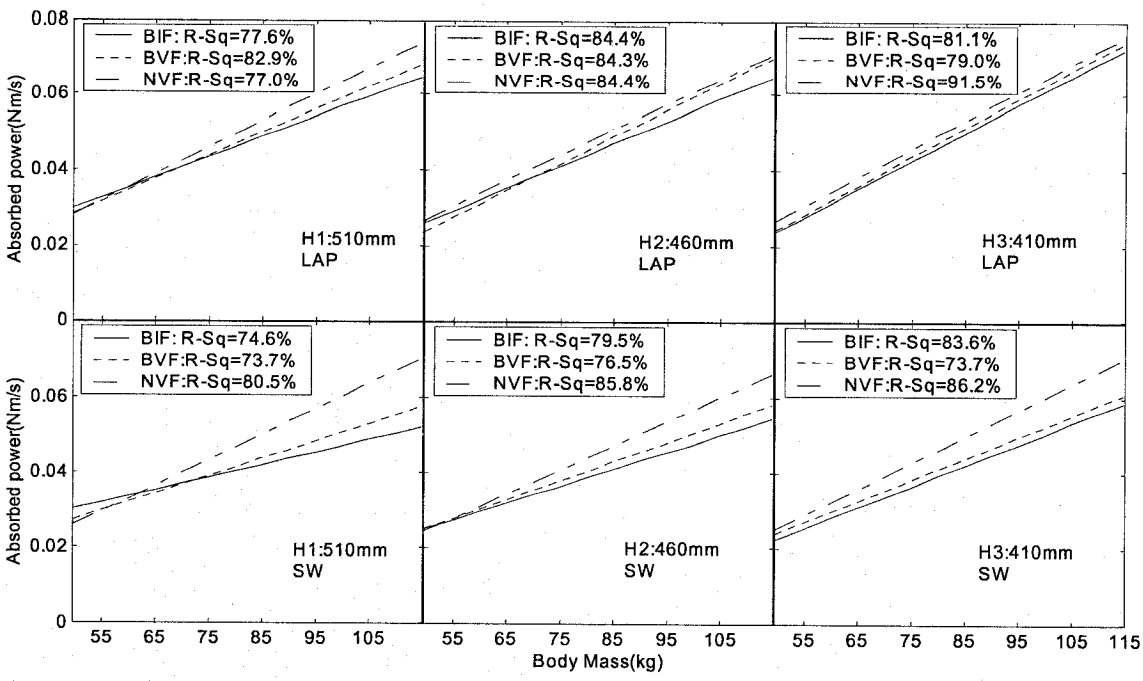

(a) Peak absorbed power vs. the body mass

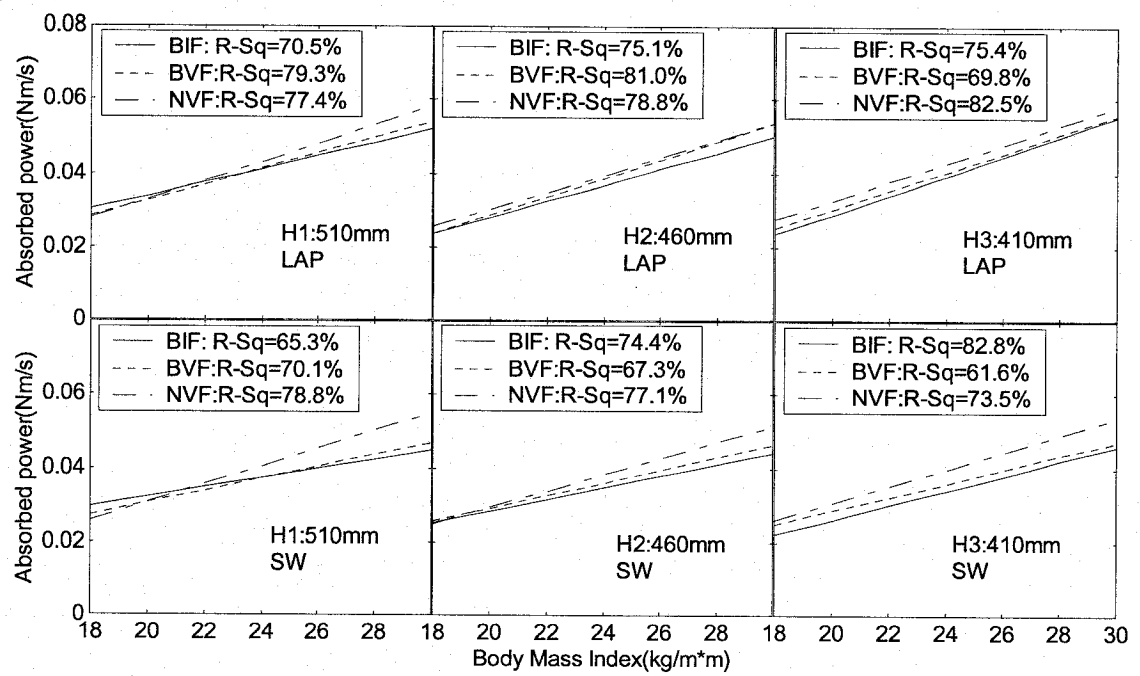

(b) Peak absorbed power vs. the body mass index

Figure 3.22: Dependence of peak absorbed power on body mass and body mass index under different sitting postures. (a) Peak absorbed power vs. body mass; (b) Peak absorbed power vs. body mass index.

Table 3.10: Energy absorption rate (mW/kg) obtained from single regression analysis between the absorbed power at the primary resonance and body mass under different postures. (Excitation: 1.0 m/s^2 rms).

Hand position	LAP			SW		
Sitting Posture	Seat Height					
	H1	H2	H3	H1	H2	H3
NVF	0.700	0.676	0.771	0.684	0.646	0.699
BVF	0.616	0.704	0.762	0.460	0.503	0.568
BIF	0.533	0.589	0.767	0.337	0.445	0.550

3.4 Discussions about absorbed power on whole body vibration

The concept of power absorbed by the human body when exposed to seat–transmitted vibration was first proposed in the mid-1960s by Lee and Pradko [85] in order to evaluate the health, safety and comfort of occupants of military vehicles. Since the 1970's, the absorbed power concept has been extensively applied to study the human hand-arm responses under hand-transmitted vibration arising from the operation of hand-held power tools [86-91]. The studies on hand-arm vibration in terms of absorbed power have established that the energy point of view encompasses a greater complexity of the biological effects of vibration than the measure of acceleration alone, as it can partly account for the influence of many potential stressors, such as grip and push forces, hand-arm posture and the magnitude of vibration [87]. Another study has established a strong correlation between the subjective annoyance data and energy absorbed into the hand-arm system under vibration [89]. Furthermore, an epidemiological study has shown that the prevalence of vibration induced white fingers is related to the amount of energy absorbed by the operators [90]. While the investigations on the hand-arm response to vibration have demonstrated the vibration energy absorbed in the hand and arm may offer a superior means of assessing the vibration-induced injuries and "Hand Arm Vibration

Syndrome" [90], only a few studies have explored the similar potential of energy absorption under WBV.

The human body, comprising a complex combination of visco-elastic properties of muscles, bones, joints etc., responds to whole-body vibration in a highly complex manner. The biological system consumes the vibratory energy by means of relative motions between the visco-elastic tissues, muscles and the skeletal system. Exposure to large motions occurring over a prolonged duration may cause physical damage or modification of the musculoskeletal system. The motion of the musculoskeletal system and the inherent damping behavior that results in energy absorption within the body, could be assessed in terms of absorbed power, or alternatively mechanical energy absorption.

It has been suggested that the energy absorption characteristics of seated human body exposed to WBV are related to both the human anthropometry and nature of vibration [43,44]. The principal vertical mode resonance of the seated body around 5Hz has been consistently identified from two different measures (STHT and APMS) [10,11]. Mansfield and Griffin [45] simultaneously measured the APMS response at the driving-point, and the vibration transmitted to various locations on the body surface, namely, the upper and lower abdominal wall near L3, over the posterior superior iliac spine and the iliac crest. Vertical motion of the lumbar spine and pelvis showed small magnitude resonant peaks at about 4 Hz, while large magnitude responses were observed in the 8 to 10 Hz range. El-Khatib *et al.* [92] investigated the seat-to-vertebrate-transmissibility of human cadavers by making simultaneous measurements at the trunk and throughout the

lumbar spine. The study observed the first lumbar transmissibility peak around 6.3 Hz, and around 7 Hz for the thorax.

It may thus be concluded that the vibration transmissibility characteristics of different segments of the musculo-skeletal structure of the seated human body are more sensitive to vibration in the 4-16 Hz frequency range. The majority of the vibration energy absorption by the seated body also occurs in the same frequency range. The results attained in this study suggest that over 80% of the total absorbed power occurs in the 4-16 Hz range. The absorbed power thus directly related to the resonant motions of the upper body, and could serve as a better method for investigating the vibration induced injuries.

The results suggest that the mechanical energy absorption characteristics of seated occupants exposed to vertical vibration require appropriate considerations of postural differences arising from variations in hands position, seated height, and inclinations of the backrest, while the role of seat pan orientation appears to be negligible. The back support conditions (back not supported, and supported against vertical and inclined backrests) were found to contribute to notable differences in power absorption. Under the same hands positions, back not supported posture (NVF) results in higher energy absorption in the lower frequency bands prior to the primary resonance, while the inclined backrest posture (BIF) causes less energy absorption. However, the inclined backrest posture (BIF) result in higher energy absorption beyond the primary resonant frequency, which is attributed to the presence of the secondary resonance around 10 Hz. The results also support the earlier findings on the influence of back support on the basis of the apparent mass magnitude, which was observed to be significant at frequencies

ranging from primary resonance to 18 Hz [93], irrespective of the hands position. Within this frequency range, the apparent mass magnitudes tend to increase when the back is supported.

Placing the hands on the steering wheels tends to slightly reduce the portion of body mass supported by the seat, when compared to that for the hands in lap postures. This difference tends to be larger with the inclined backrest than for the vertical backrest. The hands in lap postures with slightly larger portion of body mass supported by the seat could account for slightly larger total amount of absorbed power, as observed in Figures 3.18 and 3.19. The hands position, however, affects the absorbed energy only when the back is supported. This trend has also been observed for the seated body apparent mass magnitude response [93]. It may be concluded that for the inclined back support postures the hands position influences the interactions of the seated body with the seat pan, which results in considerable variations in the biodynamic responses. This may also explain the noticeable differences caused by the seat height on absorbed power around the primary resonance, only when inclined back support is employed.

Since absorbed power could be computed indirectly from the imaginary APMS, the absorbed power may also hold the advantage of APMS, namely relatively smaller measurement and inter-subject variabilities [10,36], as opposed to the STHT measurement [11]. Moreover, the absorbed power response characteristics could be applied to obtain an estimate of the cumulative energy dissipated by the exposed body over a given exposure duration. The absorbed power can thus serve as a better measure for assessing the health and safety risks associated with exposure to whole-body vertical vibration.

3.5 Summary

Owing to the severe health and safety risks posed by the exposure to WBV, considerable efforts have been made in reducing the magnitudes of transmitted vibration in vehicular applications, and in characterizing the seated human occupant response to vibration. Postural differences in vehicular situation mainly arise from variations in seat geometry, like seated height, inclinations of the seat pan and the backrest, and back support conditions. Besides hands positions also constitute another source of postural variations. For the purpose of examining the role of seat geometry and hands positions on the force-motion biodynamic functions, measurements were performed for 13 male and 14 female subjects exposed to whole-body vertical vibration. The APMS responses were initially derived, and then absorbed power quantity were computed using the indirect method described in section 2.4.

Owing to the strong dependence of the apparent mass response on the body mass, the statistical analyses are performed with body mass as a covariant in an attempt to eliminate the contributions due to body mass. From the results, it is concluded that an increase in seat height yields higher peak magnitude response attributed to larger portion of the body mass supported by the seat. The measured data revealed negligible effect of variations in the seat pan orientation on the apparent mass response. The subsequent analyses were thus limited to six sitting postures, realized from two hands positions and three back support conditions (back not supported, and supported against vertical and inclined backrests). The primary resonant frequency and bandwidth of the biodynamic responses were strongly influenced by the combined effects of hands position and back support condition, while the peak magnitude was further affected by the seat height.

Furthermore, the hands position was found to influence the APMS response only when the back is supported with an inclined backrest and at frequencies within the primary resonant frequency range. The influence of back support, irrespective of hands position, was generally significant at the frequencies ranging from primary resonance up to 18 Hz. Within this frequency range, the apparent mass magnitudes tend to increase when the back is supported. The data further revealed that the APMS magnitude response at higher frequencies is also affected by the gender.

From the computed absorbed power responses, the results show that the absorbed power is strongly influenced by excitation magnitude and individual anthropometry variables (body mass, body mass index). Owing to the strong effects of the inter-subject variability, the analyses were further performed by selecting 10 subjects from the ensemble of 27 subjects in an attempt to eliminate the contributions due to individual anthropometry variables. The computed data revealed negligible effect of variations in the seat pan orientation on the absorbed power response. Similar to APMS responses, the subsequent analyses were thus limited to six sitting postures, realized from two hands positions and three back support conditions (back not supported, and supported against vertical and inclined backrests). It was found that when the hands position was on the steering wheel, the rate of change of energy absorption within the human body is strongly influenced by the back support condition. The hands in lap postures tend to absorb more energy than those with hands on steering wheel postures when combined with the inclined backrest support. The back supported postures tend to reduce the energy dissipation by the body at low frequencies, and increase the absorption at frequencies above resonance, irrespective of the hands position.

CHAPTER 4

APPARENT MASS AND SEAT-TO-HEAD TRANSMISSIBILITY CHARACTERISTICS

4.1 Introduction

Seated occupant response to WBV has been widely evaluated using two methodologies. These include the measurement of transmission of vibration to different body segments, and measurement of force-motion relationships at the body-seat interface. The former method involves the study of 'motion-motion' vibration transmissibility through the body. The latter method involves the study of forces developed at the body-seat interface as well as the dynamic interaction of seated body with the seat. The apparent mass, computed as the ratio of the force to the acceleration, is directly proportional to the static mass of the human body supported by the seat and it provides measures of resonant frequencies of the biological system. The apparent mass of the human body is more frequently used to characterise the human biodynamic response to vertical or horizontal vibrations, since it permits greater convenience for performing the necessary corrections to account for inertia force due to the seat structure [36].

Epidemiological studies have established definite associations between the WBV exposure encountered in vehicles and the symptoms of LBP among the professional drivers [3,4]. A few studies have suggested the use of vibration transmission through the body to enhance the understanding of the adverse effects of whole body vibration. These studies have thus investigated the nature of vibration transmitted to the head, lumbar (L1,L3,L5), thoracic (T1,T5,T10) and cervical spine [42]. By using skin mounted accelerometers, it has been shown that the relative motions of the skin with respect to the

bone could modify the true responses [75]. The reported transmissibility responses at these locations generally show large inter-subject variabilities, which can be attributed in part to limitation of the measurement methods and to anthropometric differences among the subjects [42,75-77]. Moreover, the vibration transmission characteristics measured at L1, L2, L3 and L4, reported in different studies, namely by Sandover and Dupuis [77], Pope et al. [75], Magnusson [42] and Panjabi et al. [76] showed extremely large differences in both the peak values and the corresponding frequencies.

Alternatively, seat-to-head transmissibility (STHT), which describes the transmission of vibration through the body, has been used to gain a better understanding of transmission of vibration through the seated body [10,11]. It has also been shown that STHT can be directly related to the normalized APMS response to WBV, when the response can be characterized by that of a single-degree-of-freedom system [73]. The vast majority of the reported studies have focused on the STHT responses to vertical vibration excitation, while a few have also measured the head responses along the three translation and rotational axes [35, 55-57]. Demic [49] reported the STHT responses to vertical, fore-and-aft and combined vertical and fore-and-aft vibration at the seat.

Considerable differences among the reported datasets, however, have been observed due to the wide range of test conditions used in different studies, such as sitting posture, frequency and amplitude of vibration excitation, number and physical characteristics of subjects [10,11]. The ranges of the idealized values of APMS and STHT of seated body biodynamic response under vertical vibration have also been proposed in ISO-5982 [12] on the basis of a synthesis of various datasets reported under comparable test conditions. However, the ranges of idealized values presented in ISO-

5982 [12] are not intended to characterize the biodynamic response of seated human occupants under automotive postures and vibration conditions, since they are based upon data acquired with no back support and under relatively high magnitudes of vertical vibration. Paddan and Griffin [35,55-57] studied the effect of a rigid vertical backrest support on STHT under translational and rotational vibration at the seat applied independently, while the responses at the head were measured along the six directions. Under vertical excitation, they reported a decrease in the inter-subject variability with a backrest but an increase in the head vibration, especially in the mid-sagittal plane in the 5–10 Hz frequency range, when compared to those observed for the no back support.

Although both the APMS and STHT response functions relate to the seated occupant responses to whole-body vibration, the two responses have shown some differences, particularly in the resonant frequencies [10,11,73]. Such differences may be inherent to the biological systems response to vibration or may be attributed to the differences in the methods used to characterize the two measures. Compared to the APMS responses, relatively fewer studies have investigated the motion-motion response in terms of seat-to-head transmissibility [10,12,74]. Moreover, the two measures have been acquired either by different investigators or during different test sessions that may also involve different subjects. Simultaneous measurements of the two functions could thus yield considerable insight into the differences, if any, moreover, the characterization of both motion-motion and force-motion response characteristics would provide a better understanding of human response to WBV and its adverse effects.

Apart from the above, the characterization of both APMS and STHT functions is essential for deriving effective seated body models for assessing the responses to WBV

and for applications to seating dynamics. The knowledge of two target response data sets would facilitate the identification of more feasible values for the uncertain parameters of the biological system.

In this chapter, the apparent mass and seat-to-head transmissibility response characteristics are derived through simultaneous measurements of forces at the seat base and backrest and motions on the seat base and head using 12 male subjects under postural and vibration conditions representative of those applicable to automobile drivers and passengers. The measurements are performed to establish the influence of back support condition, hands position, vibration excitation magnitude on the seated body biodynamic responses. On the basis of these results, the target values of both force-motion and motion-motion biodynamic responses of seated occupants are derived for development of mechanical equivalent models.

4.2 Seat-to-head transmissibility characteristics

The acceleration data acquired on the seat and subjects' head under the selected test conditions are analyzed to derive the vertical and fore-and-aft STHT magnitudes and phases. The biodynamic response characteristics and its influential factors are described in the following sub-sections. Multi-factor ANOVA was conducted using the SPSS software to verify the statistical significance level of the main factors upon the vertical and fore-and-aft STHT responses. These included the three back support conditions (NBS, VBS and IBS), two hands positions (LAP and SW) and three excitation levels.

4.2.1 Vertical and fore-and-aft STHT responses

Figure 4.1 illustrates magnitudes of vertical (TF_z) and fore-and-aft (TF_x) STHT responses of 12 subjects seated assuming three different back support conditions and hands in lap posture, while exposed to 1 m/s^2 rms acceleration excitation along a vertical axis. The corresponding mean curves with standard deviation of the mean as the error bars are presented in Figure 4.2. Despite considerable scatter between the STHT magnitude responses of different subjects, the peak moduli of STHT in both vertical and

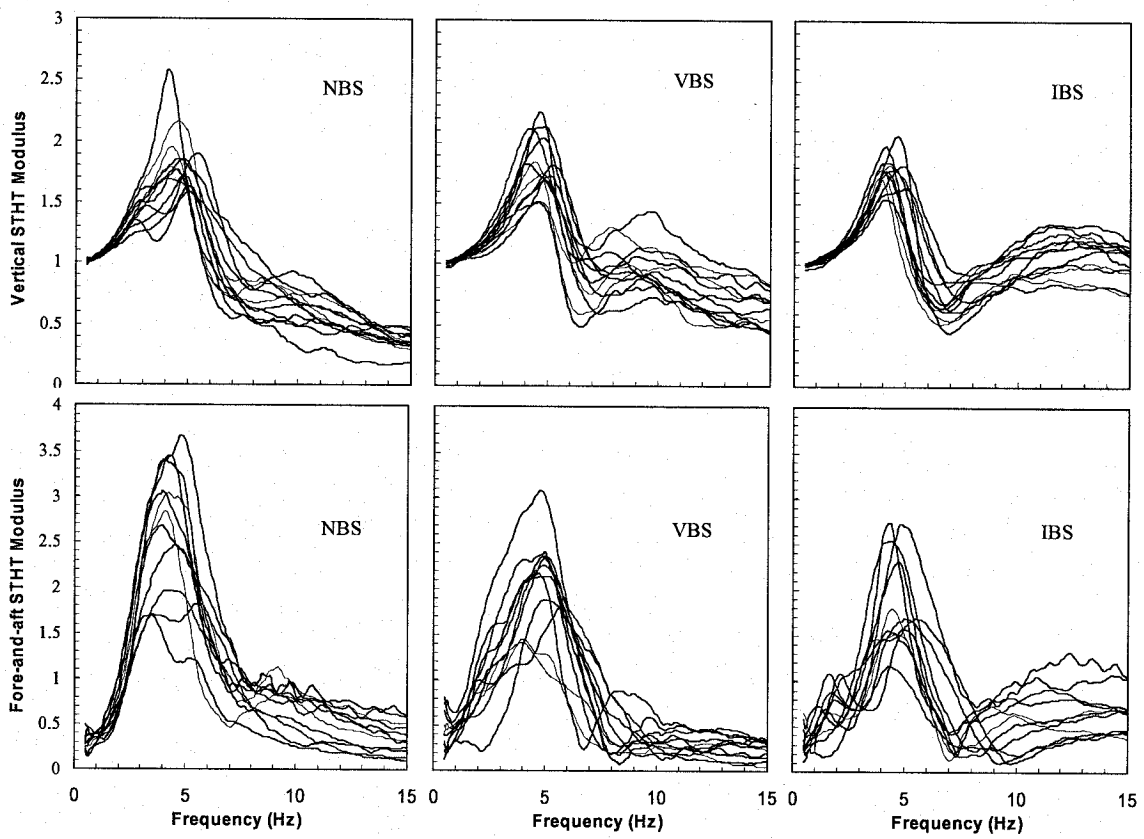

Figure 4.1: Inter-subject variability in the vertical and fore-and-aft STHT responses measured at 1.0 m/s^2 rms excitation with three back support conditions and hands in lap posture.

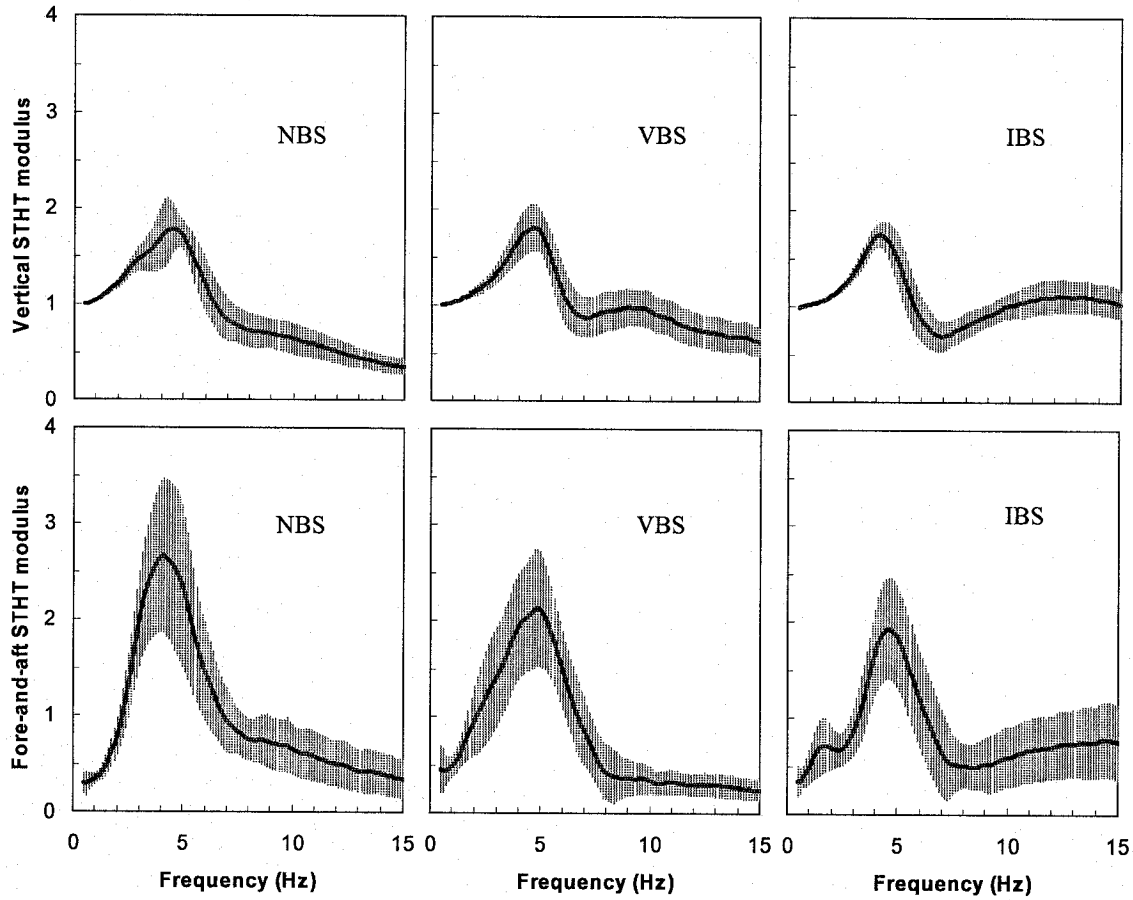

Figure 4.2: Mean curves and mean ± standard deviation scatters of the vertical STHT and fore-and-aft STHT measured for 12 subjects under 1.0 m/s^2 rms excitation and three back support conditions with hands in lap posture.

fore-and-aft axes occur in the 4 to 5 Hz frequency range for all subjects, irrespective of the back support conditions, often referred to as the primary resonant frequency of the seated body [10,12,22,23,34,36,41,42]. Similar degrees of scatter and consistent trends in the data were also observed for the other test conditions involving different excitation magnitudes and hands on steering wheel (SW).

The results further show considerable effects of the back support conditions on the magnitudes of acceleration transmitted to the head along both the vertical and fore-and-aft directions. At frequencies below the primary resonance, a larger dispersion of the moduli of the TF_z was observed for the no and vertical back support conditions than with the inclined back supported posture. The magnitudes of fore-and-aft STHT responses also exhibit considerable dispersion in the measured data as in the case of the vertical STHT, while the trends are somewhat different. A relatively larger dispersion of the moduli of TF_x around 2 Hz was revealed for the inclined back supported posture, which was observed to be the smallest in TF_z for the same posture. This is most likely caused by the body mode around 2 Hz in the fore-and-aft direction, which has been observed in APMS under horizontal vibration [94].

At frequencies around the primary resonance, both the vertical and fore-and-aft STHT responses with the inclined back support exhibit the smallest scatter, while relatively larger variations were observed under the no back support condition. The inter-subject variations in the moduli of TF_x tend to be significantly higher, which could be attributed to differences in individuals' anthropometry and muscles tension. For the NBS posture, the coefficient of variation of TF_z modulus is in the vicinity of 15% near the primary resonance, which reduces to nearly 12% and 7% for the VBS and IBS postures. The coefficient of variations of the TF_x modulus exceeds 30% for the NBS and VBS postures, and is in the order of 25% for the IBS posture.

The vertical STHT responses exhibit the presence of a second resonance in the 9-11 Hz range. The second resonant peak was noticeable only for some subjects when sitting without back support, and is thus not very clearly evident in the mean curve.

However, the magnitude of this secondary peak becomes apparent for the back supported postures, while the vertical and inclined back supports cause higher corresponding frequencies when compared to that from the NBS response. As indicated in Figure 4.1, at frequencies above 10 Hz, the inter-subject variability in vertical STHT magnitude is relatively smaller for the no back support in contrast with the back supported postures. For the fore-and-aft STHT responses, a second resonant peak is clearly evident under the inclined back supported posture. A number of reported biodynamic response studies have also suggested the presence of this secondary. Matsumoto and Griffin [42] found the second peak between 6 and 9 Hz for vertical vibration transmissibilities of seat to L4 and to the pelvis under the no back sitting posture. Similarly, Mansfield and Griffin [45] found the second resonant peak in the 8-10 Hz range, while investigating the seat to spine and pelvis acceleration transmissibilities under vertical WBV. Rakheja et al. [48] reported the second resonance frequency occurring in the vicinity of 11 Hz under the inclined back support and hands on steering wheel posture on the basis of the measured APMS biodynamic responses. Nawayseh and Griffin [51] also observed the presence of a second resonance peak of relatively small magnitude in the 10-15 Hz range in the fore-and-aft APMS response measured at both the seat and the backrest, which was considered to be consistent with the rotational mode of the pelvis and the lower upper-body (T11-L3).

The results show significant magnitudes of fore-and-aft acceleration of the head, even though the seated subjects are exposed to vertical vibration alone. This could be attributed to the angular motions of the upper body and the head, which have also been observed in a few reported studies [35,51]. The results suggest strong coupling between

the angular and vertical motions of the seated body. The peak magnitudes of TF_x are observed to be either comparable or larger than those of the TF_z. The peak mean magnitude of TF_x, however, is greater than that of TF_z for the NBS posture, which can be attributed to relatively larger angular motion of the unsupported upper body. The mean magnitudes of TF_x for the two back supported postures are only slightly larger than those of TF_z. The magnitudes of TF_x also exhibit primary peak in the 4-6 Hz frequency range, while sitting against the inclined back support yields a relatively small peak around 2 Hz. This peak is most likely attributed to the upper body response to component of vibration excitation along the fore-and-aft axis encountered at the inclined backrest. A few studies conducted on the biodynamic responses of seated occupants exposed to fore-and-aft vibration have also suggested the presence of this peak around 2 Hz, which has been attributed to considerable interactions of the upper body with the inclined backrest [94].

Figure 4.3 illustrates comparisons of the vertical STHT phase responses of individual subjects for the three back support conditions, while sitting with hands in lap. The figure also illustrates the mean responses and standard deviations of the means as the error bars. These responses also show similar degree of variability but consistent trends. The inclined back support posture yields relatively smaller dispersion in the data, as observed in the TF_z moduli data. Correspondingly, STHT phase responses show the similar results while placing the hands on the steering wheel.

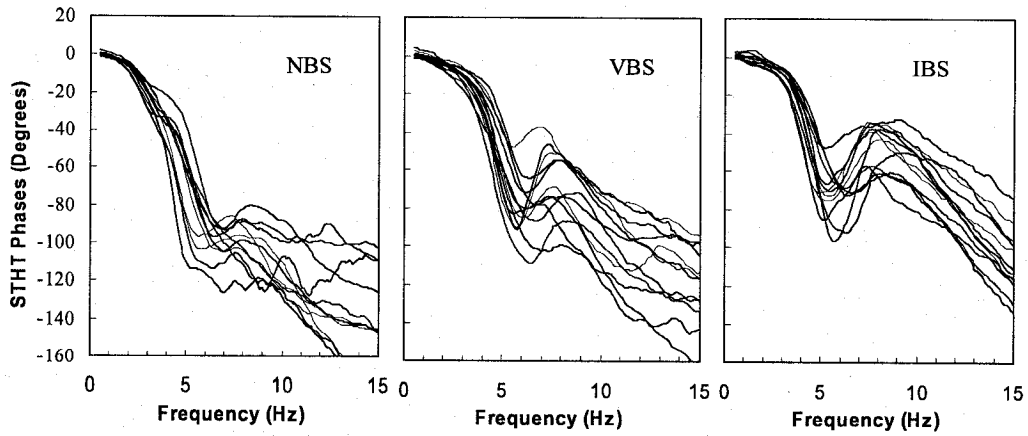

(a)

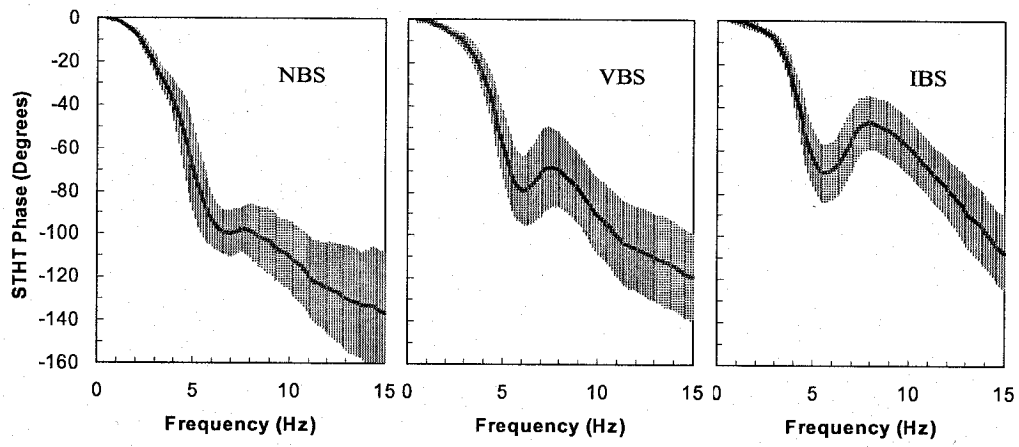

(b)

Figure 4.3: Comparison of vertical STHT phase responses of 12 subjects exposed to 1.0 m/s^2 rms acceleration excitation and seated assuming three back support conditions and hands in lap posture: (a) Phase responses of 12 subjects; and (b) mean and standard deviation of the phase responses.

As an example, Figure 4.4 illustrates the strong correlation between the seat and head acceleration signals for the condition with hands in lap posture. In the vertical direction, the coherence is close to 1 over the entire frequency range. In the fore-and-aft direction, the coherence is low in the low frequency range (below 2 Hz) due to relatively small motions of the head in that direction.

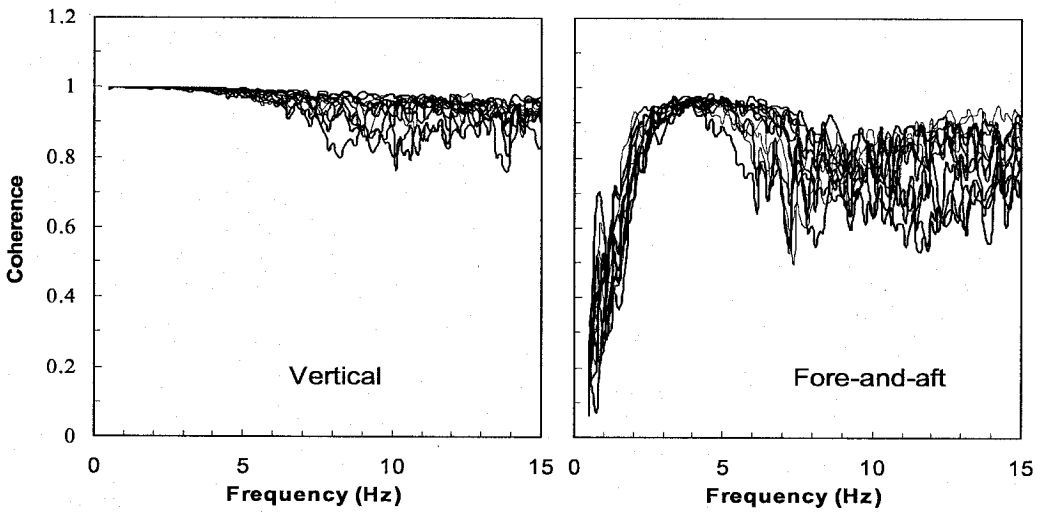

Figure 4.4: Coherence in the vertical and fore-and-aft STHT measured at 1.0 m/s^2 rms with no back support condition and hands in lap posture.

Prior to the subsequent analysis, the influence of body mass on the measured 'vertical STHT' and 'fore-and-aft STHT' responses was checked first. The results have invariably shown little effects of body mass, which was consistent with the published studies, as reviewed in section 1.3.1.

The results presented in Figures 4.1 and 4.3, however, suggest that the back support condition strongly affects the STHT in both the vertical and fore-and-aft directions. Furthermore, the hands position and vertical vibration magnitude may also influence the STHT responses, while little has been reported in the literature on the influences of such factors. The measured data were thus statistically analyzed to study the effects related to different experimental conditions considered in this study. The interpretations of these statistical results are presented on the basis of mean responses comparisons, which is justifiable in view of consistent tendencies in terms of peak response magnitudes and the corresponding frequencies.

4.2.2 Effect of vibration magnitude on STHT

The effect of vibration magnitude has been widely reported in terms of driving-point biodynamic functions [36,45,51,52]. Most studies have concluded that the primary resonance frequency decreases as the magnitude of vibration is increased. This phenomenon is known as a 'softening effect' or 'non-linearity' of the human body, while subjected to WBV. Unlike the driving-point biodynamic responses, only minimal efforts have been made to study the influence of excitation amplitude on the STHT responses of the seated human body. Mansfield and Griffin [45] demonstrated the nonlinearity of the seat vibration transmitted to various body segments of the seated body, namely the viscera, pelvis and lumbar spine. Figure 4.5 illustrates comparisons of mean vertical and fore-and-aft STHT responses attained under three different vertical vibration magnitudes: 0.25, 0.5 and 1.0 m/s^2 rms acceleration.

The results presented for the three back support conditions distinctly reveal that the primary resonance tends to shift to a lower frequency with increasing vibration magnitude. Similar trends were also observed for the phase response. The same trend is also evident for the fore-and-aft STHT, while the shift in frequency is more evident for the back supported postures. The broad secondary resonant frequency in the vertical STHT response, which is more evident with the vertical and inclined back supports, also decreases with increasing vibration magnitude. The results suggest that the mean primary resonance for the inclined back support posture decreases by approximately 0.85 Hz (from 5.55 Hz to 4.7 Hz), when vertical excitation magnitude is increased from 0.25 to 1.0 m/s^2. Besides, it is also observed that increasing of the excitation magnitude causes a

difference of approximately 0.3 Hz for the first resonance frequency around 2 Hz that occurs in the fore-and-aft direction with an inclined back support.

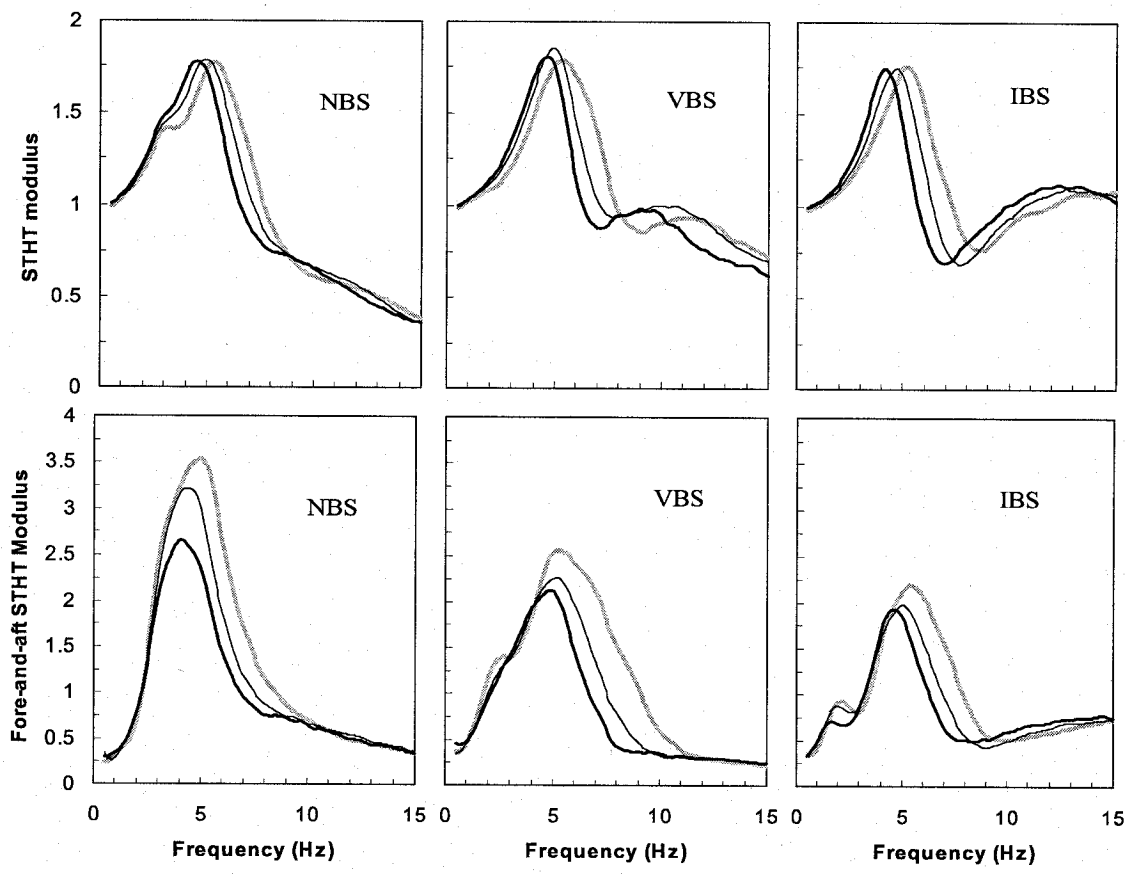

Figure 4.5: Influence of excitation magnitude on mean STHT responses of 12 subjects with hands in lap; ——1.0 m/s^2 rms; —— 0.5 m/s^2 rms; ——0.25 m/s^2 rms.

Tables 4.1 and 4.2 summarize the results attained from ANOVA of the vertical and for-and-aft STHT data, respectively, considering three main factors: back support condition *B* (NBS, VBS, IBS); excitation magnitude *E* (0.25m/s^2, 0.5m/s^2, 1.0m/s^2); and hands position *H* (LAP, SW). The tables present the *p* values corresponding to each main factor and their interactions at selected discrete frequencies. The results suggest significant effects of excitation magnitude (p <0.05) on the fore-and-aft STHT responses

in the frequency range between the two resonances (5-10.5 Hz). For the vertical STHT responses, the most significant effects of excitation magnitude (p <0.01) occur from 1-8 Hz, except at 5 Hz, while the significant effects are also evident at frequencies above 11.5 Hz (p<0.05). The influence of excitation magnitude on the primary resonance will be further discussed in the subsequent sections.

Table 4.1: p values obtained from three factor statistical analysis in view of the vertical STHT modulus over the frequency 0.5-15 Hz.

Frequency (Hz)	B	E	H	B*E	E*H	B*H	B*E*H
1	0	0	0.364	0.880	0.729	0.945	0.928
1.5	0	0	0.126	0.998	0.686	0.178	1.000
2	0	0	0.463	0.997	0.993	0.505	0.999
2.5	0	0	0.375	0.841	0.998	0.778	0.994
3	0	0	0.342	0.366	0.975	0.705	0.969
3.5	0	0	0.603	0.348	0.959	0.162	0.974
4	0.47	0	0.806	0.863	1.000	0.344	0.976
4.5	0.281	0	0.927	0.142	0.550	0.217	0.858
5	0	0.196	0.302	0	0.291	0.067	0.752
5.5	0	0	0.021	0.002	0.419	0.048	0.982
6	0	0	0.001	0.537	0.799	0.105	0.904
6.5	0	0	0	1	0.996	0.242	0.861
7	0	0	0	0.976	0.815	0.542	0.960
7.5	0	0	0	0.854	0.294	0.632	0.966
8	0	0.006	0	0.136	0.439	0.566	0.948
8.5	0	0.577	0	0.241	0.089	0.590	0.926
9	0	0.734	0	0.232	0.064	0.657	0.862
9.5	0	0.570	0.002	0.475	0.128	0.790	0.939
10	0	0.813	0.075	0.568	0.191	0.619	0.994
10.5	0	0.989	0.537	0.461	0.326	0.436	1.000
11.5	0	0.017	0.067	0.596	0.795	0.227	0.822
12	0	0.032	0.589	0.03	0.286	0.439	0.888
13.5	0	0.038	0.843	0.012	0.258	0.561	0.935
14	0	0.036	0.036	0.838	0.879	0.155	0.809

B=Back support conditions (NBS, VBS, IBS);
E=Excitation (0.25 m/s^2, 0.5 m/s^2, 1.0 m/s^2 rms);
H=Hands position (LAP, SW).

Table 4.2: *p* values obtained from three factor statistical analysis in view of the fore-and-aft STHT modulus over the frequency 0.5-15 Hz.

Frequency (Hz)	B	E	H	B*E	E*H	B*H	B*E*H
1	0	0.197	0.624	0.711	0.853	0.677	0.983
1.5	0	0.490	0.452	0.712	0.830	0.02	0.948
2	0	0.073	0.954	0.012	0.910	0.001	0.801
2.5	0	0.208	0.108	0.272	0.763	0.005	0.781
3	0	0.583	0.012	0.461	0.876	0.042	0.841
3.5	0	0.516	0.021	0.028	0.980	0.854	0.988
4	0	0.783	0.015	0.025	0.802	0.844	0.978
4.5	0	0.308	0.035	0.033	0.324	0.543	0.996
5	0	0.002	0.120	0.056	0.297	0.250	0.997
5.5	0	0	0.201	0.028	0.371	0.074	0.984
6	0	0	0.332	0.267	0.562	0.057	0.930
6.5	0	0	0.464	0.828	0.753	0.082	0.789
7	0	0	0.620	0.606	0.703	0.102	0.752
8	0	0	0.604	0.001	0.911	0.440	0.899
8.5	0	0	0.413	0	0.972	0.47	0.798
9	0	0	0.288	0.001	0.983	0.402	0.717
9.5	0	0	0.209	0.016	0.691	0.689	0.784
10	0	0.002	0.185	0.228	0.468	0.646	0.882
10.5	0	0.043	0.214	0.350	0.337	0.578	0.883
11.5	0	0.867	0.473	0.732	0.383	0.164	0.984
13.5	0	0.984	0.837	0.756	0.497	0.037	0.990
14	0	0.958	0.587	0.862	0.582	0.033	0.990

B=Back support conditions (NBS, VBS, IBS);
E=Excitation (0.25 m/s^2, 0.5 m/s^2, 1.0 m/s^2 rms);
H=Hands position (LAP, SW).

4.2.3 Peak variation analysis of STHT

Table 4.3 summarizes the mean values of the primary resonant frequencies observed from the measured vertical and fore-and-aft STHT responses attained under different combinations of experimental conditions, together with the standard deviations on the means. The mean primary resonant frequencies decrease with increasing excitation magnitude, suggesting nonlinear response and a softening effect, which has been widely reported [36,45,51,52]. This softening effect seems to be greater for the IBS posture. The

Table 4.3: Primary resonance frequencies (Mean, SD values) for both vertical and fore-and-aft STHT responses.

Back support condition		No back support			Vertical back support			Inclined back support		
Excitation (m/s^2 rms)		0.25	0.5	1.0	0.25	0.5	1.0	0.25	0.5	1.0
Vertical STHT	LAP	5.63	5.06	4.66	5.58	4.94	4.69	5.43	4.83	4.30
		0.59	0.43	0.43	0.63	0.33	0.36	0.74	0.47	0.35
	SW	5.97	5.25	4.89	6.08	5.22	4.76	5.59	4.97	4.30
		0.58	0.32	0.33	0.86	0.62	0.46	0.73	0.40	0.37
Fore-and-aft STHT	LAP	4.89	4.39	4.24	5.54	5.38	4.83	5.55	4.97	4.67
		0.48	0.54	0.48	0.67	0.44	0.45	0.81	0.46	0.29
	SW	4.96	4.59	4.49	5.73	5.54	4.95	5.65	5.14	4.66
		0.57	0.51	0.47	0.85	0.67	0.33	0.78	0.43	0.37

difference in mean primary resonant frequency attained under lowest and highest excitation amplitude is 1.13 Hz for the vertical STHT with hands in lap and about 0.9 Hz for the fore-and-aft STHT responses. For the identical back support condition, the SW posture yields even larger difference compared with the LAP posture except for the fore-and-aft STHT response under NBS. For the hands in lap posture, the mean resonance frequency of the vertical STHT generally tends to be highest for the NBS and lowest for the IBS, while these increase slightly for the SW posture, which may be attributed to slightly lower effective body mass on the seat [48,54]. The difference in the frequencies between the LAP and SW postures diminishes under higher excitations, which suggest greater softening effect of increasing magnitude for the SW posture. The same trends are also evident in the mean frequencies of fore-and-aft STHT responses, while the frequencies for the NBS posture are considerably lower than those observed for vertical STHT responses.

The standard deviation on the primary resonance tends to increase as the excitation magnitude decreases, and it is also decreasing in the order of no back support, vertical back support and inclined back support. The standard deviations of the means for both vertical and fore-and-aft STHT frequencies generally tend to be considerably higher under lower excitation magnitude of 0.25 m/s^2, when compared to those under higher excitations, irrespective of the hands position and back support condition. Moreover, back supported postures exhibit relatively higher standard deviations of the means compared to those for the NBS posture. This tendency is opposite to that observed for the peak transmissibility magnitudes. The above trends observed in the primary resonance data may suggest that the 'softening effect' of the seated body would also be influenced by the back support condition and hands position.

Table 4.4 summarizes the results attained from three factors ANOVA of the vertical and fore-and-aft peak transmissibility moduli and primary resonances in view of the back support condition (*B*), hands position (*H*) and excitation magnitude (*E*), and their interactions. The results clearly show significant effects (p <0.005) of the back support condition upon the peak moduli and the corresponding frequencies. Excitation magnitude was found to have a significant influence (p <0.005) on the fore-and-aft moduli and resonant frequencies of both responses, while it was insignificant in view of the vertical STHT modulus. This is also evident from the mean responses presented in Figure 4.5. The hands position was only found to be significant for the vertical mode resonance (p <0.005) but relatively less significant for the corresponding peak modulus. The results further show insignificant interactions among the main factors.

Table 4.4: *p* values obtained from three factor statistical analysis in view of the peak STHT modulus and primary resonance.

	B	E	H	B*E	E*H	B*H	B*E*H
Vertical Peak modulus	0.004	0.243	0.014	0.752	0.826	0.015	0.972
Vertical Primary resonance	0	0	0.003	0.687	0.391	0.522	0.938
Fore-and-aft Peak modulus	0	0.001	0.1	0.431	0.472	0.405	0.999
Fore-and-aft Primary resonance	0	0	0.069	0.446	0.936	0.867	0.958

B=Back support conditions (NBS, VBS, IBS);
E= Excitation (0.25 m/s^2, 0.5 m/s^2, 1.0 m/s^2 rms);
H=Hands position (LAP, SW).

4.2.4 Effect of hands position on STHT

Figure 4.6 compares the STHT responses measured with two hands position (in lap and on the steering wheel) for the 12 subjects while exposed to excitation level of 1.0 m/s^2 rms. The influences of hands position on the mean STHT responses appear to be generally small for the postures and excitation level considered. The effects on the vertical STHT responses can be observed (p <0.05) at frequencies above the primary resonance (5.5-9.5 Hz). For the fore-and-aft STHT responses, the hands position can be considered as a slightly significant factor (p <0.05) in the 3-5.5 Hz frequency range. No significant interactions were detected between the hands position and excitation magnitude as well as among the back support condition, excitation magnitude and the hands position in both the STHT responses. The hands position reveals relatively larger differences in the modulus occurring around the primary resonance for the NBS condition, as opposed to the VBS and IBS conditions (Figure 4.6). For the back supported postures, the differences in the vertical modulus are observed in the 6 to 9 Hz frequency range.

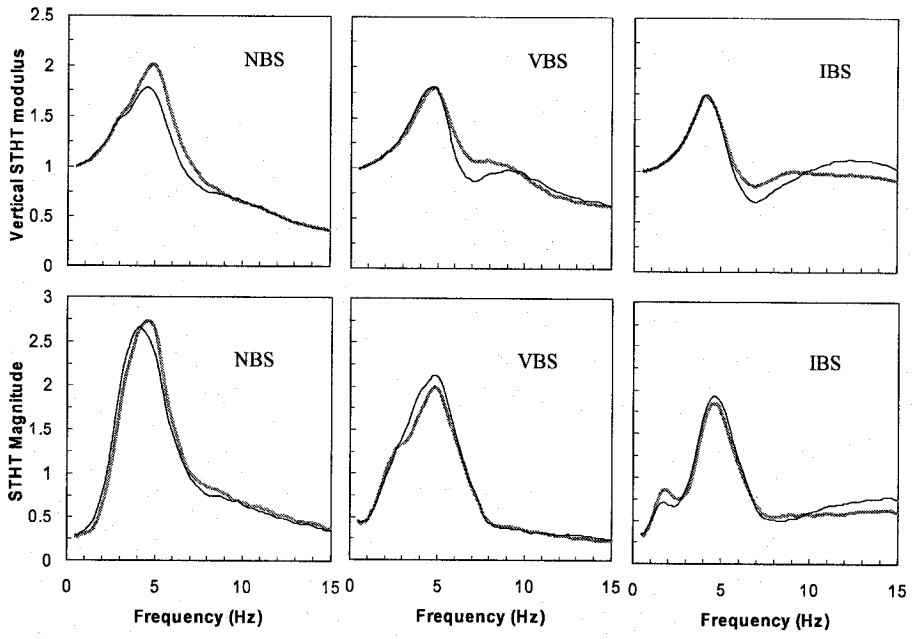

Figure 4.6: Influence of two hands position on mean STHT responses of 12 subjects under different back supported conditions. —— Hands in lap; —— hands on steering wheel (Excitation: 1.0 m/s^2 rms).

Unlike the STHT responses, the hands position tends to strongly affect the APMS response under vertical WBV exposure [48,54,92], particularly when the seated subject utilizes an inclined backrest support. The reported study utilized relatively lower magnitudes of white noise vibration in the 0.5-40 Hz range and slightly different steering column geometry. The observed differences in the effects of hands position on the STHT and APMS responses could be attributed to the differences in the column geometry and the excitation level.

4.2.5 Effect of back support condition on STHT

Figure 4.7 and 4.8 illustrates the comparisons of mean STHT magnitude responses attained for the three back support conditions (NBS, VBS and IBS) under

exposure to 1.0 m/s^2 rms excitation and the LAP. Figure 4.8 provides the same as that of the SW posture. At frequencies around the primary resonance, the variations arising from the back support conditions appear to be most important for the fore-and-aft STHT TF_x than that for the vertical STHT TF_z, which conforms to the results obtained from the peak variation analysis. The p values obtained for the back support conditions on the peak TF_z moduli (p <0.005) are higher than those for the peak TF_x moduli (p <0.00001), as evident in Table 4.4. These results thus suggest that a back support contributes greatly to the fore-and-aft motion of the body near the primary resonance, most likely the angular motion of the upper body, when compared with the vertical head motion. The use of a back support tends to reduce the angular motion of the upper body and thus the fore-and-aft motion of the head most significantly.

For the vertical TF_z modulus, the primary resonance of the body with IBS occurs at a lower frequency compared to that with NBS and VBS, this trend is somehow opposite to that observed from the reported APMS responses [93], which may be attributed to the differences in seat geometry dependent postures and excitation magnitudes. The broad secondary resonance for the IBS, on the other hand, occurs at a relatively higher frequency than those for the NBS and VBS postures. The peak modulus of TF_z corresponding to this secondary resonance is significantly higher than those for the other support conditions, and approaches values near 1.0. The IBS posture also shows similar effect on the TF_x modulus, while the peak value remains below 1.0. In the 1-3 Hz frequency range, the NBS posture yields a relatively higher value of TF_z modulus. At frequencies above 10 Hz, both the TF_z and TF_x moduli increase for the back supported postures.

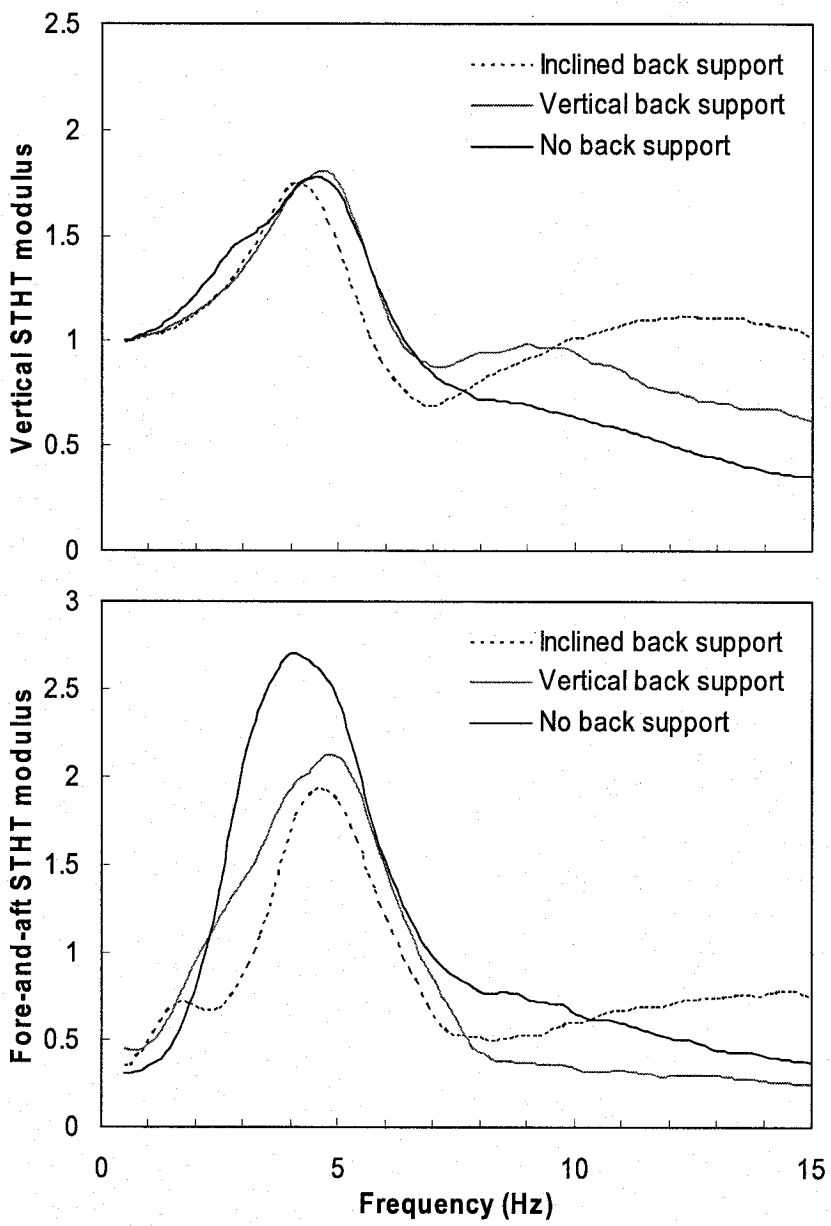

Figure 4.7: Influence of three back support conditions on mean STHT responses of 12 subjects. —— No back support; —— vertical back support;------ Inclined back support (Hands in lap: excitation: 1.0 m/s^2 rms).

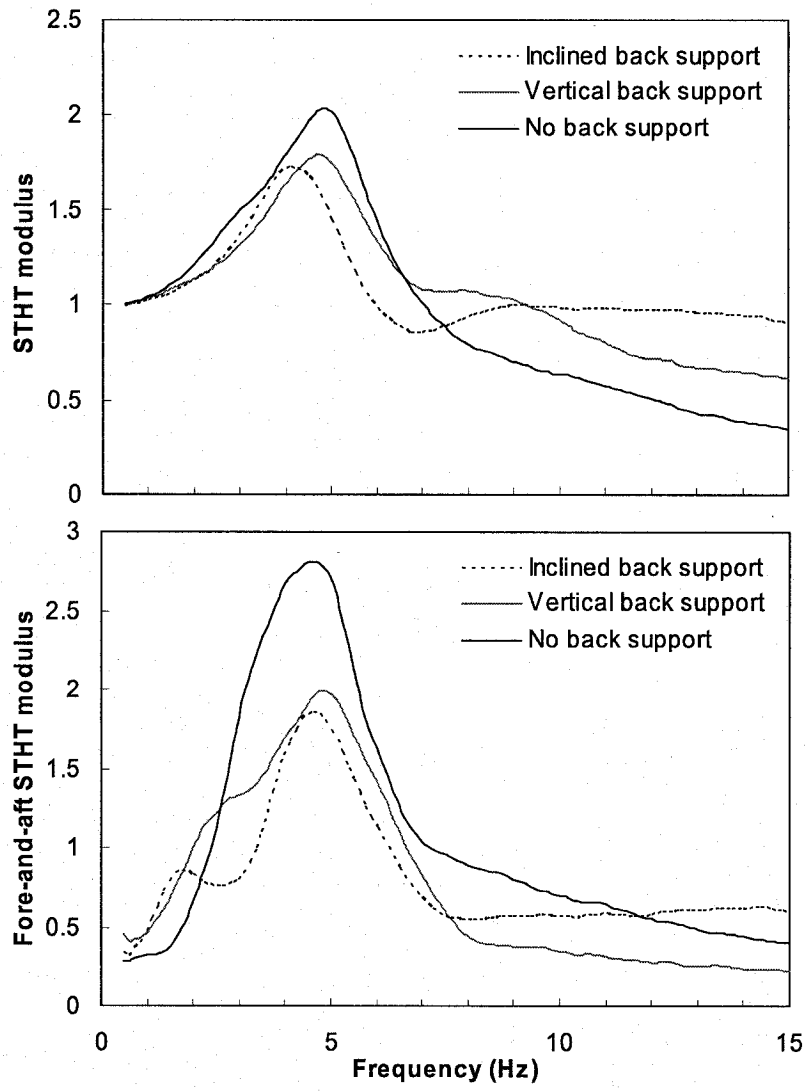

Figure 4.8: Influence of three back support conditions on mean STHT responses of 12 subjects. —— No back support; —— vertical back support;------ Inclined back support (Hands on steering wheel: excitation: 1.0 m/s^2 rms).

The ANOVA results, summarized in Tables 4.1 and 4.2, reveal rather strong significance of the back support condition over the entire frequency range 0.5-15 Hz (p <0.00001), except for the vertical STHT response in the 4-4.5 Hz range, where the effect of the back support condition is insignificant. The slightly strong interaction between the back support condition and the hands position (p <0.05) can be observed for the TF_x

modulus in the lower frequency range (1.5-3 Hz). Slight interactions (p <0.05) between the back support and the excitation magnitude could also be observed for both the moduli in the small frequency intervals of 5-5.5 Hz and 12-13.5 Hz for the vertical, as well as 3.5-5.5 Hz and 8-9.5 Hz for the fore-and-aft STHT responses.

The STHT biodynamic responses obtained with the use of a rigid backrest may be compared with those reported by Paddan and Griffin [35]. In that study, the STHT responses were measured using 12 male subjects, who assumed a comfortable upright posture or were leaning against an upright backrest, while exposed to vertical WBV. The study concluded that the backrest increased the rms values of head vibration, and provided a stiffening effect for the body resulting in an increase in the primary resonance frequency. The results presented in Figure 4.7 and 4.8 show only a slightly higher mean primary resonant frequency for the VBS posture when compared to that for NBS posture. The VBS posture, however, yielded considerably larger magnitude of vertical STHT at frequencies above 7 Hz, which would yield higher rms values of head vibration, as reported in [35]. The peak magnitude of TF_x is considerably larger for the NBS posture, when compared to those for the back supported posture. This trend is opposite to that reported by Paddan and Griffin [35], which may be attributed to the differences in the measurement system, namely the bite-bar vs. the helmet-strap mounted accelerometer mounting system.

The results presented in Figure 4.7 and 4.8 also exhibit the highest magnitude of TF_x *and* TF_z for the IBS posture at frequencies above 10 Hz. This is also evident from the effects of back support on the APMS magnitude and absorbed power [93,95]. These

studies have shown that both the APMS and absorbed power magnitudes in the vicinity of the secondary resonance tend to be higher for the back supported postures.

4.3 APMS responses characteristics

Wu et al. [73] performed analyses of STHT and APMS responses and concluded that for a single–DOF biodynamic model, both measures exhibit identical primary resonance frequencies. Another study on the analyses of various reported models suggested the frequencies corresponding to peak APMS and STHT magnitudes differ [19]. Such differences are also evident in the idealized values of STHT and impedance responses presented in ISO-5982 [12]. Considering that both measures characterize the response behaviour of the same body, one may expect similar resonance frequencies. On the other hand, the two measures describe considerably different response characteristics, and may thus yield some differences by emphasizing different modes. The reported studies have attributed these differences to a few primary factors [10]. The two measures have been mostly measured in separate experimental sessions mostly likely involving different subject population and measurement methods. Simultaneous measurement of these two measures using identical subjects is thus essential to gain insight into the similarity of two measures. Moreover, the APMS and STHT measures relate to 'to-the body' and 'through-the-body' characteristics. The data acquired in this study are initially analyzed to derive the two measures, which are subsequently evaluated to identify the similarities and differences between them.

The force and acceleration data acquired on the seat are analyzed to derive the force-motion biodynamic response in term of vertical apparent mass measured at the seat

pan, cross-axis apparent mass at the backrest support. The APMS responses measures acquired under automotive postures, employed in simultaneous measurement, are discussed in relation to those attained for a commercial vehicle seat posture presented in previous chapter.

4.3.1 Vertical and cross-axis APMS responses

Figure 4.9 illustrates magnitude and phase responses of vertical APMS (M_v) responses of 12 subjects seated assuming three different back support conditions and hands in lap posture, while exposed to 1 m/s^2 rms acceleration excitation along a vertical axis. The results show mean responses for each subject derived from data acquired for two repeats under each test condition. The scatter in the M_v magnitude response tends to be higher at lower frequencies prior to the primary resonance, which can be mostly attributed to variations in the body masses, as illustrated earlier in section 3.2.1. But at frequencies above the primary resonance, the scatter in the magnitude responses is relatively small irrespective of the back support conditions. The corresponding scatter in the phase response, as presented in Figure 4.9, however, shows the opposite trend compared with magnitude response, irrespective of the back support conditions. Similar degrees of scatter and consistent trends in the phase data were also observed for other test conditions involving different excitation magnitudes and hands on steering wheel (SW).

Figure 4.10 illustrates magnitude and phase responses of 'cross-axis APMS' (M_{vb}), responses of 12 subjects seated assuming two different back support conditions and hands in lap posture, while exposed to 1 m/s^2 rms acceleration excitation along a vertical axis. As defined in section 2.3, 'cross-axis APMS' was derived from the force

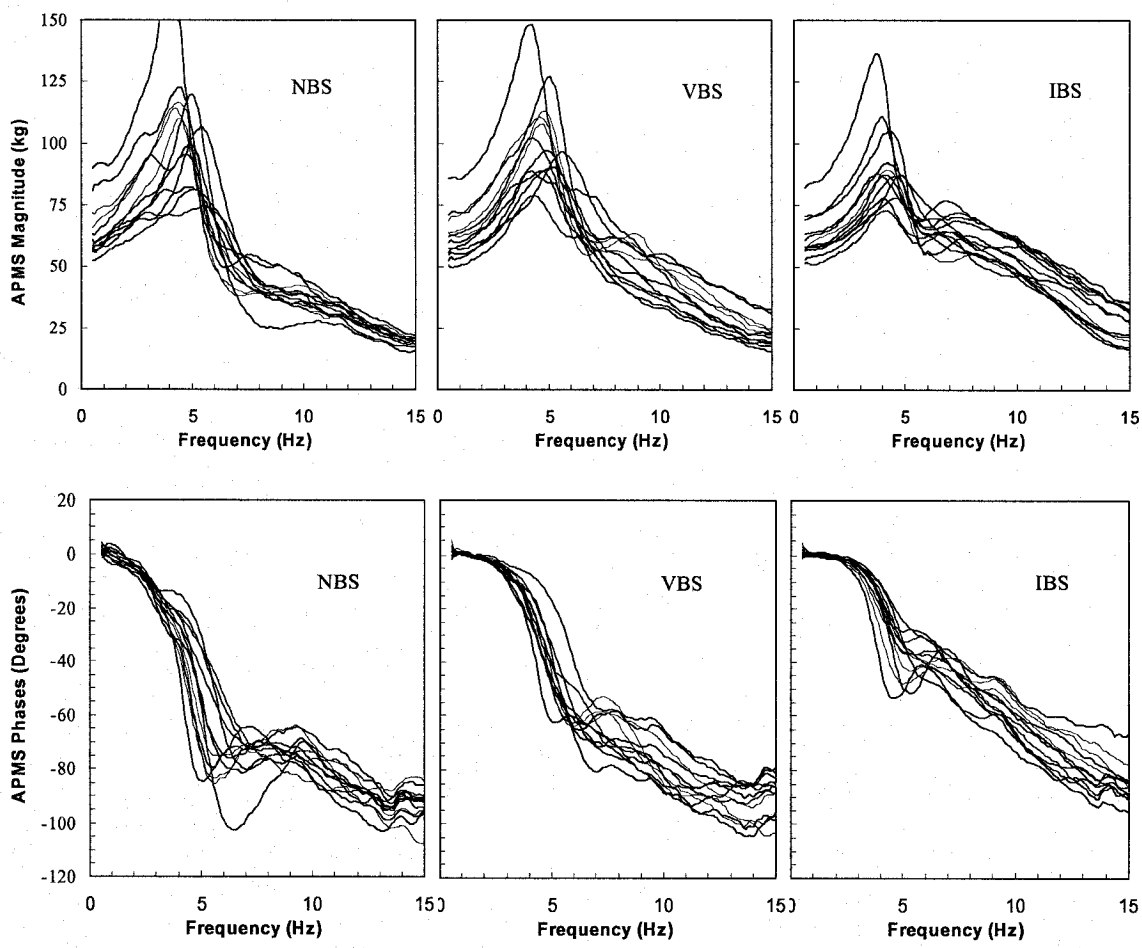

Figure 4.9: 'Vertical APMS' magnitude and phase responses of 12 subjects measured under 1.0 m/s^2 rms excitation with three back support and hands in lap posture.

measured at the backrest and acceleration measured at the seat base. The scatter in the M_{vb} magnitude and phase responses under the vertical back support tends to be higher over the entire frequency range compared with that acquired from the inclined back support condition, which may partly have resulted from the contact condition between the upper body and backrest. The seated upper body tends to make full use of backrest in

an inclined position and maintain a stable relaxed sitting posture, while VBS support may yield inconsistent interaction with the backrest.

The scatter in the M_{vb} magnitude response under the inclined back support tends to be higher at frequencies until around 7 Hz, which may be partly attributed to the variations arising from the static body masses interacting with the backrest, and partly to the variations in the primary and secondary resonance.. The scatter in the M_{vb} magnitude response under the vertical back support reveals a different trend, the greatest scatter occurs around the primary resonance from 5 to 7 Hz. Compared to the inclined back support posture, the scatter of M_{vb} response at lower frequencies under vertical back support is relatively small, which may be due to the reduced static body weight supported by the backrest.

Despite the considerable scatter between the APMS magnitude responses of different subjects, the peak magnitude of M_v occur around 3.75 to 5.5 Hz frequency range for all test subjects, irrespective of the back support condition, often referred to as the primary resonant frequency of the seated body [36,41,42,58]. The peak magnitude of M_{vb}, occurs at a relatively higher frequency, ranging from 4.5 to 7 Hz.

The 'vertical APMS' responses (M_v) exhibit a noticeable second resonance in the 7.5-11 Hz frequency range only for some subjects when sitting without back or for vertical back support. The magnitude responses of all the subjects reveal a distinct second peak in the 6-8 Hz frequency range under the inclined backrest support. Moreover, the magnitude of this secondary peak become higher for the back supported postures as compared with the no back support posture. The 'cross-axis APMS' responses (M_{vb}) also

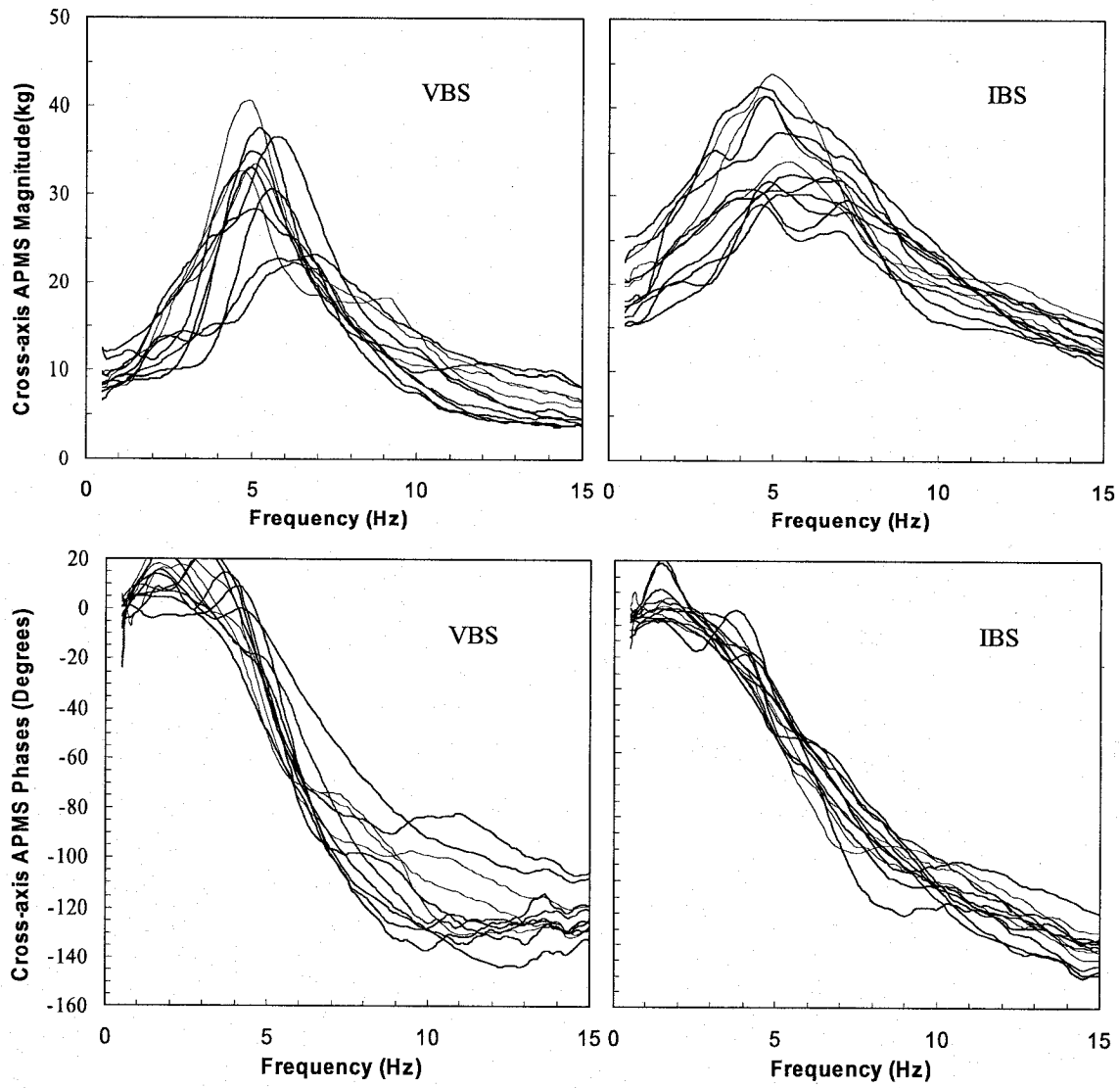

Figure 4.10: 'Cross-axis APMS' magnitude and phase responses of 12 subjects measured at the backrest under 1.0 m/s^2 rms excitation with three back support and hands in lap posture.

reveal a higher magnitude of secondary peak in the 6-8 Hz frequency range for all the subjects when sitting against the inclined backrest. However, this second peak was not observed for the cross-axis responses of 12 subjects under the vertical back support, although the magnitude responses exhibit relatively larger scatter.

The mean 'vertical APMS' and 'cross-axis APMS' responses, where the standard deviations are shown with error bars, are presented in Figures 4.11 and 4.12, respectively. For the NBS posture, the coefficient of variation of M_v magnitude is in the vicinity of 47% near the primary resonance, which reduces to nearly 20% and 22% for the VBS and IBS postures respectively. The coefficient of variations of the M_{vb} magnitude in the vicinity of primary resonance reaches 83% for the VBS posture, and is in the order of 34% for the IBS posture. Moreover the coefficient of variations of the M_{vb} magnitude is considerably larger when sitting with upright back support compared with the inclined back support over the entire frequency range except at frequencies below 3 Hz. Moreover the coefficient of variations of the M_{vb} phase is considerably larger when sitting with upright back support compared with the inclined back support over the entire frequency range. This suggests that a vertical back support may cause considerable inter-subject variability for the cross-axis APMS responses, and that a vertical back support yields a less constrained and controlled upper body posture.

4.3.2 Static forces at the inclined backrest

As introduced in chapter 2, the static forces at the backrest have been recorded before and after each experiment corresponding to different postures to ensure consistent sitting posture during a trial. The overall mean values of the static forces at the inclined backrest for all 12 subjects, are obtained as 20.87 kg and 19.27 kg, with standard deviation of 3.19 and 2.75 kg respectively for hands-in-lap and hands on the steering wheel positions. The static forces at the inclined backrest are also estimated from the reported anthropometric data [96]. While sitting against the backrest, the upper body that

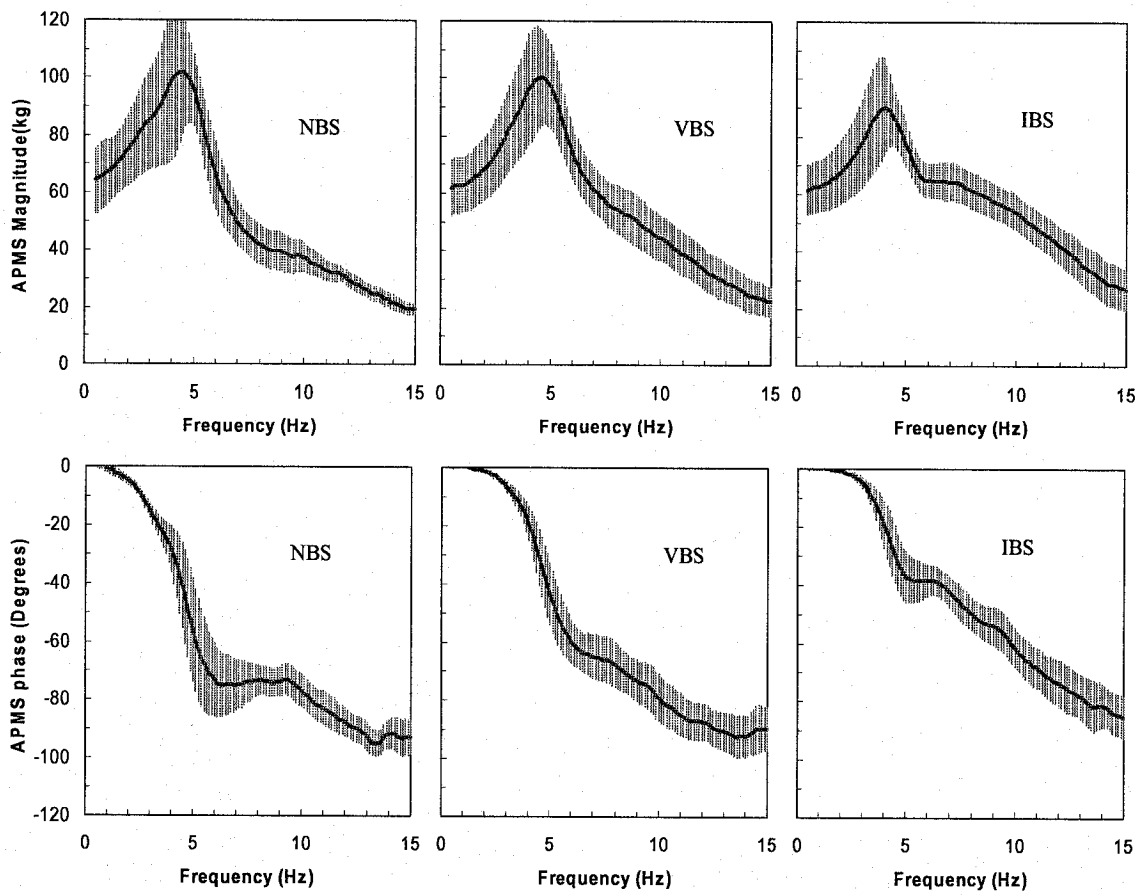

Figure 4.11: Mean curves and mean ± standard deviation scatters of the vertical APMS magnitude and phase responses for 12 subjects measured at 1.0 m/s^2 rms excitation under three back support conditions with hands in lap posture.

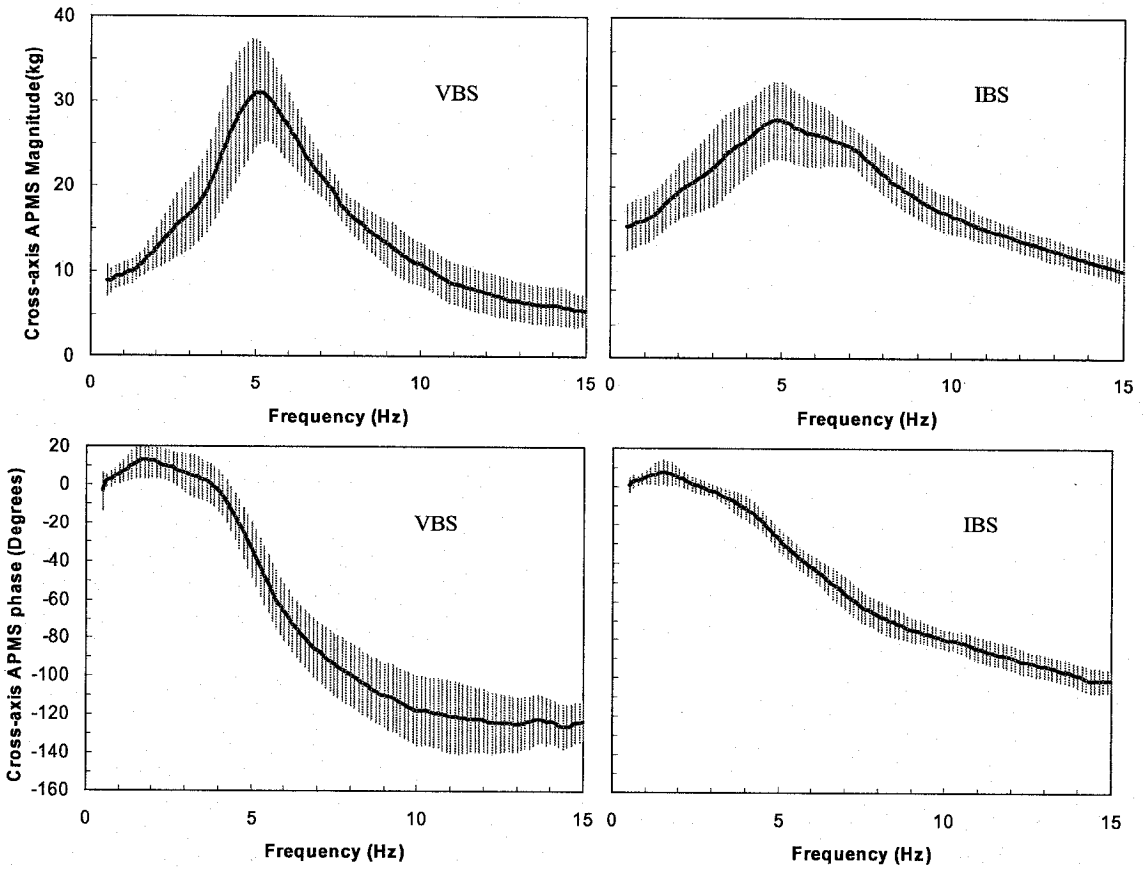

Figure 4.12: Mean curves and mean ± standard deviation scatters of the cross-axis APMS magnitude and phase responses for 12 subjects measured at 1.0 m/s^2 rms excitation under three back support conditions with hands in lap posture.

includes the trunk, head, neck, and arms is interacting with the backrest. The anthropometry suggests that the human upper body mass, including the masses due to head, neck, trunk and arms, accounts for nearly 67.8% of the total body mass for the hands-in-lap position, and 65.6% of the total body mass for the hands-on-steering wheel position [54]. The normal component of the upper body mass acting on the backrest is obtained by multiplying the upper body mass with the sine function of inclination angle (24°). This estimation assumes that the entire upper body is supported against the backrest. Table 4.5 presents comparisons of the measured static forces at the inclined

backrest for all the subjects with the estimated values. The table also lists the ratios of the measured static force to the estimated force for the hands in lap and hands on steering wheel postures. The results show reasonably good agreement between the estimated and measured values. The mean values of ratio of static measured to estimated forces are obtained as 0.98 and 0.99, respectively, for the hands in lap (LAP) and hands on the steering wheel (SW) postures. The overall percentage values of the body weight supported by the backrest, computed for all 12 subjects, are obtained as 27% of the total body mass, with standard deviation of 4.13% for hands-in-lap position; 24.93% with standard deviation of 3.56% for hands on the steering wheel position.

Table 4.5: Estimated and measured static forces at the backrest.

Subject ID	Body Mass (kg)	Static forces at the backrest (kg)					
		LAP			SW		
		Measured	Computed	Ratio	Measured	Computed	Ratio
1	72	17.29	19.85	0.87	16.91	18.09	0.93
2	87	21.54	23.98	0.90	21.03	21.86	0.96
3	74.2	19.04	20.45	0.93	18.77	18.64	1.01
4	88	24.47	24.26	1.01	21.66	22.11	0.98
5	77.2	19.65	21.28	0.92	17.74	19.40	0.91
6	77.3	21.91	21.31	1.03	19.31	19.42	0.99
7	66.6	19.32	18.36	1.05	18.68	16.73	1.12
8	99.6	28.24	27.45	1.03	25.62	25.02	1.02
9	79.6	22.71	21.94	1.04	20.19	20.00	1.01
10	66.4	16.73	18.30	0.91	14.42	16.68	0.86
11	73.2	20.12	20.18	1.00	18.19	18.39	0.99
12	66	19.38	18.19	1.07	18.72	16.58	1.13
Mean	77.3	20.87	21.3	0.98	19.27	19.41	0.99
Stdev	10.1	3.19	2.79	1.15	2.75	2.54	1.08

4.3.3 The APMS data normalization

Since the force-motion biodynamic functions are strongly dependent upon the body weight, as illustrated in section 3.2.1, it is often desirable to normalize the magnitude responses with respect to the seated mass [36,46]. Several methods of normalization have been used in the reported studies. Fairley and Griffin [36] derived the "normalized apparent mass" for each subject by dividing the apparent mass of the same subject measured at a low frequency of 0.5 Hz. Holmlund et al. [46] and Wu et al. [73], normalized the measured data for each subject corresponding to each posture with respect to the respective static mass supported by the seat. Both the approaches yield comparable results, since the APMS response at 0.5 Hz is close to the static mass on the seat. In this study, the normalization of both 'vertical APMS and 'cross-axis APMS' are carried out by dividing the magnitude responses by the corresponding values measured at 0.5 Hz.

Unlike the inclined backrest, the static forces at the vertical backrest were not related to anthropometric characteristics of human body. Also from Figure 4.10 and 4.12, a greater inter-subject variability was generated due to this posture. Therefore, the subsequent analysis for the normalized cross-axis APMS will exclude this case. Although in the previous chapter, the normalized data was not suggested to characterize the various factors from the postural variation, the dimensionless characteristics would facilitate the overall analysis of simultaneous biodynamic responses since the seat-to-head transmissibility is a non-dimensional quantity.

Figure 4.13 illustrates the normalized magnitude responses of 'vertical APMS'. The corresponding mean curves with standard deviation on the mean as the error bars are presented in Figure 4.14. Figure 4.13 clearly reveals that the normalization greatly

reduces the scatter of the magnitude responses at frequencies below the primary resonances. Figure 4.14 further shows the coefficient of variation of normalized APMS magnitude is below 20% after the primary resonances, irrespective of the sitting postures and excitation magnitudes, which are believed to considerably reduce the scatter among the data acquired for different subjects compared with the non-normalized APMS data.

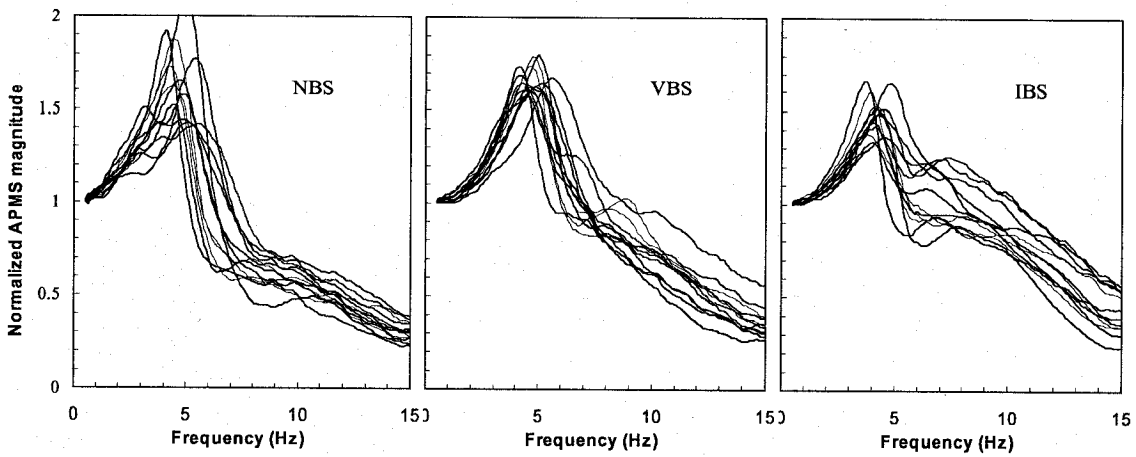

Figure 4.13: 'Vertical APMS' normalized magnitude responses of 12 subjects under 1.0 m/s^2 rms excitation with three back support conditions and hands in lap postures.

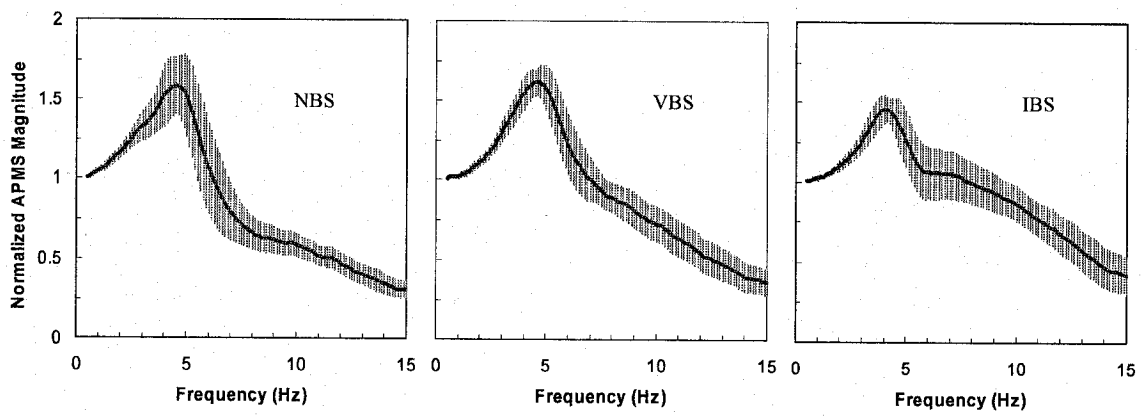

Figure 4.14: Mean curves and standard deviation scatters of 12 subjects in the normalized vertical APMS responses under 1.0 m/s^2 rms excitation with three back support conditions and hands in lap postures.

Figure 4.15 illustrates normalized magnitudes of 'cross-axis APMS' (M_{vb}) responses of 12 subjects seated assuming two hands position with the inclined back support, while exposed to 1 m/s^2 rms acceleration excitation along a vertical axis. It is evident that scatter for the SW posture is much greater than that for the hands in lap posture, especially around the primary resonance.

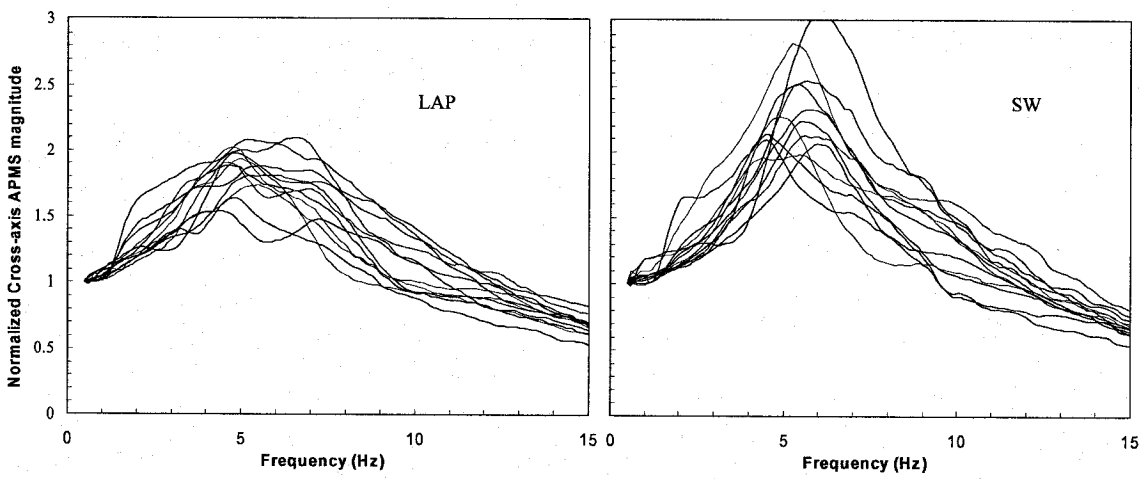

Figure 4.15: 'Cross-axis APMS' normalized magnitude and responses of 12 subjects measured at 1.0 m/s^2 rms with the inclined backrest.

The cross-axis biodynamic behaviour of the seated body has not been characterized, only one single study has reported the back supported forces for the vertical back support with hand in lap [51]. The results presented in Figures 4.15, however, suggest that the two hands positions may strongly affect the cross-axis APMS responses.

The results presented in Figure 4.9 suggest that the back support condition strongly affects the vertical APMS responses. Furthermore, the hands position and vertical vibration magnitude may also influence the APMS responses, while little has

been reported in the literature on the influences of such factors. The measured data were thus analyzed to study the effects related to different experimental conditions considered in this study.

Owing to the strong dependence of the APMS on the body mass, the analyses are performed for a subset of datasets containing the data acquired for a smaller subject population of comparable body mass. For this purpose, the data acquired for a total of 6 subjects with body mass ranging from 70.5 to 79.96 kg (mean= 75.58kg; standard deviation =2.90 kg) are selected from the ensemble of 12 subjects in order to examine the influence of postural factors variations. The analyses based on this selected subset of data are expected to eliminate the strong inter-subject variability arising from variations in the anthropometric variables, such as the body mass. The effects of excitation levels and posture-related factors are characterized by analyzing the normalized APMS of 6 selected data sets in the following sections.

4.3.4 Peak variation of APMS responses

Table 4.6 summarizes the mean values of the primary resonant frequencies observed from the measured 'vertical APMS' and 'cross-axis APMS' responses attained under different combinations of experimental conditions, together with the standard deviations of the means. The mean primary resonant frequencies decrease with increasing excitation magnitude, as observed in earlier results. This softening tendency seems to be greater for the VBS posture for both 'vertical APMS' and 'cross-axis APMS' responses than that for the other two back support conditions. Only one exception was observed for the 'cross-axis APMS' responses with the inclined back support while hands were

placing on the steering wheel. The difference in mean primary resonant frequency attained under lowest and highest excitation amplitude is 1.23 Hz for the 'vertical APMS' and about 1.35 Hz for the 'cross-axis APMS' responses. For identical back support condition, the SW posture yields relatively larger difference compared with the LAP posture except for 'vertical APMS' response under VBS. The difference in the frequencies between the LAP and SW postures diminishes under higher excitations for the inclined back support for both 'vertical APMS' and 'cross-axis APMS' responses, as it was observed in the STHT responses. The above findings again suggest greater softening effect of increasing magnitude for the SW posture.

The standard deviation of the primary resonance tends to increase as the excitation magnitude decrease for both 'vertical APMS and 'cross-axis APMS' frequencies. The standard deviations tend to be considerably higher for 'cross-axis APMS' frequencies when compared to those for the 'vertical APMS', irrespective of the hands position and back support condition. The same trend was also revealed in vertical and fore-and-aft STHT responses, as shown in Table 4.3.

Table 4.6: Primary resonance frequencies (mean and SD values) for both 'vertical APMS' and 'cross-axis APMS' responses.

Back support condition		No back support			Vertical back support			Inclined back support		
Excitation (m/s^2 rms)		0.25	0.5	1.0	0.25	0.5	1.0	0.25	0.5	1.0
Vertical APMS	LAP	5.61	4.99	4.76	5.92	5.19	4.69	5.29	4.70	4.22
		0.48	0.69	0.46	0.60	0.48	0.43	0.48	0.42	0.28
	SW	5.78	5.11	4.84	6.26	5.77	5.07	5.51	4.91	4.23
		0.45	0.59	0.36	0.76	0.73	0.43	0.63	0.51	0.31
Cross-axis APMS	LAP				6.35	5.68	5.34	5.93	5.17	5.16
					0.68	0.71	0.70	1.22	0.74	0.64
	SW				6.60	5.96	5.25	6.82	5.85	5.36
					0.77	0.75	0.54	1.05	0.83	0.50

4.3.5 Effect of excitation magnitude on APMS

Figure 4.16 compares the normalized vertical APMS responses measured with hands in lap for the 6 subjects while exposed to three excitation levels under three back support conditions. The results shown in Figure 4.16 distinctly reveal that the primary resonance tends to shift to a lower frequency with increasing vibration magnitude, irrespective of the back support condition. Similar trends were also observed for the phase response, while the shift in frequency is more evident for the back supported postures. The secondary resonant frequency in the vertical APMS response, which is more evident with the vertical and inclined back supports, also decreases with increasing vibration magnitude. The shift in the secondary resonance frequency for the IBS was larger than that of VBS posture. The results also suggest that the mean primary resonance for the inclined back support posture decreases by approximately 1.01 Hz (from 5.29 Hz to 4.22 Hz), when vertical excitation magnitude is increased from 0.25 to 1.0 m/s^2 rms. The same trends are also observed in the STHT responses (Figure 4.5).

The 'softening effect' of the seated body is also evident for the 'cross-axis APMS' under the inclined back support posture with the two hands positions, as shown in Figure 4.17. The results suggest that the mean primary resonance decreases by approximately 0.77 Hz and 1.46 Hz for the hands in lap and hands on the steering wheel, respectively, when vertical excitation magnitude is increased from 0.25 to 1.0 m/s^2 rms.

4.3.6 Effect of hands position on APMS

Figure 4.18 compares the normalized vertical APMS responses measured with two hands position (in lap and on the steering wheel) for the 6 subjects while exposed to

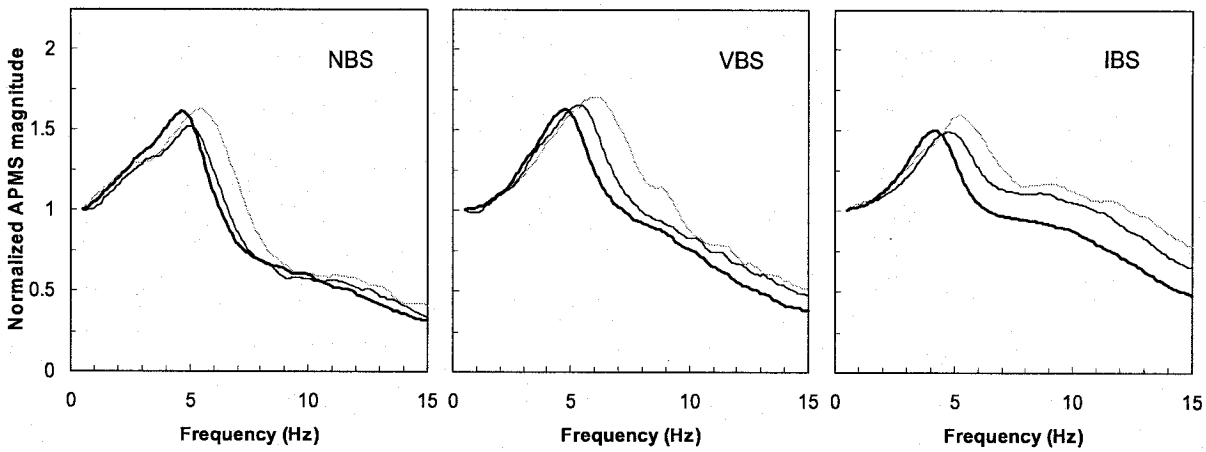

Figure 4.16: Influence of excitation magnitude on mean vertical APMS responses of 6 subjects with hands in lap posture: —1.0 m/s^2 rms; — 0.5 m/s^2 rms; ····· 0.25 m/s^2 rms.

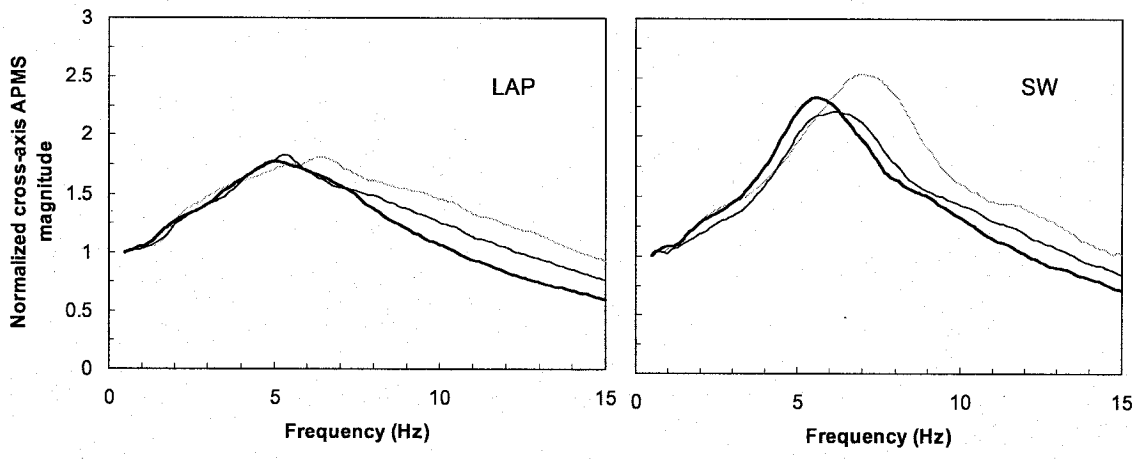

Figure 4.17: Influence of excitation magnitude on mean cross-axis APMS responses of 6 subjects with hands in lap posture: —1.0 m/s^2 rms; — 0.5 m/s^2 rms; ····· 0.25 m/s^2 rms.

excitation level of 1.0 m/s^2 rms. The hands position reveals relatively larger differences in the normalized APMS magnitude occurring around the primary resonance for the NBS condition, as opposed to the VBS and IBS conditions (Figure 4.18). For the back supported postures, the differences in the normalized APMS magnitude are observed in

the 6 to 9 Hz frequency range. Figure 4.18 also compares the normalized cross-axis APMS responses measured with two hands position (in lap and on the steering wheel) for the 6 subjects while exposed to excitation level of 1.0 m/s^2 rms. The hands position reveals relatively larger differences in the magnitude occurring around the primary resonance. Hands on the steering wheel posture result in a higher peak magnitude and primary resonance. This may suggest that the hands position strongly influences the cross-axis APMS under the inclined back support, and due to the manner in which the upper body interacts with the backrest, while the hands position on 'vertical APMS' was considered to be negligible.

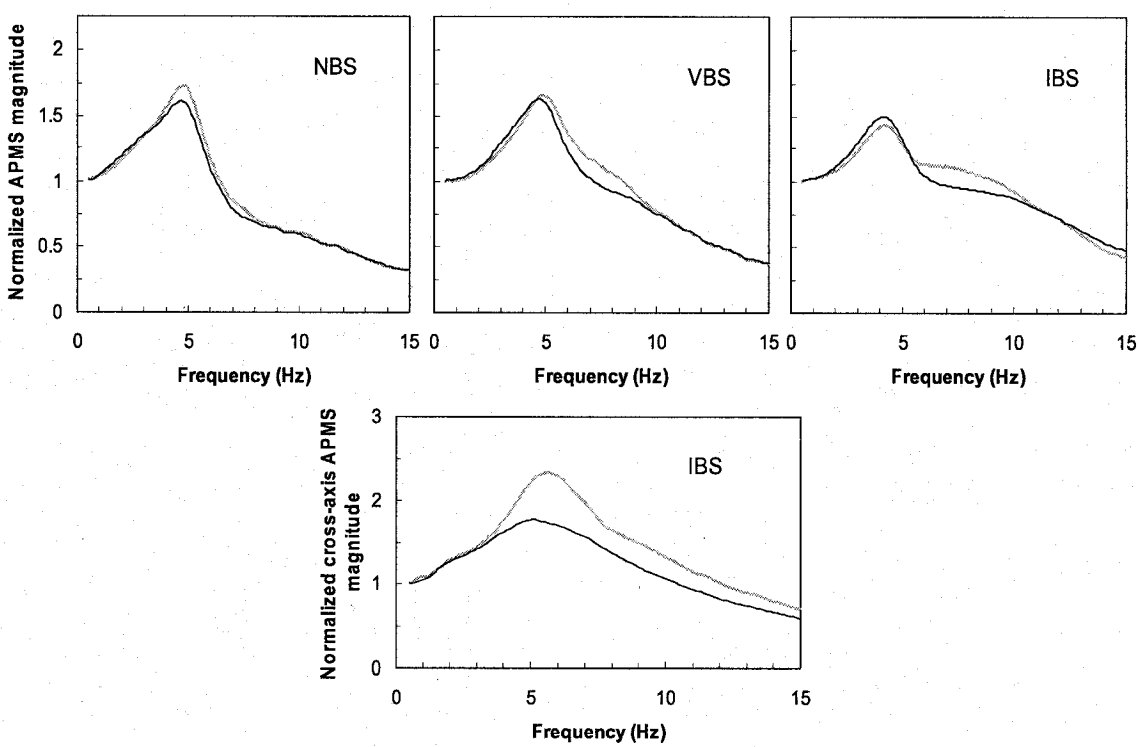

Figure 4.18: Influence of hands position on mean vertical and cross-axis APMS responses of 6 subjects under different back supported conditions: ——Hands in lap; ——hands on steering wheel (Excitation: 1.0 m/s^2 rms).

In the previous Chapter, the hands position tends to strongly affect the APMS and absorbed power response under vertical WBV exposure, particularly when the exposed subject utilizes an inclined backrest support. The observed differences in the effects of hands position on the simultaneous force-motion and motion-motion responses as well as the single driving-point force-motion could be attributed to the differences in the column geometry and the excitation level.

4.3.7 Effect of back support condition on APMS

Figure 4.19 illustrates the comparisons of mean normalized APMS magnitude responses attained for the three back support conditions (NBS, VBS and IBS) under exposure to 1.0 m/s^2 rms excitation and the LAP posture. For the vertical APMS (M_v), the primary resonance of the body with IBS occurs at a lower frequency compared to that with NBS and VBS, this trend is somehow opposite to that observed from the reported APMS responses [93], which may be attributed to the differences in seat geometry dependent postures and excitation magnitudes. The secondary resonance for the IBS, on the other hand, occurs at a relatively higher frequency than those for the NBS and VBS postures. The peak normalized magnitude of vertical APMS (M_v) corresponding to this secondary resonance is significantly higher than those for the other support conditions. In the 0.5-3 frequency Hz range, the NBS posture yields relatively higher value of normalized APMS modulus. The results presented in Figure 4.19 also exhibit the highest modulus of M_v for the IBS posture at frequencies above 9 Hz. At frequencies above 9 Hz, the normalized APMS magnitude increase for the back supported postures. The same finding was also revealed in the vertical STHT magnitude, as shown in Figure 4.7.

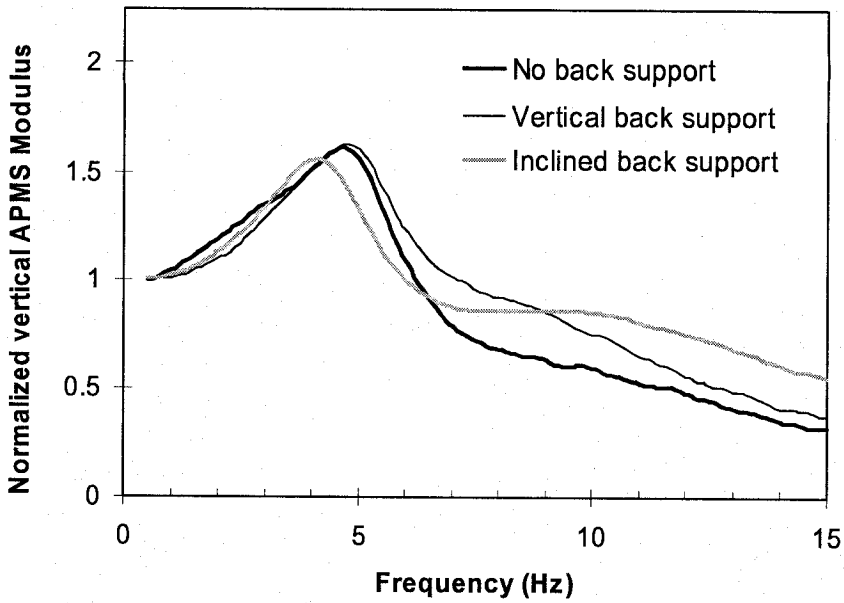

Figure 4.19: Influence of three back support conditions on mean APMS responses of 6 subjects; —— No back support; —— Vertical back support; —— Inclined back support (Hands in lap; excitation: 1.0 m/s^2 rms).

Similar to single-driving point force-motion biodynamic responses [93,95], those studies have shown that both the APMS and absorbed power magnitudes in the vicinity of the secondary resonance tend to be higher for the back supported postures. The same conclusion was also established in simultaneously measured APMS and STHT responses.

4.3.8 Comparison of vertical APMS responses of body seated on two different seats

As introduced in Chapter 2, the single force-motion and simultaneously biodynamic characterizations have employed two different rigid seats. The former test seat represents a commercial seat geometry, while the latter represents an automobile seat

structure. In order to investigate the effect of seat design factors on the biodynamic responses, the mean APMS responses were derived for both two seats. For the commercial seat, the data acquired for a total of 7 subjects with body mass ranging from 72.2 to 78 kg (75.1±2.38 kg) were selected from the ensemble of 27 subjects. The subjects were exposed to 1.0 m/s^2 rms in the 0.5-40 frequency Hz with the lowest seat height (410 mm). For the automobile seat, the data acquired for a total of 6 subjects with body mass ranging from 70.5 to 79.96 kg (75.58±2.90 kg) were selected from the ensemble of 12 subjects. The subjects were exposed to 1.0 m/s^2 rms in the 0.5-15 frequency Hz. Considering the different steering column configuration employed in two measurements, only hands in lap posture responses were selected. It should be noted that effective excitation for the commercial seat is considerably small that employed for the automobile seat due to differences in the excitation frequency bands.

Figure 4.20 illustrates comparisons of the mean vertical APMS magnitude responses derived for the two test seats. Corresponding to each back support condition, the peak magnitudes of APMS could be considered comparable. The responses, however, in the primary resonances, exhibit notable differences, which became larger with the back supported postures. With the inclined backrest support, the primary resonance observed from the peak APMS response for the automobile seat, in the order of 4.25 Hz, increases to nearly 6Hz acquired for the commercial seat. This may be partly attributed to the difference in the excitation magnitude. However, the contributions due to seat design factors, such as differences in backrest inclination and seat height can not be neglected. The comparisons thus suggest that the biodynamic response characterization of the seated body exposed to WBV necessitates considerations of the seat design factors.

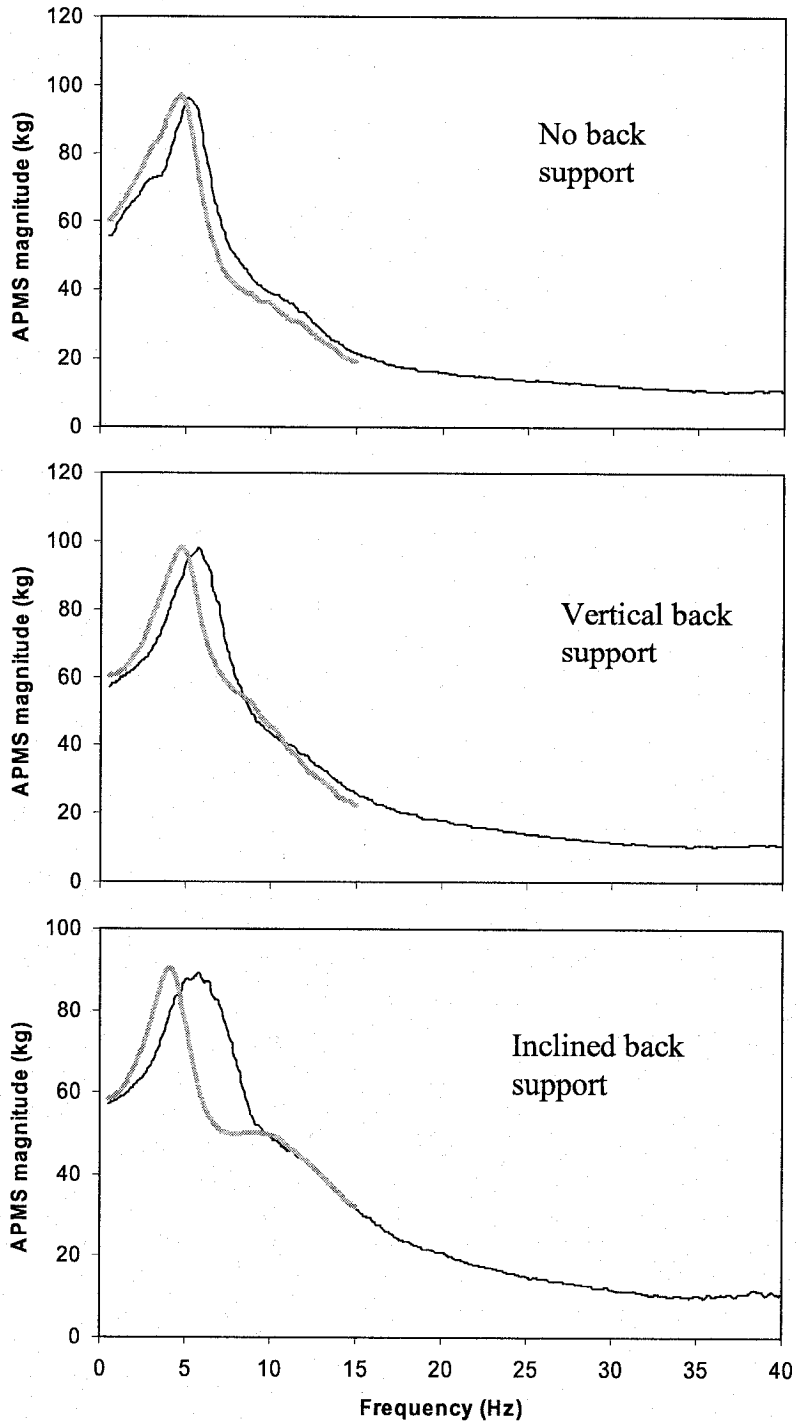

Figure 4.20: Comparison of vertical APMS magnitude responses acquired from the different seats under three back support conditions with hands in lap posture; ——7 subjects seated in commercial seat (Backrest inclination: 12°; seat height: 410 mm; excitation: 1.0 m/s^2 rms and 0.5-40 Hz); —— 6 subjects seated in automobile seat (Backrest inclination: 24°; seat height: 220 mm; excitation: 1.0 m/s^2 rms and 0.5-15 Hz).

4.4 Relationship between the simultaneously measured APMS and STHT responses

Figure 4.21 provides the comparisons of the normalized vertical APMS and vertical STHT moduli measured under hands in lap posture with 1.0 m/s^2 rms excitation. It is evident, that for all the back support conditions, the primary resonances are nearly identical. For the no back support posture, the measured modulus of STHT tends to be

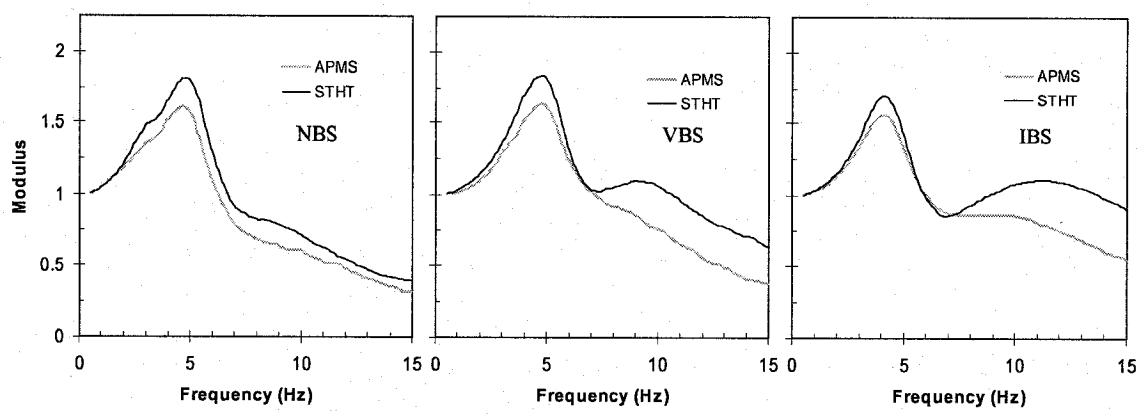

(a)

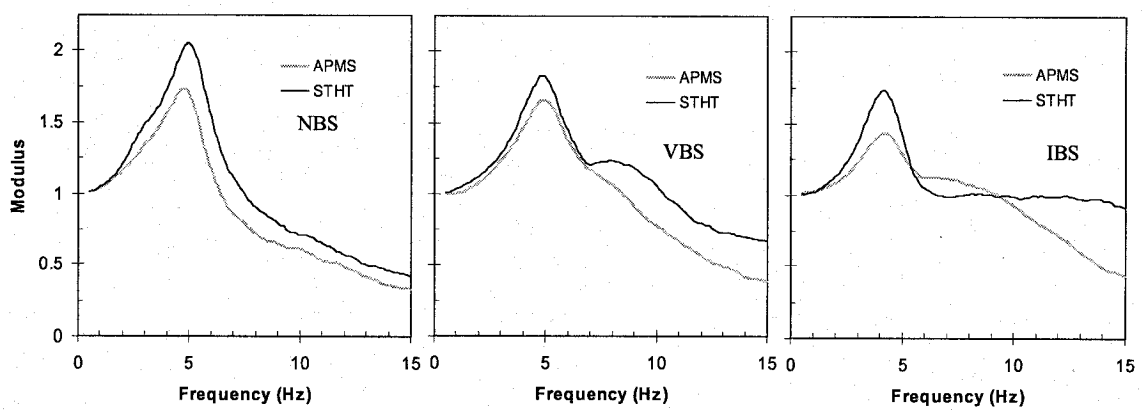

(b)

Figure 4.21: Comparison of STHT and normalized APMS moduli responses (excitation: 1.0 m/s^2 rms): (a) Hands in lap; (b) Hands on the steering wheel.

relatively higher than measured normalized APMS magnitude over the entire frequency range. For the two back support postures, similar trends occur only from 0.5-6 Hz, which cover the first primary resonance. At higher frequencies, there are quite large differences between the normalized APMS and STHT magnitudes for the two back supported postures. It could be clearly observed that the STHT responses are more sensitive to the secondary resonance compared to the APMS responses.

Figure 4.22 further shows the good agreements between the normalized APMS and STHT as far as the primary resonances are concerned. For both APMS and STHT responses, standard deviations of primary resonance is relatively larger for the no back support posture with the values of 0.43 Hz and 0.46 Hz respectively, the smallest standard deviations in the primary resonance were observed for the inclined back support posture, which were 0.28 Hz for APMS responses and 0.35 Hz for STHT responses. This may suggest that the subjects tend to maintain a more stable sitting posture with the use of backrest.

Figure 4.23 reveals a similar trend in both vertical STHT modulus and normalized vertical APMS moludus for the three back support conditions. The results suggest the same important role of seat geometry on simultaneously measured force-motion and motion-motion biodynamic responses. Wu et al. [73] have investigated the relationship between the APMS and STHT based upon the models validated using the APMS measurement. A close agreement between the normalized APMS and STHT functions was also established in terms of the magnitudes and the primary resonant frequency of the seated body. However the models used in that study do not describe a direct

biomechanical representation of the head. Therefore, the estimation of STHT in that study was under-evaluated, and caution must be exercised in interpreting these results.

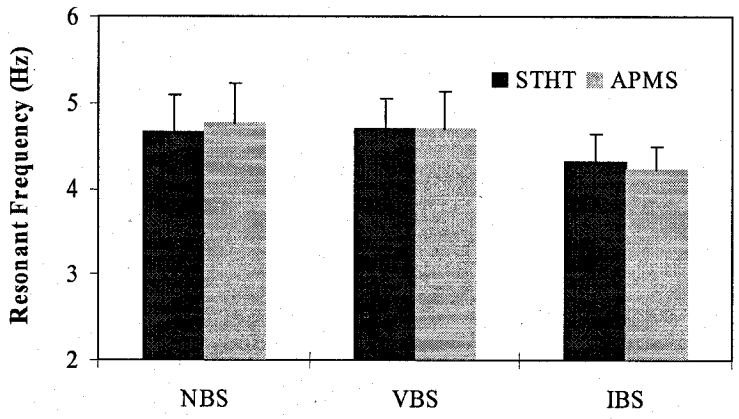

(a)

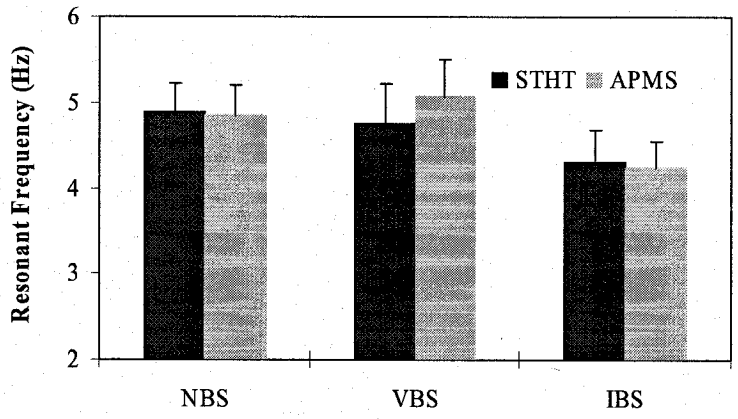

(b)

Figure 4.22: Comparison of primary resonance frequency derived from the STHT and APMS (excitation: 1.0 m/s^2 rms), (a) Hands in lap; (b) Hands on the steering wheel.

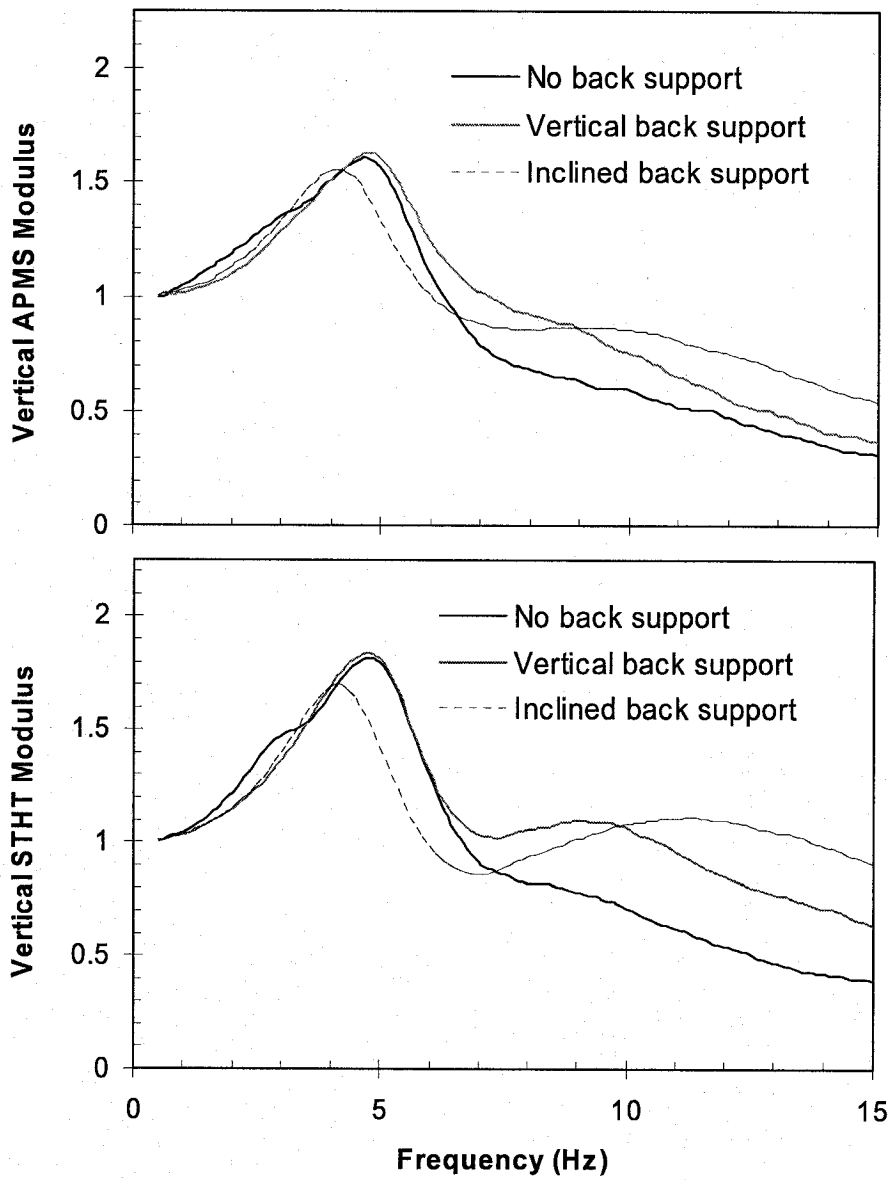

Figure 4.23: Influence of three back support conditions on simultaneous mean APMS and vertical STHT responses of 6 subjects; ——No back support; ——— vertical back support;------- Inclined back support (Hands in lap: excitation: 1.0 m/s^2 rms).

4.5 Comparison with ISO 5982

As stated in Chapter 1, the STHT responses of vibration-exposed seated human subjects show extreme variabilities. The data reported in different studies show most significant inter- and intra-subject variabilities, which are greatly attributable to differences in the experimental conditions [11], apart from the measurement and data analyses methods. The reported datasets may thus be applicable only for the chosen experimental conditions. The syntheses of the reported datasets therefore must involve careful considerations of the test conditions.

ISO 5982 [12] presents the ranges of STHT responses on the basis of a synthesis of datasets reported under somewhat comparable conditions that were considered to represent those applicable for vehicle driving. Owing to the lack of data for the back supported postures, the data synthesis was limited to only no back support postures. The reported synthesis thus resulted in significantly smaller variabilities than those reported by Paddan and Griffin [35]. Figure 4.24 shows comparisons of the mean 'vertical STHT' responses acquired for the three back supports with hands in lap posture and exposure to 1 m/s^2 excitation with the standardized range. The results show good agreement with the standardized range in view of the primary resonance, while the peak moduli tend to be closer to the upper bound of the standardized values, irrespective of the back support condition. While the magnitude response for the NBS posture remains well below the lower bound at frequencies above 6 Hz, the response for the IBS posture exceeds the upper bound at frequencies above 12 Hz. The magnitude response for the VBS posture remains within the bounds in the entire frequency range, except in the vicinity of 6.5 Hz, although the standardized values are considered applicable only for the NBS posture.

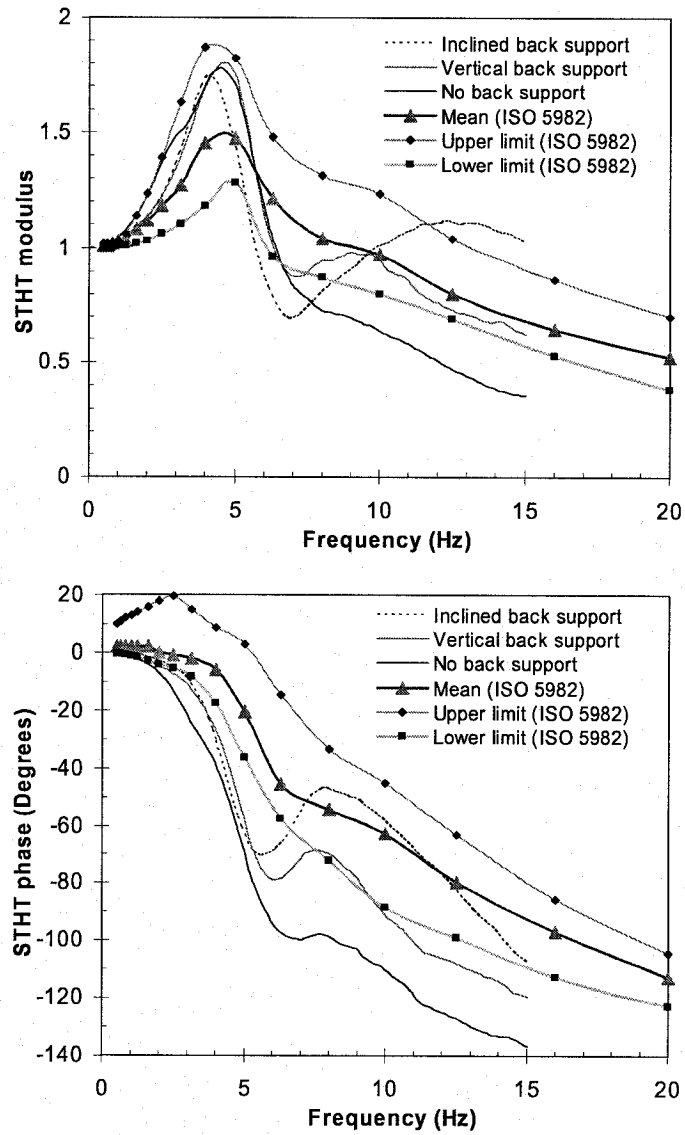

Figure 4.24: Comparison between the idealized ranges of STHT responses provided in ISO 5982 with the mean responses of 12 subjects under three back support conditions and hands in lap posture (excitation: 1.0 m/s^2 rms).

Considering that the standardized values were derived from the synthesis of only a few datasets, a number of which were acquired under relatively higher levels of

vibration, further efforts in acquiring the STHT responses would be desirable to deduce more reliable ranges. Moreover, the vehicle seats are invariably designed to provide enhanced support for the occupant back through an inclined backrest, which poses constraints on the upper-body movements, and thereby tends to limit the angular and fore-and-aft motions of the upper body in the vicinity of the primary resonance. Additionally, an inclined backrest serves as a supplementary source of horizontal movement to the upper body and thus alters the body interactions with the seat pan and the backrest. Additional data on the nature of vibration transmission with an inclined back support under representative vibration excitations would be highly desirable to assist in the standardization efforts.

Figure 4.25 shows comparisons of the mean 'vertical APMS' responses acquired for the three back support conditions with hands in lap and exposed to 1 m/s^2 rms excitation with the standardized range. The results show reasonably good agreement with the standardized range in view of the primary resonance, while the peak moduli tend to be closer to the upper bound of the standardized values for no back and vertical back postures. While the magnitude response for the IBS posture remain beyond the upper bound at frequencies above 7 Hz, The magnitude response for the NBS and VBS postures remain within the bounds in the entire frequency range, except in the vicinity of 6.5 Hz, although the standardized values are considered applicable only for the NBS posture.

Unlike the magnitude responses, the phase responses tend to be closer but out of the lower bound of the standardized values for VBS and NBS postures at frequencies above 9 Hz. At frequencies above 8 Hz, the phase response falls between the mean and

upper bound for the IBS posture, and at the frequency interval of 5-8 Hz, the phase response is beyond the upper bound for IBS posture.

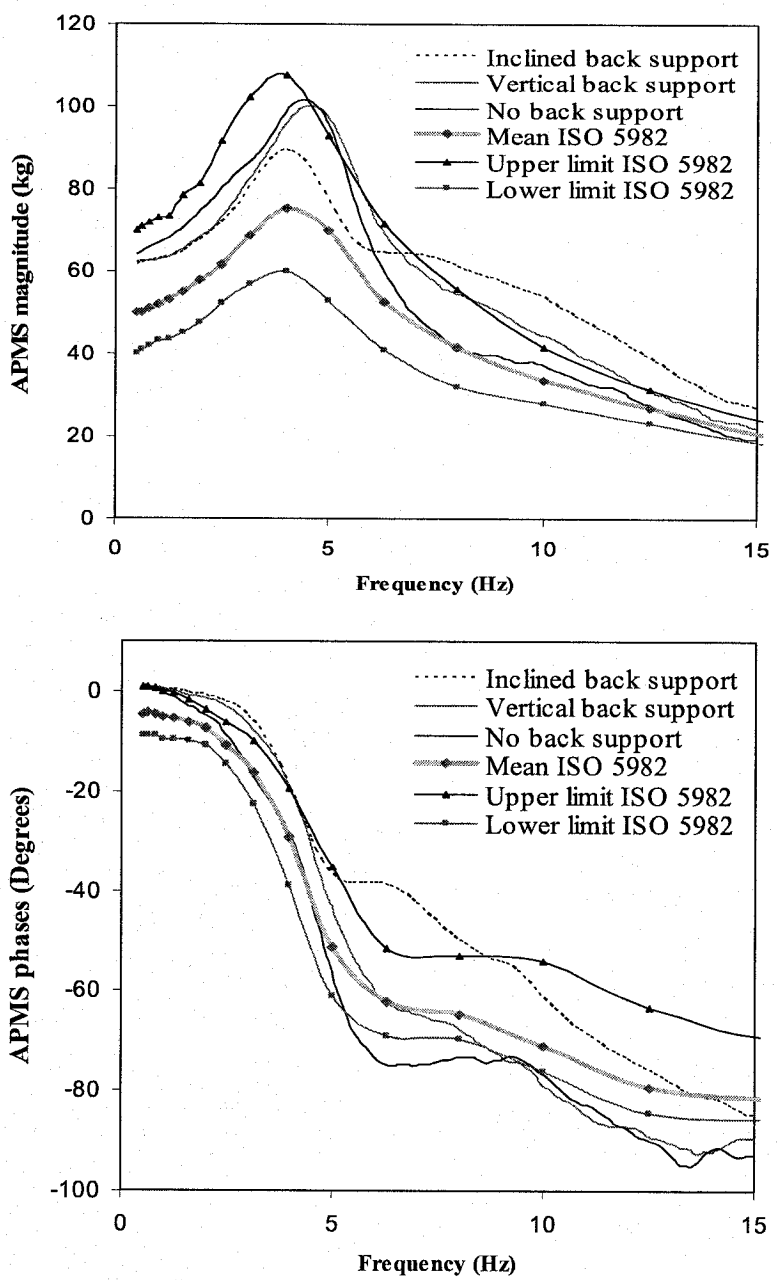

Figure 4.25: Comparison between the idealized ranges of APMS responses provided in ISO 5982 with the mean responses of 12 subjects under three back support conditions and hands in lap posture (excitation: 1.0 m/s^2 rms).

Figure 4.26 reveals the difference between the normalized APMS response and STHT response of the ISO 5982. At frequencies above 5 Hz, the modulus of STHT is much higher than that of APMS, and even around the primary resonance, the difference is

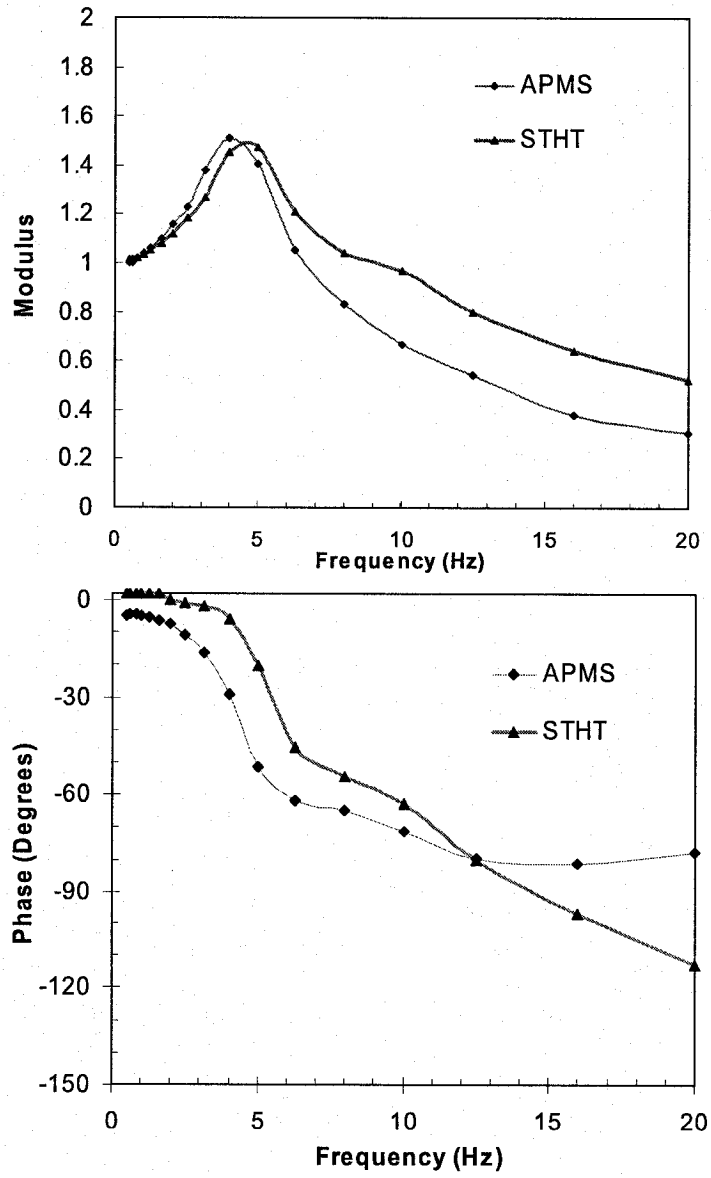

Figure 4.26: Comparison of modulus and phase responses of STHT and normalized APMS magnitude and phase responses (derived from ISO 5982).

observed for two biodynamic responses. The phase difference between two responses was evident over the entire frequency range. Although the datasets selected in ISO-5982 were mainly for the no back support condition, the differences between two responses were much higher than those derived from the simultaneous measurements conducted in this study. This may suggest that simultaneous measurements of force-motion and motion-motion biodynamic functions would be significant for enhancing understanding and characterization of biodynamic responses, and model development of seated human body subject to WBV would be more constructive based upon the simultaneous measurements.

4.6 Summary

Simultaneous measurements of the apparent mass and seat-to-head vibration transmission characteristics of seated occupants exposed to whole-body vertical vibration were investigated through measurements performed with 12 adult male subjects. A strap-mounted accelerometer was employed to measure the vertical vibration transmitted to the head. The proposed approach to measuring the head motion could facilitate the adjustment and monitoring of the accelerometer orientation, while reducing the discomfort caused by a 'bite-bar' system, and the inertial force contributions arising from the helmet-mounted measurement systems. Measured seat-to-head biodynamic response in both vertical and fore-and-aft directions were further statistically characterized to examine the effects of three main factors: back support condition (no back, vertical back, inclined back support), excitation magnitude (0.25, 0.5, 1.0 m/s^2 rms white noise in the frequency range 0.5-15 Hz) and two hands position (Hands in lap and hands on the

steering wheel). The measured data suggest that the back supported postures generally yield lesser inter-subject variability of the data in the vicinity of the primary resonance. The secondary resonant peak becomes apparent for the back supported postures, which occurs in the 9-11 Hz range. The results show significant magnitudes of fore-and-aft head acceleration even though the vibration excitation is limited to the vertical axis alone, which is most likely attributed to pitch motions of the upper body. The peak magnitude of fore-and-aft STHT tends to be considerably higher than that of the vertical STHT for the no back support posture. The peak magnitude of fore-and-aft STHT for the back supported postures are comparable with the vertical STHT magnitude. The results also suggest that backrest tends to constrain the upper-body movements, which alters the body interactions with the seat. The peak magnitude of fore-and-aft STHT in the vicinity of the primary resonance is most significantly affected by the back support conditions. The use of an inclined back support can help suppress the fore-and-aft motion of the head most notably near the primary resonance. This support, however, causes significantly higher vertical and fore-and-aft motion of the head near the secondary resonant frequency. The results of the ANOVA have further shown the strong influence of the three back support conditions on both vertical and fore-and-aft STHT responses over the entire frequency ranges. Both the vertical and fore-and-aft STHT responses exhibit the non-linearities. The influence of hands position on both vertical and fore-and-aft STHT was considered to be negligible in this study.

'Vertical APMS' and 'cross-axis APMS' responses were analyzed to reveal the dynamic interaction between the seated body and seat for the back supported conditions. Without back support, only 'vertical APMS' responses were obtained. Owing to the

strong effects of the body mass, the analyses of measured APMS responses are performed on a subset of data attained for 6 subjects with body mass 70.5 to 79.96 kg. The results reveal the non-linearites for both 'vertical APMS' and 'cross-axis APMS' responses, as widely reported in force-motion biodynamic responses. The hands position yields relatively larger differences in peak magnitude and primary resonant frequency on 'cross-axis APMS' magnitude responses, while the hands position on 'vertical APMS' responses was considered to be negligible. The results also reveal that the vertical APMS magnitudes in the vicinity of the secondary resonance tend to be higher for the back supported postures.

Simultaneously measured APMS and STHT responses showed good agreements as far as the primary resonances are concerned irrespective of the back support condition, while the considerable differences between the normalized APMS and STHT magnitudes were found in the secondary resonance range for the back supported postures. The following model development will emphasize the effects of back support condition on the force-motion and motion-motion biodynamic responses.

CHAPTER 5

DEVELOPMENT OF SEATED HUMAN BODY MODEL

5.1 Introduction

The human body is a complex active dynamic system, the physical, biological and mechanical properties of which vary from moment to moment and from one individual to another. The vibration performance of a seat relies upon the biodynamic behavior of the seated body. Considerable efforts have thus been made to develop mechanical-equivalent models of the seated body to facilitate analyses of the coupled occupant-seat system. The development of the seated body model necessitates thorough knowledge of whole-body biodynamics. Considerable efforts are also being made in developing anthropodynamic manikins for effective experimental assessments of seat-occupant system [64]. The construction of a mechanical dummy generally relies on the biodynamic responses of models which derived under particular sitting conditions. A lumped-parameter mechanical-equivalent biodynamic model coupled with the seat model could serve as effective assessment and suspension design tool.

The reported biodynamic responses, in terms of force-motion (APMS/DPMI) and motion-motion (STHT) relationships, have invariably shown resonant behavior of the body, and extreme variations with vibration excitation and seating conditions, as observed in the previous chapters. The development of a biodynamic model is thus a complex task to reflect adequately the complexity of human biodynamics. A number of lumped-parameter seated human models, comprising interconnection of masses, springs and dampers, have been proposed on the basis of the measured biodynamic responses [71]. The parameters of these models have been identified from either measured

mechanical impedance or vibration transmissibility response characteristics of the seated human subjects exposed to whole-body vertical vibration. The vast majority of those models, with only a few exceptions [54,71], consider the data acquired for the subjects seated without a back support. A few studies have also attempted to derive models to satisfy both measures, APMS and STHT [8,9,71], in order to identify more reliable model parameters. These studies, however, employed the APMS and STHT data acquired in different laboratories and most likely acquired under different conditions. Consequently, these models revealed poor agreement with the measured STHT, while good agreement with APMS was evident [8,9,71].

The important influences of anthropometric variables and sitting postures on the biodynamic responses have been widely recognized. Furthermore, the role of seat geometry on the biodynamic response has been thoroughly characterized in this dissertation. The results clearly show that the back support conditions contribute tremendously to both force-motion (APMS) and motion-motion (STHT) biodynamic functions. The development of biodynamic models of seated body thus needs to consider the contribution arising from the back support condition so that the dynamic interaction between the seated body and seat could be fully revealed. Since the contribution due to back support are more clearly evident in the STHT responses, it is desirable to consider both STHT and APMS datasets for model development. Moreover, consideration of the two datasets is expected to identify more reliable model parameters.

In this chapter, modeling the seated body applicable to automotive environment was investigated with consideration of the seat geometry, particularly the use of backrest. Both one-dimensional and two-dimensional analytical models are proposed to satisfy

both APMS and STHT responses which were simultaneously measured under vertical vibration, as described in the previous chapters. The model formulation also considers the dynamic interactions of the upper body with the back support. A constrained optimization based identification approach was applied to identify the model parameters.

5.2 One-dimensional modeling

Seat-to-head transmissibility (STHT) and mechanical impedance (APMS/DPMI) characteristics of seated human body exposed to vertical WBV have been widely measured. The measured data generally reveal two peaks in the magnitude responses in the concerned frequency range. Some researchers have thus employed as little as two-degrees-of-freedom models to fit these frequency response functions [25,65]. Other studies have employed higher degrees-of-freedom of lumped parameter models to match the measured responses [9,19,28,66,69].

Majority of the models proposed in the literature are one-dimensional lumped-parameter models with little consideration of the body anatomy. Only a few models, such as those proposed by Boileau [19], Mertens [28], Payne and Band [66], Amirouche and Ider [69], were defined with the consideration of biomechanical properties of the human body. However, the validity of none of these models with the exception of Mertens' model, was verified by satisfying both vibration transmissibility and mechanical impedance biodynamic responses, however, has not been demonstrated with the exception of the model proposed by Merten [28].

A biodynamic model should not only describe the essential features of the data on which it is based, but also reflect some attributes of anatomical parts of the body. For

example, it is desired the model derived to satisfy the seat-to-head transmissibility response, at best, provide the representation of the human head. Since the biodynamic measurements are still predominantly conducted under one directional excitation, the biodynamic data mainly represent the human response in the direction along the excitation.

In this section, a relatively simple one-dimensional model structure is proposed for simulating the vertical APMS and STHT biodynamic responses under vertical WBV. The model parameters are identified on the basis of the mean normalized vertical APMS and vertical STHT magnitude data that will be further described in section 5.2.2.

5.2.1 One-dimensional 4-DOF model

Figure 5.1 illustrate the structure of the proposed one dimensional model, which is formulated upon the consideration of the seated body anatomy in the vertical direction only. The proposed model comprises five masses, coupled by linear elastic and damping elements. Similar to Payne and Band model [66], a simple dynamic representation of the viscera mass is applied in the model. The model components can be related to anatomical structures of the human body. Specifically, m_3 represent the head; m_4 represent the viscera mass, m_1 and m_2 may represent lower and upper body torso respectively. The lower mass m_0 represents the body portion in contact with the seat pan. The model neglects the dynamic interactions between the upper body and back support.

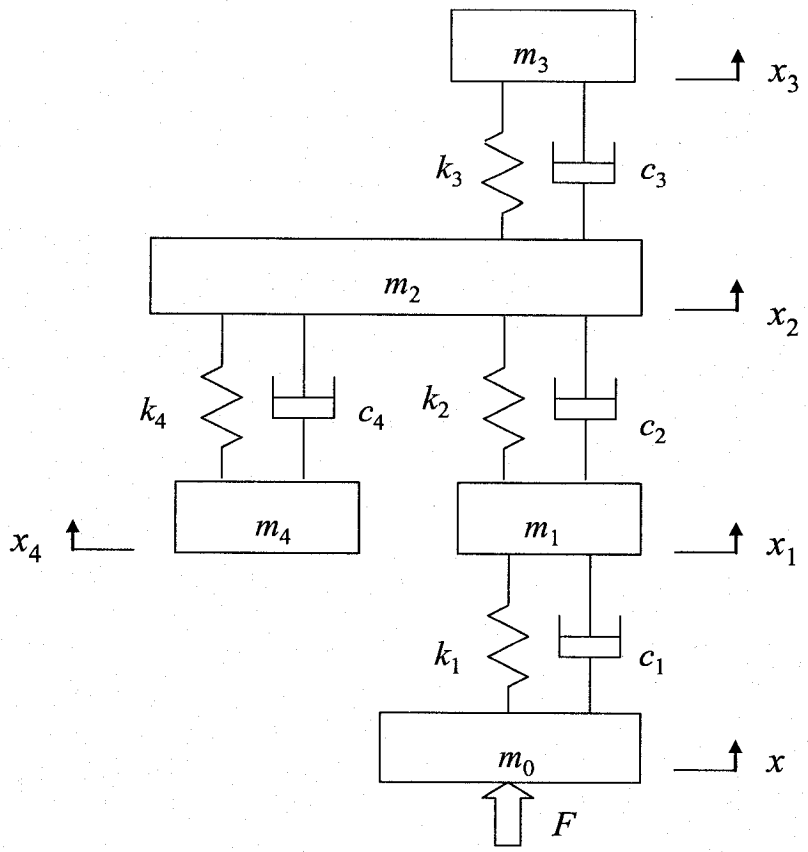

Figure 5.1: Proposed one-dimensional four-DOF seated body biodynamic model.

Assuming linear properties of the elastic and damping elements, the motions of the masses along the vertical direction can be described by the following differential equations of motion:

$$\begin{cases} m_1\ddot{x}_1 + c_1(\dot{x}_1 - \dot{x}) + k_1(x_1 - x) + c_2(\dot{x}_1 - \dot{x}_2) + k_2(x_1 - x_2) = 0 \\ m_2\ddot{x}_2 + c_2(\dot{x}_2 - \dot{x}_1) + k_2(x_2 - x_1) + c_3(\dot{x}_2 - \dot{x}_3) + k_3(x_2 - x_3) \\ \qquad + c_4(\dot{x}_2 - \dot{x}_4) + k_4(x_2 - x_4) = 0 \\ m_3\ddot{x}_3 + c_3(\dot{x}_3 - \dot{x}_2) + k_3(x_3 - x_2) = 0 \\ m_4\ddot{x}_4 + c_4(\dot{x}_4 - \dot{x}_2) + k_4(x_4 - x_2) = 0 \end{cases} \tag{5.1}$$

Where m_i, c_i, and k_i (i=1,2,3,4) are the masses, damping coefficients and stiffness coefficients respectively. The above equations could be rewritten in the matrix format as.

$$[M]\{\ddot{u}\} + [C]\{\dot{u}\} + [K]\{u\} = \{q\} \tag{5.2}$$

Where $[M]$ is (4×4) mass matrix; [C] and $[K]$ are (4×4) damping and stiffness matrices, respectively. $\{u\}$ is vector of response coordinates, such that:

$$\{u\} = \{x_1, x_2, x_3, x_4\}^T$$

Where 'T' designates the transpose;

In the above equation, $\{q\}$ represents the forcing vector, given by:

$$\{q\} = \{k_1 x + c_1 \dot{x}, 0, 0, 0\}^T$$

Applying the Laplace transform, and assuming zero initial conditions, equation (5.2) could be rewritten as:

$$\{s^2[M] + s[C] + [K]\}\{U(s)\} = \{Q(s)\} \tag{5.3}$$

Where s is Laplace variable; $\{U(s)\}$ and $\{Q(s)\}$ are Laplace transforms of $\{u(t)\}$ and $\{q(t)\}$ respectively, given by:

$$\{U(s)\}=\{X_1(s),X_2(s),X_3(s),X_4(s)\}^T \text{; and } \{Q(s)\}=\{(k_1+c_1s)X(s),0,0,0\}^T$$

Equation (5.3) is solved to yield the transfer function vector, *H(s)*, as:

$$\{H(s)\}=\begin{Bmatrix} X_1(s)/X(s) \\ X_2(s)/X(s) \\ X_3(s)/X(s) \\ X_4(s)/X(s) \end{Bmatrix}=[Z(s)]^{-1}\begin{Bmatrix} c_1s+k \\ 0 \\ 0 \\ 0 \end{Bmatrix} \tag{5.4}$$

Where the system matrix *Z(s)* is derived from (5.3), such that:

$$Z(s)=s^2[M]+s[C]+[K] \tag{5.5}$$

The STHT responses of the to excitation *X(s)* is directly obtained from the transfer function, such that:

$$T(s)=\frac{X_3(s)}{X(s)} \tag{5.6}$$

Where *T(s)* is the transfer function relating the motion of the head $X_3(s)$ to the motion at the seat *X(s)*.

The resultant force developed at the human-seat interface can also be computed from the equation of motion for the base mass m_0:

$$m_0\ddot{x}+c_1(\dot{x}-\dot{x}_1)+k_1(x-x_1)=F \tag{5.7}$$

Equation (5.1) and (5.7) yield the following relationship for the resulting force:

$$F=m_0\ddot{x}\ +m_1\ddot{x}_1+m_2\ddot{x}_2+m_3\ddot{x}_3+m_4\ddot{x}_4 \tag{5.8}$$

The Laplace transform of the above equation yields APMS and STHT functions of model could be derived as:

$$M(s)=\frac{F(s)}{s^2X(s)}=m_0+m_1H_1(s)+m_2H_2(s)+m_3H_3(s)+m_4H_4(s) \tag{5.9}$$

Where $H_1(s)=\frac{X_1(s)}{X(s)}$; $H_2(s)=\frac{X_2(s)}{X(s)}$; $H_3(s)=T(s)=\frac{X_3(s)}{X(s)}$; $H_4(s)=\frac{X_4(s)}{X(s)}$

The above relationship reveals that the APMS response of the seated body *M(s)* is directly related to STHT function, *T(s)*.

By substituting for $s=j\omega$ in equations (5.6) and (5.9), the APMS and STHT function could be expressed by their magnitude and phase in the frequency domain.

The normalized APMS response of the model can also be computed from:

$$\overline{M}(s)=\frac{1}{m_s}[m_0+m_1H_1(s)+m_2H_2(s)+m_3H_3(s)+m_4H_4(s)] \qquad (5.10)$$

Where $\overline{M}(s)$ is the normalized APMS, m_s is sitting weight of the human body derived from the mechanical equivalent model, and can be expressed as:

$$m_s=\sum_0^4 m_i \qquad (5.11)$$

The mass values for the proposed model are expressed as fraction of the total body mass M_t on the basis of anthropometric data for male subjects [96]. The normalized five masses corresponding to the different body segments are thus expressed as:

$$\mu_i=m_i/M_t \ \ (i=0,1,2,3,4) \qquad (5.12)$$

5.2.2 Identification of a target data set

Force-motion and vibration transmission properties of seated body have been characterized by performing the simultaneous measurements that involve differences in subjects' mass, posture arising from back support condition and hands position, and excitation frequency and magnitude. Since the reported biodynamic models of seated occupants [19,73] have been mainly derived on the basis of mean response of a population of subjects, where the individual subject masses are known to vary within a

certain range. These models may thus be shown to provide a close estimate of the mean response of occupants whose masses correspond to mean mass of groups of subjects employed in the test. Moreover, majority of the reported one-dimensional models are based upon the data acquired with the hands in lap posture, and under relatively high magnitude of vertical vibration. Owing to the important contribution of the magnitude of vibration, sitting posture and body mass, it is desirable to develop a nonlinear model that may predict the biodynamic responses within the ranges of important variations. This task, however, would be extremely complex due to nonlinear effects of various contributory factors. It would thus be reasonable to consider the model developments for different body masses, representing 5^{th}, 50^{th} and 95^{th} percentile population. The model development in this study, however, is limited in the vicinity of 50^{th} percentile population, while the total body mass is fixed to 75.58 kg on the basis of the available measured data. Furthermore, the magnitude of vibration is limited to 1.0 m/s^2 rms, which is close to that of vibration encountered in many road vehicles, such as urban buses, trucks and low-spaced earth moving machinery [97-99]. The methodology can be further applied to derive models for different body masses and excitation levels. This is quite convenient since the model masses are considered to represent a particular body segment, while each mass is expressed by its fraction of the total body mass. Considering the most significant influence of back support conditions, the model development is undertaken for all the three conditions, namely, no back support (NBS), vertical back support (VBS) and the inclined back support (IBS), while the hands position are considered to be in the lap. The corresponding target datasets comprising both APMS and STHT responses, used in the model development, have been illustrated in Figure 4.21 (a).

5.2.3 4-DOF model parameters estimation

The parameters for the proposed 4DOF model are identified through minimization of a weighted error function of the model and measured 'vertical APMS' (M_v) and 'vertical STHT' (TF_z) responses using the optimization function *fmincon* available within MATLAB [98]. The weighted error function is defined as:

$$E(\chi) = \min[\alpha\, E_{APMS}(\chi) + \beta\, E_{STHT}(\chi)] \tag{5.13}$$

Where $\chi = \{\mu_0, \mu_1, \mu_2, \mu_3, \mu_4, k_1, k_2, k_3, k_4, c_1, c_2, c_3, c_4\}$ is the model parameters vector to be identified. $E(\chi)$ is the total error function, and $E_{APMS}(\chi)$ is the error function arising from the APMS response, and $E_{STHT}(\chi)$ is the error function in seat-to-head transmissibility response. α and β are the weighting factors used to ensure comparable contributions of the error functions, $E_{APMS}(\chi)$ and $E_{STHT}(\chi)$, and two factors satisfy the following relationship :

$$\alpha + \beta = 1 \tag{5.14}$$

$E_{APMS}(\chi)$ and $E_{STHT}(\chi)$ are the squared errors resulting from APMS and STHT responses respectively, taken at various discrete frequencies in the 0.5-15 Hz range, given by:

$$\begin{cases} E_{APMS}(\chi) = \sum_{i=1}^{N} \lambda_1 \left| \overline{M}^*(\omega_i) - \overline{M}(\omega_i) \right|^2 + \sum_{i=1}^{N} \psi_1 \left| \phi^*(\omega_i) - \phi(\omega_i) \right|^2 \\ E_{STHT}(\chi) = \sum_{i=1}^{N} \lambda_2 \left| T^*(\omega_i) - T(\omega_i) \right|^2 + \sum_{i=1}^{N} \psi_2 \left| \varphi^*(\omega_i) - \varphi(\omega_i) \right|^2 \end{cases} \tag{5.15}$$

Where $\overline{M}^*(\omega_i)$ and $\overline{M}(\omega_i)$ are the moduli of normalized apparent masses derived from the model and the measured data, respectively; $\phi^*(\omega_i)$ and $\phi(\omega_i)$ are the

corresponding APMS phase responses; $T^*(\omega_i)$ and $T(\omega_i)$ are the moduli of STHT derived from the model and the measured data, respectively; $\varphi^*(\omega)$ and $\varphi(\omega)$ are the corresponding STHT phase responses. All the above magnitude and phase responses are corresponding to discrete frequency ω_i, and N is the number of discrete frequencies selected in the 0.5 to 15 Hz frequency range. $\lambda_i\ (i=1,2)$ and $\psi_i\ (i=1,2)$ are the weighting factors applied to attain comparable contributions of the magnitude and phase errors, respectively, in the error functions of $E_{APMS}(\chi)$ and $E_{STHT}(\chi)$. Table 5.1 provides the selected weighting factors for each error function. These weighting factors assume higher values around the primary resonance than those in the remaining frequency range in order to attain a better agreement within the primary resonance range for both APMS and STHT magnitude functions. As observed from the measured data (Figure 4.22), the normalized APMS and STHT reveal good agreements in the vicinity of the primary resonances, irrespective of the back support conditions and excitation conditions. It should be noted that the weighting factors were selected on the basis of solutions attained with various values of weighting factors. The selected weighting factors resulted in consistent values of the error functions and the model parameters, when different values for the staring vector were considered.

Table 5.1: Weighting factor values used in the error minimization.

$\lambda_i(i=1,2)$	λ_i =100 (3.5 ≤f ≤ 6.125 Hz) λ_i =1 (f<3.5; f>6.125 Hz)
$\psi_i(i=1,2)$	ψ_i =1 (0.5 ≤f ≤ 15 Hz)

The error function in equation (5.13) was minimized subject to a number of inequality constraints imposed on the model parameters. Irrespective of the back support conditions, the head mass is ensured to maintain around 6.88% of the total body mass [96]; The seated upper body (trunk, head, neck, arms and visceral mass) is maintained around 67.8% [96], while the total model mass is close to the sitting mass for each back support condition. The above anthropometric limit constraints were defined to allow these masses to vary within a narrow band of $\pm 4\%$, such that:

$$\begin{cases} 0.066 \le \mu_3 \le 0.0716 \\ 0.65 \le \sum_{i=1}^{4} \mu_i \le 0.705 \\ 0.72 \le \sum_{i=0}^{4} \mu_i \le 0.78 \ ; \text{for no back support} \\ 0.74 \le \sum_{i=0}^{4} \mu_i \le 0.80 \ ; \text{for vertical back support} \\ 0.745 \le \sum_{i=0}^{4} \mu_i \le 0.805 \ ; \text{for inclined back support} \end{cases} \tag{5.16}$$

The error minimization problem is also subjected to additional inequality constraints for the stiffness and damping coefficients, such that:

$$\begin{cases} k_1 > 0;\ k_2 > 0;\ k_3 > 0; k_4 > 0 \\ c_1 > 0;\ c_2 > 0;\ c_3 > 0;\ c_4 > 0 \end{cases} \tag{5.17}$$

The parameter vector χ corresponding to each back support condition is identified through the error function defined in equation (5.13). The minimization problem was solved using a nonlinear parameter search method (*fmincon*) provided by MATLAB. Weighting factors (α and β) in equation (5.13) together with the starting

values were varied systematically, and the resulting function values were thoroughly examined to identify a more reliable and consistent parameter set.

The solutions were initially obtained on the basis of the target APMS response by letting α =1 and β =0. The solutions based on STHT response alone were also attained by letting α =0 and β =1. Finally, α and β values were determined arbitrarily such that parameter vector would provide an overall fit to both the target responses. For this purpose, the solutions were obtained for many different values of α and β . The following section illustrates the solutions attained for different values of weighting factors imposed on the two biodynamic functions.

5.2.4 Model parameters analysis and discussions

Table 5.2 summarizes the model parameters identified for the no back support conditions, when either APMS (α =1, β =0) or STHT (α =0, β =1) target function is considered. The table also presents the parameters values when both target functions are considered in the weighted error (α =0.3, β =0.7). The results show considerable differences in some of the model parameters identified for different target functions, although a number of model parameters converge to comparable values. Figures 5.2 to 5.4 provide comparisons between the measured target data and model responses for the two functions subject to different weighting factor combinations. Although the differences in parameters can be clearly observed for the single objective function (α =1, β =0; and α =0, β =1). It may be concluded that the identification based upon either APMS or STHT biodynamic function could lead to model parameters set that could provide reasonably good agreement in both the two biodynamic functions. The

results, however, suggest that consideration of APMS target function alone yields relatively larger error in STHT responses (Figure 5.3). Consideration of both the response functions in the weighted error sum yields better agreement in APMS as well as STHT response magnitudes (Figure 5.4). The phase responses show reasonably good agreements, irrespective of the target function considered. The results thus suggest that the minimization of the weighted composite error function could result in identification of more reliable model parameters.

Table 5.2: Model parameters identified on the basis of APMS, STHT and both biodynamic functions (no back support condition).

Functions / Parameters	**APMS only**	**STHT only**	**APMS & STHT**
m_0 (kg), u_0	5.77(0.076)	5.03(0.067)	4.53(0.06)
m_1 (kg), u_1	21.03(0.278)	19.56(0.259)	17.45(0.231)
m_2 (kg), u_2	16.68(0.221)	17.66(0.234)	19.96(0.264)
m_3 (kg), u_3	4.99(0.066)	4.99(0.071)	4.99(0.066)
m_4 (kg), u_4	10.48(0.139)	10.20(0.135)	10.20(0.135)
k_1 (kN/m)	151.46	151.4	201.25
k_2 (kN/m)	43.80	43.77	43.60
k_3 (kN/m)	300.24	302.4	300.83
k_4 (kN/m)	16.65	17.28	22.55
c_1 (Ns/m)	836.46	1160.5	1015.2
c_2 (Ns/m)	979.93	954.57	1029.7
c_3 (Ns/m)	799.7	786.96	800
c_4 (Ns/m)	506.51	500.08	575.62
Weighting factor	α =1 β =0	α =0 β =1	α =0.3 β =0.7

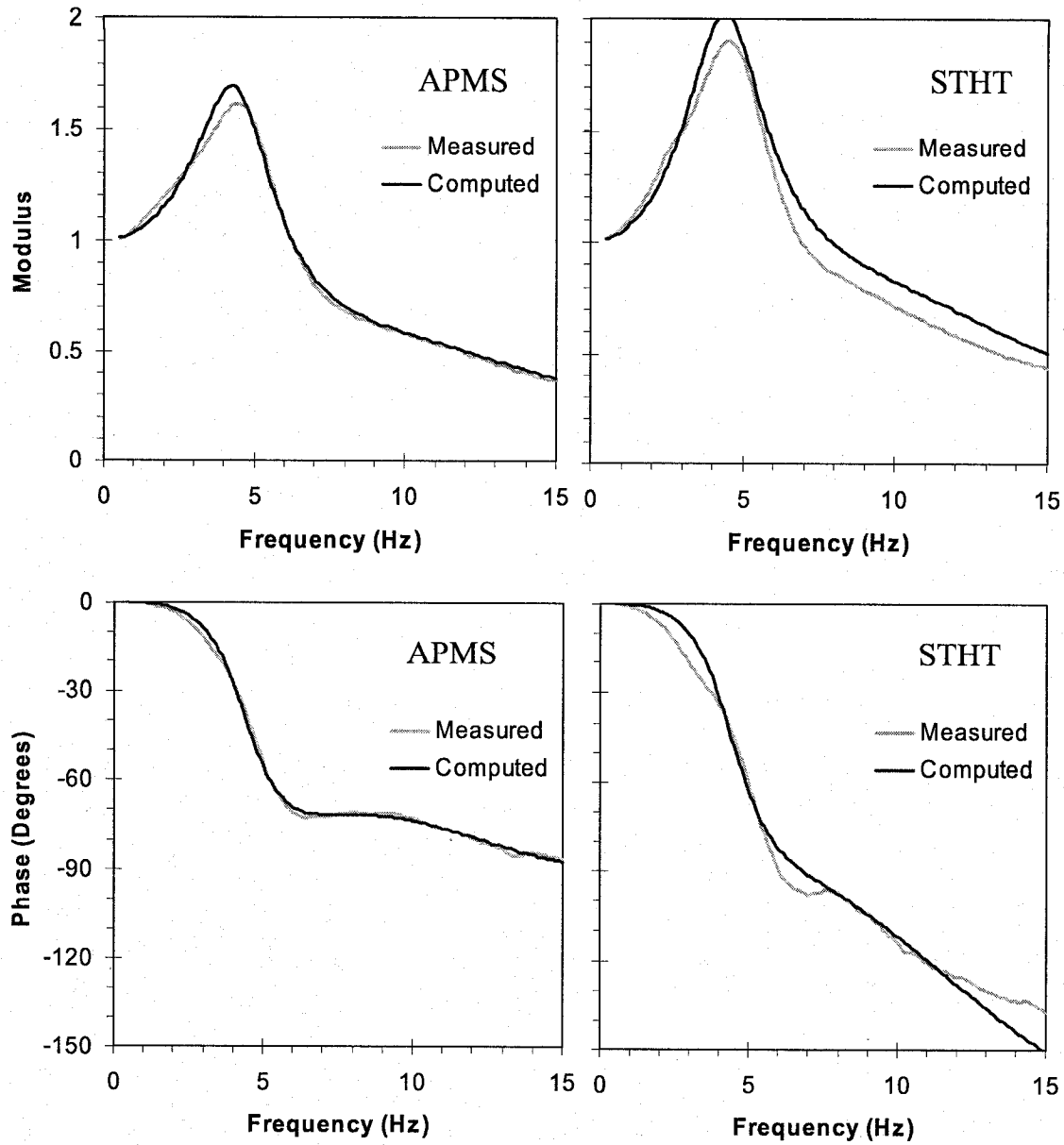

Figure 5.2: Comparison of the computed moduli and phases responses of apparent mass and seat-to-head transmissibility with the measured data (α=1; β=0; No back support).

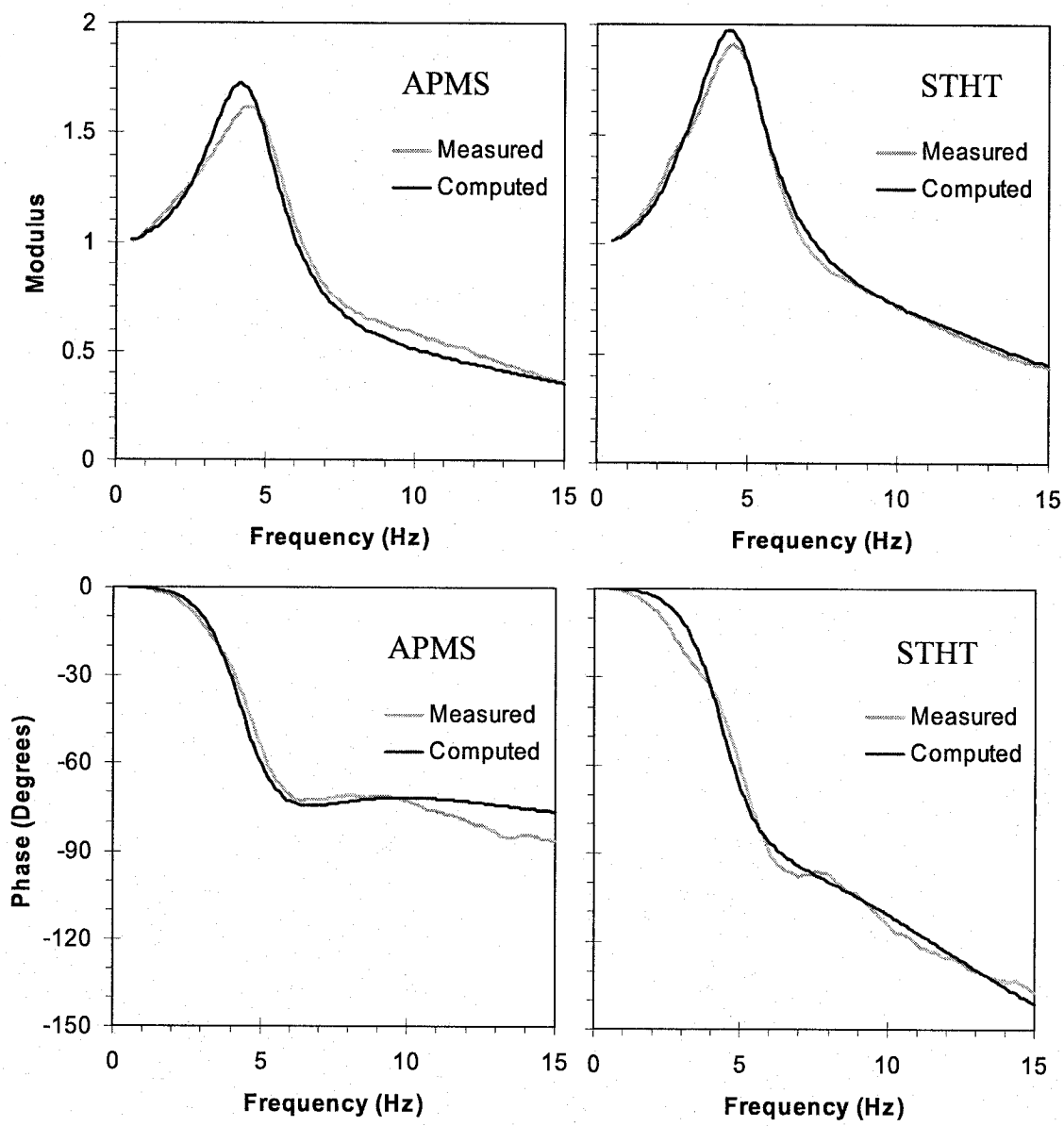

Figure 5.3: Comparison of the computed moduli and phases responses of apparent mass and seat-to-head transmissibility with the measured data (α=0; β=1; No back support)

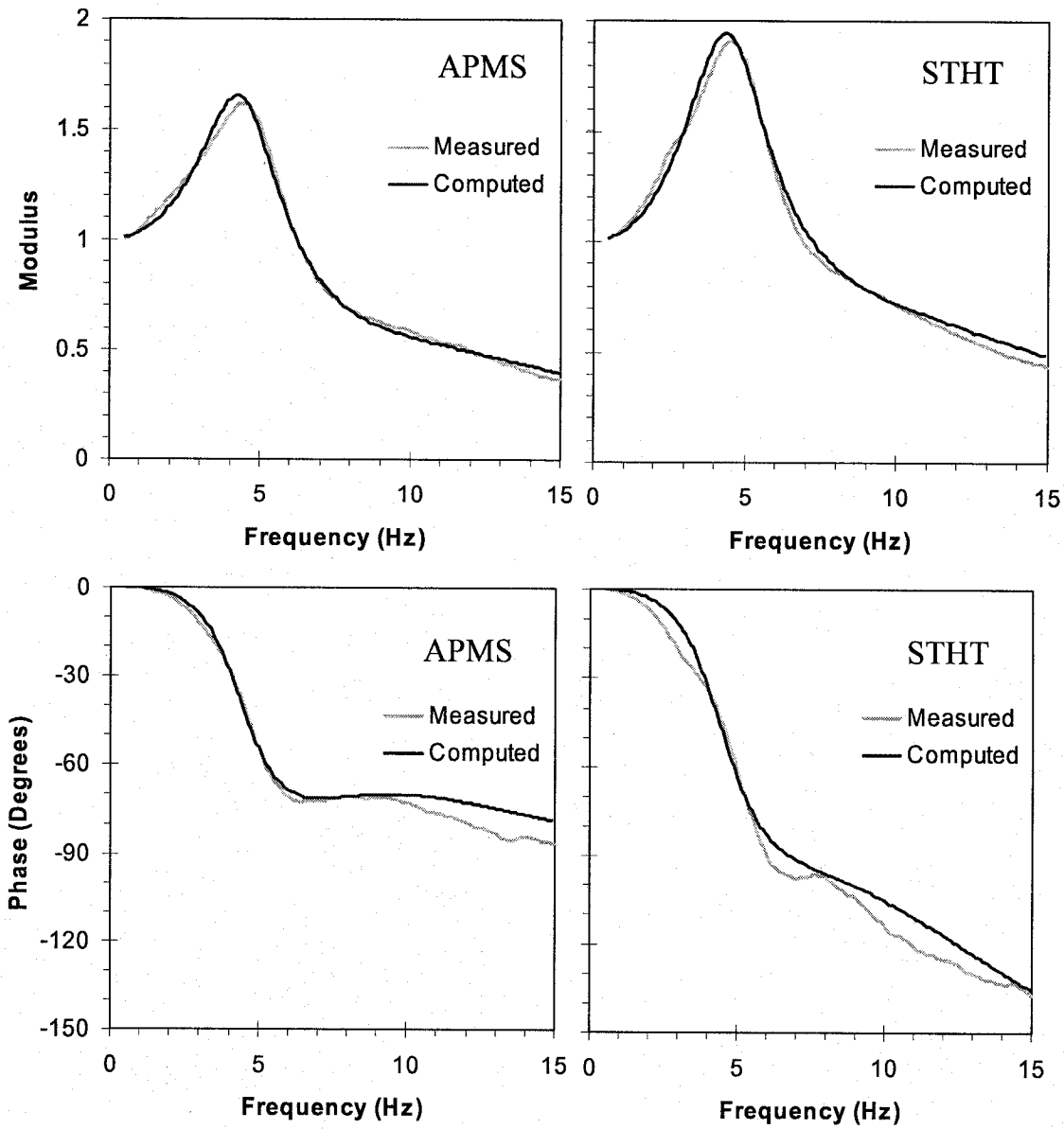

Figure 5.4: Comparison of the computed moduli and phases responses of apparent mass and seat-to-head transmissibility with the measured data (α=0.3; β=0.7; No back support)

Table 5.3 summarized the model parameters derived on the basis of target data sets for the vertical back support conditions using the same three sets of weighting factors. Figures 5.5 to 5.7 provide comparisons between the measured data and computed data for the two functions subject to different weighting factors combinations. Table 5.4, in a similar manner, summarizes the model parameters identified for the inclined back support conditions. The resulting model responses are compared with the target responses in Figures 5.8 to 5.10, respectively for (α =1, β =0); (α =0, β =1) and (α =0.3; β=0.7). The parameter values summarized in Table 5.2 and 5.3 for the back support conditions again reveal notable differences depending upon the target function or weighting considered, as observed for the no back support condition. The result again confirm that consideration of APMS target data alone (α =1, β =0) can provide good agreement only in APMS, while considerable error in STHT response is evident (Figures 5.5 and 5.8). The magnitude of error between the model and target STHT response can be substantially reduced when the model parameters are identified on the basis of STHT target data alone (Figures 5.6 and 5.9). A better compromise in errors in both the functions can be attained when the weighted composite error function (α =0.3, β =0.7) is minimized, as seen in Figures 5.7 and 5.10.

Since the APMS and STHT data characterize response behaviors of the seated body exposed to vertical WBV, it would be appropriate to expect that mechanical equivalent model satisfy both the biodynamic responses. The results clearly suggest that consideration of either one function alone yields appreciable errors in the other response function. The model parameters identified on the basis of either APMS or STHT target data thus can not be considered reliable. This is particularly apparent for the back

supported postures. For the two back supported conditions, the model parameters identified on the basis of APMS error alone show considerably larger errors in the STHT magnitude response, particularly at frequencies above the primary resonant frequency (Figures 5.5 and 5.8). The models derived through minimization of STHT error alone yield better agreement in STHT response but larger errors in the APMS response (Figures 5.6 and 5.9).

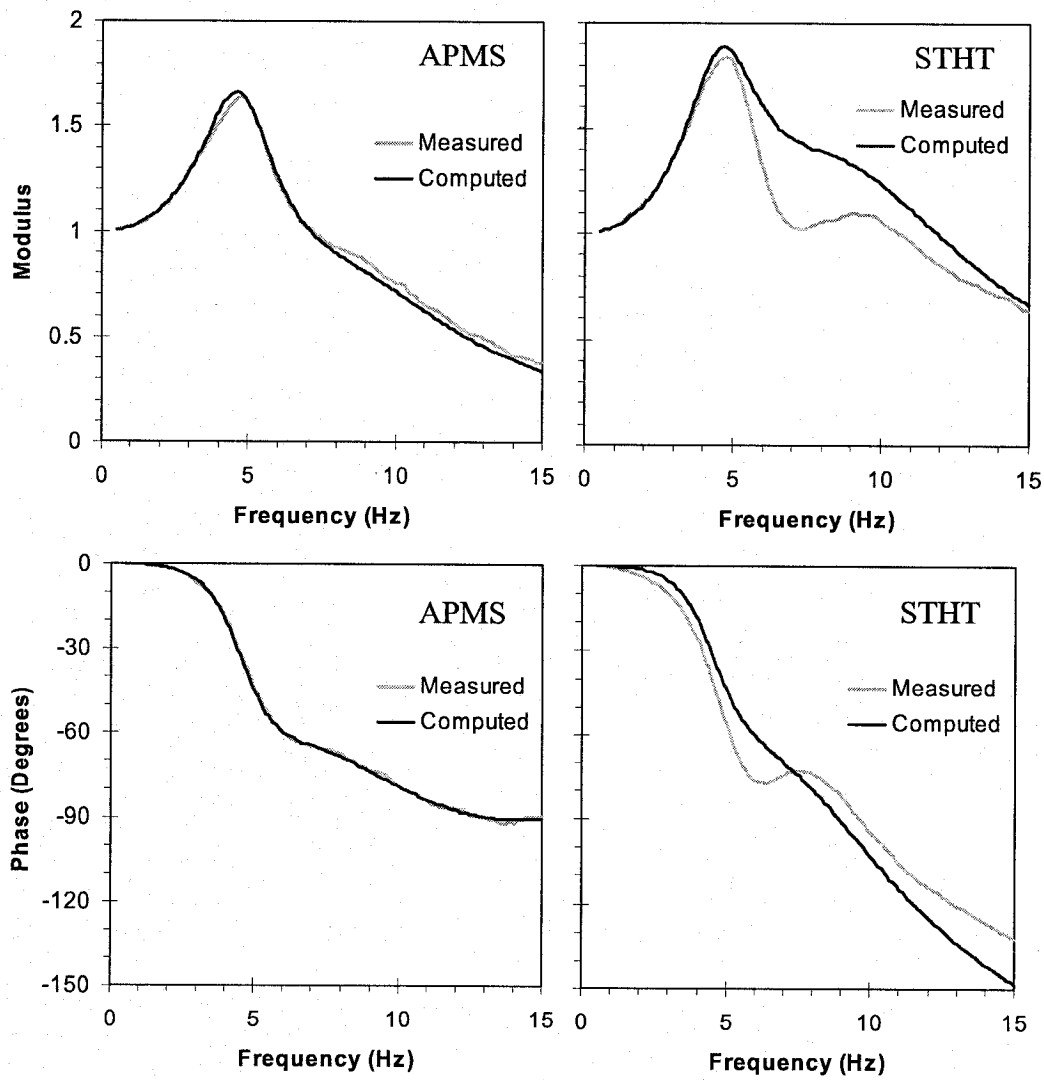

Figure 5.5: Comparison of the computed moduli and phases responses of apparent mass and seat-to-head transmissibility with the measured data (α=1; β=0; Vertical back support).

Table 5.3: Model parameters identified on the basis of APMS, STHT and both biodynamic functions (vertical back support condition).

Functions / Parameters	**APMS only**	**STHT only**	**APMS & STHT**
m_0 (kg), u_0	7.01(0.11)	5.03(0.06)	4.53(0.06)
m_1 (kg), u_1	21.03(0.278)	19.56(0.245)	22.30(0.295)
m_2 (kg), u_2	16.18(0.214)	17.66(0.228)	13.60(0.180)
m_3 (kg), u_3	4.99(0.066)	4.99(0.066)	4.99(0.066)
m_4 (kg), u_4	10.48(0.16)	10.20(0.16)	10.2(0.135)
k_1 (kN/m)	147.29	154.2	181.11
k_2 (kN/m)	74.68	64.17	42.65
k_3 (kN/m)	300.77	300.9	303.38
k_4 (kN/m)	15.19	19.39	20.0
c_1 (Ns/m)	750.11	1100	969.62
c_2 (Ns/m)	1250	1250	1210
c_3 (Ns/m)	800	800	802.5
c_4 (Ns/m)	399.61	326.00	325.00
Weighting factor	α =1 β =0	α =0 β =1	α =0.3 β =0.7

Table 5.4: Model parameters identified on the basis of APMS, STHT and both biodynamic functions (inclined back support condition).

Functions / Parameters	**APMS only**	**STHT only**	**APMS & STHT**
m_0 (kg), u_0	4.54(0.06)	4.53(0.06)	4.53(0.06)
m_1 (kg), u_1	23.59(0.312)	22.34(0.296)	20.85(0.276)
m_2 (kg), u_2	14.98(0.198)	12.80(0.169)	15.18(0.202)
m_3 (kg), u_3	5.37(0.071)	4.99(0.066)	4.99(0.066)
m_4 (kg), u_4	9.80(0.13)	11.71(0.155)	11.71(0.155)
k_1 (kN/m)	171.13	193.5	180.00
k_2 (kN/m)	41.55	37.33	39.55
k_3 (kN/m)	302.6	302.7	303.75
k_4 (kN/m)	21.65	21.07	19.89
c_1 (Ns/m)	902.96	1167.2	814.25
c_2 (Ns/m)	1200	1106.1	1200
c_3 (Ns/m)	800.24	865.88	800
c_4 (Ns/m)	274.12	237.8	273.06
Weighting factor	α =1 β =0	α =0 β =1	α =0.3 β =0.7

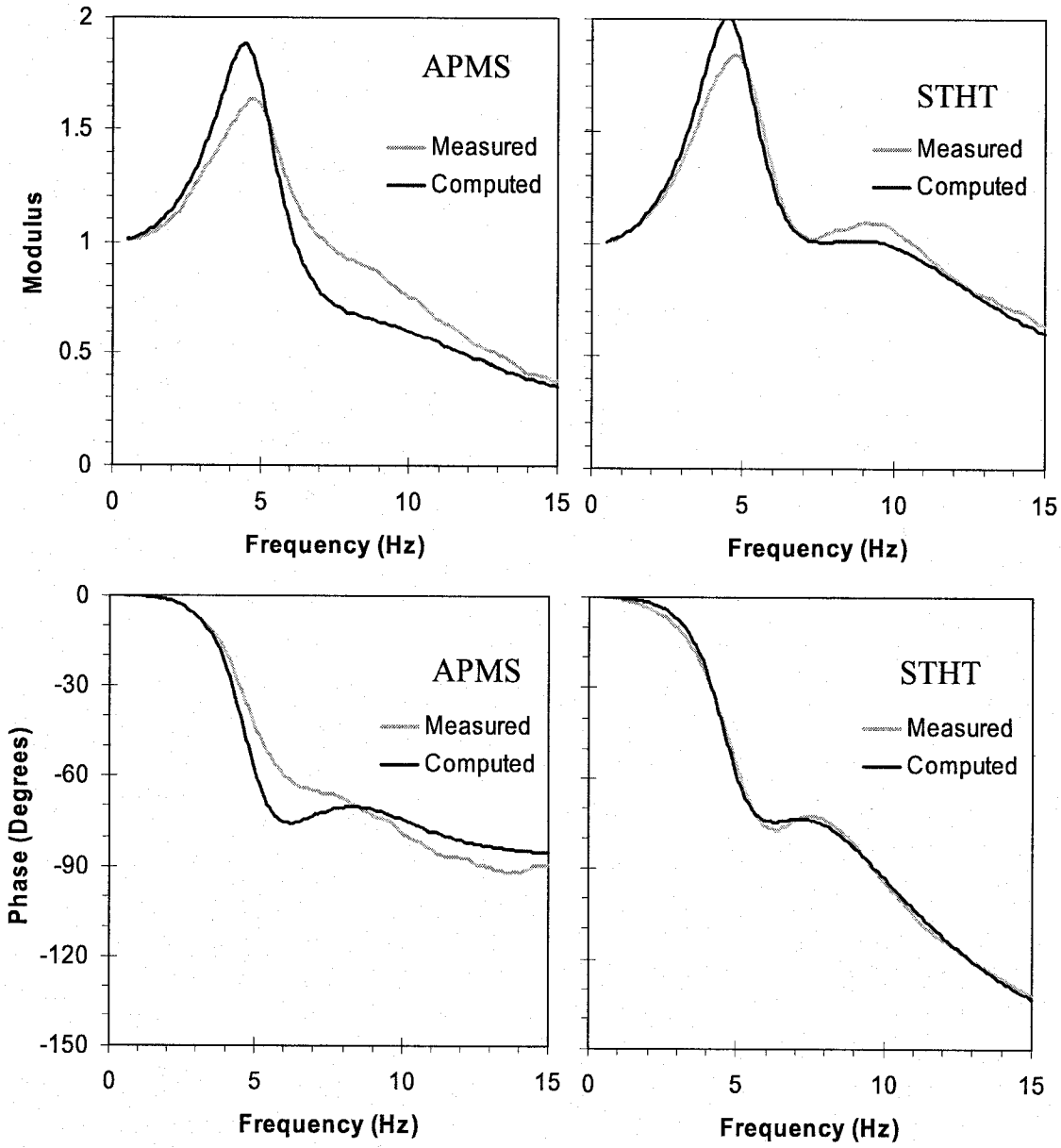

Figure 5.6: Comparison of the computed moduli and phases responses of apparent mass and seat-to-head transmissibility with the measured data (α=0; β=1; Vertical back support)

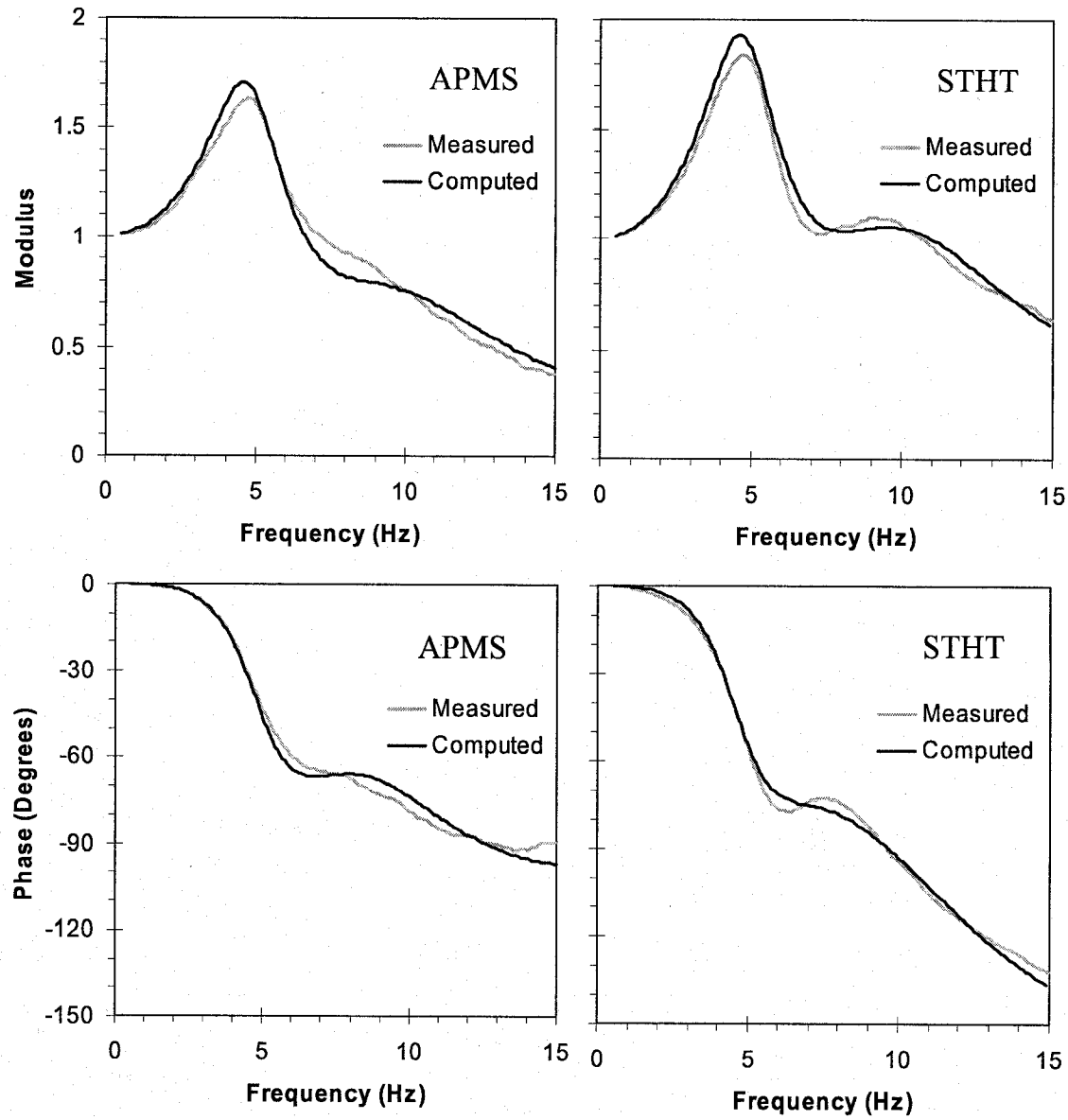

Figure 5.7: Comparison of the computed moduli and phases responses of apparent mass and seat-to-head transmissibility with the measured data (α=0.3; β=0.7; Vertical back support)

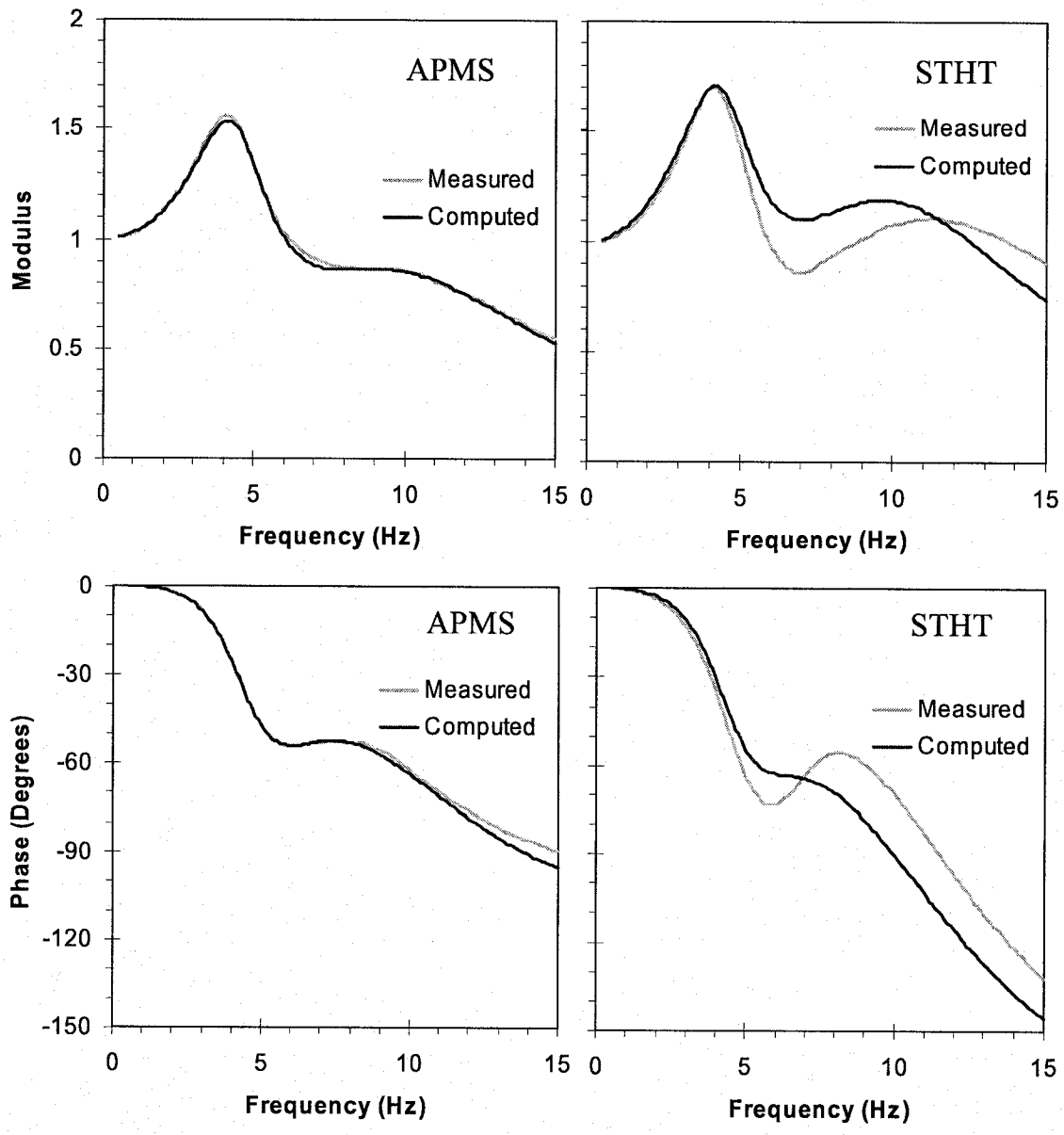

Figure 5.8: Comparison of the computed moduli and phases responses of apparent mass and seat-to-head transmissibility with the measured data (α=1; β=0; Inclined back support).

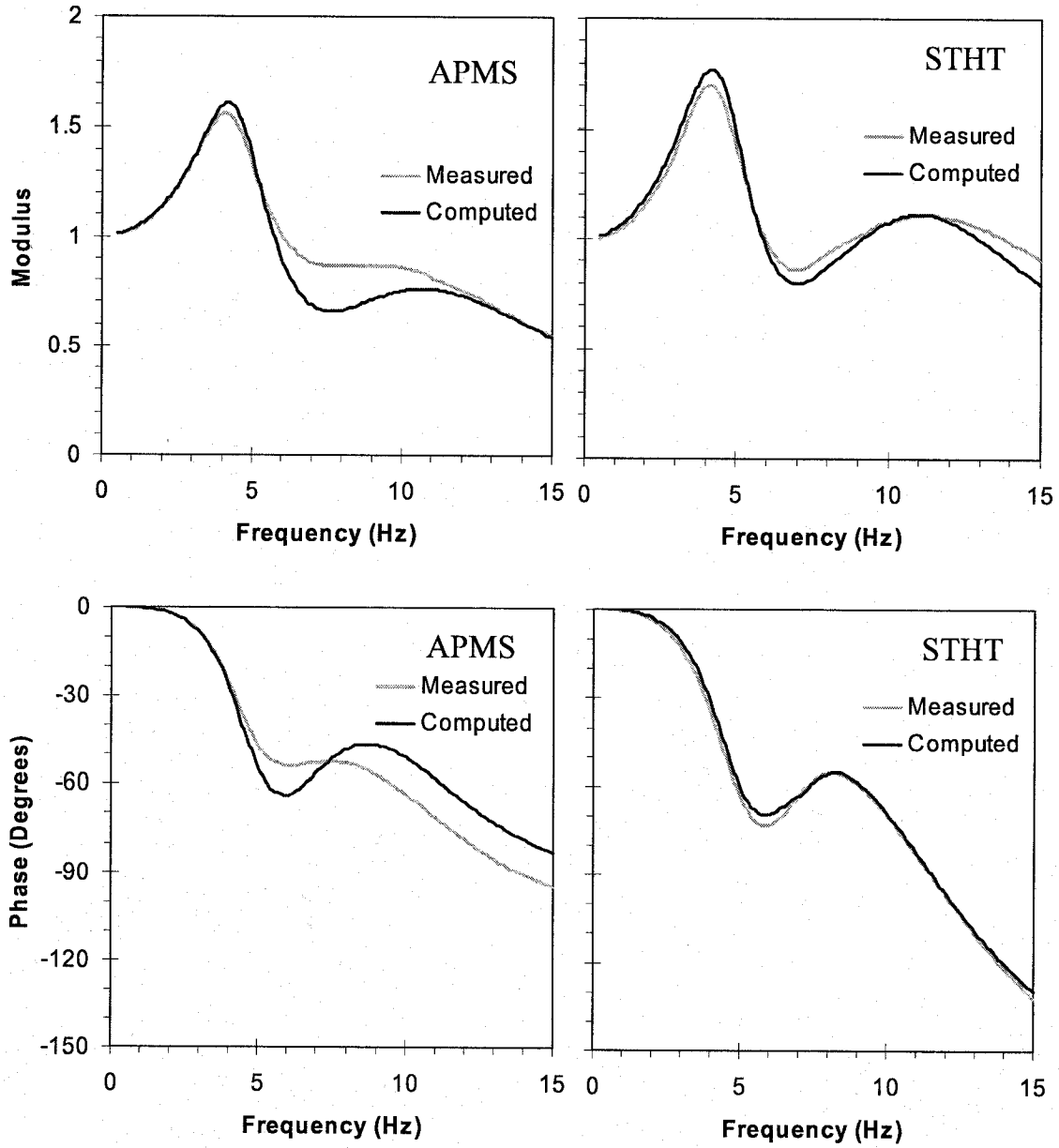

Figure 5.9: Comparison of the computed moduli and phases responses of apparent mass and seat-to-head transmissibility with the measured data (α=0; β=1; Inclined back support).

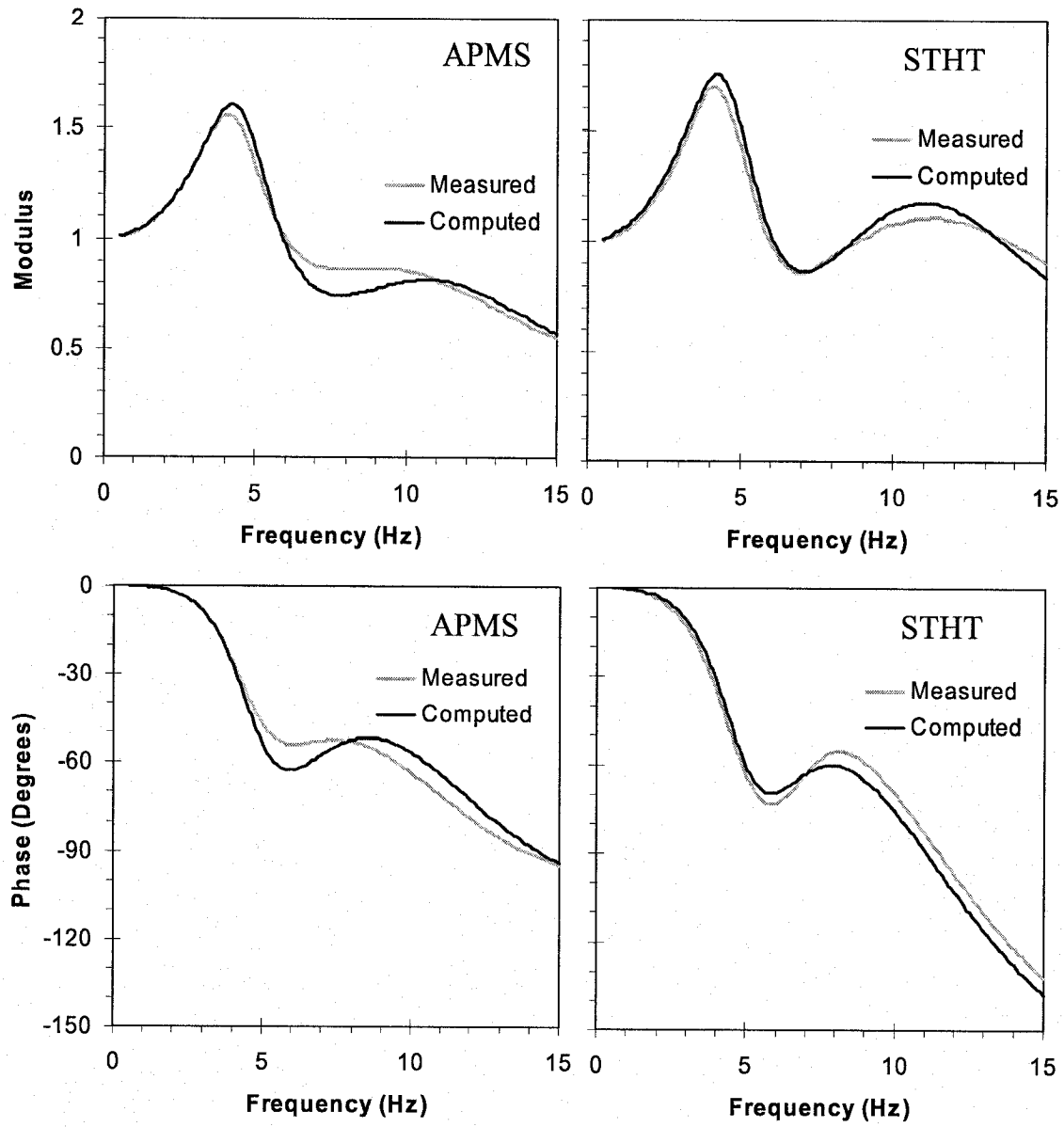

Figure 5.10: Comparison of the computed moduli and phases responses of apparent mass and seat-to-head transmissibility with the measured data (α=0.3; β=0.7; Inclined back support).

The model parameters attained for the three back support conditions are compared in Table 5.4. There are larger differences between the STHT and normalized APMS magnitude responses for the two back supported postures at frequencies above 6 Hz. The difference, however, is relatively small for the no back support postures, as observed in the experimental data. The model parameters identified for the three back support condition are also observed to be considerably different. The APMS and STHT responses of the models thus also differ, and confirm the trends observed from the measured data (Figure 4.21) on the role of back support.

The mass parameters attained form the three postures suggest that the masses (m_0 and m_3), attributed to buttocks and the head, respectively, remain unchanged irrespective of the back support conditions. The stiffness and damping properties of elements coupling the head to the upper body torso also remain quite similar for all these back support conditions. The effective mass representing the upper body torso (m_2), however, decreases considerably when a back support is introduced. The effective masses due to lower body (m_1) and viscera (m_4) however, increase with the back support. The two back supported postures yield quite comparable values of the model masses. The model results show that the back support postures yield relatively lower stiffness of the lower and upper body torso and viscera component (k_1, k_2, k_4). This suggests that seated upper body tends to stiffen in the absence of back support. The model results also particularly show the damping element coupling the lower body and the buttocks (c_1) and varies considerably as the back support condition changed. Without back support, this damping element reveals a relatively higher value compared to that of back supported postures. The inclined back support results in the lowest damping coefficient (c_1). This may be

attributed to relatively higher movement of the unsupported torso. This is further supported by the lower absorbed power density of the back supported postures near the primary resonance (Figures 5.15 to 5.17). Moreover, it is found that the back support condition yields considerably lower damping coefficient (c_4) of the viscera component of upper body. The two back supported postures yield quite closer values of the damping coefficients.

Table 5.5: Model parameters identified on both APMS and STHT biodynamic functions under three back support conditions.

Postures / Parameters	NBS	VBS	IBS
m_0 (kg), u_0	4.53(0.06)	4.53(0.06)	4.53(0.06)
m_1 (kg), u_1	17.45(0.231)	22.30(0.295)	20.85(0.276)
m_2 (kg), u_2	19.96(0.264)	13.60(0.18)	15.18(0.201)
m_3 (kg), u_3	4.99(0.066)	4.99(0.066)	4.99(0.066)
m_4 (kg), u_4	10.58(0.135)	10.2(0.135)	11.71(0.155)
k_1 (kN/m)	201.25	181.11	180.00
k_2 (kN/m)	43.60	42.65	39.55
k_3 (kN/m)	300.83	303.38	303.75
k_4 (kN/m)	22.55	20.0	19.89
c_1 (Ns/m)	1015.2	969.62	814.25
c_2 (Ns/m)	1029.7	1210	1200
c_3 (Ns/m)	800	802.5	800
c_4 (Ns/m)	575.62	325.00	273.06

The results presented in Figure 5.1 through 5.10 show reasonably good validity of the model for the three back support conditions, when both the biodynamic target data sets are considered. The models, however, are derived for mean body mass of 75.58 kg in the vicinity of the 50th percentile male population. Owing to the strong influence of the back support condition, it is essential to derive models applicable to a particular back condition. The validated models can be effectively applied for design and assessment of

coupled occupant seat system. Moreover, the validated models may find application in absorbed power prediction for the seated body, which is introduced in the subsequent section.

5.2.5 Prediction of absorbed power distribution

The vibration energy absorbed within the exposed seated body, has been suggested as a potential measure for assessing the risk of injury due to whole body vibration. As described in Chapter 2, the absorbed power may not only be derived from the 'Co-spectrum direct method', but also indirectly from the force-motion biodynamic functions (APMS/DPMI). The suitability of the proposed mechanical equivalent models in estimating the absorbed power is thus investigated. For this purpose, the absorbed power characteristics of seated subjects exposed to vibration in the applied excitation direction were directly derived from force-motion measures performed in simultaneous in measurements the frequency range 0.5-15 Hz.

Owing to the strong effect of body mass on the force-motion relationships, the data acquired for six subjects with body mass ranging from 70.5 kg to 79 kg alone are considered. Moreover, the force-motion data acquired under 1.0 m/s^2 rms acceleration excitation and three back support condition are applied to derive the mean absorbed power responses. Figures 5.11, 5.12 and 5.13 illustrate the absorbed power density measured for the six subjects seated with no back, vertical back and inclined back support, respectively. The figures also show the mean absorbed power responses corresponding to each back support condition. The results suggest that peak power absorption occurs in the

vicinity of the primary resonant frequency, as observed from the data presented in section 3.3.3. The significant effect of the back support condition is evident from the results.

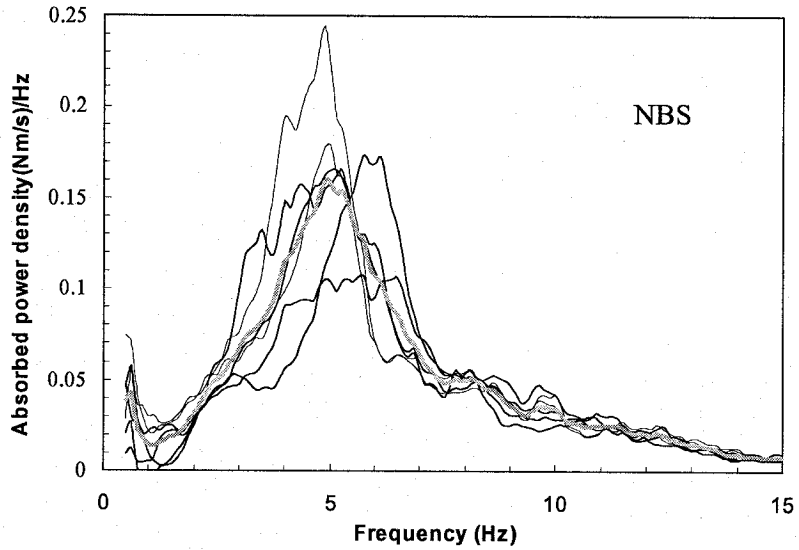

Figure 5.11: Comparison of measured absorbed power density responses of 6 subjects and corresponding mean values; —— individual responses; ——— mean response (No back support posture).

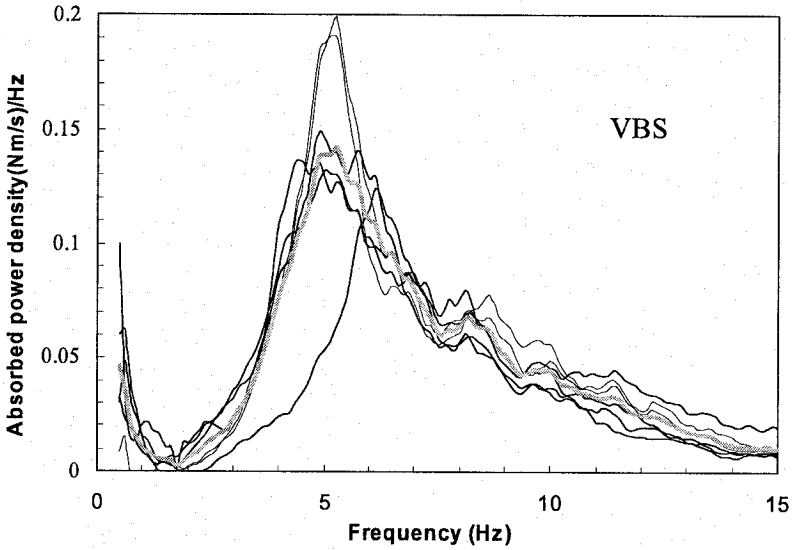

Figure 5.12: Comparison of measured absorbed power density responses of 6 subjects and corresponding mean values; —— individual responses; ——— mean response (Vertical back support posture).

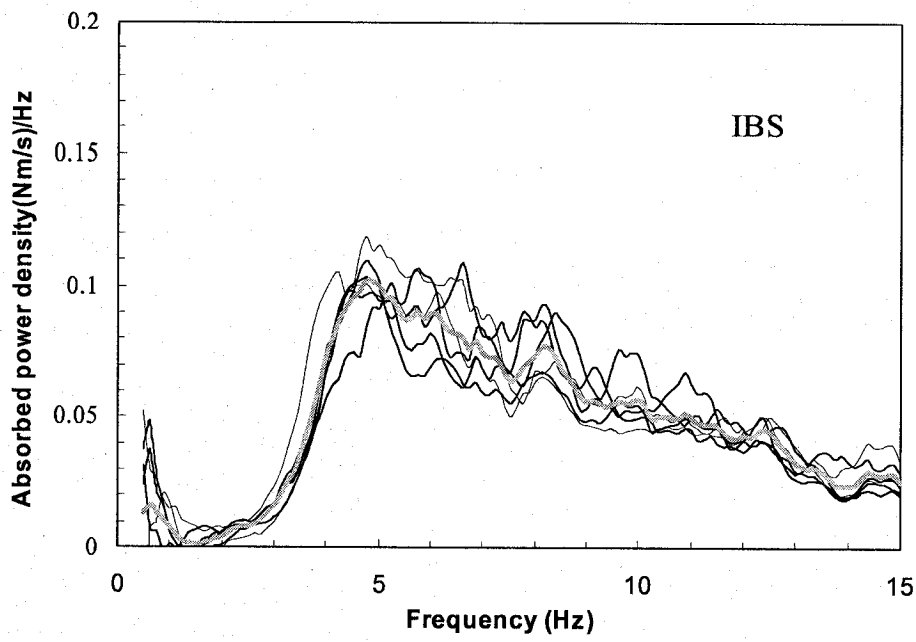

Figure 5.13: Comparison of measured absorbed power density responses of 6 subjects and corresponding mean values; —— individual responses; —— mean response (Inclined back support posture).

The proposed one-dimensional models are further applied to compute the total power absorbed within the model for different back support conditions. Moreover, the model can also be applied to obtain relative power absorption of the body segments employed in the model. Such analysis can provide considerable insight into the distribution of absorbed power within the body, and may provide additional guidance on the health and safety risks of vibration exposure.

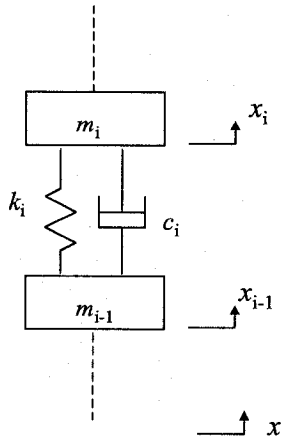

Figure 5.14: Spring-mass-damping unit in lumped parameter model structures

The power absorbed or distributed by the model can be formulated through consideration of a typical spring-mass-damping unit in widely used lumped parameter model structures, as illustrated in Figure 5.14. Where $\dot{\zeta}_i = \dot{x}_i - \dot{x}_{i-1}$ is the relative velocity across the viscous element, and c_i is the damping coefficient. The damping force developed by the linear viscous element is given by:

$$F_d = c_i \dot{\zeta}_i \tag{5.18}$$

The dissipated power can be expressed as:

$$P = F_d \frac{d\zeta_i}{dt} = c_i \dot{\zeta}_i^{\,2} \tag{5.19}$$

Under stochastic excitation, the mean square value of the relative velocity is related to the relative velocity transfer function and the excitation power spectral density, such that:

$$\dot{\zeta}_i^{\,2} = \int_0^\infty \left| H_{\dot{\zeta}_i}(j\omega) \right|^2 S_{\dot{x}}(j\omega) d\omega \tag{5.20}$$

Where $S_{\dot{x}}(j\omega)$ is the auto-spectral density of excitation velocity at the human seat interface. $H_{\dot{\zeta}_I}(j\omega)$ is the complex relative velocity transfer function.

The velocity spectral density, $S_{\dot{x}}(j\omega)$, is related to the auto-spectral density of excitation acceleration $S_{\ddot{x}}(j\omega)$ at the human seat interface [14], such that :

$$S_{\dot{x}}(j\omega) = \frac{S_{\ddot{x}}(j\omega)}{\omega^2} \tag{5.21}$$

Furthermore, for linear system the transfer function, $H_{\dot{\zeta}_I}(j\omega)$, can be expressed by the displacement transfer function, such that;

$$S_{\dot{\zeta}_I}(j\omega) = \left|H_i(j\omega) - H_{i-1}(j\omega)\right|^2 \frac{S_{\ddot{x}}(j\omega)}{\omega^2} \tag{5.22}$$

Where $H_i(j\omega)$ is the complex displacement transfer function relating the human seat interface motion (x) to that of body mass m_i (x_i).

The absorbed power density of each damping element in a lumped parameter model can thus be expressed as:

$$p_i(\omega) = c_i \left|H_i(j\omega) - H_{i-1}(j\omega)\right|^2 \frac{S_{\ddot{x}}(j\omega)}{\omega^2} \tag{5.23}$$

The total absorbed power density of the model is the sum of those due to each damping element, and expressed as:

$$p_{total}(\omega) = \sum_{i=1}^{NC} p_i(\omega) \tag{5.24}$$

Where NC is the total number of damping element in the model.

On the basis of the above finding, the validated one-dimensional models were applied to predict the total absorbed power density of the seated body and local absorbed

power density distributed in each viscous damping element, which may represent particular body segments. Figures 5.15 to 5.17 illustrate comparisons of total absorbed power density estimated from the model with the measured mean absorbed power density of six subjects under 1 m/s^2 rms excitation, and three back support conditions, respectively. The energy dissipated by each viscous element was further computed to gain some insight into the distribution of absorbed power within the body. The results revealed very small energy dissipation due to c_3 coupling the head and neck to the upper torso mass m_2. The figure thus present the dissipated energy due to c_1 coupling the lower torso to the buttocks, c_2 coupling the upper and lower torso, and c_4 coupling the upper torso to the viscera mass.

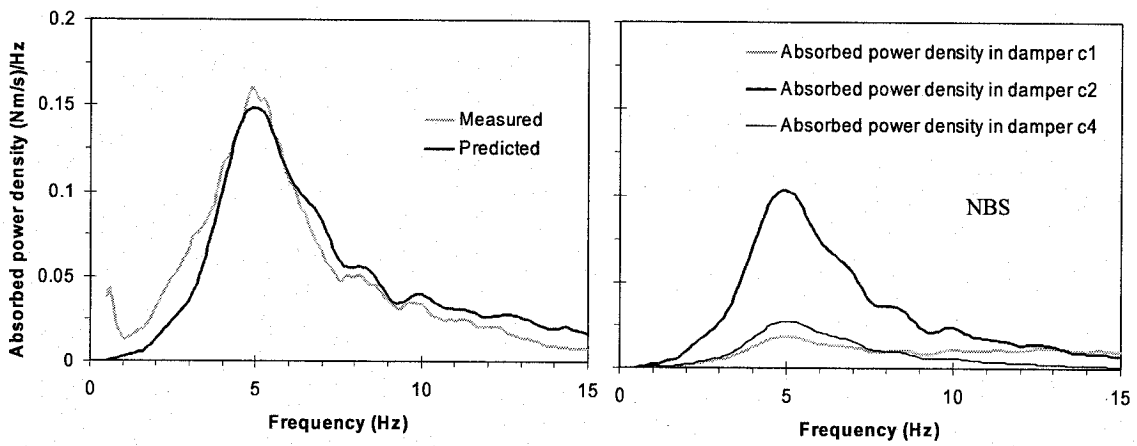

Figure 5.15: Prediction of absorbed power density from the model derived for no-back support condition: (a) Comparison between measured mean absorbed power density of six subjects and predicted total absorbed power density of the 4-DOF model; (b) Prediction of localized absorbed power density (1m/s^2 rms acceleration excitation).

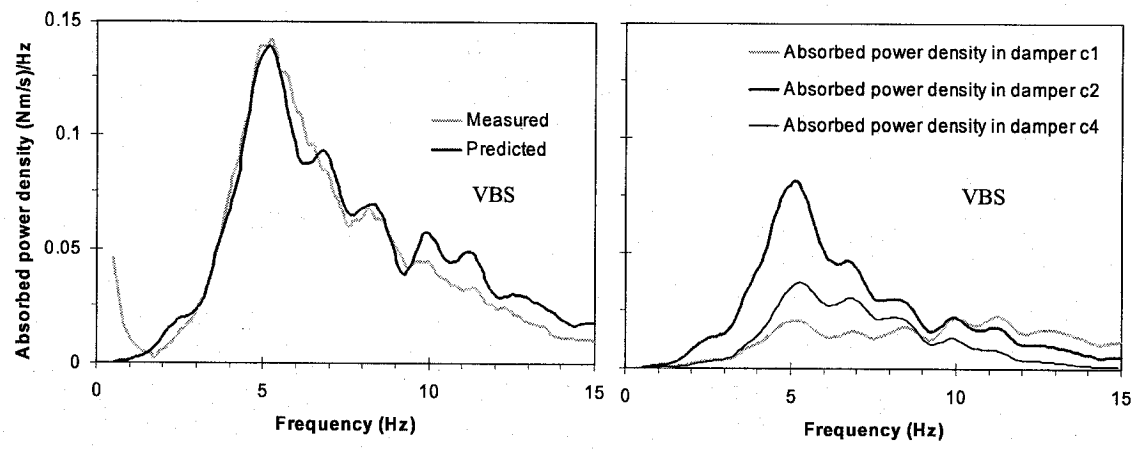

(a) (b)

Figure 5.16: Prediction of absorbed power density from the model derived for vertical back support condition: (a) Comparison between measured mean absorbed power density of six subjects and predicted total absorbed power density of the 4-DOF model; (b) Prediction of localized absorbed power density (1m/s^2 rms acceleration excitation).

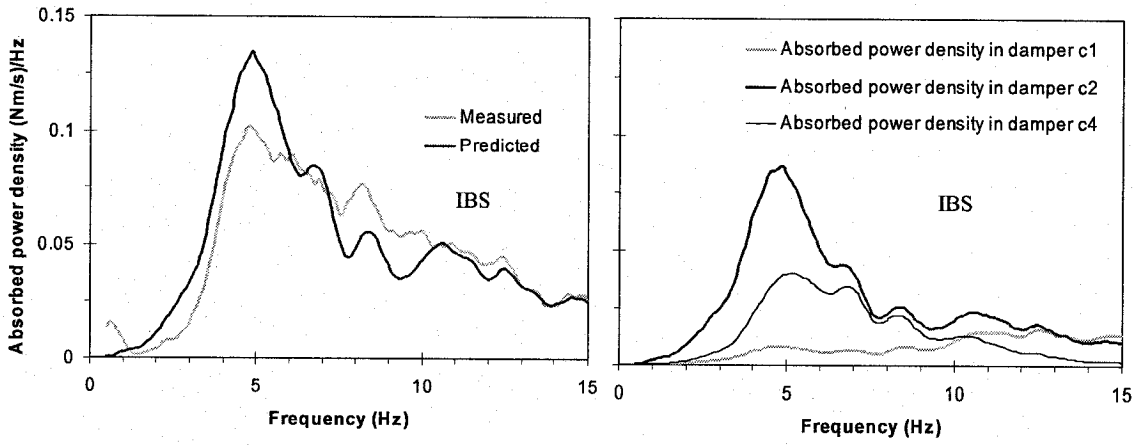

(a) (b)

Figure 5.17: Prediction of absorbed power density from the model derived for inclined back support condition: (a) Comparison between measured mean absorbed power density of six subjects and predicted total absorbed power density of the 4-DOF model; (b) Prediction of localized absorbed power density (1m/s^2 rms acceleration excitation).

The results, in general, show reasonably good agreements in the total power derived from the model and the mean measured power for all three back support conditions. The model, however, yields an overestimate of the peak power density in the vicinity of the primary resonance for the inclined back support posture (Figure 5.17). The results further suggest that a large portion of the power is dissipated by c_2 coupling the upper and lower torso, irrespective of the back support condition. The absorbed power density due to energy dissipated within the torso is in the order of 60% of the total power density. The no back support posture yields highest proportion of dissipated energy within the torso, which can be attributed to relatively larger motion of the unsupported torso. The energy dissipated within the viscera is also considerable and the peak absorbed power density ranges from nearly 20% for NBS posture to nearly 30% for the IBS posture.

5.3 Two-dimensional 5-DOF model

The seated human body exhibits motions in two dimensions (in the mid-sagittal plane) under the WBV vertical vibration [42], which may arise from angular motion of the upper body and upper body interactions with the backrest. Moreover, the occupant-seat system represents multiple driving points formed by the buttock-pan, upper body-backrest, hands-steering column, and feet-pedal interfaces. Studies on biodynamic responses to vibration, however, have invariably considered the single driving-point formed by the seat pan-buttock interface, with only one exception [54]. Those studies would be applicable for NBS posture, hands in lap and negligible contribution due to feet-pedal/floor interactions. However, the interactions with the back support may be

relatively significant, since the backrest supports nearly 30% of the total body weight [54]. Moreover, the dynamic interactions of the upper body with the backrest have been clearly observed from the measured data presented in section 4.3 in terms of cross-axis apparent mass.

Since the biodynamic forces developed at the backrest interface occur along a direction normal to the back support, the one-dimensional model formulated in the previous section would not be applicable. The same would also apply to the reported one-dimensional biodynamic models [19]. Zhang [54] introduced sliding visco—elastic elements between the upper body masses and the back support to study the biodynamic response reflected at the second driving-point (backrest). The study showed significant dynamic interactions between the upper body and the back support, as it was observed from the measured data. A two-dimensional model would thus be desirable in order to provide an appropriate description of the biodynamic behavior of the seated human body with the back support.

A two-dimensional model of the seated human body is formulated upon consideration of the anatomical structure and anthropometry, as it was described for the one-dimensional model in section 5.2.1. The major assumptions associated with the model formulation are listed below:

(i) The upper body is assumed to constitute four lumped masses constrained to slide along a massless ro d oriented along the direction parallel to the back support. The four centered masses represent the head, upper torso, lower torso and viscera mass, as shown in Figure 5.18.

(ii) It was assumed that the upper-body structure is coupled with the greater trochanteric point '**o**' [96] through a revolute joint with rotational viscosity and elasticity.

(iii) It was assumed that the upper body is always in contact with the backrest, and there is sufficient frictional force at the contact zone.

(iv) The body part contacted with the seat pan is attached to the seat pan, and is constrained to move along the vertical axis only.

Base upon the above assumptions, a two-dimensional 5-DOF model structure is formulated, as shown in Figure 5.18, to account for dynamic interactions of the seated body with the backrest while exposed to vertical vibration. Owing to negligible interactions of the upper body with a vertical backrest [51], the modeling task is carried out for the inclined back support posture alone. The model structure also incorporates the geometric parameters of the seated body against an inclined backrest. The rotational stiffness and damping characteristics of the body are introduced to describe the two-dimensional motion of seated body or cross-axis biodynamic response. The entire upper body structure thus undergoes vertical as well as rotational motions.

The model comprises 5 masses, similar to the one-dimensional model. The mass (m_3) may be considered to represent head and neck mass, while m_1 and m_2 are due to lower and upper torso, respectively, m_4 may be attributed to the viscera, and m_0 is the mass due to buttocks and pelvis in contact with the seat. The masses m_1 to m_4 are constrained to move along the direction parallel to the back support. The coordinates r_1 to r_4 define the motions of four masses, respectively, with respect to the origin, considered as the greater

trochanteric point. Parallel combinations of elastic and viscous elements are introduced for coupling the lower and upper torso masses with the backrest, as shown in Figure 5.18. Compared with the 4-DOF model shown in Figure 5.1, the proposed 5-DOF model merely introduce one more rotational degree-of-freedom. The five massed in the model still maintain the same anthropometry characteristics as described for the one-dimensional 4-DOF model. Geometric characteristics of four upper body segments are also introduced in the 5-DOF model. The distances from the greater trochanteric point to each mass (m_1, m_2, m_3, m_4) are represented by *a, b, c,* and *d* respectively. The inclination of the backrest is given by angle ϕ with respect to the horizontal axis. The distance from greater trochanteric point to the center of force generated at the backrest is given by *L*. The masses and geometric parameters of the model were determined from the anthropometric data by Winter [96], for male population of 75.58 kg body mass and 1.76m standing height.

5.3.1 Equations of motion of 5-DOF model

The equations of motion for the proposed five-degree-of-freedom model are derived by using the D'Alembert's principle using the r - θ coordinates, where θ describes the rotational motion of entire upper-body about "O", and r_1, r_2, r_3 and r_4 are the relative motions of four masses to "O" respectively. The equation of motions for the model are summarized as follows:

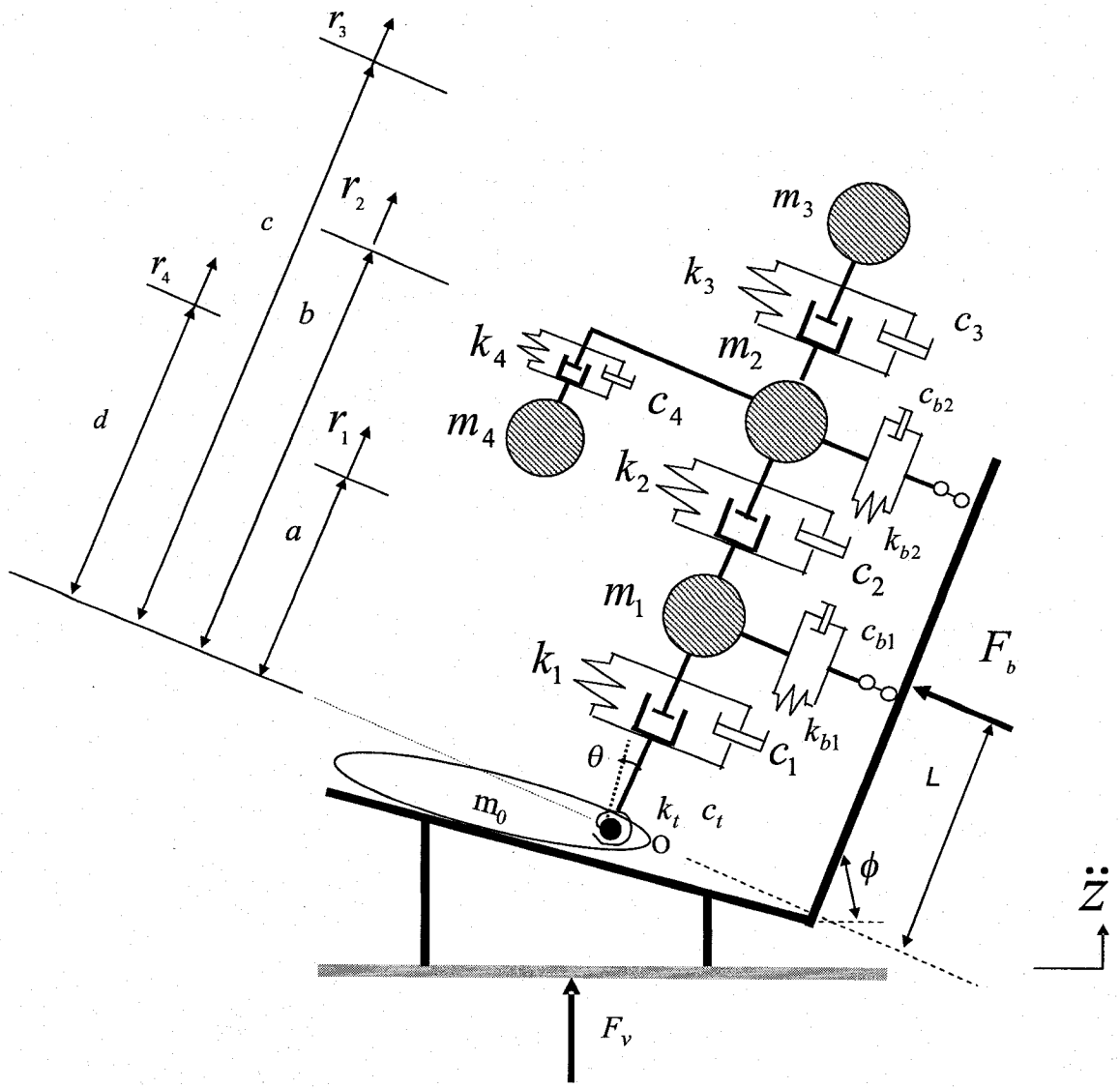

Figure 5.18: Structure of the proposed 5-DOF two-dimensional seated human biodynamic model.

$$\begin{cases} J'\ddot{\theta} + C'\dot{\theta} + K'\theta = -(m_1 a + m_2 b + m_3 c + m_4 d)\ddot{z}\cos\phi \\ m_1\ddot{r}_1 + (c_1 + c_{2)}\dot{r}_1 - c_2\dot{r}_2 + (k_1 + k_2)r_1 - k_2 r_2 = -m_1\ddot{z}\sin\phi \\ m_2\ddot{r}_2 + (c_2 + c_3 + c_4)\dot{r}_2 - c_2\dot{r}_1 - c_3\dot{r}_3 - c_4\dot{r}_4 \\ +(k_2 + k_3 + k_4)r_2 - k_2 r_1 - k_3 r_3 - k_4 r_4 = -m_2\ddot{z}\sin\phi \\ m_3\ddot{r}_3 + c_3\dot{r}_3 - c_3\dot{r}_2 + k_3 r_3 - k_3 r_2 = -m_3\ddot{z}\sin\phi \\ m_4\ddot{r}_4 + c_4\dot{r}_4 - c_4\dot{r}_2 + k_4 r_4 - k_4 r_2 = -m_4\ddot{z}\sin\phi \end{cases} \tag{5.25}$$

$$\text{Where} \quad \begin{cases} J' = m_1 a^2 + m_2 b^2 + m_3 c^2 + m_4 d^2 \\ C' = C_t + C_{b1} a^2 + C_{b2} b^2 \\ K' = K_t + K_{b1} a^2 + K_{b2} b^2 \end{cases} \tag{5.26}$$

Equation (5.26) describes the effective mass moment of inertia, rotational damping element and rotational stiffness, respectively, of upper-body structure.

Equation (5.25) could be rewritten in the matrix form as:

$$\begin{bmatrix} J' & 0 & 0 & 0 & 0 \\ 0 & m_1 & 0 & 0 & 0 \\ 0 & 0 & m_2 & 0 & 0 \\ 0 & 0 & 0 & m_3 & 0 \\ 0 & 0 & 0 & 0 & m_4 \end{bmatrix} \begin{Bmatrix} \ddot{\theta} \\ \ddot{r}_1 \\ \ddot{r}_2 \\ \ddot{r}_3 \\ \ddot{r}_4 \end{Bmatrix} + \begin{bmatrix} C' & 0 & 0 & 0 & 0 \\ 0 & c_1 + c_2 & -c_2 & 0 & 0 \\ 0 & -c_2 & c_2 + c_3 + c_4 & -c_3 & -c_4 \\ 0 & 0 & -c_3 & c_3 & 0 \\ 0 & 0 & -c_4 & 0 & c_4 \end{bmatrix} \begin{Bmatrix} \dot{\theta} \\ \dot{r}_1 \\ \dot{r}_2 \\ \dot{r}_3 \\ \dot{r}_4 \end{Bmatrix}$$
$$+ \begin{bmatrix} K' & 0 & 0 & 0 & 0 \\ 0 & k_1 + k_2 & -k_2 & 0 & 0 \\ 0 & -k_2 & k_2 + k_3 + k_4 & -k_3 & -k_4 \\ 0 & 0 & -k_3 & k_3 & 0 \\ 0 & 0 & -k_4 & 0 & k_4 \end{bmatrix} \begin{Bmatrix} \theta \\ r_1 \\ r_2 \\ r_3 \\ r_4 \end{Bmatrix} = \ddot{z} \begin{Bmatrix} q_1 \\ q_2 \\ q_3 \\ q_4 \\ q_5 \end{Bmatrix} \tag{5.27}$$

$$\text{Where} \quad \begin{cases} q_1 = -(m_1 a + m_2 b + m_3 c + m_4 d)\cos\phi \\ q_2 = -m_1 \sin\phi \\ q_3 = -m_2 \sin\phi \\ q_4 = -m_3 \sin\phi \\ q_5 = -m_4 \sin\phi \end{cases} \tag{5.28}$$

Then above equation could be written as:

$$[M]\{\ddot{u}\}+[C]\{\dot{u}\}+[K]\{u\}=\{q\}\ \ddot{z} \tag{5.29}$$

Where $[M]$ is (5×5) mass matrix; [C] and $[K]$ are (5×5) damping and stiffness matrices, respectively. $\{u\}$ and $\{q\}$ the generalized position coordinate and consultant vectors, given by: is vector of response coordinates, such that:

$$\{u\}=\{\theta, r_1, r_2, r_3, r_4\}^T;\ \{q\}=\{q_1, q_2, q_3, q_4, q_5\}^T$$

Where T designates the transpose.

Applying Laplace transform, and assuming zero initial conditions, then Equation (5.29) could be rewritten as:

$$(s^2[M]+s[C]+[K])\{U(s)\}=s^2 Z(s)\{q\} \tag{5.30}$$

Where $\{U(s)\}=\{\Theta(s), R_1(s), R_2(s), R_3(s), R_4(s)\}^T$; $Z(s)$ and $\Theta(s)$ are Laplace transform of $z(t)$ and $\theta(t)$, respectively, $R_i(s)$ is that of $r_i(t)$, i=1,2,3,4.

Then transfer function vector for the system is further derived from equation (5.30), and such that:

$$\{H(s)\}=\begin{Bmatrix} H_\theta(s) \\ H_1(s) \\ H_2(s) \\ H_3(s) \\ H_4(s) \end{Bmatrix}=\begin{Bmatrix} \Theta(s)/Z(s) \\ R_1(s)/Z(s) \\ R_2(s)/Z(s) \\ R_3(s)/Z(s) \\ R_4(s)/Z(s) \end{Bmatrix}=s^2\left[s^2[M]+s[C]+[K]\right]^{-1}\begin{Bmatrix} q_1 \\ q_2 \\ q_3 \\ q_4 \\ q_5 \end{Bmatrix} \tag{5.31}$$

The vertical component of force generated at the human-seat interface, F_v can be by derived by using the D'Alembert's principle, such that:

$$F_v - \sum_{i=0}^{4} m_i \ddot{z} - (m_1 a + m_2 b + m_3 c + m_4 d)\cos\phi\ddot{\theta}$$
$$-(m_1 \ddot{r}_1 + m_2 \ddot{r}_2 + m_3 \ddot{r}_3 + m_4 \ddot{r}_4)\sin\phi = 0 \quad (5.32)$$

$$F_b = \frac{1}{L}[J'\ddot{\theta} + C_t\dot{\theta} + K_t\theta + (m_1 a + m_2 b + m_3 c + m_4 d)\cos\phi\,\ddot{z}] \quad (5.33)$$

Vertical and cross-axis APMS responses of the model are derived as:

$$M_v(s) = \frac{F_v(s)}{s^2 Z(s)} = \sum_{0}^{4} m_i + (m_1 a + m_2 b + m_3 c + m_4 d)H_\theta(s)\cdot\cos\phi +$$
$$m_1 H_1(s) + m_2 H_2(s) + m_3 H_3(s) + m_4 H_4(s) \quad (5.34)$$

$$M_{vb}(s) = \frac{F_b(s)}{s^2 Z(s)} = \frac{(m_1 a + m_2 b + m_3 c + m_4 d)\cos\phi}{L} + \frac{1}{L}(J' + \frac{C_t}{s} + \frac{K_t}{s^2})H_\theta(s) \quad (5.35)$$

Where M_v and M_{vb} are the vertical and cross-axis APMS.

The 'vertical STHT' response of the model is derived upon consideration of resulting vertical motions of the head and neck mass as:

$$T(s) = 1 + c\ H_\theta(s)\cos\phi + H_3(s)\sin\phi \quad (5.36)$$

Similarly the 'fore-and-aft STHT' response of the model is derived upon consideration of horizontal motions of the head and neck mass as:

$$T_x(s) = H_3(s)\cos\phi - cH_\theta(s)\sin\phi \quad (5.37)$$

5.3.2 Model parameters identification

Similar to the one-dimensional model, the model parameters are identified on the basis of the target data representing the biodynamic responses of the seated male subjects with mean body mass of 75.58 kg, which is close to that of 50th percentile population, while exposed to vertical random vibration of 1.0 m/s^2 rms acceleration (0.5-15Hz), and

seated with hands in lap posture. The target biodynamic functions are 'vertical STHT', and 'vertical STHT', as described for the one-dimensional model. Apart from these, a third target function in 'cross-axis APMS' is introduced to ensure model applicability for back supported posture. The 'cross-axis APMS' target dataset has been illustrated in Figure 4.17. Considering the considerable inter-subject variability revealed in the 'fore-and-aft STHT' responses, as illustrated in Figure 4.2, the parameter identification is performed upon excluding the 'fore-and-aft STHT'.

The parameters for the proposed 5-DOF model are identified through minimization of a weighted error function of the model and measured 'vertical APMS' (M_v), 'vertical STHT' (TF_z) and 'cross-axis APMS' (M_{vb}) magnitude and phase responses. The weighted error function is thus formulated as:

$$E(\eta) = \min[\alpha\, E_{VAPMS}(\eta) + \beta\, E_{STHT}(\eta) + \gamma\, E_{VBAPMS}(\eta)] \tag{5.38}$$

Where $\eta = \{\mu_0, \mu_1, \mu_2, \mu_3, \mu_4, k_1, k_2, k_3, k_4, c_1, c_2, c_3, c_4, k_{b1}, k_{b2}, k_t, c_{b1}, c_{b2}, c_t\}$ is the model parameters vector to be identified. $E(\eta)$ is the total weighted error function, and $E_{VAPMS}(\eta)$ relates to the error arising from the 'vertical APMS' response. Similarly, $E_{STHT}(\eta)$ and $E_{VBAPMS}(\eta)$ relate to the error functions in vertical seat-to-head transfer function and 'cross-axis APMS' respectively. The constants α , β and γ are the weighting factors used to ensure comparable contributions of the error functions in$E_{VAPMS}(\eta)$, $E_{STHT}(\eta)$ and $E_{VBAPMS}(\eta)$, and three factors satisfy the following relationship:

$$\alpha + \beta + \gamma = 1 \tag{5.39}$$

$E_{VAPMS}(\eta)$, $E_{STHT}(\eta)$ and $E_{VBAPMS}(\eta)$ are the squared errors resulting from vertical APMS, vertical STHT and cross-axis APMS responses, respectively, taken at various discrete frequencies in the 0.5-15 Hz range, and are expressed as:

$$\begin{cases} E_{VAPMS}(\chi) = \sum_{i=1}^{N} \lambda_1 \left| \overline{M}_v^*(\omega_i) - \overline{M}_v(\omega_i) \right|^2 + \sum_{i=1}^{N} \psi_1 \left| \phi_v^*(\omega_i) - \phi_v(\omega_i) \right|^2 \\ E_{STHT}(\chi) = \sum_{i=1}^{N} \lambda_2 \left| T^*(\omega_i) - T(\omega_i) \right|^2 + \sum_{i=1}^{N} \psi_2 \left| \varphi^*(\omega_i) - \varphi(\omega_i) \right|^2 \\ E_{VBAPMS}(\chi) = \sum_{i=1}^{N} \lambda_3 \left| \overline{M}_{vb}^*(\omega_i) - \overline{M}_{vb}(\omega_i) \right|^2 + \sum_{i=1}^{N} \psi_3 \left| \phi_{vb}^*(\omega_i) - \phi_{vb}(\omega_i) \right|^2 \end{cases} \quad (5.40)$$

Where $\overline{M}_v^*(\omega_i)$, $\overline{M}_v(\omega_i)$, $\overline{M}_{vb}^*(\omega_i)$ and $\overline{M}_{vb}(\omega_i)$ are the moduli of normalized apparent masses derived from the model and the measured data, respectively; $\phi_v^*(\omega_i)$, $\phi_v(\omega_i), \phi^*_{vb}(\omega_i)$ and $\phi_{vb}(\omega_i)$ are the corresponding APMS phase responses; $T^*(\omega_i)$ and $T(\omega_i)$ are the moduli of STHT derived from the model and the measured data, respectively; $\varphi^*(\omega)$ and $\varphi(\omega)$ are the corresponding STHT phase responses. All the above magnitude and phase responses are attained corresponding to discrete frequency ω_i, and N is the number of discrete frequencies selected in the 0.5 to 15 Hz frequency range. $\lambda_i\,(i=1,2,3)$ and $\psi_i\,(i=1,2,3)$ are the weighting factors applied to attain the comparable contributions of the magnitude and phase errors in the error functions of $E_{VAPMS}(\eta)$, $E_{STHT}(\eta)$ and $E_{VBAPMS}(\eta)$. The weighting factors were selected using the methodology described for the one-dimensional model. Table 5.6 provides the selected weighting factors for the magnitude responses of each error function. These weighting factors assume higher values around the primary resonance than those in the remaining frequency range in order to attain a better agreement within the primary resonance range for both APMS and STHT functions.

Table 5.6: Weighting factor values used in the error function for the 5-DOF model.

$\lambda_i (i=1,2,3)$	λ_i=100 (3.5 ≤f≤ 6.125 Hz) λ_i=1 (f<3.5; f>6.125 Hz)
$\psi_i (i=1,2,3)$	ψ_i =1 (0.5 ≤f≤ 15 Hz)

The error function in equation (5.38) was minimized subject to a number of limit and inequality constraints imposed on the model parameters. The limit constraints imposed on the model masses are identical of those described for the one-dimensional 4-DOF model, corresponding to the inclined back support condition. The minimization problem in equation (5.38) was also subjected to the same inequality constrains on the model stiffness and damping coefficients.

The minimization problem was solved using the nonlinear parameter optimization method (*fmincon)* provided in MATLAB. Several solutions were obtained for different values of weighting factors. The resulting model parameters and the error function were examined to attain weighting factors that yield consistent parameter vector and an overall fit to the target dataset. The weighting factors (α =0.3; β =0.4; and γ=0.3) provide a better fit with all the target functions. The identified parameter values are summarized in Table 5.7. The Table 5.7 also lists the parameter values for the one-dimensional model applicable to the inclined back support condition, as derived in session 5.2.2 .

The results show that solution of equation (5.38) for the two-dimensional model converges to nearly identical parameter values of the one-dimensional model, when common parameters are considered. The damping property of the viscera, however, forms the only exception, which tends to be lower when interactions with the back support are considered. This is most likely attributed to the additional rotational degree-

of-freedom and damping properties of the rotational and backrest interface damping elements.

Table 5.7: Comparison of model parameters for the one- and two-dimensional models for the inclined back support condition.

Values / Parameters	**IBS (5-DOF)**	**IBS (4-DOF)**
m_0 (kg), u_0	4.53(0.06)	4.53(0.06)
m_1 (kg), u_1	20.85(0.276)	20.85(0.276)
m_2 (kg), u_2	15.18(0.201)	15.18(0.201)
m_3 (kg), u_3	4.99(0.066)	4.99(0.066)
m_4 (kg), u_4	11.71(0.155)	11.71(0.155)
k_1 (kN/m)	175.80	180.00
k_2 (kN/m)	37.55	39.55
k_3 (kN/m)	302.72	303.75
k_4 (kN/m)	19.49	19.89
c_1 (Ns/m)	725.25	814.25
c_2 (Ns/m)	1150	1200
c_3 (Ns/m)	800	800
c_4 (Ns/m)	225.25	273.06
k_{b1} (N/m)	9182.9	
k_{b2} (N/m)	4917.7	
k_t (Nm/rad)	8894	
c_{b1} (Ns/m)	133.4	
c_{b2} (Ns/m)	265.1	
c_t (Nms/rad)	146.1	

5.3.2 Model validation

The validity of the identified model is examined by comparing the model responses with the mean measured APMS and STHT responses, as illustrated in Figures 5.19-5.21. The responses of the models show reasonably good agreements with the mean measured data for the inclined back support. Although some deviations are observed at the frequencies above 6 Hz for all moduli and phase responses, which were most likely

attributed to the relatively high inter-subject variations around the secondary resonance. Relatively larger deviation in the frequency corresponding to peak is also evident in Figure 5.21. This is most likely attributed, in part, to the variations in backrest contact condition between the seated human subjects.

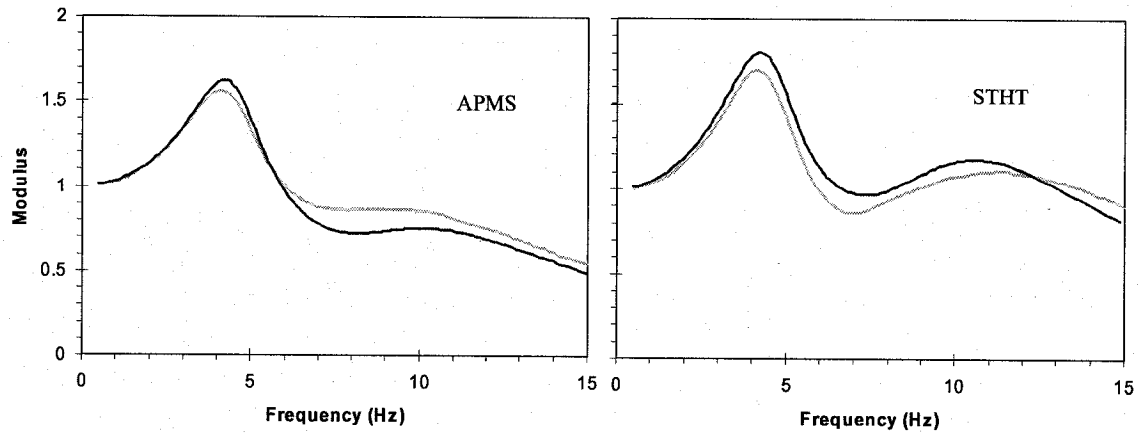

Figure 5.19: Comparison of the computed modulus of vertical apparent mass and seat-to-head transmissibility with the measured data under the inclined back support: —Computed, —Measured.

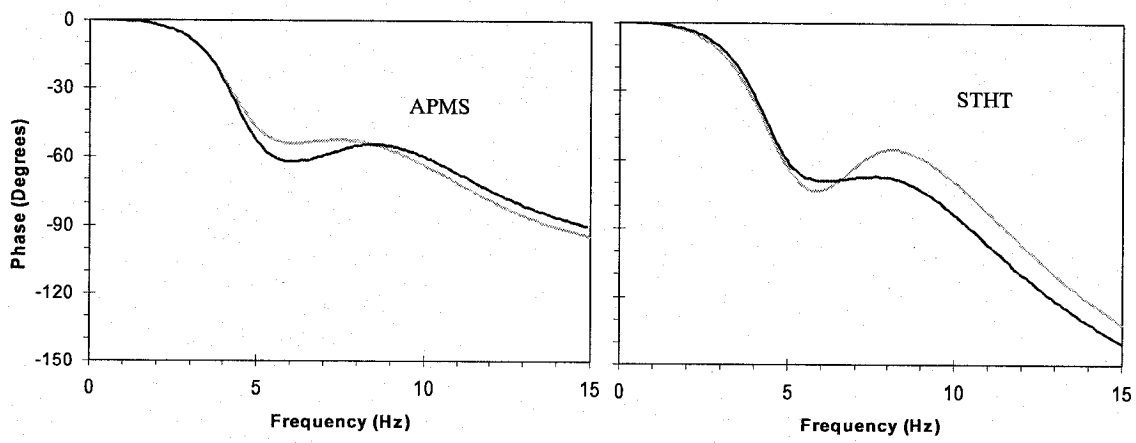

Figure 5.20: Comparison of the computed phase responses of vertical apparent mass and seat-to-head transmissibility with the measured data under the inclined back support: —Computed, —Measured.

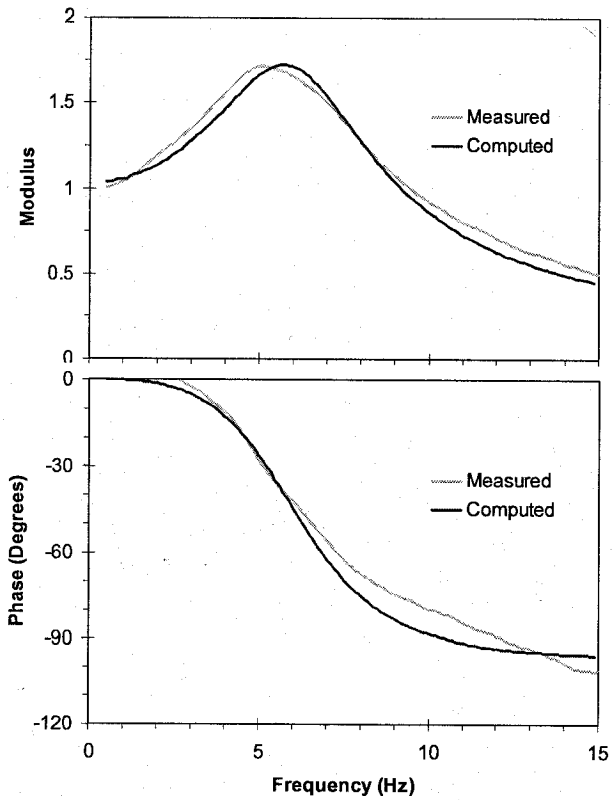

Figure 5.21: Comparison of the computed responses of cross-axis apparent mass with the measured data under the inclined back support: ——Computed;——Measured.

The model was further evaluated to derive the fore-and-aft STHT transmissibility magnitude. The result is compared with the mean measured data in Figure 5.22, which show very poor agreement between the model results and the measured data. Extreme difference in the peak magnitude and corresponding frequency are clearly evident. Moreover, the measured data reveals relatively higher transmissibility magnitude at frequencies beyond 7 Hz (>0.5), while the model response diminishes at higher frequencies. Such great discrepancy in the fore-and-aft STHT response can be mostly attributed to the lack of consideration of the pitch flexibility of the head and neck.

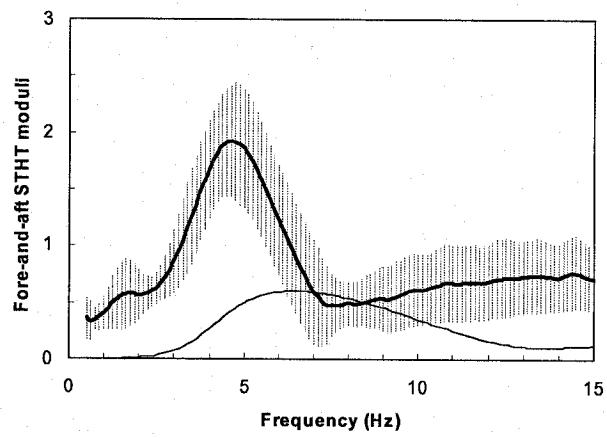

Figure 5.22: Mean curves and mean ± standard deviation scatters of the fore-and-aft STHT measured for 6 subjects under 1.0 m/s^2 rms excitation with hands in lap posture. ——— Measured data, —— Computed data.

5.3.4 Prediction of absorbed power of the two-dimensional model

The validity of two-dimensional model is also examined by computing its absorbed power response with the measured response, as described in section 5.2.5 for the one-dimensional model. The model is further analyzed to compute the local absorbed power density distributed in each viscous damping element in two-dimensional 5-DOF model. Figure 5.23 (a) illustrates a comparison of total absorbed power density estimated from the model with the measured mean absorbed power density of six subjects under 1 m/s^2 rms excitation. There results reveal reasonably good agreement between the two, while notable deviation are evident near the primary resonance, as it was observed for the one-dimensional model. Figure 5.23 (b) illustrates the distributed absorbed power density or energy dissipation by the individual viscous elements, namely, c_1, c_2 and c_4. The energy dissipated by the element coupling the head and neck to the upper body torso is

not presented due to is very low magnitude. The results also revealed very small energy dissipation due to, c_{b1}, c_{b2}, c_t. Therefore, the predicted responses for the two-dimensional model are quire similar to those attained for the one-dimensional model.

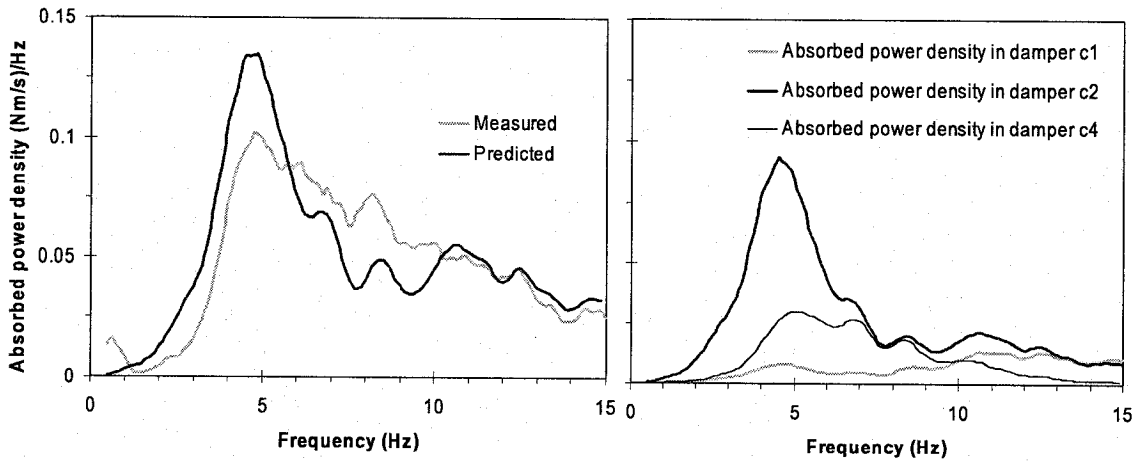

(a) (b)

Figure 5.23: Prediction of absorbed power density from the model derived for inclined back support condition: (a) Comparison between measured mean absorbed power density of six subjects and predicted total absorbed power density of the 5-DOF model; (b) Prediction of localized absorbed power density ($1m/s^2$ rms acceleration excitation).

5.4 Summary

The biodynamic response characteristics of seated occupants under whole-body vehicle vibration have been described in terms of either force-motion relationship at the human-seat interface, or motion-motion relationship through the body. The seated occupant models are derived to characterize both force-motion and motion-motion relationships under a set of representative postural and vibration conditions.

Since the role of seat geometry on both force-motion and motion-motion dynamic responses of seated vehicle occupants exposed to whole-body vibration have been

thoroughly characterized, it is necessary for the mechanical equivalent models to provide the reasonable explanations for the observed biodynamic responses. One-and two-dimensional models are formulated to simulate the APMS and STHT responses to emphasize the effects of back support conditions. The target biodynamic responses are limited to those representing mean body mass of 75.58 kg in the excitation of $1m/s^2$ rms acceleration (0.5-15 Hz) with the hands in lap posture. Specifically, the one-dimensional 4-DOF model is developed using simultaneously measured vertical APMS and STHT response. The model parameters are identified for the three back support conditions respectively. The model parameter analysis suggest that both the force-motion and motion-motion measures need to be satisfied in order to obtain a more reliable model parameter set. The two-dimensional 5-DOF model was developed to describe the cross-axis APMS responses encountered with the inclined backrest support. This allows for the consideration of the upper body dynamic interaction with the backrest. The identified models show good agreements with the measured target responses in APMS measured at the seat pan and the backrest, and vertical STHT.

The model validity is further demonstrated in terms of the absorbed power property of the seated body. Considering that the physical responses of the tissues are more directly related to localized responses, alternate methods that can predict the distributed absorbed power property in body segment are realized in both one-dimensional and two-dimensional models.

In combination with the synchronizing experimental studies, the developed models in this study would provide a better mathematical representation of force-motion and motion-motion biodynamic behaviors of seated human body under vertical whole body

vibration. The validated models would provide an essential basis for an enhanced anthropodynamic manikin.

CHAPTER 6

CONCLUSION AND RECOMMENDATIONS FOR FUTURE WORK

6.1 Highlights and contributions of the Study

The primary focus of this dissertation research is on the study of vertical whole-body vibration biodynamic response characterization of seated occupants through measurements and model development. The dissertation research is conducted in five systematic phases including: (i) Measurement of the vertical apparent mass response characteristics under vehicular vibration environment with different seat geometry-dependent postures; (ii) Characterization of role of seat geometry on biodynamic responses of seated occupants in terms of both apparent mass and absorbed power. (iii) Simultaneous measurements of apparent mass and seat-to-head transmissibility characteristics under vehicular vibration environment with different seat geometry-dependent postures; (iv) Characterization of seat geometry on simultaneous biodynamic responses of seated occupants in terms of both apparent mass and seat-to-head transmissibility; (v) Development and validation of biodynamic models of the seated occupant in one- and two dimensions. The major contributions and highlights of this investigation are summaries below:

a) The apparent mass (APMS) responses of seated vehicle occupants are measured and characterized in relation to several contributory factors, which include anthropometric features, variations in hands position (in lap and on steering wheel), three seat heights, and seat design factors involving two different pan orientations and three different back support conditions (no support, and support with vertical and inclined backrest), and excitation magnitude. The measurements

were taken at a single driving point, the force at the human-seat interface was measured in the applied excitation direction.

b) The absorbed power characteristics of the seated body exposed to vertical WBV was analyzed was performed in frequency domain. The relationship between the absorbed power and apparent mass (driving point mechanical impedance) was revealed. The validity of the indirect method for computing absorbed power was demonstrated.

c) Thorough analyses of the measured APMS data were performed to identify significant factors influencing the biodynamic responses, such as body mass, pan orientations, back support conditions, hands positions, seat heights, excitation magnitude and gender effect.

d) Thorough analyses of the computed absorbed power data were performed to identify significant factors affecting the power absorption, such as body mass, body mass index, body fat, pan orientations, back support conditions, hands positions, seat heights and excitation magnitude.

e) A light weight head-strap measurement system was developed to measure the vibration transmitted to the seated subjects head in a more accurate and repeatable manner.

f) The apparent mass (APMS) and seat-to-head transmissibility (STHT) responses of seated vehicle occupants were measured simultaneously and characterized in relation to several factors, which included variations in hands position, three different back support conditions and excitation magnitudes. The head acceleration was measured in both vertical and fore-and-aft directions. The force

measurements were taken at two driving-points, formed the upper body backrest and buttock-pan interface, as opposed to the single driving-point, invariably considered in previous studies. The 'vertical STHT', 'fore-and-aft STHT', 'vertical APMS', and 'cross-axis APMS' were thus derived from the measured data.

g) Thorough analyses of the measured 'vertical STHT', 'fore-and-aft STHT', 'vertical APMS', and 'cross-axis APMS' data were performed to identify significant factors contributing to these biodynamic responses.

h) The relationship between the simultaneously measured APMS and STHT responses was established with the consideration of role of seat geometry.

i) A four degree-of-freedom biodynamic one-dimensional model was developed to simulate 'vertical STHT' and 'vertical APMS' responses for three different back support conditions. The target datasets are limited to those representing mean body mass of 75.58 kg (in the vicinity of 50^{th} percentile population) in the excitation of $1 m/s^2$ rms acceleration (0.5-15 Hz).

j) The 4-DOF model parameter analysis was performed by satisfying single biodynamic response (APMS or STHT) and both corresponding to three different back support conditions.

k) The identified 4-DOF model parameters were discussed with the consideration of anthropometry aspects both corresponding to three different back support conditions.

l) Analytical method that can predict the distributed absorbed power property in lumped parameter models was derived.

m) The identified 4-DOF model was further validated by predicting the energy dissipation in body segments corresponding to three different back support conditions.

n) A 5-DOF two-dimensional model was developed for the consideration of the seated upper body interactions with the inclined backrest support.

o) The identified 5-DOF two-dimensional model satisfied the measured target responses in APMS measured at the seat pan and the backrest, and vertical STHT.

p) The 5-DOF two-dimensional model was further validated by predicting the total and distributed power property into the body segments.

6.2 Conclusions

On the basis of the results attained in this dissertation, the following major conclusions are drawn:

a) From the study of reported biodynamic characteristics of seated body exposed to vertical WBV, it is apparent that the DPMI/APMS and STHT are influenced by many factors related to subject characteristics, such as body mass and test conditions, excitation magnitudes and postural variations.

b) The absorbed power characteristics of the vibration-exposed body can be effectively derived from the force-motion biodynamic functions, such as APMS or DPMI.

c) Measured vertical apparent mass characteristics at the single driving-point generally exhibit relatively higher primary resonant frequencies when compared

to those widely reported 5 Hz, irrespective of sitting postures. This difference is attributed to the relatively smaller excitation magnitude applied in this study (0.5, 1.0 m/s^2 rms in the frequency range 0.5-40 Hz). The non-linear nature of the APMS response can thus be concluded.

d) Measured vertical apparent mass characteristics at the driving-point reveal a secondary resonance in the 10 -12 Hz frequency range. This secondary peak could be vaguely discerned for the no back supported postures, while it is more pronounced for the inclined back supported posture.

e) The absorbed power is strongly dependent upon the individual's anthropometry characteristics than APMS/DPMI. The absorbed power is strongly correlated with body mass and body mass index, and less strongly correlated with body fat, and body height.

f) The majority of the power absorption in all postures could be attributed to the motion of the upper body. The results further revealed that about 60% of the total absorbed power appears in the lower frequency range of 4-16 Hz.

g) The absorbed power is extremely sensitive to excitation magnitude, while the APMS responses exhibit slight increase in primary resonant frequency with increasing by increasing the excitation magnitude. The APMS responses thus may not be adequate for assessing the risks associated with vibration exposure. However, the absorbed power increases approximately quadratically with the excitation magnitude.

h) From the single driving-point force-motion biodynamic data, it is concluded that seat pan orientation considered in this study has negligible effect on the APMS and absorbed power responses.

i) The seat height affects the sitting posture and the portion of the body weight supported by the seat. The results suggest that the body mass supported by the seat increases with increasing seat height, while the higher seat height yields larger variations in the seated mass for all postures as observed from the standard deviations. The peak APMS magnitude is thereby strongly affected by the seat height.

j) Placing the hands on the steering wheels tends to slightly reduce the portion of body mass supported by the seat, when compared to that for the hands in lap postures. The hands position was found to influence the APMS response only when the back is supported with an inclined backrest and at frequencies in the vicinity of the primary resonant frequency. The hands in lap postures tend to absorb more energy than those with hands on steering wheel postures. This difference tends to be larger with the inclined backrest than for the vertical backrest.

k) The APMS and absorbed power responses out of single driving-point force-motion measurement are strongly affected by the back support condition. At frequencies prior to primary resonance, the APMS magnitude with no back support is higher than that of back supported postures. At the frequencies above the primary resonance to 18 Hz, the APMS magnitude is increasing in the order of no back support, vertical back support and inclined back support. Similarly, the

back supported postures tend to reduce the energy dissipation by the seated body at frequencies prior to primary resonance, and increase the energy absorption after the primary resonance to 18 Hz.

l) A strap-mounted accelerometer was employed to measure the vertical vibration transmitted to the head. The proposed methodology could facilitate the adjustment and monitoring of the accelerometer orientation, while reducing the discomfort caused by the widely-used 'bite-bar' system, and the inertial force contributions arising from the helmet-mounted measurement systems. Compared to the reported STHT responses, the results attained in this study greatly reduce the inter-subject variability.

m) 'Non-linearities' of the human body is distinctly observed for both 'vertical STHT' and 'fore-and-aft STHT' responses irrespective of the back support condition, which is also observed in the vertical and cross-axis APMS responses.

n) The measured STHT data suggest that the back supported postures generally yield lesser inter-subject variability of the data in the vicinity of the primary resonance.

o) Significant magnitudes of fore-and-aft head acceleration are shown even though the vibration excitation is limited to the vertical axis alone, which is most likely attributed to pitch motions of the upper body. The peak magnitudes of fore-and-aft STHT tend to be considerably higher than those of the vertical STHT for the no back support posture. The peak magnitudes of fore-and-aft STHT for the back supported postures were comparable with the vertical STHT magnitude.

p) The 'cross-axis APMS' response data provide important quantitative information on the upper-body interactions with the backrest. The frequency corresponding to peak magnitude occurs relatively larger than that of 'vertical APMS' under the same test condition.

q) The second resonance peak could be observed in the 9-11 Hz from the 'vertical APMS' and 'vertical STHT' responses. This peak becomes more apparent for the back supported postures.

r) Motion-motion biodynamic response out of simultaneous measurement revealed the strong effect of back support condition over the entire frequency range. The peak magnitude of fore-and-aft STHT in the vicinity of the primary resonance is most significantly affected by the back support condition. The use of an inclined back support can help suppress the fore-and-aft motion of the head most notably near the primary resonance. This support, however, causes significantly higher vertical and fore-and-aft motion of the head near the secondary resonant frequency.

s) Similar to the single driving-point force-motion biodynamic responses, the vertical APMS magnitudes in the vicinity of the secondary resonance tend to be higher for the back supported postures.

t) The comparison between the normalized vertical APMS modulus and vertical STHT showed identical primary resonances for all the back support postures, the primary resonances are identical. For the no back support posture, the measured modulus of STHT tends to be relatively higher than the measured normalized APMS magnitude over the entire frequency range. For the two back support

postures, similar trends occur only from 0.5-6 Hz, which cover the primary resonance range. At higher frequencies, there are quite larger differences between the APMS and STHT for the two back supported postures. The STHT responses tend to emphasize the secondary resonance compared to the APMS responses.

u) The hands position yields relatively larger differences in peak magnitude and primary resonant frequency on 'cross-axis APMS' magnitude responses, while the hands position on vertical APMS and STHT responses as well as fore-and-aft STHT responses is considered to be negligible.

v) Comparison of vertical APMS responses of body seated on two different seats, namely the commercial seat vs. automobile seat, suggest that the biodynamic response characterization of the seated body exposed to WBV necessitates considerations of the seat design factors.

w) The one-dimensional 4-DOF model parameters analyses suggest that both the force-motion and motion-motion measures need to be satisfied in order to obtain a more reliable model parameter set.

x) The one-dimensional 4-DOF model results show that the back support postures yield relatively lower stiffness of the lower and upper body torso and viscera component. It suggests that seated upper body tends to stiffen in the absence of back support.

y) The one-dimensional 4-DOF model results show the damping element coupling the lower body and the buttocks and varies considerably as the back support condition changed. Without back support, this damping element reveals a

relatively higher value compared to that of back supported postures. Moreover, it is found that the back support condition yields considerably lower damping coefficient of the viscera component of upper body. The two back supported postures yield quite closer values of the damping coefficients.

z) The identified two-dimensional 5-DOF model show good agreements with the measured target responses in APMS measured at the seat pan and the backrest, and vertical STHT.

aa) The predictions of the total absorbed power density derived from the one-and two-dimensional models show reasonably good agreements with the mean measured power for all three back support conditions.

bb) The predictions of power distribution in body segments suggest that nearly 60% of total power is absorbed within the viscous elements coupling the upper and lower body torso. The energy dissipated within the viscera is also considerable and the peak absorbed power density ranges from nearly 20% for NBS posture to nearly 30% for the IBS posture.

6.3 Recommendations for the future work

Owing to the considerable complexities associated with the seated human and occupant-seat systems, the present study is considered to constitute an important attempt toward quantifying the whole body vibration responses under typical vehicular sitting postures, and the role of various seat design factors. Further efforts need to be undertaken to fully quantify the biodynamic responses in terms of the STHT, APMS and absorbed

power of seated occupant exposed to whole-body vibrations, and the influence of various environmental and postural factors. Although a vast number of fundamental explorations are needed for measurements, analyses, and interpretations of the biodynamic responses in view of risk assessment or injury potentials, and seat design factors, some of the important steps for further research are suggested below:

- Number of subjects: current study considered only 12 male subjects for simultaneous measurement, it is recommended to perform the study with a larger sample of subjects to enhance interpretation of the biodynamic responses, and to quantify the body mass and gender effects more accurately. This would be important considering the large inter-subject variability of the data, and strong dependence of the responses on the body anthropometry.
- Multi-driving point measurements: The biodynamic measurements at different vibration entry points, like the hand-steering wheel, feet platform, are vital for understand the multi-driving point biodynamic behavior, and entry absorption properties of the seated body. The forces along three-axis at each driving point should be acquired in order to fully characterize the biodynamic responses.
- Analyses of multi-axis force-motion and motion-motion biodynamic responses under multi-axes vibration excitations would be extremely important to characterize the human responses to realistic vibration environment of vehicles.
- While force-motion responses relate to the biodynamics at the point of entry, the motion-motion response could yield considerable insight into the nature of vibration transmitted to different body segments. It is thus recommended to

characterize the nature of vibration transmitted to various body segments, namely, the lumbar, thoracic and cervical region of spine.

- EMG: the seated human exposed to whole vibration displays diverse psychological and physiological reactions. It is recommended to analyze the spinal muscle-activities under vibration environment along with the force-motion and motion-motion biodynamic functions to develop a correlation among the musculoskeletal loading and biodynamic response.
- Posture: the present study suggests strong contributions due to inclination of the backrest. It is recommended that the role of backrest under different inclinations of the backrest and pan should be thoroughly investigated to identify the design guidance for seats.
- Further studies in two-dimensional model may consider the pitch flexibility of head and neck in order to better describe the fore-and-aft STHT responses.
- Further studies in the seated human body modeling are desirable to consider multi-axis and motion-motion biodynamic response measurements. The consideration of development of anthropodynamic manikins may be brought together with the modeling issues. Moreover, multi-body modeling approach would be beneficial to study three-dimensional dynamic responses.

REFERNCES

1. Griffin, M.J., 1990. Handbook of Human Vibration, Academic Press Limited, London.

2. Seidel, H., 2005. On the relationship between whole-body vibration exposure and spinal health risk. Industrial Health, 43, 361-377.

3. Seidel, H., Blüthner R., Hinz B., Schust, M., 1998. On the health risk of the lumbar spine due to whole-body vibration — theoretical approach, experimental data and evaluation of whole-body vibration, Journal of Sound and Vibration 215 (4), 723-741.

4. Bovenzi, M., Hulshof, C. T. J., 1998. An updated review of epidemiologic studies on the relationship between exposure to whole-body vibration and low back pain. Journal of Sound and Vibration 215 (4), 595-612.

5. Hulshof, C., Van Zanten, B.V., 1987. Whole-body vibration and low back pain. A review of epidemiologic studies. International Archives of Occupational and Environmental Health 59, 205-220.

6. Magnusson, M. L., Pope, M. H., Hulshof, C., and Bovenzi, M., 1998. Development of a protocol for epidemiological studies of whole-body vibration and musculoskeletal disorders of the low back. Journal of Sound and Vibration 215 (4), 643-651.

7. Seidel, H., Heidel, R., 1986. Long term effects of whole-body vibration — a critical survey of literature. International Archives of Occupational and Environmental Health 58, 1-26.

8. Boileau, P.-É., 1995. A study of secondary suspension and human driver response to whole-body vehicular vibration and shock. Ph.D., Thesis, Concordia University, Montreal, Canada.

9. Wu, X., 1998. Study of driver-seat interactions and enhancement of vehicular ride vibration environment. Ph.D. Thesis, Concordia University, Montreal, Canada.

10. Boileau, P.-É. Wu, X. and Rakheja, S., 1998. Definition of a range of idealized values to characterize seated body biodynamic response under vertical vibration. J. Sound and Vibration, 215 (4), 841-862.

11. Paddan, G.S. and Griffin, M.J., 1998. A review of the transmission of translational seat vibration to the head. Journal of Sound and Vibration, 215 (4), 863-882.

12. International Organization for Standardization, ISO-5982: 2001. Mechanical vibration and shock range of idealized values to characterize seated-body biodynamic response under vertical vibration.

13. Rakheja et al., 1997. Estimation of vibration transmission of the seat-human system though measurements of the seat-load system. Research Report, CONCAVE Research Center, Concordia University.

14. Bendat, J.S., Piersol A.G., 1992. Random data-analysis and measurement procedures. New York, John Wiley & Sons.

15. Lee, R.A., Pradko, F., 1968. Analytical analysis of human vibration, SAE paper 680091.

16. International Organization for Standardization ISO 2631-1, 1997. Mechanical vibration and shock – evaluation of human exposure to whole – body vibration. Part 1, General Requirements.

17. Lewis, C.H., Griffin, M.J., 1998. A comparison of evaluations and assessments obtained using alternative standards for predicting the hazards of whole-body vibration and repeated shock. Journal of Sound and Vibration, 215 (4), 915-926.

18. Mansfield, N.J., Holmlund, P., Lundström, R., 2000. Comparison of subjective responses to vibration and shock with standard analysis methods and absorbed power. Journal of Sound and Vibration 230 (3), 477-491.

19. Boileau, P.E. Rakheja, S. Yang, X. and Stiharu, I., 1997. Comparison of biodynamic response characteristics of various human body models as applied to seated vehicle drivers. Noise & Vibration Worldwide, October, 7-14.

20. Seidel, H., Griffin, M.J., 2001. Modeling the responses of the spinal system to whole-body vibration and repeated shock. Clinical Biomechanics 16 (Supplement 1), S3–S7.

21. Griffin, M.J., 2001. The validation of biodynamic models. Clinical Biomechanics 16 (Supplement 1), S81–S92.

22. Coermann, R.R., 1962. The Mechanical Impedance of the Human Body in Sitting and Standing Position at low frequencies. Human Factors, 227-253.

23. Miwa, T., 1975. Mechanical impedance of human body in various postures. Industrial Health, 13, 1-22.

24. Vogt, H.L., Coermann, R.R. and Fust, H.D., 1968. Mechanical impedance of the sitting human under sustained acceleration. Aerospace Medicine, 39, 675-679.

25. Suggs, C.W., Abrams, CF Stikeleather, L.F., 1969. Application of a Dynamic Simulator in Seat Testing. Transaction of ASAE, Vol.13, 378-381.

26. Griffin, M.J., 1975. Vertical vibration of seated subjects, effects of posture, vibration level and frequency. Aviation Space Environmental Medicine 46, 269-276.

27. Cohen, H.H., Wasserman, D.E., Hornung, R.W., 1977. Human performance and transmissibility under sinusoidal and mixed vertical vibration. Ergonomics 20,207-216.

28. Mertens H., 1978. Nonlinear behavior of sitting humans under increasing gravity. Aviation, Space, and Environmental Medicine, 287-298.

29. Griffin, M.J. and Whitham, E.M., 1978. Individual variability and its effect on subjective and biodynamic response to whole-body vibration. Journal of Sound and vibration 58, 239-250.

30. Griffin, M.J., Lewis, C.H., Parsons K.C. and Whitham, E.M., 1979. AGARD Conference Proceedings CP-253. Paper A28 in Models and analogues for the evaluation of human biodynamic response, performance and protection. The biodynamic response of the human body and its application to standards.

31. Sandover, J., 1982. Measurements of the frequency response characteristics of man exposed to vibration. Ph.D Thesis, Loughborough University of Technology.

32. Donati, P.M. and Bonthous, C., 1983. Biodynamic response of the human body in the sitting position when subjected to vertical vibration. Journal of Sound and Vibration, 90, 423-442.

33. Hagena, F.W., Piehler, J., Wirth, C.J., Hofmann, G.O. and Zwingers, T.H., 1986. The dynamic response of the human spine to sinusoidal Gz-vibration. In-vivo-experiments. Neuro-Orthopedics 2, 29-33.

34. Hinz, B., and Seidel, H., 1987. The non-linearity of the human body's dynamic response during sinusoidal whole body vibration. Industrial Health 25, 169-181.

35. Paddan, G.S. and Griffin, M.J., 1988. The transmission of translational seat vibration to the head -I. Vertical seat vibration. Journal of Biomechanics, 21, 191-197.

36. Fairley, T. E. and Griffin, M.J., 1989. The apparent mass of the seated human body, vertical vibration. Journal of Biomechanics, 22, 81-94.

37. Smith, S.D., 1993. Comparison of the driving-point impedance and transmissibility techniques in describing human response to whole-body vibration. Proceedings U.K. Informal Group Meeting on Human Response to Vibration, APRE, Farnborough,

United Kingdom.

38. Seidel, H., 1996. A contribution to the revision of ISO 5982. Mechanical driving point impedance and transmissibility of the human body. Personal communications to A. J. Brammer.

39. Zimmennann, C.L. and Cook, T.M., 1997. Effects of vibration frequency and postural changes on human responses to seated whole-body vibration exposure. Archives of Occupational and Environmental Health, 69, 165-179.

40. Boileau, P.-É. & Rakheja, S., 1998. Whole-body vertical biodynamic response characteristics of the seated vehicle driver, Measurement and model development. International Journal of Industrial Ergonomics, 22, 449-472.

41. Kitazaki, S. and Griffin, M.J., 1998. Resonance behaviour of the seated human body and effects of posture. Journal of Biomechanics, 31, 143-149.

42. Matsumoto, Y. and Griffin, M.J., 1998. Movement of the upper-body of seated subjects exposed to vertical whole-body vibration at the principal resonance frequency. Journal of Sound and Vibration, 215(4), 743-762.

43. Lundstrom, R. and Holmlund P., 1998. Absorption of energy during whole-body vibration exposure. Journal of Sound and Vibration, 215 (4), 789-799.

44. Mansfield N. J. and Griffin M.J., 1998, Effect of magnitude of vertical whole-body vibration on absorbed power for the seated human body. Journal of Sound and Vibration, 215 (4), 813 - 825.

45. Mansfield, N.J. and Griffin M.J., 2000. Non-linearities in apparent mass and transmissibility during exposure to whole-body vertical vibration. Journal of Biomechanics, 33, 933-941.

46. Holmlund, P., Lundstrom, R. and Lindberg, L., 2000. Mechanical impedance of the human body in vertical direction. Applied Ergonomics, 31,415-422.

47. Hinz, B., Seidel, H., Menzel, G. and Bluthner, R., 2002. Effects related to random whole-body Vibration and posture on a suspended seat with and without backrest. Journal of Sound and Vibration, 253 (1), 265-282.

48. Rakheja, S., Boileau, P.-E. and Stiharu, I., 2002. Seated occupant apparent mass characteristics under automotive postures and vertical vibration. Journal of Sound and Vibration, 253(1), 57-75.

49. Demic, M., Lukic, J. and Milic, Z., 2002. Some aspects of the investigation of random vibration influence on ride comfort. Journal of Sound and Vibration, 253 (1), 109-129.

50. Nawayseh, N. and Griffin, M.J., 2003. Non-linear dual-axis biodynamic response to vertical whole-body vibration. Journal of Sound and Vibration, 268 (3), 503-523.

51. Nawayseh, N. and Griffin, M.J., 2004. Tri-axial forces at the seat and backrest during whole-body vertical vibration. Journal of Sound and Vibration, 277 (1-2), 309-326.

52. Nawayseh, N. and Griffin, M.J., 2005. Absorbed power at the seat, backrest and feet of subjects exposed to Whole-body vertical vibration. 40th United Kingdom Conference on Human Response to Vibration, 13-15 September, Liverpool, England.

53. Nawayseh, N. and Griffin, M.J., 2005. Effect of seat surface angle on forces at the seat surface during whole-body vertical vibration. Journal of Sound and Vibration, 284 (3-5), 613-634.

54. Zhang, H., 2005. Biodynamic response and body interactions with the seat pan and the backrest under vertical vibration. Master thesis, Concordia University, Montreal, Canada.

55. Paddan, G.S., Griffin, M.J., 1988. The transmission of translational seat vibration to the head II. Horizontal seat vibration, Journal of Biomechanics 21,199–206.

56. Paddan, G.S., Griffin, M.J., 1994. Transmission of roll and pitch seat vibration to the head, Ergonomics 37, 1513–1531.

57. Paddan, G.S., Griffin, M.J., 2000. Transmission of yaw seat vibration to the head, Journal of Sound and Vibration 229, 1077–1095.

58. Mansfield, N.J. and Griffin, M.J., 2002. Effects of posture and vibration magnitude on apparent mass and pelvis rotation during exposure to whole-body vertical vibration. Journal of Sound and Vibration 253(1), 93-107.

59. Magnusson, M. Pope, M. Rostedt, M. Hansson, T., 1993. Effect of backrest inclination on the transmission of vertical vibrations through the lumbar spine. Clinical Biomechanics 8, 5–12.

60. Griffin, M.J., Whitham, E.M. and Parsons, K.C., 1982. Vibration and comfort. II. Translational seat vibration, Ergonomics 25, 603-630.

61. Parsons, K.C. and Griffin, M.J., 1982. Vibration and comfort, II. Rotational seat vibration, Ergonomics 25, 631-644.

62. Laurent, R., 1996. A study of the effect of gender on the transmissibility of car seats. UK Informal Group Meeting on Human Response to Vibration.

63. International Standard for Standardization ISO 10326-1, 1994. Mechanical vibration laboratory method for evaluating vehicle seat vibration. Part 1, Basic requirements.

64. Toward M.G.R., 2000. Use of an anthropodynamic dummy to measure seat dynamics. Proceedings of the 35th UK Group Meeting on Human Response to vibration 13-15 September, 39-48, ISPR, University of Southampton, England.

65. Allen, G., 1978. A critical look at biodynamic modeling in relation to specifications for human tolerance of vibration and shock. AGARD Conference Proceedings No.253. A25-5.

66. Payne, P.R. and Band, E.G.U., 1971. A 4-DOF lumped parameter model of the seated human body. Aerospace Medical Research Laboratories Report AMRL-TR-70-35, Wright-Patterson Air Force Base, Ohio, USA.

67. ISO Committee Draft CD 5982, 1993. Mechanical Driving Point Impedance and Transmissibility of the Human body. Document ISO/TC 108/SC 4 N226, 21p.

68. Payne, P.R., 1978. Method to Quantify Ride Comfort and Allowable Accelerations. Aviation, Space, and Environmental Medicine, 262-269.

69. Amirouche, F.M. and Ider, S.K., 1988. Simulation and Analysis of a Biodynamic Human model Subjected to Low Accelerations – a Correlation Study. Journal of Sound and Vibration, 123, 281-292.

70. Patil, M.K. and Palanichamy, M.S., 1988. A mathematical model of tractor-occupant system with a new seat suspension for minimization of vibration response. Applied Mathematical Modeling, 12, 63-71.

71. Matsumoto, Y. and Griffin, M.J., 2001. Modeling the dynamic mechanisms associated with the principal resonance of the seated human body. Clinical Biomechanics, 16 (1), S31-S44.

72. Kitazaki, S. and Griffin, M.J., 1997. A modal analysis of whole body vertical vibration, using a finite element model of the human body. Journal of Sound and Vibration 200 (1), 83–103.

73. Wu, X. Rakheja, S. and Boileau, P.-É., 1999. Analyses of the relationships between biodynamic response function. Journal of Sound and Vibration, 226 (3), 595-606.

74. Mansfield, N.J., 2005. Impedance methods (apparent mass, driving point mechanical impedance and absorbed power) for assessment of the biomechanical response of the seated person to whole-body vibration. Industrial Health 43(3), 378-389.

75. Pope, M.H., Svensson, Broman, M.H. and Anderson, G.B.J., 1986. Mounting of the transducers in measurement of segmental motion of the spine. Journal of Biomechanics, 19, 675-677.

76. Panjabi, M.M., Anderson, G.B.J., Jorneus, L., Hult, E. and Mattsson, L., 1986. In vivo measurements of spinal column vibrations. Journal of Bone and Joint Surgery, Incorporated 1986, 68A, 695-702.

77. Sandover, J. and Dupuis, H., 1987. A reanalysis of spinal motion during vibration Ergonomics, 30, 975-985.

78. Lewis, C.H. and Griffin, M.J., 1980. Predicting the effects of vibration frequency, and axis, and seating conditions on the reading of numeric displays. Ergonomics, 23, 485-501.

79. Woodman, P.D., 1995. The influence of skin tissue on the relative motion between the head and a helmet. United Kingdom Conference on Human Response to Vibration, 18-20 September.

80. Woodman, P.D., 1996. The effect of the head-helmet coupling on the relative acceleration between head and helmet. United Kingdom Conference on Human Response to Vibration, 18-20 September.

81. Smith, S.D. et al., 2000. Helmet system performance in vibration environments. United Kingdom Conference on Human Response to Vibration, 13-15 September.

82. International Organization for Standardization ISO-4253, 1977. Agricultural Tractors – Operator Seating Accommodation – Dimensions.

83. Burström L., 1990. Absorption of vibration energy in the human hand and arm, Ph.D. Thesis, Lulea University of Technology, Lulea, Sweden.

84. Munro, H.B., 1997. Statistical methods for health care research. 3rd ed. Philadelphia, Lippincott.

85. Lee, R.A. and Pradko, F., 1968. Analytical analysis of human vibration. SAE transactions (77), Paper No. 680091.

86. Cundiff, J.S., 1976. Energy dissipation in human hand-arm exposed to random vibration. Journal of Acoustics Soc Am (59), 212-214.

87. Lidstrom, I.M., 1977. Vibration injury in rock drillers, chiselers, and grinders, some views on the relationship between the quantity of energy absorbed and the risk of occurrence of vibration injury. Proceedings of the international Conference on Hand-Arm Vibration, Cincinnati, OH, 77-83.

88. Anderson, J.S., 1978. Measurement of the energy dissipated in the hand and arm whilst using vibratory tools. Applied Acoustics (11), 219-224.

89. Burström L., Lundström R., 1988. Mechanical energy absorption in human hand-arm exposed to sinusoidal vibration, Int. Arch. Occupational Environ. Health 61, 213–216.

90. Burström L., 1990. Measurement of the mechanical energy absorption in the hand and arm whilst using vibrating tools. Journal of Low Frequency, Noise and Vibration Control (9), 1-14.

91. Kihlberg S., 1995. Biodynamic response of the hand-arm system to vibration from an impact and a grinder. International Journal of Industrial Ergonomics (16), 1-8.

92. El-khatib, A., Guillon, F., and Domont, A., 1998. Vertical vibration transmission through the lumbar spine of the seated subject-first results. Journal of Sound and Vibration, 215 (4), 763-773.

93. Wang, W., Rakheja, S., and Boileau, P.-É., 2004. Effects of sitting posture on biodynamic response of seated occupants under vertical vibration, International Journal of Industry Ergonomics 34 (4), 289-306.

94. Mandapuram, S.C., Rakheja, S., Ma, S., Demont, R.G. and Boileau, P-É., 2005. Influence of back support conditions on the apparent mass of seated occupants under horizontal vibration. Industrial Health, 43, 421–435.

95. Wang, W., Rakheja, S., and Boileau, P.-É., 2006. The role of seat geometry and posture on the mechanical energy absorption characteristics of seated occupants under vertical vibration International Journal of Industrial Ergonomics, 36 (2) 171-184.

96. Winter, D.A., 1990. Biomechanics and Motor Control of Human Movement. Wiley Inc., New York.

97. European Standard prEN 13490, 2001. Mechanical Vibration-Industrial Trucks-Laboratory evaluation and specification of operator seat vibration.

98. Boileau, P-E., Rakheja, S., 2000. Rapport IRSST Caractérisation de l'environnement vibratoire dans différentes catégories de véhicules: industriels, utilitaires et de transport urbain.

99. International Organization for Standardization ISO 7096:2000. Earth-moving machinery-Laboratory Evaluation of Operator Seat Vibration.

100. Optimization Toolbox for Use with MATLAB, MATHWORKS Inc. 1997